Leeds Liverpool Newcastle Sheffield
MRC DiMeN Doctoral Training Partnership
Discovery Medicine North

# Using *Drosophila* to characterise the role of *amo/PKD2* and associated pathways in the context of immune cell function and ADPKD modelling

**Elliot Charles Brooks**

A thesis submitted in partial fulfilment of the requirements for the degree of Doctor of Philosophy

The University of Sheffield
Faculty of Medicine, Dentistry and Health
Department of Infection, Immunity and Cardiovascular Disease (IICD)
Submitted June 2022

# Acknowledgments

First and foremost, I would like to dedicate this thesis to anyone who has put up with me, helped me, comforted me and/or amused me for over 3 and a half years. I have met and leant on some truly wonderful people in my time in Sheffield, and I genuinely would not have been able to do this without them. A special mention to Charlotte Higgins who for 3 years was not only my house mate, but my very good mate.

My entire family have been incredible throughout these past few years, while my parents, Roz and Richard Brooks, have been there for me not just throughout this PhD, but my entire life, and I want to thank them for everything they have done for me.

Both my supervisors, Iwan Evans and Albert Ong, have been extremely patient, kind and supportive to me throughout this project, for which I will be eternally grateful. Iwan especially has supported me in countless ways, and I would not be at this point without him. He is a fine scientist and an even better person, and we could do with a lot more people like him, both in science and the world. All members of both the Evans and Ong labs, past and present, have been wonderful to work with, and it's a shame my project didn't involve more mammalian work, as it would have been a pleasure to work more closely with the Kidney Genetics Group. Even so, Lisa Chang and Andrew Streets offered plenty of help and guidance during my forays into cell culture, for which I am grateful.

As for the fly guys, I have to mention and thank Emma Armitage for her patience during my early days of fly pushing, and for many lunchtime chats in the Bateson room, as well as Juliette Howarth for her excellent assistance with the subtypes work. An unbelievably special mention to one of the finest humans I have ever met, Olivier Tardy, without whom I would have imploded several times over. He is truly a remarkable person the like of which I have never met, and I consider myself extremely lucky to have crossed paths with him. Without him, I would not have made many of the other friends who have helped keep me sane these few years, namely Dan Bennison, Jacqui Chalakova, Jacob Rudman and Ffion Hammond, among many other people in the Bateson Centre and beyond.

Special thanks to the MRC Discovery Medicine North (DiMeN) DTP for funding me for the past few years and for providing excellent training courses. Particular thanks to Emily Goodall, who does such a wonderful job at making DiMeN a fine environment for young scientists to thrive in, and to everyone within the DTP who has offered their camaraderie.

I would also like to offer my thanks to many of the technical staff I have relied on these past few years, namely Darren Robinson and Nick Van Hateren of the Light Microscopy Facility, and Kath Whitley and the rest of the Sheffield Fly Facility, without whom I would have been too busy preparing fly food to carry out any experiments.

Finally, I would like to thank the best person in the world, Kayleigh Scotcher. I started this PhD with an amazing partner, and I now submit my thesis with an amazing wife. I can't stress enough how amazing Kayleigh has been to me throughout the past few years, and I count myself incredibly lucky every single day of my life.

# Abstract

Autosomal Dominant Polycystic Kidney Disease (ADPKD) is one of the most common monogenic disorders, affecting between 1:400 and 1:1000 people, and accounting for over 12 million patients worldwide. It is known to be caused by mutations in the genes *PKD1* or *PKD2,* which encode Polycystin-1 and Polycystin-2, respectively. However, the exact molecular mechanisms involved in the pathogenesis remain poorly understood, partly due to the high levels of allelic heterogeneity both *PKD1* and *PKD2* possess. The fruit fly *Drosophila melanogaster* possesses a homolog of *PKD2* known as *almost there/amo*, which is required for male fertility, smooth muscle contractility and the macrophage-mediated phagocytosis of apoptotic cells, known as efferocytosis. Interestingly, the polycystic kidney microenvironment is associated high levels of uncleared apoptotic cells, and macrophage influx into nascent cysts is known to drive expansion. In this thesis, I have exploited *Drosophila* in order to characterise the impact of *amo* mutations to help further understanding of ADPKD pathogenesis. I have taken three approaches, firstly to develop *Drosophila* as a model with which to screen clinically relevant missense variants of *amo/PKD2*. Secondly, I have investigated if the presence of uncleared apoptotic cells, due to loss of Amo-mediated efferocytosis, is sufficient to impair macrophage function and behaviour. Finally, I investigated the role of apoptotic cell clearance and other pathways related to Amo in the specification of putative pro-inflammatory macrophage subpopulations in *Drosophila*. Through the use of mutants with a high apoptotic background, as well as various apoptotic cell receptor mutants I have shown that Amo prevents the appearance of these putative pro-inflammatory macrophages in the developing embryo. Furthermore, results suggest that Amo regulates acidification of the internalised phagosomes during efferocytosis, rather than engulfment of apoptotic cells. I have also shown how the calcium-binding chaperone protein Calnexin14D seems to be involved in the priming of *Drosophila* macrophages to mount an effective wound response. Overall, these data implicate potentially novel pathways in the pathogenesis of ADPKD, while validating the use of *Drosophila* as a model with which to understand processes underlying macrophage heterogeneity, which was previously thought restricted to vertebrate macrophage populations.

# Abbreviations

Acute myeloid leukaemia 1/Runt related transcription factor 1 – AML1/RUNX1
Adenosine triphosphate – ATP
Almost there – Amo
Angiotensin converting enzyme – ACE
Autosomal Dominant Polycystic Kidney Disease – ADPKD
Bone marrow-derived macrophage – BMDM
Bovine serum albumin – BSA
c-Jun N-terminal Kinase – JNK
Calcium induced calcium release – CICR
Calcium-sensing receptor – CaSR
Calnexin14D – Cnx14D
Chronic obstructive pulmonary disease – COPD
Croquemort – Crq
Cyclic Adenosine Monophosphate – cAMP
Daughterless – Da
Death-associated inhibitor of apoptosis-1 – Diap-1
Debris buster – Dsb
Deoxyribonucleic acid – DNA
DNA adenine methyltransferase – DAM
Draper – Drpr
Dual oxidase – DUOX
Ecdysone receptor – EcR
End-stage renal disease – ESRD
Endoplasmic reticulum – ER
Epidermal growth factor – EGF
Epidermal growth factor receptor – EGFR
Foetal calf serum – FCS
GAL4 activation domain – AD
GAL4 DNA binding domain – DBD
Glial cells missing – Gcm
Green fluorescent protein – GFP
Head involution defective – Hid
Human influenza hemagglutinin – HA
Inhibitors of apoptotic proteins – IAPs
Inositol 1,4,5-triphosphate receptor – IP3R
Interferon gamma – IFNγ
Interleukin-4 – IL-4
Janus kinase – JAK
Kidney injury molecule-1 – KIM-1
Kupffer's vesicle – KV
Lipopolysaccharide – LPS
Lozenge – Lz
Luria broth – LB
Lysosomal associated membrane protein – LAMP

Mechanistic target of rapamycin – mTOR
Mitochondrial outer membrane permeability – MOMP
Monocyte chemoattractant protein-1 – MCP-1
Monocyte-derived macrophage – MDMs
Nimrod B4 – NimB4
Open reading framer – ORF
Paraformaldehyde – PFA
Pathogen-associated molecular patterns – PAMPs
PDGF and VEGF-related factor – Pvf
Peripheral blood mononucleated cells – PBMCs
Phagocytic index – PI
Phosphate buffered saline – PBS
Phosphatidylinositol 3-phosphate – PI3P
Phosphatidylserine – PS
Polycystic Kidney Disease 1 – PKD1
Polycystic Kidney Disease 2 – PKD2
Polycystin-1 – PC-1
Polycystin-2 – PC-2
Polymerase chain reaction – PCR
Red fluorescent protein – RFP
Reversed polarity – Repo
Ribonucleic acid – RNA
Ryanodine receptor – RyR
Sarcoplasmic reticulum – SR
Serpent – Srp
Signal transducer and activator or transcription – STAT
Six microns under – Simu
Store operate calcium entry – SOCE
Systemic lupus erythematous – SLE
Tetragonal opening for Polycystins domain – TOP domain
Total kidney volume – TKV
Transforming growth factor beta – TGF-β
Transient receptor potential mucolipin – Trpml
Tris-acetate-EDTA – TAE
Triton-x100 in 1x PBS – PBTx
Undertaker – Uta
Upstream activator sequence – UAS
Vascular endothelial growth factor – VEGF
Ventral midline – VML
Ventral nerve cord – VNC
Vienna Tiles – VT

# Table of contents

# Table of figures

# Table of tables

# Chapter 1: Introduction

## 1.1 Autosomal dominant polycystic kidney disease

### 1.1.1 Disease background

Autosomal Dominant Polycystic Kidney Disease (ADPKD) is the most common inherited cause of end stage renal disease (ESRD) and one of the most common monogenic disorders, affecting between 1 in 400 and 1 in 1000 people worldwide, accounting for over 12 million patients (Iglesias et al., 1983; Leuenroth & Crews, 2009). It is characterised by the bilateral formation of cysts on the kidneys, causing marked increases in total kidney volume and kidney to bodyweight ratio, ultimately causing end stage renal disease (ESRD) in most cases (Torres et al., 2007). Cysts typically originate from individual epithelial cells of the renal tubules within the nephron, which rapidly proliferate and detach from the tubule to form distinct cysts which continue to expand. ADPKD is often, although not always, also associated with the formation of cysts on other organs, primarily the liver and, less commonly, the pancreas (Kim et al., 2016; Milutinovic et al., 1980). It is usually not diagnosed in patients until later in life, generally between 40 and 60 years of age, although more severe cases can be diagnosed as early as 30 (Hateboer et al., 1999).

For nearly three decades it has been known that ADPKD is caused by loss-of-function mutations in the genes *PKD1* and *PKD2*, which encode the proteins Polycystin-1 (PC-1) and Polycystin-2 (PC-2), respectively (Hughes et al., 1995; Peters et al., 1993). Mutations in *PKD1* cause type 1 ADPKD, accounting for around 85% of ADPKD cases. Type 1 patients are associated with a more severe phenotype and a median onset of ESRD of 53 years of age, although this is dependent on the nature of the mutation, as discussed below. Mutations in *PKD2* cause type 2 ADPKD, accounting for the remaining 15% of all ADPKD cases, and these are associated with a milder phenotype and a later median onset of ESRD at 79 years of age (Cornec-Le Gall et al., 2013).

For a number of years there was some debate about the possible existence of a third gene associated with ADPKD, tentatively titled '*PKD3*', following independent familial cases of

ADPKD apparently lacking mutations in *PKD1* or *PKD2* (Ariza et al., 1997; Bogdanova et al., 1995; Daoust et al., 1995; de Almeida et al., 1995; Turco et al., 1996). The use of more up-to-date mutation screening technologies allowed Paul *et al.* to reanalyse data from these studies and identify mutations in *PKD1* or *PKD2* in 4 of these 5 families, casting doubt on the existence of '*PKD3'* (Paul et al., 2014). However, a 2016 study did indeed identify *GANAB* (encoding the Glucosidase II alpha subunit) as a third ADPKD causing gene responsible for mild cases associated with highly variable Autosomal Dominant Polycystic Liver Disease (ADPLD), following whole exome sequencing of 6 genetically unresolved ADPKD familial cases (Porath et al., 2016). Since the discovery of *GANAB,* 3 more genes have been identified as ADPKD causing, 2 of which are also associated with ADPLD (*ALG8*, encoding Alpha-1,3-gluocsyltransferase and *SEC61B*, encoding transport protein Sec61 subunit beta), while the other, *DNAJB11* (encoding DnaJ heat shock protein family member B11), is associated with autosomal-dominant tubulointerstitial disease (Cornec-Le Gall et al., 2018a; Cornec-Le Gall et al., 2018b).

Despite knowing that mutations in the Polycystin genes are the genetic cause of ADPKD, we are still unsure of the exact role these mutant proteins have in the pathogenesis of ADPKD. Indeed, the precise structure and function of wild type PC-1 still attracts debate to this day, although our knowledge of PC-2 is somewhat clearer, with the protein known to function as a non-selective cation channel (González-Perrett et al., 2001). There are many pathways implicated in cystogenesis; I will now discuss many of these, focusing on a possible role in the clearance of apoptotic cells, also referred to as efferocytosis.

### 1.1.2 The Polycystin proteins

The gene *PKD1*, encoding PC-1, maps to human chromosome 16p13.3, covering a region of approximately 52kb, with around 14kb of this region encoding 46 exons (Harris et al., 1995). The first 32 exons of *PKD1* have undergone multiple duplication events, and there are 6 pseudogenes flanking *PKD1*; these are actively transcribed, but are not thought to form any protein products (Kirsch et al., 2008).

PC-1 is a large and complex protein, with a molecular mass of over 460kDa. It is thought to be

an integral membrane protein with a cytosolic C-terminal domain and extracellular N-terminal domain separated by many different motifs, including 11 transmembrane domains (Sandford et al., 1997; Nims et al., 2003). Roughly 30% of the total protein is comprised of 16 extracellular so called 'PKD domains', 15 of which are adjacent to each other with the 16$^{th}$ being closer to the N-terminal domain (Bycroft et al., 1999). These domains enable remarkable flexibility in the extracellular region of the protein, adding substance to theories that PC-1 functions as a mechanosensory protein, involved in cell-cell and/or matrix-cell signalling (Forman et al., 2005).

As well as the multiple transmembrane and PKD domains, PC-1 also possesses numerous other domains (figure 1.1). These include the G-protein coupled receptor autoproteolysis-inducing (GAIN) regulatory domain, which contains a 50-residue G protein-coupled receptor proteolysis site – the activation of which results in cleavage of PC-1 into 2 separate products (Yu et al., 2007). Though the function of this cleavage remains unclear, failure in this cleavage causes severe type 1 ADPKD in mouse models (Yu et al., 2007). PC-1 also contains a C-terminal coiled-coil domain, as well as numerous other functional motifs, including phosphatase-binding sites (Parnell et al., 2012,).

N-glycosylation occurs when oligosaccharides are added to the nitrogen in the side chain of asparagine residues in proteins, forming glycosidic bonds, a feature that is able to modify protein structure and function (Imperiali & O'Connor, 1999). PC-1 is readily N-glycosylated at 60 asparagine residues (Newby et al., 2002), a feature that has made it even harder to establish a concrete function for the protein. Interestingly, aberrant glycosylation of PC-1 has been reported in Aquaporin 11 knockout mice models, which develop polycystic kidneys independent of *PKD1* gene mutations (Inoue et al., 2014). The structural complexity of PC-1 has made it particularly difficult to elucidate the function of this protein, and there are no universally accepted theories into how loss of PC-1 function causes ADPKD. Though we are similarly unclear as to how loss of PC-2 function causes ADPKD, the protein is significantly simpler, smaller (approximately 110kDa) and relatively more is known about its structure and function. Encoded by *PKD2*, covering just under 70kb on chromosome 4q22 and encoded by 15 exons (Hayashi et al., 1997), PC-2, also known as TRPP2, was first identified as an integral membrane protein possessing 6 transmembrane domains by Mochizuki *et al.* in 1996, who also

first proposed its potential function as a non-selective cation channel permeable to calcium, which was confirmed 6 years later (Mochizuki et al., 1996; Hayashi et al., 1997; Koulen et al., 2002). PC-2 possesses significantly fewer functional domains than PC-1 (**figure 1.1**), primarily a coiled-coil domain and calcium-binding EF hands, and unlike PC-1, both the N- and C-terminal domains remain within the cytosol. The calcium-binding EF hand was long hypothesised to be responsible for regulating the permeability of PC-2 to calcium ions in a process dubbed 'calcium-dependent modulation' (Ćelić et al., 2012; Koulen et al., 2002; Petri et al., 2010). This claim was supported by the identification of pathogenic mutations, both truncating and non-truncating, within this domain (S. Rossetti et al., 2012). A recent study generated mice with mutations in conserved residues of the EF hand. Interestingly, while these mutations did disrupt the affinity for calcium of the EF hand, the permeability of PC-2 was unaffected, and the mice developed no PKD-related phenotypes, showing how poorly understood the

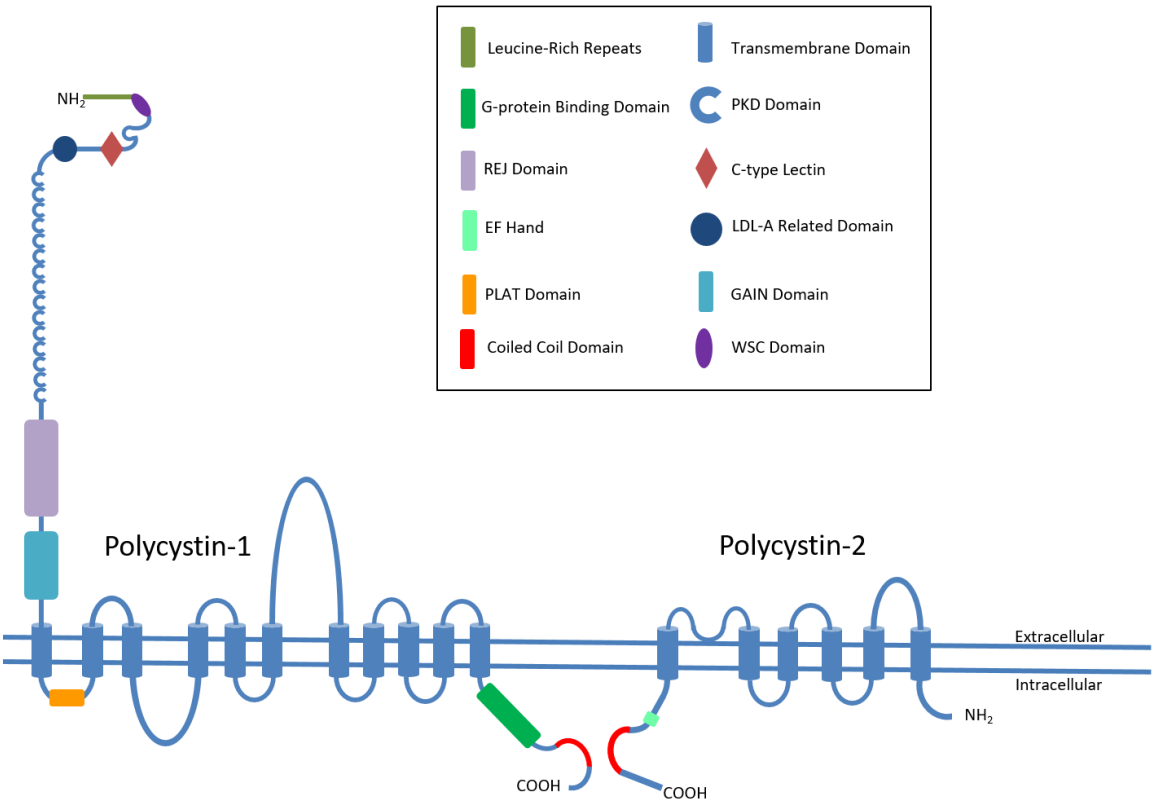


*Figure 1.1 – The Polycystin proteins*
Cartoon schematics of the Polycystins including functional domains and motifs. Note the intracellular coiled-coil domains towards the C-terminal domain present in both Polycystins, where interaction between the two proteins takes place. Adapted from Ong and Harris 2015.

modulation of the PC-2 channel remains (Vien et al., 2021).

PC-1 and PC-2 interact through their intracellular coiled-coil domains to form the Polycystin complex, consisting of 3 PC-2 polypeptides for every 1 PC-1 (Qian et al., 1997; Yu et al., 2009). This complex localises to primary cilia of kidney epithelial cells, and functions as a mechanosensory, calcium-permeable, non-selective cation channel, thought to have different properties to standalone PC-2 (Hanaoka et al., 2000; Yoder et al., 2002; Nauli et al., 2003). The *GANAB* (i.e., 'PKD3') gene product, which encodes glucosidase II subunit α, is essential for the correct localisation of the Polycystin complex, showing the importance of this localisation, as loss of *GANAB* function is associated with ADPKD (Porath et al., 2016). As well as forming a complex, the Polycystins can be expressed independently of one another. *PKD2* is constitutively expressed throughout life, localising to the endoplasmic reticulum as a homotetramer, where it mediates calcium homeostasis via calcium-induced calcium release, releasing ER stores of calcium into the cytosol in a process that has been shown to be important in determining sensitivity to cell death (Chauvet et al., 2002; Guillaume & Trudel, 2000; Koulen et al., 2002; Shen et al., 2016; Wegierski et al., 2009). Expression of *PKD1* however peaks during embryonic development, possibly explaining the earlier manifestation of the disease seen in patients with *PKD1* mutations (Chauvet et al., 2002; Guillaume & Trudel, 2000; Koulen et al., 2002; Shen et al., 2016).

We do not currently know the mechanism by which loss of either PC-1 or PC-2 function causes ADPKD. It is however known that *PKD1* mutations cause a more severe phenotype than *PKD2*, with the most severe cases of ADPKD associated with *PKD1* truncating mutations. These are associated with a median age of ESRD of 55 years, compared to 67 years for type 1 patients with a non-truncating mutation (Cornec-Le Gall et al., 2013). This could be explained by the potential involvement of PC-1 in modulating multiple signalling pathways, disruption of which may contribute to onset of ADPKD, with PC-2 having a somewhat more restricted function as a non-selective cation channel, possibly explaining the milder phenotype. Furthermore, *PDK1* is expressed more highly at embryonic stages suggesting that the pathways leading to cystogenesis may be initiated earlier, causing the more severe phenotype associated with type 1 ADPKD. However, this does not explain the fact that ESRD typically does not set in until the patient is around 50 years old, further showing how poorly understood this disease is.

### 1.1.3 ADPKD pathogenesis and pathophysiology

#### 1.1.3.1 Two hit hypothesis vs gene dosage model for ADPKD

As mentioned previously, remarkably little is known about the molecular mechanisms leading to the polycystic phenotype despite the association with mutated Polycystin proteins. Indeed, there is even a degree of disagreement regarding the genetic basis of the disease, with some researchers favouring a 'gene dosage model' wherein heterozygous patients have lower functional Polycystin proteins than wild-type individuals, and cystogenesis occurs when functional protein levels fall below a critical threshold (Eccles & Stayner, 2014).

The alternate, and generally more widely accepted hypothesis is that of a 'two-hit' mechanism, with the inherited mutant allele acting as the first 'hit', with the inactivation of the remaining function allele via somatic mutation later in life being the second 'hit'. Of the millions of cells within the kidney, only a small fraction end up cystic, and it has since been shown that cysts are clonal in origin, deriving from expansion of a single cell, giving credibility to this two-hit mechanism (Watnick et al., 1998; Pei et al., 1999). However, the identification of incompletely penetrant *PKD1* alleles lends more credibility towards the gene dosage model showing the complexity of ADPKD pathogenesis (Rossetti et al., 2009).

Elucidating the mechanisms leading to ADPKD is further complicated by the allelic heterogeneity displayed by both Polycystin genes, with new mutations constantly being identified. At the turn of the century *PKD1* and *PKD2* had around 200 and 50 reported disease variants respectively (Magistroni et al., 2003; Sandro Rossetti et al., 2001); there are now 868 and 162 known pathogenic variants of *PKD1* and *PKD2* respectively, with many more likely pathogenic variants reported by the ADPKD Mutation Database (available at: http://pkdb.pkdcure.org). Mutations are generally contained within a single-family pedigree, with a study on 98 Chinese families identifying 93 distinct mutations in either *PKD1* or *PKD2* (Xu et al., 2018). The most common of these loss-of-function alleles are truncating mutations caused by non-sense mutations or indels causing premature stop codons, although non-truncating missense mutations have also been reported, as have splice variant mutations and nonstop mutations (Deltas, 2001; Audrézet et al., 2012). Interestingly, the functional effect of

many pathogenic missense mutations remain to be understood, despite knowing that they ultimately cause the disease (see **table 1.1** for a summary of pathogenic missense *PKD2* variants.)

#### 1.1.3.2 Mechanisms involved in ADPDKD

Despite a lack of understanding regarding the exact molecular mechanisms leading to ADPKD, cysts arise from a single tubular epithelial cell that suffers a second 'hit', inactivating the remaining functional *PKD1/2* allele. This cell then proliferates and detaches from the tubule, where it continues to proliferate and switches to a secretory phenotype, ultimately leading to the rapid expansion of fluid-filled cysts (Grantham et al., 1987). Interestingly, fluid derived from cysts of patients is capable to induce cystic phenotypes in renal cell lines *in vitro* (Ye et al., 1992). These cysts continue to grow until they ultimately impair kidney function and eventually result in end stage renal disease. Many other pathways have been implicated in cyst initiation and expansion, such as loss of apicobasal polarity, planar polarity and cell-cell adhesion (Russo et al., 2005; Fischer et al., 2006).

ADPKD patients also exhibit high blood pressure, or hypertension, often prior to any loss of renal function (Chapman et al., 2010). PC-2 has been implicated in hypertension, with an inducible *PKD2* knockout in arterial smooth muscle cells lowering blood pressure in mouse models. PC-2 therefore functions to increase blood pressure (Bulley et al., 2018). This contrasts with the pathophysiology of ADPKD, wherein loss of protein function causes hypertension, whereas the mouse model would suggest loss of PC-2 function should decrease blood pressure. This difference is possibly explained by the fact that type 2 ADPKD patients have a global loss of PC-2 dosage, as opposed to a knockout specific to arterial myocytes, or it could simply reflect functional divergence of the PC-2 protein over millions of years of evolution between mice and humans. Nonetheless, this discrepancy is another example of how complicated pathogenesis is, and how much more there is to understand about the Polycystins and their function.

*Table 1.1 A selection of known pathogenic missense PKD2 variants*

Table showing pathogenic missense variants of *PKD2* and their effect on the protein (if known). All mutations affect residues which are conserved in Amo, with the equivalent Amo residue shown for each variant. Compiled using the Autosomal Dominant Polycystic Kidney Disease Mutation Database (available at http://pkdb.pkdcure.org). TOP = tetragonal opening for Polycystins.

| Variant | Location on PC-2 | Effect | Amo residue | Reference |
|---|---|---|---|---|
| W280R | Helix 2, TOP domain | Unknown | W299 | Grieben et al., 2017 |
| R322W | Beta pleated sheet 1 | Decreased PC-1 maturation | R341 | Gainullin et al., 2015 |
| R322Q | Beta pleated sheet 1 | Prevents PC-1 maturation and surface localisation | R341 | Gainullin et al., 2015 |
| R325P | TOP domain | Unknown | R444 | Grieben et al., 2017 |
| C331S | Polycystin domain | Abolished disulphide bonding thought to disrupt channel assembly | C450 | Shen et al., 2016 |
| Y345C | Unannotated | Unknown | Y464 | Yu et al., 2011 |
| W414G | TOP domain | Abolished ciliary trafficking, decreased ER PC-2 channel activity | W529 | Cai et al., 2014, Pavel et al., 2016 |
| R420G | Beta pleated sheet 3, TOP domain | Decreased ER PC-2 channel activity | R535 | Pavel et al., 2016 |
| D511V | Transmembrane span 3 | Thought to be targeted for lysosomal degradation | D627 | Hoffher et al., 2016 |
| R638C | Pore Helix 1 | Disrupts pore helix 1 structure | R754 | Shen et al., 2016 |

It is thought that the main function of the Polycystin complex is to maintain calcium homeostasis, and this is therefore considered the most likely factor contributing to cystogenesis. Decreased intracellular calcium signalling causes an increase in adenylyl cyclase activity, producing more cAMP, which in turn causes an increase in ATP production, fluid secretion and proliferation (Belibi et al., 2004; Hanaoka & Guggino, 2000; Pinto et al., 2012). $Ca^{2+}$ signalling in response to the binding of Wnt ligands is also regulated by the Polycystin complex (Kim et al., 2016). Wnt signalling is a highly-conserved pathway essential for proper development of various tissues and organs, and defective Wnt signalling is well known to be associated with kidney disease, suggesting a potential role for Wnt signalling in the onset of ADPKD (Wang et al., 2018).

As mentioned previously, both Polycystin proteins are known to localise to base of the primary cilia, a single, non-motile hair-like projection found on the surface of most mammalian cells (Sorokin, 1962). Genetic disorders resulting from failures in primary cilia assembly are known as cilipoathies, and these are often associated with the development of renal cysts, with one such example being Joubert syndrome, caused by mutations in the centrosomal protein CEP290 (McConnachie et al., 2021). ADPKD itself is considered a ciliopathy, with various ciliary defects having been reported in ADPKD models. For example, mice with a pathogenic *PKD1* missense variant are reported to have significantly elongated cilia of collecting duct cells in the heterozygous state, with the effect even more pronounced when this allele was in trans to a *PKD1* null (Hopp et al., 2012).

PC-1, possibly in the context of the Polycystin complex, has been shown to be important in regulating the cell cycle. It interacts with the JAK/STAT pathway to upregulate p21Waf1, a cyclin-dependent kinase inhibitor, thereby promoting cell cycle arrest and quiescence (Bhunia et al., 2002). Disruption of this process leads to cystogenesis through aberrant proliferation, a hallmark of the polycystic phenotype, with increased JAK/STAT activity reported in ADPKD models both *in vitro* and *in vivo* as reviewed by Weimbs and Talbot (2013). On a similar theme, ER-resident PC-2-mediated calcium homeostasis is known to prevent apoptosis *in vitro*, and loss-of-function PKD2 mutations disrupt this, leading to aberrant apoptosis, another hallmark of ADPKD (Lanoix et al., 1996; Wegierski et al., 2009).

Both PC-1 and PC-2 have been implicated in autophagy, and there is an argument to suggest that failures in autophagy contribute to the establishment of the polycystic phenotype (Wang & Dong, 2020). Indeed, activators of autophagy such as rapamycin and the mTOR-independent carbamazepine, have been shown to attenuate cyst growth in *Pkd1* mutant zebrafish models (Zhu et al., 2017). In the context of autophagy, PC-1 is required for the fusion of autophagosomes and lysosomes, with loss of PC-1 resulting in activation of Calpains, a family of calcium-dependent proteases. Calpain activation leads to the degradation of lysosomal associated membrane protein-1 (LAMP1), a glycoprotein expressed on the surface of lysosomes required for autophagolysosomal fusion, preventing effective degradation of autophagosomes in *Pkd1* knockout murine inner medullary collecting ducts cells (Mrschtik & Ryan, 2015; Peintner et al., 2020). PC-2 however, is thought to be required for the formation of the autophagosome itself, forming a complex with Beclin-1 (BECN1), an essential autophagic protein, in a manner dependent on PC-2 calcium channel activity (Peña-Oyarzun et al., 2021)

The polycystic kidney is a highly inflamed environment, suggesting a possible role for the inflammatory response in pathogenesis (Karihaloo, 2015). Inflammation is largely driven by the action of macrophages and other innate immune cells. However, neither PC-1 or PC-2 have been shown to have a function in mammalian macrophages, although PC-2 has been shown to be involved in T lymphocyte function (Magistroni et al., 2019) so it is possible that PC-2 may play a similar role in macrophages. Regardless, there is a wealth of evidence implicating macrophages in ADPKD pathogenesis. For example, expression of monocyte chemoattractant protein 1 (MCP1) is upregulated in ADPKD, and there is evidence suggesting that macrophage influx directly correlates with cyst expansion (Karihaloo et al., 2011; Cassini et al., 2018). It was also shown in an inducible murine *PKD1* knockout that proinflammatory macrophages (often known as M1-like macrophages) infiltrate early cysts and induce inflammation before switching to an alternate phenotype (also known as M2-like) associated with increased proliferation (Karihaloo, 2015; Karihaloo et al., 2011).

A role for macrophages and innate immune cells in contributing to the pathogenesis of the polycystic kidney is further supported by the presence of many uncleared apoptotic cells present in the microenvironment, and the fact that failures in apoptotic cell clearance are associated with chronic inflammatory conditions as will be discussed below (Lanoix et al., 1996;

Peintner and Borner, 2017; Doran et al., 2020). Innate immune cells such as macrophages are largely responsible for clearing apoptotic cells. Thus, it could be that macrophages infiltrate nascent cysts in order to clear apoptotic cells, but an increased apoptotic burden results in an inflammatory response and subsequent compensatory proliferation promotes cyst expansion. However, this is purely speculative at this time.

Despite these numerous pathways implicated in ADPKD, there is still a large degree of uncertainty about the exact mechanisms. What is known is that calcium signalling and homeostasis are involved in many of these pathways, highlighting this facet as a potential key component driving pathogenesis. See figure 1.2 for a schematic summary of the pathways associated in cystogenesis.

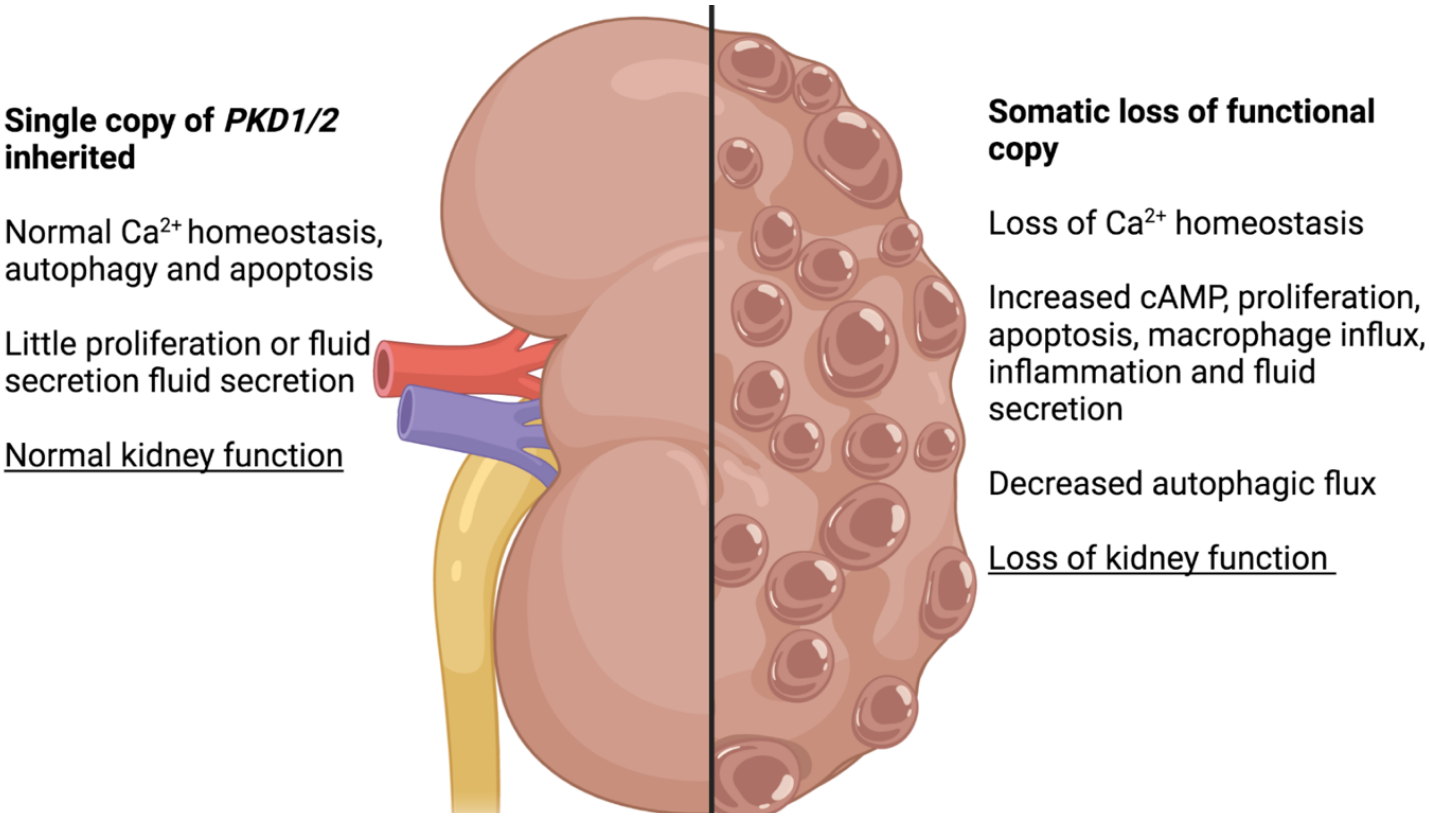


*Figure 1.2 – A summary of specific pathways implicated in ADPKD*

Cartoon showing certain pathways and processes occurring in a healthy kidney (left) and how they are disrupted in ADPKD (right). It is thought that inheritance of a single copy of PKD1/2 initially results in a healthy kidney, until somatic mutations affecting the functional copy of PKD1/2 occur in cyst progenitor cells. These cells then exhibit loss of calcium homeostasis, resulting in increased cAMP levels that drive proliferation, with cysts expanding until ultimately causing ESRD.

### 1.1.4 Current and potential treatment for ADPKD

There is no current treatment to stop kidneys becoming polycystic in patients possessing Polycystin gene mutations, although it is possible to treat the various symptoms associated with ADPKD. For example, ADPKD patients typically exhibit hypertension, which can be treated with Angiotensin-converting enzyme (ACE) inhibitors as well as through dietary adjustments (Schrier, 2016). CRISPR-Cas9 genome editing could theoretically be used to 'cure' families of ADPKD, by 'cutting out' the mutant PKD1/2 allele and replacing it with a wild-type allele in an embryo possessing an ADPKD associated allele (Ma et al., 2017). However, there are naturally many ethical issues associated with this technique, and any advances into higher vertebrates are not likely to be seen for a number of decades.

Following a successful clinical trial, in which it slowed cyst growth, several countries approved the use of Tolvaptan to treat patients shown to have, or be at risk of developing, rapidly progressing disease (Gansevoort et al., 2016; Torres et al., 2012). These include patients with truncating *PKD1* mutations, or those exhibiting hypertension before 30 years of age. Tolvaptan targets the vasopressin V2 receptor, which, when bound by vasopressin (also known as antidiuretic hormone) initiates a cAMP-dependent signalling cascade resulting in expression of aquaporin-2 channels and their transport to the plasma membrane of the collecting duct, increasing water reabsorption from the filtrate (Nielsen et al., 1995). Tolvaptan functions as a competitive vasopressin V2 receptor antagonist, binding the receptor and inhibiting the signalling cascade, suppressing water reabsorption in the collecting duct and resulting in more dilute urine. Tolvaptan antagonism of the vasopressin V2 receptor is thought to inhibit cystogenesis by decreasing cAMP levels in the collecting duct (figure 1.3), as increased cAMP levels are associated with increased proliferation and subsequent cystogenesis (Devuyst & Torres, 2013; Reif et al., 2011). As with any aquaretic therapy, Tolvaptan treatment naturally causes increased urination in patients, as well as an insatiable thirst (Devuyst et al., 2017). However, Tolvaptan has also been associated with more severe side effects: 5% of patients involved in one clinical trial exhibited increased serum alanine transaminase levels, indicative of serious liver injury (Watkins et al., 2015).

The fact that Tolvaptan is only effective on a small subset of APDKD patients and can be associated with severe side effects clearly shows how urgently alternative treatments are needed. Indeed, many clinical trials are on-going, often trying to exploit pathways deregulated in ADPKD. For example, various calcimimetic (calcium mimicking) compounds are being studied to test their effectiveness at ameliorating cystic phenotypes, as calcium homeostasis is defective in ADPKD (Gattone et al., 2009). One such calcimimetic compound, known as R-568,

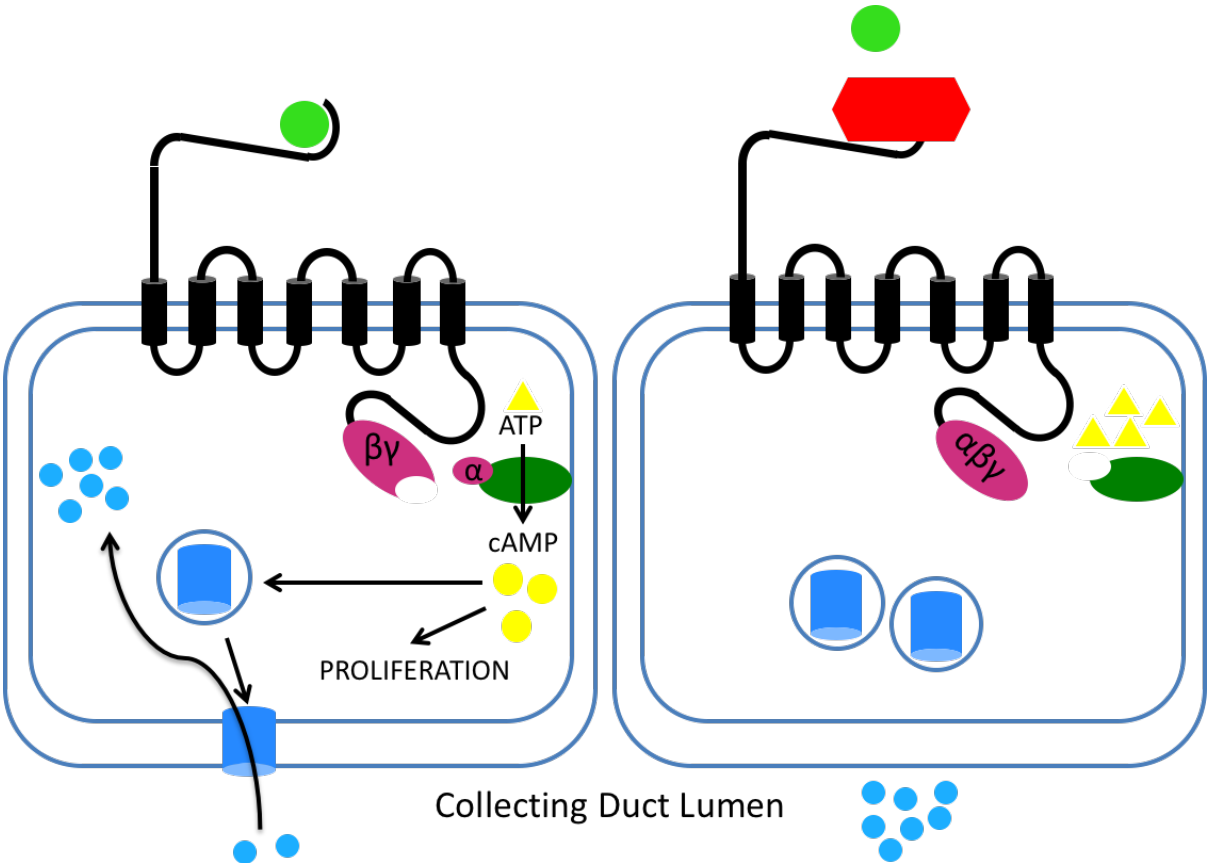


*Figure 1.3 – Mechanism of action of Tolvaptan*

Binding of vasopressin (ADH, Green circle) to the Vasopressin-2-Receptor (V2R, in black) results in the cleavage of the receptor-coupled G-protein (magenta ovals). The alpha subunit then binds and activates adenylyl cyclase (green oval), which converts ATP (yellow triangles) into cAMP (yellow circles). cAMP then initiates a signaling cascade resulting in the translocation of Aquaporin-2 to the luminal membrane, allowing reabsorption of water (blue circles) from the collecting duct, as well as driving proliferation and fluid secretion in the context of ADPKD. Tolvaptan (red hexagon) acts as an antagonist, blocking the binding of Vasopressin to the V2R. This prevents the activation of adenylyl cyclase, resulting in decreased cAMP and therefore decreased proliferation and secretion. This also results in the decreased translocation of Aquaporin-2 to the luminal membrane, and therefore reduces the amount of water reabsorbed, causing the polyuria experienced by Tolvaptan patients.

activates the calcium-sensing receptor (CaSR) in immortalised proximal tubular epithelial cells lacking *PKD1*. This increases intracellular calcium concentration and decreases cAMP levels, recovering both to wild-type levels (Di Mise et al., 2018). Other compounds that target cAMP production are being investigated, such as analogues of Somatostatin, a peptide hormone that functions to decrease cAMP through inhibition of Growth Hormone release, thereby preventing proliferation (Kokudo et al., 1991; Mascardo & Sherline, 1982). Clinical trials using Somatostatin analogues have been carried out, reporting a smaller increase in total kidney volume (TKV) compared to placebo groups, but this was not statistically significant suggesting the need for a greater number of patients in future trials (Caroli et al., 2013).

A separate signalling pathway associated with cellular proliferation and survival is the mTOR (mechanistic target of rapamycin) pathway (Schmelzle & Hall, 2000). This is regulated by PC-1 (Shillingford et al., 2006), and deregulation is therefore thought to be involved in cystogenesis. Furthermore, mTOR negatively regulates effective autophagy, a Polycystin-dependent process known to be downregulated in ADPKD (Peña-Oyarzun et al., 2021; Wang & Dong, 2020). It has been shown that treating both zebrafish and mouse ADPKD models with rapamycin, an inhibitor of mTOR signalling, significantly ameliorates the cystic phenotype by selectively inducing autophagy and apoptosis of cyst-lining epithelial cells (Shillingford et al., 2006; Zhu et al., 2017). mTOR inhibitors were therefore identified as potential therapeutic targets, and rapamycin/sirolimus was the subsequent subject of a clinical trial which proved to be unsuccessful. However new trials are currently taking place with a modified dosage (Riegersperger et al., 2015; Ruggenenti et al., 2016).

As mentioned above, the JAK/STAT pathway is significantly upregulated in ADPKD (Strubl et al., 2020). It has been shown that curcumin and tofacitinib, inhibitors of JAK2, significantly reduce cyst growth and expansion in *in vivo* mouse models and in *in vitro* human cell culture (Leonhard et al., 2011; Patera et al., 2019). Indeed, curcumin is known to modulate not just the JAK/STAT pathway, but other pathways implicated in cystogenesis, such as mTOR and Wnt, and it is currently in a Phase 4 clinical trial investigating vascular defects in young ADPKD patients (Leonhard et al., 2011; Nowak et al., 2022).

As well as pharmaceutical interventions, recent evidence suggests that lifestyle changes could

be capable of ameliorating the polycystic phenotype, albeit in rodent models. Dietary restriction of rat models, wherein food was only available for 8 hours a day, significantly reduced proliferation via downregulation of mTOR signalling (Torres et al., 2019). Similarly, a high fat, low carb, ketogenic diet significantly reduced disease progression in juvenile models, and reversed the polycystic phenotype in treated adults, as did acute fasting (Torres et al., 2019). This ties in with work suggesting a role in disease progression for autophagy, as mTOR downregulation is known to activate autophagy in response to nutrient starvation (Jung et al., 2010).

It has recently been shown that cystic kidneys have the capacity for plasticity, with re-expression of *PKD1* and *PKD2* successfully reversing the polycystic phenotype in murine models (Dong et al., 2021). Re-expression of *PKD1* or *PKD2* in 13-week-old mice resulted in decreased proliferation, increased autophagy and a decrease in TKV to near wild-type levels within 3 weeks. A similar recovery, albeit less complete, was again observed following re-expression in 16-week-old, suggesting that the kidney is capable of repairing itself following gross restructuring, and this ability is dependent on the actions of the Polycystin proteins (Dong et al., 2021). For a relatively recent review summarising potential therapeutic targets in ADPKD see Weimbs et al., 2018.

### 1.1.5 *PKD2* homologs and *Drosophila melanogaster* as a model

Around 85% of ADPKD patients have *PKD1* mutations, therefore cell lines used to model ADPKD typically derive from these type 1 patients. As such, there is limited ability to study *PKD2* function *in vitro,* given the relative lack of type 2 patients available, though mutations can of course be introduced. However, *PKD2* is evolutionarily conserved and present in both invertebrates and vertebrates, providing model organisms in which the function of this protein can be investigated *in vivo*. The nematode *Caenorhabditis elegans,* fruit fly *Drosophila melanogaster* and zebrafish *Danio rerio* have all been used to study the function of PC-2, while mice possessing *PKD2* mutations can be used to model the disease in a mammalian system (Wu *et al.*, 1998; Watnick *et al.*, 2003; Schottenfeld *et al.*, 2007; Knobel *et al.,* 2008).

In *C. elegans*, pkd-2 and the *PKD1* homolog lov-1, interact in the same pathway in male sensory neurons, co-localising at cilia and the cell body (Barr et al., 2001), showing the evolutionary conservation of the Polycystin complex. The *PKD2* homologue in zebrafish (*Pkd2*) is required in the Kupffer's Vesicle (KV), a 'ciliated organ of asymmetry' (Essner et al., 2005), to establish left-right asymmetry of the developing embryo (Bisgrove et al., 2005; Schottenfeld et al., 2007; Hofherr et al., 2018). The channel activity of ciliary *Pkd2,* in response to asymmetric fluid flow within the KV, restricts expression of *Southpaw*, part of the Nodal signalling cascade, to the left-hand side of the KV, determining left-right asymmetry; this is abolished in *Pkd2* morphants and heterozygous mutants, which exhibit randomised heart looping and *Southpaw* expression (Hofherr et al., 2018; Long et al., 2003; Pennekamp et al., 2002; Schottenfeld et al., 2007).

Recent work suggests that Pkd2 is required for the generation of asymmetry in the first place, as *Pkd2* morphants exhibit significantly shorter cilia which are unable to generate the flow required for ciliary Pkd2 to initiate asymmetric *Southpaw* expression (Jacinto et al., 2021). *Pkd2* zebrafish morphants have been shown to develop kidney cysts, and this system has been used to test compounds that can inhibit cyst formation (Obara et al., 2006; Schottenfeld et al., 2007; Chang et al., 2017). However, somewhat confusingly *Pkd2* null mutants exhibit no such renal phenotypes, with the authors speculating there could be maternal *Pkd2* present in mutants that would otherwise be knocked down in morphants (Schottenfeld et al., 2007).

The short generation time, lack of ethical concerns and its ease of genetic manipulation compared to other animal models have allowed the fruit fly *Drosophila melanogaster* to be used as a model organism for well over a century, with *Drosophila* research contributing towards 6 Nobel prizes. *Drosophila* possess homologs of roughly 75% of all known human disease genes, which has enabled it to be used to model and understand a wide range of diseases and the processes driving the pathology, such as various cancers and neurological disorders (Halder & Mills, 2011; Lu & Vogel, 2009; Reiter et al., 2001).

One example of a human disease gene found as a homolog is *PKD2*, allowing *Drosophila* to be used to characterise various functions of *Pkd2.* At the amino acid level, *Drosophila* and human PKD2 share 26% identity, which is relatively low for homologous proteins. However, of the 12 amino acid residues associated with pathogenic missense variants 10 are present within

*Drosophila*, suggesting the functional importance of these residues may be conserved (**figure 1.4)**. *Drosophila* males homozygous for *Pkd2* loss of function mutations produce motile sperm, but these are unable to be hyperactivated by the female uterus. Consequently, sperm are not transported to the spermatheca, the sperm storage organ (Watnick *et al.*, 2003). This phenotype provides the rationale for the alternate name of *Drosophila Pkd2* (*almost there*/*amo*), which it will be referred to from now on to avoid confusion with human *PKD2*. Sperm hyperactivation in *Drosophila* is mediated by calcium signalling, requiring a functional *amo* channel to allow calcium influx, initiating a signalling cascade resulting in flagellar beating of the sperm. Homozygous male *amo* mutants are therefore sterile (Watnick et al., 2003; Köttgen et al., 2011).

As well as male fertility, Amo also mediates smooth muscle contraction throughout the digestive system, with mutations significantly decreasing rates of excretion rates in first instar (i.e., newly hatched) *Drosophila* larvae during pulse-chase experiments (Gao et al., 2004). Interestingly, *amo* mutant heterozygotes are reported to be haploinsufficient for this smooth muscle contractility, with the remaining wild-type allele unable to produce enough protein to maintain normal function in heterozygote mutants (Gao et al., 2004). The nature of the allele in this study was not characterised, so it is possible they generated a dominant negative mutation, wherein the mutant allele impairs the action of the wild-type allele and the reported haploinsufficiency could be due to this phenomenon as opposed to a gene dosage effect. However, *amo* haploinsufficiency is consistent with a *PKD2* haploinsufficiency reported in mammalian vascular smooth muscle cells, where inactivation of one *PKD2* allele is sufficient to alter intracellular calcium homeostasis (Qian et al., 2003). These results suggest gene dosage can be responsible for *PKD2* mutant phenotypes, although the 'two-hit' hypothesis is still preferred with respect to ADPKD pathogenesis.

In addition to sperm hyperactivity and smooth muscle contractility, Amo is important in the phagocytic clearance of apoptotic cells, a process also known as efferocytosis. Van Goethem et al., identified *amo* mutant fly plasmatocytes (the functional *Drosophila* equivalent of the vertebrate macrophage) as having a 50% reduction in phagocytic index relative to wild types (Van Goethem et al., 2012). In mammalian macrophages the concentration of intracellular $Ca^{2+}$

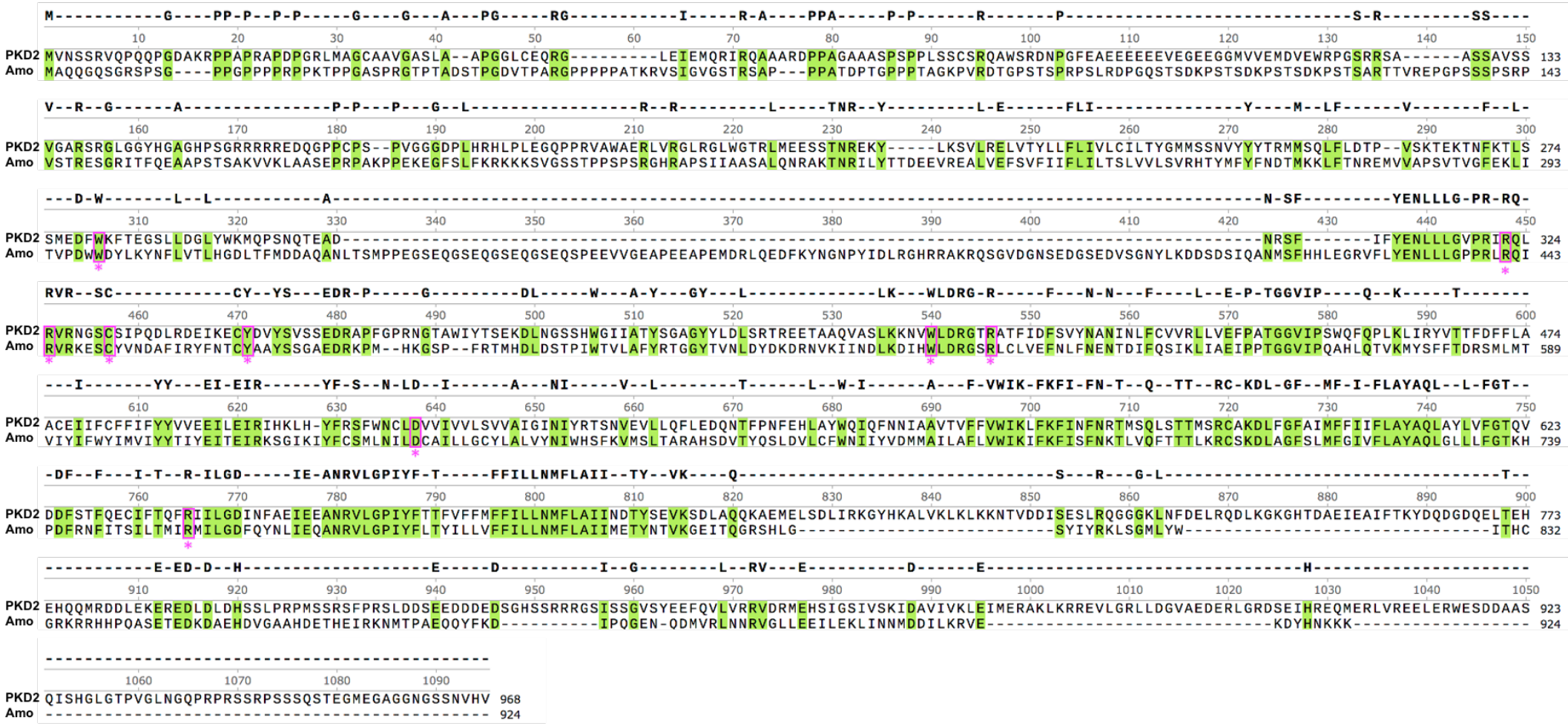


*Figure 1.4 – Alignment of human and Drosophila PKD2 protein*

Pairwise alignment comparing the protein sequence of human PKD2 and *Drosophila* Amo, with conserved residues highlighted in green and displayed as a consensus sequence at the top. Residues associated with pathogenic missense variants that are conserved in *Drosophila* are highlighted in pink

increases during phagocytosis (Rubartelli et al., 1997; Dewitt and Hallett, 2002) and calcium homeostasis is important to the function and phagocytic activity of *Drosophila* macrophages (Cuttell et al., 2008; Weavers et al., 2016). It is therefore possible that PC-2/Amo are required to mediate calcium homeostasis during these processes, and that mutations affect this process explaining the impaired phagocytosis, although this has yet to be confirmed

Despite not possessing kidneys, flies and other insects possess two structures which together function analogously to the kidney: the filtrating nephrocytes, which are functionally equivalent to glomeruli, and Malpighian tubules, representing the equivalent of renal tubules, mediating osmoregulation (Dow et al., 2022; Weavers et al., 2008). Unlike the vertebrate nephron, wherein the filtrating and osmoregulatory components of the excretory system are physically linked, nephrocytes and Malpighian tubules remain apart, with most nephrocytes surrounding the dorsal vessel (the *Drosophila* heart), while Malpighian tubules are found at the boundary between the mid-gut and hindgut. Failures in excretion and osmoregulation result in a characteristic bloating phenotype in adult flies though no such phenotypes have been reported in *amo* mutant *Drosophila*, suggesting *amo* is not involved in invertebrate renal tubule function (Cabrero et al., 2014; Denholm et al., 2013). However, it has been shown that loss of Bicaudal C (BicC), an RNA-binding protein whose mammalian homolog is implicated in ADPKD, results in the presence of cyst-like growths on Malpighian tubules, due in part to the activation of the TOR pathway (the invertebrate equivalent of mTOR) (Gamberi et al., 2017; Rothé et al., 2020). This shows how *Drosophila* could potentially be a viable model to investigate pathways associated with cystogenesis in the future.

## 1.2 Macrophages and innate immunity

### 1.2.1 Macrophages and the innate immune system

Despite the exact pathogenesis of ADPKD remaining something of a mystery, there is undoubtedly a substantial immune component, with innate immune cells implicated in both cyst initiation and expansion (Cassini et al., 2018; Karihaloo et al., 2011). Including physical

barriers such as the skin and certain epithelia, the innate immune system represents the first line of defence against infection and parasitism in almost all metazoans. The cellular arm of the innate immune system comprises of various white blood cells, known as leukocytes, which include macrophages, neutrophils and eosinophils. These cells all derive from a common myeloid progenitor cell differentiated to become a myeloblast, which itself is capable of differentiating into neutrophils, eosinophils, basophils or monocytes. Monocytes themselves have the capacity to differentiate further, into antigen presenting dendritic cells or into monocyte-derived macrophages (MDMs) (Jakubzick et al., 2017; Liebermann & Hoffman, 2002).

The highly phagocytic, short lived neutrophil represents the most abundant innate immune cell, accounting for up to 70% of circulating leukocytes, while the macrophage is the other major phagocytic innate immune cell (McCracken & Allen, 2014). Macrophages are much longer lived than the neutrophil, which typically exist no longer than 24 hours before undergoing apoptosis (McCracken & Allen, 2014), and represent a much more heterogeneous population of cells which will be discussed below. Briefly, macrophages are either tissue resident macrophages, highly specialised to the environment of a certain tissue or organ with distinct hematopoietic origins, or monocyte-derived macrophages (MDMs), differentiated from circulating monocytes in response to injury or infection (Gordon & Plüddemann, 2017; Ito et al., 2022; Jakubzick et al., 2017). Despite their independent origins, both tissue resident macrophages and MDMs generally carry out the same vital functions - namely phagocytosis, tissue homeostasis and repair.

### 1.2.2 Macrophage heterogeneity and polarisation

Owing to the wide range of functions carried out in numerous different environments, macrophages are a highly heterogeneous population of cells, with this macrophage heterogeneity conserved across vertebrates (London et al., 2013; Nguyen-Chi et al., 2015). Heterogeneity is underpinned by the presence of tissue resident macrophages, which are highly specialised to their micro-environments, such as Kuppfer cells in the liver and microglia in the brain, and circulating macrophages that are capable of polarising to different activation

states in response to different environmental stimuli (Li & Barres, 2018; Murray, 2017; Orecchioni et al., 2019; Wardle, 1987). For example, in response to LPS and other pathogen-associated molecular patterns (PAMPs), or cytokines such as IFNγ, circulating macrophages are polarised towards a pro-inflammatory 'M1 like' activation state to facilitate the phagocytic killing of the infecting pathogen (Nathan et al., 1983; Orecchioni et al., 2019). Contrastingly, cytokines such as interleukin-4 (IL4) and transforming growth factor beta (TGF-β) inhibit polarisation towards this activation state, and instead polarise macrophages towards an anti-inflammatory 'M2-like' activation state, associated with tissue repair, removal of apoptotic cells and proliferation (Gordon & Martinez, 2010; Stein et al., 1992). Tissue resident macrophages are thought to generally be polarised towards this anti-inflammatory state, facilitating their role in mediating tissue homeostasis (Murray & Wynn, 2011).

Though previously thought to be binary, the M1-M2 paradigm is now thought to be more of a spectrum, with macrophages existing on a spectrum of different activation states in response to different stimuli (Hume, 2015). Critically, it is now known that macrophages are capable of shifting activation states, with 'M1-like' cells having been observed shifting towards a more 'M2-like' activation state, often to facilitate the resolution of inflammation (Chen et al., 2018; Kim et al., 2019; Kohno et al., 2021).

### 1.2.3 Macrophage polarisation and disease

Macrophage polarisation is a fundamental facet of the vertebrate innate immune system. As such, aberrant macrophage polarisation often causes or exacerbates chronic inflammatory diseases (Parisi et al., 2018). Atherosclerosis is a chronic inflammatory condition affecting blood vessels, wherein a build-up of fatty plaques results in the narrowing of the lumen. There is a large macrophage influx into the developing plaques, and increased levels of 'M1-like' markers are associated with more severe symptoms (de Gaetano et al., 2016). Chronic obstructive pulmonary disease (COPD) refers to a group of diseases wherein the airways have been progressively damaged and remodelled, often as a result of inflammation (Barnes et al., 2015). Cigarette smoke is a leading risk factor in the development of COPD, and interestingly smokers exhibit significantly higher levels of 'M2-like' macrophage markers, associated with proliferation and remodelling, relative to controls, suggesting that an 'M2-like' activation state

is in some part responsible for driving pathogenesis of COPD (Cornwell et al., 2018; Shaykhiev et al., 2009).

ADPKD is another inflammatory disease associated with aberrant macrophage polarisation; during early cystogenesis, Mcp1 attracts circulating macrophages, which polarise to a pro-inflammatory activation state, before anti-inflammatory cytokines stimulate a shift towards an anti-inflammatory, pro-proliferative state, driving expansion of the nascent cyst (Karihaloo *et al.*, 2011; Harris and Torres, 2014; Cassini *et al.*, 2018). This shows the importance of macrophage function and polarisation in driving ADPKD pathogenesis, and highlights these areas as being worthy of further investigations.

### 1.2.4 *Drosophila* hemocytes

The cellular arm of the *Drosophila* innate immune system comprises of a population of blood cells known as hemocytes, consisting of plasmatocytes, crystal cells and lamellocytes (Wood & Jacinto, 2007). Crystal cells functionally resemble a cross between platelets and mast cells, and are required for melanisation during the wound healing process, while lamellocytes are large encapsulating cells differentiated only in response to parasitism of organisms too large to phagocytose (Wood & Jacinto, 2007). The plasmatocyte is the dominant hemocyte across development. Indeed, they are the only functional hemocyte during embryogenesis, and account for roughly 95% of all hemocytes in healthy adults (Meister & Lagueux, 2003; Tepass et al., 1994). These cells are highly migratory, phagocytic and responsive to both wounding and infection, acting as the *Drosophila* equivalent of the vertebrate macrophage, and making them a suitable model to study macrophage behaviour and regulation *in vivo* (Wood & Jacinto, 2007; Wood & Martin, 2017). They migrate to sites of wounding and infection using extensions of the cell membrane known as lamellipodia; GTPases and actin regulators are required for the reorganisation of cytoskeletal components of the lamellipodia, enabling migration to these sites of pathology, where they mediate phagocytosis of bacteria or cellular debris (Stramer et al., 2005; Tucker et al., 2011).

Similarities between plasmatocytes and vertebrate macrophages are apparent not just at the functional level, but also molecularly: various homologs of myeloid specific genes are present

in *Drosophila*, where they are required for the correct specification of blood cells. For example, the fate of mesodermal cells destined to become plasmatocytes is determined by Serpent (Srp), a homolog of vertebrate GATA transcription factors that are required for vertebrate hematopoiesis (Lebestky et al., 2000), whilst the scavenger receptor Croquemort, homologous to the vertebrate macrophage marker CD36, is expressed on the surface of plasmatocytes, where it is required for phagocytosis (Franc et al., 1996; Guillou et al., 2016). These functional and molecular similarities make *Drosophila* plasmatocytes a truly excellent model with which to study macrophage and behaviour, and the ease of *Drosophila* as a model has allowed us to dissect the processes involved in their specification as will be discussed below.

### 1.2.5 Hematopoiesis in *Drosophila*

The first wave of *Drosophila* hematopoiesis occurs at around stage 10 of embryogenesis, where hemocytes begin to differentiate from head mesoderm cells (Tepass et al., 1994), and lineage tracing experiments have shown that this population persists to later stages of development (Holz et al., 2003; Sanchez Bosch et al., 2019). These cells are specified from pro-hemocytes by the GATA transcription factor Serpent into hemocytes, which are then specified further into either crystal cells or plasmatocytes (**figure 1.5**). Crystal cells are differentiated via Lozenge (Lz), a transcription factor related to AML1/RUNX1 which is involved in the differentiation of myeloid progenitors in humans and implicated in acute myeloid leukaemia, while plasmatocytes are specified via the transcription factor Glial cells missing (Gcm) (**figure 1.5,** Lebestky et al., 2000; Okuda et al., 1996). Following differentiation, plasmatocytes then follow chemotactic gradients, principally the VEGF-related ligands Pvf2 and Pvf3, along well-defined migration routes into the extended germband and along the developing ventral nerve cord (VNC), and are typically dispersed across the entire embryo by the end of stage 15 (Cho et al., 2002; Evans et al., 2010; Siekhaus et al., 2010).

During larval stages some embryonic hemocytes circulate in the hemolymph, pumped around by the dorsal vessel (the *Drosophila* heart), while others adhere to the body wall and form sessile clusters of cells (Márkus et al., 2009). These clusters form “hematopoietic pockets”, with hemocytes proliferating rapidly in these pockets under control of Activin-β produced by

nearby neurons. These cells then differentiate into plasmatocytes and crystal cells (Leitão & Sucena, 2015; Makhijani et al., 2017; Márkus et al., 2009).

A second hematopoietic wave occurs in the larval lymph gland, a multi-lobed structure surrounding the dorsal vessel (Jung et al., 2005). In the most anterior of these lobes, progenitor cells differentiate into plasmatocytes and crystal cells, primarily under the control of Notch signalling (Blanco-Obregon et al., 2020; Duvic et al., 2002), in a process that takes place throughout larval development. However, these cells remain within the lymph gland until metamorphosis, when the lymph gland ruptures and allows this new pool of hemocytes to be released into circulation (Lanot et al., 2001).

Though hematopoiesis takes place during embryonic and larval stages, whether any hematopoiesis occurs in adult *Drosophila* remains a source of some debate, with various

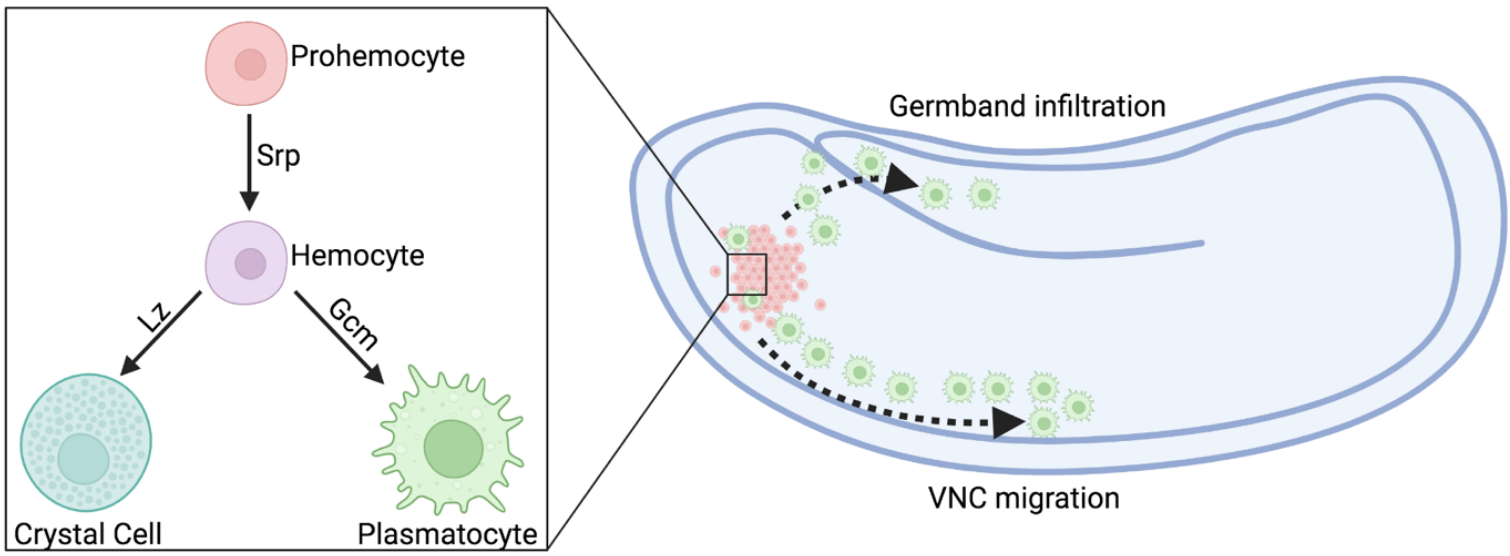


*Figure 1.5 – Drosophila embryonic hematopoiesis and plasmatocyte dispersal*

Prohemocytes arise from mesodermal cells in the developing head around stage 9 of embryogenesis. The GATA transcription factor Serpent (Srp) drives differentiation of prohemocytes into hemocytes, which then differentiate into crystal cells or plasmatocytes through the action of the transcription factors Lozenge (Lz) or Glial cells missing (Gcm) respectively. Following their differentiation, plasmatocytes (green) disperse across the embryo (right – lateral view of developing embryo, anterior left) by infiltrating the extended germband and migrating down the ventral nerve cord (VNC)

conflicting papers having been published. For example, one study identified hematopoietic hubs on the dorsal side of the adult abdomen, while a subsequent study showed that adults lack hematopoiesis, and instead rely on a 'reservoir' of hemocytes, primarily of the embryonic lineage, located at respiratory epithelia (Ghosh et al., 2015; Sanchez Bosch et al., 2019). However, a more recent study identified progenitor cells in the adult capable of differentiation and proliferation in response to bacterial infection, suggesting that hematopoiesis may indeed occur in adults (Boulet et al., 2021). Irrespective of whether hematopoiesis occurs in adults or not, the evidence shows *Drosophila* hematopoiesis is clearly a more complicated process than first thought and justifies the use of *Drosophila* as a model with which to study this fundamental process.

### 1.2.6 Macrophage heterogeneity and polarisation in *Drosophila*

Despite the undoubted similarities between *Drosophila* plasmatocytes and the vertebrate macrophage, a major limitation of the use of plasmatocytes to model macrophage behaviour is that they have historically been considered a homogenous population of cells, in stark contrast to vertebrate macrophages. However, studies investigating the *in vivo* behaviour of plasmatocytes suggest that these cells do not behave uniformly. For example, imaging embryonic plasmatocytes undergoing random migration on the ventral midline (VML) at stage 15 reveals a wide range of different migration speeds (Evans et al., 2013; Roddie et al., 2019). Likewise, macrophages within similar distances to sites of epithelial wounding do not necessarily respond equally to the wound, suggesting certain hemocytes preferentially engage in this inflammatory response (Evans et al., 2015; Roddie et al., 2019). This also appears to be observed with M2-like behaviours of plasmatocytes, namely apoptotic cell clearance, as plasmatocytes exhibit a wide range of phagocytic indices when counting vacuoles containing apoptotic corpses. This hints that some populations may be programmed to be more adept at mediating efferocytosis (Evans et al., 2015).

These incidental observations of heterogeneous behaviour were followed up by Coates *et al*. who identified, from a publicly available large scale reporter database (available at http://enhancers.starklab.org/), non-coding enhancer elements apparently active in distinct subpopulations of macrophages within *Drosophila* (Coates et al., 2021; Kvon et al., 2014). It

was shown that plasmatocytes with active enhancer activity were associated with not only an enhanced wound response, potentially an M1-like relevant behaviour, but also decreased rates of efferocytosis, an M2-like behaviour, evidence of distinct, potentially pro-inflammatory plasmatocyte subpopulations in *Drosophila.* Furthermore, misexpression of *Calnexin14D* (*Cnx14D*), a gene closely linked to one of these non-coding enhancer elements, was capable of shifting the entire population of macrophages to a more wound-responsive state, with the overall macrophage population resembling the more pro-inflammatory subpopulation associated with the *Cnx14D*-linked enhancer. *Cnx14D* encodes a calcium binding chaperone protein known to localise to the ER (Christodoulou et al., 1997). The fact that overexpression of this gene enhances wound responsiveness in the fly potentially implicates ER-resident calcium stores in the establishment of this pro-inflammatory subpopulation.

There is also increasing evidence that plasmatocytes exhibit not only heterogeneity, but plasticity and potentially polarisation depending on the environment of the surrounding tissues. The number of plasmatocytes within putative pro-inflammatory subpopulations varies greatly at different developmental stages, suggesting that plasmatocytes are capable of being polarised to differential activation states (Coates et al., 2021). Furthermore, high levels of uncleared apoptotic cells on the VML dampen the wound-responsiveness of the overall plasmatocyte population, suggesting that 'find-me' cues released from these dying cells could be causing a shift towards a more anti-inflammatory activation state, dampening this pro-inflammatory behaviour (Roddie et al., 2019). This is supported by recent work showing that the overexpression of the EGFR ligand *spitz*, a putative 'find me' cue, specifically within plasmatocytes, lowers inflammatory wound responses (Tardy et al., 2021). This further suggests both plasmatocyte heterogeneity and plasticity, as plasmatocytes more proximal to the wound are still able to respond, suggesting a shift into a more pro-inflammatory activation state in response to wound signals, which are most potent immediately at the wound site, even in the presence of Spitz (Razzell et al., 2013; Tardy et al., 2021).

Further evidence of plasticity can be shown by increasing exposure of plasmatocytes to apoptotic cells. Glial cells function as the other major phagocyte during embryogenesis, with plasmatocytes and glia working in concert to remove apoptotic corpses during CNS development (Sonnenfeld & Jacobs, 1995). Mutations in the transcription factor *repo* prevent

effective terminal differentiation of glia, and result in an increased apoptotic burden placed upon plasmatocytes. Despite plasmatocyte differentiation not being affected, the migratory and wound-responsive capacities are severely impaired in this mutant background, which is thought to be due to the presence of increased levels of apoptotic cells (Xiong et al., 1994; Shklyar et al., 2014; Armitage et al., 2020). Using *repo* mutants to increase the apoptotic burden placed upon plasmatocytes, it was shown that numbers of plasmatocytes within putative pro-inflammatory subpopulations significantly decrease in *repo* mutants compared to controls (Coates et al., 2021). This suggests that overexposure to apoptotic cells causes an 'anti-inflammatory shift' out of plasmatocyte subpopulations. This is consistent with the vertebrate macrophage, as phagocytosis by macrophages of apoptotic neutrophils leads to the downregulation of pro-inflammatory cytokines, suggesting a shift towards an anti-inflammatory activation state (Fadok et al., 1998).

Additional plasmatocyte plasticity can be seen at the onset of metamorphosis. During this developmental change, the action of the receptor for the steroid hormone Ecdysone drastically changes plasmatocyte behaviour, which become highly migratory, phagocytic and wound responsive (Regan et al., 2013). This is in stark contrast to how plasmatocytes behave during the preceding larval stages, where they are typical sessile and non-migratory (Leitão & Sucena, 2015; Márkus et al., 2009). Indeed, culturing *ex vivo* larval plasmatocytes with Ecdysone is sufficient to induce this behavioural shift, further showing hints that plasmatocytes are plastic and may exhibit activation changes relevant to polarisation (Sampson et al., 2013).

Evidence of heterogeneity in plasmatocytes is apparent not just at the behavioural level, but also transcriptionally. RNA sequencing (RNAseq) studies have been carried out on plasmatocytes obtained from third instar larvae, and two independent studies from Cattenoz et al. and Tattikota et al. identified 13 and 12 clusters of plasmatocytes sharing similar transcriptional profiles, respectively, further hinting at robust heterogeneity within *Drosophila* macrophages (Cattenoz et al., 2020; Tattikota et al., 2020). One of these studies also carried out RNA sequencing on embryonic hemocytes, allowing transcriptomic comparisons between embryonic and larval hemocytes, and revealing further evidence of plasticity within plasmatocytes, due to differential gene expression between embryonic and larval populations.

A separate scRNAseq study on circulating larval hemocytes actually identified two novel hemocyte types, dubbed thanacytes and primocytes, populations of cells which were both *srp* positive but lacked various other plasmatocyte-specific markers (Fu et al., 2020). The authors speculated that thanacytes are involved in distinct responses to specific types of bacteria, while primocytes were thought to be circulating progenitor cells, similar to those found in hematopoietic sites within the larval lymph gland (Fu et al., 2020; Makki et al., 2010).

In summary, *Drosophila* plasmatocytes are an effective model with which to study macrophage behaviour and function *in vivo*. Despite previously having been considered homogenous, there is continually increasing evidence that they are in fact heterogeneous, plastic and capable of undergoing polarisation. *Drosophila* plasmatocytes therefore offer the opportunity to study these processes in an *in vivo* system, which could help shine a light on the pathogenesis of ADPKD, given the association of this disease with altered macrophage phenotypes.

## 1.3 Apoptosis and Efferocytosis

### 1.3.1 Apoptosis

Cells within all multicellular organisms undergo a type of programmed cell death known as apoptosis, with billions of cells dying in the human body on a daily basis. Apoptosis is essential both during development, for example in the removal of interdigital webs, and during adulthood for tissue homeostasis and the normal functioning of the immune system (Zakeri et al., 1994).

There are two canonical apoptotic pathways, known as the intrinsic and extrinsic pathways. These differ in their initiation, with the intrinsic pathway activated within the cell, in response to mitochondrial outer membrane permeability (MOMP), typically caused by Bcl-2 family proteins, releasing proteins that would otherwise be contained within the mitochondrial intermembrane space into the cytosol (Chipuk et al., 2006). Release of Cytochrome c from the mitochondria into the cytosol triggers the formation of the apoptosome, a multimeric protein complex which ultimately leads to the activation of a signalling pathway involving a family of

cysteine proteases known as caspases (Cohen, 1997). The extrinsic pathway however, is initiated by the binding of extracellular FAS ligands, such as the FAS ligand often expressed by T-lymphocytes, to the external domain of transmembrane FAS receptors, commonly referred to as 'death receptors' (Siegel et al., 2000). Following binding of FAS ligands, the receptor undergoes conformational changes that leads to the recruitment of various adapter proteins that ultimately leads to caspase activation, where the extrinsic and extrinsic pathways converge.

Upon activation of apoptosis via the caspase cascade, cells undergo many distinct morphological changes, starting with cell shrinkage and pyknosis, the irreversible condensation of chromatin. The cell then undergoes distinct morphological changes in a process known as blebbing, wherein the plasma membrane forms multiple protrusions, which ultimately separate from the cell in a process known as budding. This results in multiple membrane-bound apoptotic bodies, containing cytosol, organelles and nuclear fragments (Kerr et al., 1972). Persistence of these apoptotic bodies is associated with secondary necrosis and subsequent inflammation (Silva et al., 2008); their swift and effective removal is therefore vital.

### 1.3.2 Efferocytosis

As mentioned previously, the human body produces billions of apoptotic cells every single day. It is therefore essential that these are removed rapidly and efficiently in a process called efferocytosis. This is carried out by phagocytic cells, which can be professional phagocytes, i.e., macrophages, or neighbouring non-professional phagocytes, such as epithelial cells (Ichimura et al., 2008; Fadeel et al., 2010).

Cells that are undergoing apoptosis release 'find-me' signals to attract phagocytes (**figure 1.6a**), and display 'eat-me' signals on their surface. Eat-me signals are bound by phagocytic receptors on the phagocytes. The most well characterised eat-me signal is phosphatidylserine (PS), a phospholipid whose function is evolutionarily conserved across metazoans (Van Den Eijnde et al., 1998; Venegas & Zhou, 2007). PS is an integral component of the plasma membrane, where the action of flippases restricts its localisation to the intracellular leaflet of the membrane of healthy cells (Fadok et al., 2001). Upon activation of apoptosis, flippases are

cleaved by activated caspases, and phospholipid scramblases are activated in a calcium-dependent process, resulting in the presence of PS within the extracellular leaflet of the membrane (Bassé et al., 1996; Segawa et al., 2014; Suzuki et al., 2013).

PS and other eat-me signals exposed on apoptotic cells are bound by both professional and non-professional phagocytes directly, via phagocytic receptors, or indirectly (**figure 1.6b**). Indirect binding depends on the binding of so called 'bridging molecules', such as MGF-E8, to

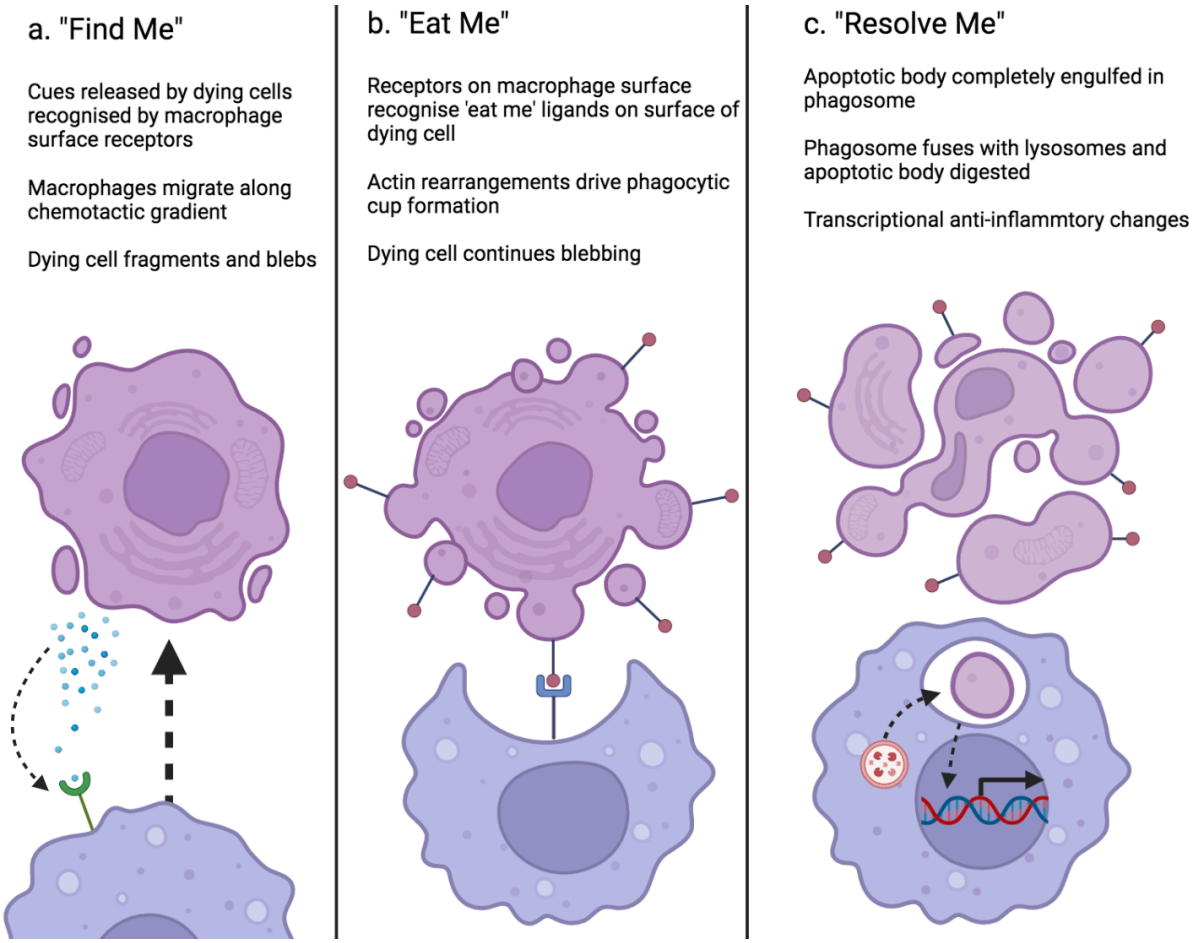


*Figure 1.6 – Key stages of efferocytosis*

(a) cells undergoing apoptosis (upper cell) release find-me cues (blue spheres) which are recognised by receptors on macrophages (bottom cell), initiating a chemotactic response towards the dying cell. (b) dying cells express eat-me ligands (e.g., PS – red circles) on their plasma membrane, which are recognised by receptors on the surface of macrophages, initiating cytoskeletal rearrangements and phagocytic cup formation. (c) the apoptotic body is then completely engulfed by the macrophage in a phagosome, which then fuses with lysosomes (pink organelle within macrophage), typically inducing anti-inflammatory effects (e.g., TGF-β signalling)

both the eat-me signal and phagocytic cell (Hanayama et al., 2002). Eat-me signal receptors can be expressed constitutively, such as Tim4 within peritoneal macrophages (i.e., professional phagocytes), or in response to a stimulus, such as KIM-1 (Wong et al., 2010). KIM-1 is a PS receptor expressed on proximal tubular epithelial cells only in response to acute kidney injury; this establishes a phagocytic phenotype and interacts with P85 to down regulate the NF-κB pathway, preventing an inflammatory response (Ichimura et al., 2008; Yang et al., 2015)

Binding to PS and other eat-me signals triggers actin polymerisation to form a 'phagocytic cup', ultimately leading to complete encapsulation (engulfment) and the formation of a phagosome containing an apoptotic body (Miller et al., 2001). The phagosome is surrounded and protected by the plasma membrane of the 'doomed' cell; subsequent phagosomal maturation occurs via fusion of phagosomes with lysosomes (figure 1.6c). This event leads to lowering of phagosomal pH and the degradation of phagosomal contents via cathepsins and other proteases active at low pH (Kinchen & Ravichandran, 2008). These events depend on a rapid increase in intracellular calcium, possibly from the ER, further suggesting a potential role for PC-2 in mammalian efferocytosis (Lundqvist-Gustafsson et al., 2000).

### 1.3.3 Apoptosis and efferocytosis in disease

In the human body new cells are constantly being created, whilst older cells are undergoing programmed cell death, primarily apoptosis. It therefore makes sense that failures in apoptosis, both too much and too little, are associated with various diseases. Numerous cancers are associated with failures in the apoptotic machinery, resulting in the uncontrolled proliferation associated with malignancies (Adams & Cory, 2007). On the other hand, increased levels of apoptosis are causative of many neurodegenerative diseases. One such example is Alzheimer's disease, which is often associated with increased caspase activity in hippocampal neurons, resulting in their death by apoptosis (Gervais et al., 1999; Smale et al., 1995).

The phagocytic removal of apoptotic cells by efferocytosis is an immunologically silent process; it occurs without initiating an inflammatory reaction where it is happening (Kurosaka et al., 2003). Defects in efferocytosis are therefore also implicated in a number of diseases, particularly autoimmune disease. Failure to phagocytose an apoptotic corpse results in a cell

undergoing what is known as 'secondary necrosis', whereby the plasma membrane ruptures, releasing the components of the cell triggering an immunological response. For example, the release of nucleosomes via secondary necrosis stimulates an autoimmune response in systemic lupus erythematous patients (Holdenrieder et al., 2006); the failure to phagocytose apoptotic corpses results in endothelial inflammation of the arteries, contributing to atherosclerosis progression (Schrijvers et al., 2005). For a recent review of efferocytosis in disease, see Morioka et al., 2019.

Evidence suggests that apoptosis, subsequent immune responses and compensatory proliferation are associated with ADPKD progression (Karihaloo et al., 2011; Peintner & Borner, 2017). It is possible therefore that efferocytosis is also implicated in this process when considering its roles in progression of other diseases. Find-me cues release by uncleared apoptotic cells attract macrophages, and macrophage influx directly correlates with disease progression in ADPKD (Karihaloo et al., 2011; Cassini et al., 2018). It is thus possible that uncleared apoptotic cells initiate an inflammatory response, as seen in other diseases, explaining the inflammation seen in the polycystic microenvironment.

### 1.3.4 Apoptosis in *Drosophila*

As with all multicellular organisms, apoptosis and efferocytosis play a crucial role throughout *Drosophila* development. For example, apoptosis is essential for the development of the nervous system during embryogenesis, as well as the gross morphological changes which occur during metamorphosis (Abrams et al., 1993; Rogulja-Ortmann et al., 2007; Zirin et al., 2013). The ease of genetically manipulating *Drosophila*, together with the imaging capabilities this model offers, has allowed us to develop an excellent understanding of apoptosis and efferocytosis (Wood & Martin, 2017; Zheng et al., 2017)

*Drosophila* apoptosis is regulated via the activity of inhibitors of apoptotic proteins (IAPs), such as Diap-1. These bind caspases, resulting in their ubiquitination and subsequent proteasomal degradation, impairing the induction of apoptosis (Herman-Bachinsky et al., 2007). However, cells destined to die actively transcribe 3 pro-apoptotic genes *reaper*, *grim* and *head involution defective (hid)*, whose protein products all function as IAP antagonists (Goyal et al., 2000). Hid

for example causes auto-ubiquitination of Diap-1, which is subsequently degraded via the proteasome, releasing the inhibition of caspases, allowing them to mediate initiation of apoptosis (Yoo et al., 2002).

### 1.3.5 Efferocytosis in *Drosophila*

In *Drosophila,* the removal of dying cells via efferocytosis is carried out primarily by hemocytes, specifically plasmatocytes (Wood & Jacinto, 2007). However, *Drosophila* efferocytosis is also mediated by other phagocytes, both professional (e.g., glial cells) and non-professional (e.g., epithelia) (Zheng et al., 2017). Co-ordinated interaction between plasmatocytes and glial cells is essential for the development of the central nervous system in *Drosophila*, with both cell types sharing the apoptotic burden during embryogenesis (Serizier & McCall, 2017; Sonnenfeld & Jacobs, 1995).

As in vertebrate systems, *Drosophila* efferocytosis is dependent on the recognition of eat-me ligands expressed on the surface of dying cells (**figure 1.7**). Phosphatidylserine is a conserved eat-me ligand, which is recognised by the receptor Six-microns-under (Simu), present on the surface of plasmatocytes (Kurant et al., 2008). Simu is thought to function upstream of the phagocytic receptor Draper as a bridging molecule, linking Draper and the apoptotic cell. However, a physical interaction between Simu and Draper has not yet been shown, suggesting Simu may function as a phagocytic receptor in its own right (Kurant et al., 2008). This is supported by a recent study that identified a protein secreted by plasmatocytes (NimB4) that binds apoptotic cells, promoting their uptake and degradation via phagosome maturation (**figure 1.7**, Petrignani et al., 2021). *NimB4* mutant plasmatocytes phenocopy *draper* mutants, exhibiting increased numbers of apoptotic corpses within the plasmatocyte, suggesting that NimB4 and Draper could be functioning in the same pathway, and that Simu could function in an independent pathway (Evans et al., 2015; Petrignani et al., 2021).

Mutations in both *draper* and *simu* significantly impair the random migration and wound responsiveness of plasmatocytes, thought to be due to the presence of excess uncleared apoptotic corpses 'distracting' plasmatocytes, while Simu is also thought to be required for retention of plasmatocytes at the wound sites (Evans et al., 2015; Roddie et al., 2019). The

genetic removal of apoptosis using *Df(3L)H99*, a genomic deletion removing three pro-apoptotic genes *head involution defective (hid), reaper (rpr)* and *grim* rescues these phenotypes in *simu* mutants, showing that they are likely due to interactions between plasmatocytes and apoptotic cells (Roddie et al., 2019; White et al., 1994).

In addition to Simu and Draper, *Drosophila* possess a third major phagocytic receptor found on the surface of plasmatocytes, Croquemort (crq), which is homologous to the CD36 scavenger receptor (figure 1.7, Franc et al., 1996). In the presence of apoptotic cells, expression of *crq* is upregulated via a recently discovered co-factor of Serpent, Bfc (Booster for croquemort) (Zheng et al., 2021). Following efferocytosis, Bfc directly binds to the zinc finger domain of Srp which increases the affinity of Srp to the promoter of *crq*, thus resulting in increased *crq* expression (figure 1.7, Zheng et al., 2021). This study also showed that, in the presence of apoptotic cells, both *drpr* and *crq* mRNA levels are increased, while there was no change in *simu*. *bfc* mutants exhibited significantly lower levels of Crq, while *drpr* mRNA appeared to increase, showing that Bfc is specific to *crq*, and that *drpr* expression could be upregulated by an as yet uncharacterised cofactor (Zheng et al., 2021). This is consistent with previous reports showing that *crq* mutant plasmatocytes exhibit increased numbers of phagocytosed apoptotic bodies, showing a degree of redundancy in apoptotic cell receptors in *Drosophila* (Franc et al., 1999).

As well as in plasmatocytes, Crq is involved in the efferocytosis of degenerating dendrites by epidermal epithelial cells (as non-professional phagocytes) during metamorphosis (Han et al., 2014). Interestingly, this study showed that Crq, along with another CD36-related protein, Dsb (Debris buster), is actually required downstream of engulfment, during phagosomal maturation, in these non-professional phagocytes. A requirement for Crq in phagosome maturation in plasmatocytes has not yet been determined, and it is still thought that Crq is required for the recognition and binding of apoptotic cells in these professional phagocytes.

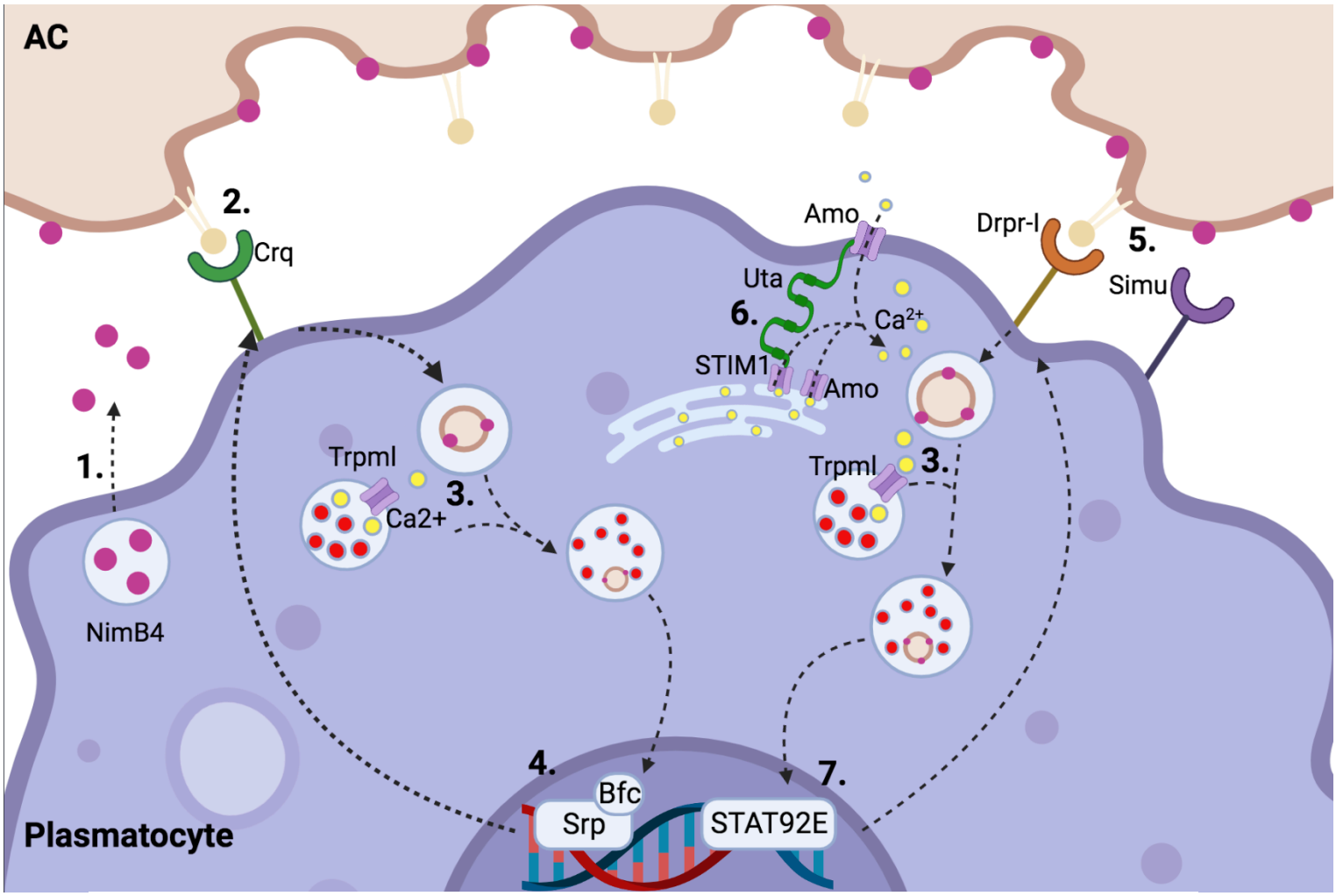


*Figure 1.7 – Drosophila apoptotic cell receptors and clearance*

1. Plasmatocytes secrete moledule NimB4 (pink circles), a putative bridging which binds to apoptotic cells (AC).
2. Following recognition of eat-me ligands on the surface of apoptotic cells (e.g., Phosphatidylserine; beige) by Crq, phagocytosis is initiated via actin rearrangements (machinery not shown)
3. Lysosomes release Calcium ions (yellow circles) via Trpml1, to facilitates fusion of the phagosome with lysosomes, resulting in phagosome maturation and the degradation of the apoptotic corpse via lysosomal enzymes (red circles).
4. Downstream of Crq-mediated phagocytosis, Bfc binds to the Zn-finger domain of Srp, increasing its affinity for the Crq promoter and upregulating expression of *crq*.
5. Simu/Drpr-I also recognise eat-me ligands on the surface of apoptotic cells, initiating actin rearrangements and phagocytosis (machinery not shown)
6. Following engulfment, Undertaker (Uta) links Calcium-release channels at the ER (e.g., STIM1, Amo) with those on the plasma membrane (e.g., Amo) to allow an influx of Calcium ions (yellow) via Store-Operated Calcium-Entry (SOCE) to maintain Calcium homeostasis.
7. Downstream of Draper-mediated phagocytosis, STAT92E is activated, resulting in increased transcription of *draper*

### 1.3.6 Calcium in *Drosophila* efferocytosis and plasmatocyte functions

Calcium signalling and homeostasis appears to play an important role in efferocytosis, and also in modulating other plasmatocyte behaviours. Downstream of Simu/Draper mediated phagocytosis, the junctophilin protein Undertaker (Uta) forms a close physical connection between the ER and plasma membrane (**figure 1.7,** Cuttell et al., 2008). It is thought that this close linking is required to maintain effective calcium homeostasis post-phagocytosis, via ER calcium channels such as STIM1 and the *Drosophila* Ryanodine receptor Rya-r44F (Cuttell et al., 2008). Interestingly, Amo/PKD2 is also thought to be involved in this process (**figure 1.7**), which is consistent with interactions between human PC-2 and Ryanodine Receptors (RyR), with human PC-2 involved in modulating RyR calcium permeability (Anyatonwu et al., 2007; Van Goethem et al., 2012). A 50% reduction in the phagocytic capacity of embryonic *amo* mutant plasmatocytes was recorded at stage 12, suggesting that calcium homeostasis is essential for effective efferocytosis (Van Goethem et al., 2012). Furthermore, the fact that *amo* is required for efferocytosis in *Drosophila* suggests *PKD2* may similarly be involved in efferocytosis mediated by mammalian macrophages.

As well as ER-resident calcium, lysosomal calcium has also been implicated in efferocytosis. Calcium release from the lysosomal channel Transient Receptor Potential Mucolipin (Trpml) was shown to be essential for effective fusion between phagosomes and lysosomes (**figure 1.7**), with *trpml* mutant plasmatocytes exhibiting a build-up of unprocessed apoptotic corpses (Edwards-Jorquera et al., 2020). Intriguingly, lysosomal calcium was also required for effective plasmatocyte migration, by controlling actomyosin contractility at the rear of the cell, showing that lysosomal calcium is capable of modulating cytoskeletal dynamics (Edwards-Jorquera et al., 2020).

Calcium is also involved in the 'priming' of plasmatocytes to be able to mount an effective wound response. Immediately following efferocytosis, bursts of intracellular calcium activate JNK signalling, which leads to upregulated expression of *draper*, which is required for the wound response (Evans et al., 2015; Weavers et al., 2016). Embryos lacking core components of the apoptotic machinery possess plasmatocytes that mount a less effective wound

response, showing how efferocytosis is an important prerequisite for the inflammatory wound response. Critically, the pan-plasmatocyte expression of *Parvalbumin*, a protein that binds to and sequesters calcium, phenocopies the impaired response, showing the importance of intracellular calcium flashes in this priming (Celio & Heizmann, 1982; Weavers et al., 2016)

As well as intracellular flashes, global calcium waves are required for the inflammatory wound response by plasmatocytes (Razzell et al., 2013). Following wounding of the epithelium, a calcium flash appears instantaneously, and propagates as a wave to neighbouring cells via gap junctions (Razzell et al., 2013). This calcium wave leads to the activation of DUOX, an enzyme that leads to the production of $H_2O_2$, a conserved wound chemoattractant, and the prevention of calcium waves results in an impaired response (Niethammer et al., 2009; Razzell et al., 2013).

In summary, *Drosophila* plasmatocytes represent an excellent *in vivo* model with which to study macrophage function and behaviour. Calcium signalling and homeostasis have been implicated in both efferocytosis and other important plasmatocyte functions, and *Drosophila Pkd2* has been directly implicated in efferocytosis. Taken together with the aberrant apoptosis and altered macrophage phenotypes seen in the polycystic kidney, an important role for efferocytosis in the pathogenesis of ADPKD is suggested, and *Drosophila* can be used as a viable model with which to characterise this involvement.

## 1.4 Hypothesis and Aims

The evidence stated above indicates clearly that, despite the exact pathogenesis of ADPKD remaining unclear, there is clearly a large immune component in this disease, with aberrant macrophage influx, cell death and inflammation all readily apparent in the polycystic kidney. I therefore sought to use *Drosophila* as an *in vivo* model with which to determine the impact of *Pkd2/amo* mutations in the context of immune cell function, particularly how efferocytosis can impair these behaviours. Furthermore, I investigated the effect of *amo*-related pathways, such as efferocytosis and calcium signalling, on macrophage subpopulations in *Drosophila*, in a bid to understand macrophage polarisation and the role it could be playing in the context of ADPKD. Finally, due to the ease of genetic manipulation of *Drosophila,* I wished to overexpress

pathogenic missense variants of *PKD2* in this model to generate functional readouts of these mutations, in order to elucidate how they might contribute to the pathogenesis of ADPKD.

## Hypotheses

1. Pathogenic missense variants of *PKD2* affect the calcium permeability of the PC-2 channel, disrupting calcium homeostasis and driving pathogenesis of ADPKD. These variants can be expressed in *Drosophila* in order to characterise their functional impact.

2. Loss of PC-2-mediated calcium homeostasis causes failures in apoptotic cell clearance, which leads to macrophage influx, inflammatory responses and compensatory proliferation, all of which contribute to the pathogenesis of ADPKD.

3. PC-2-mediated efferocytosis and calcium homeostasis modulate macrophage polarisation. Failures in these processes result in aberrant macrophage polarisation, which contributes towards the pathogenesis of ADPKD.

## Aims

1. Use *Drosophila* as a model with which to characterise the functional effect of pathogenic *PKD2* missense variants, by exploiting the *GAL4-UAS* system to drive expression of such variants in an *amo/PKD2* null background.

2. Characterise the precise defects associated with *amo* mutations in respect to apoptotic cell clearance and investigate how this can affect other immune cell functions *in vivo* and *in vitro*, to identify potential new players in the pathogenesis of ADPKD.

3. Investigate the regulation and establishment of macrophage subpopulations in *Drosophila*, by manipulating various processes with a focus on apoptotic cell clearance and other pathways related to both Amo function and macrophage polarisation.

# Chapter 2: Materials and methods

## 2.1 *Drosophila* husbandry and genetics

### 2.1.1 *Drosophila* husbandry

Stocks of *Drosophila melanogaster* were maintained at 18°C in vials containing 5mL fly food (recipe in appendix). Larger straight-sided bottles containing 20mL fly food were used at 25°C for amplifying lines and collection of virgin females, which were subsequently kept at 18°C until enough had been collected for use in crosses. All crosses were carried out using virgin females which were then kept at 25°C, with flies being tipped into a fresh vial every 2-3 days to amplify progeny. Fly stocks kept at 18°C were tipped on to fresh vials every month, whilst bottles kept at 25°C were discarded after a maximum of 3 weeks. $CO_2$ was used to anesthetise flies for up to 10 minutes during virgin collections and genotype selection, with the use of a light microscope and a paintbrush to manoeuvre flies. To collect embryos and first instar larvae, at least 20 male and 20 female flies were placed in a 100mL beaker which was sealed with a 5cm apple juice agar plate (recipe in appendix) supplemented with a small amount of yeast (50% in $dH_2O$), secured with an elastic band and placed upside down at 22°C for embryo collections, and 25°C for larval collections.

### 2.1.2 *Drosophila* lines

The following *Drosophila* drivers and constructs were used: *crq-GAL4* (Stramer et al., 2005), *srp-GAL4* (Brückner et al., 2004), *VT17559-GAL4, VT32897-GAL4, VT57089-GAL4, VT62766-GAL4* (Coates et al., 2021; Kvon et al., 2014), *daughterless-GAL4* (Wodarz et al., 1995), *24b-GAL4* (Gao et al., 2004). When exploiting the split GAL4 system (Pfeiffer et al., 2010), the GAL4 activation domain (*AD*) was expressed via *serpent-Hemo-AD,* while the GAL4 DNA binding domain (*DBD*) was expressed via *serpent-Hemo-DBD, VT17559-DBD, VT32897-DBD, VT57089-DBD* and *VT62766-DBD* (all Coates et al., 2021).

The following *UAS* lines were used: *UAS-stinger* (Barolo et al., 2000), *UAS-eGFP* (Bloomington *Drosophila* stock centre), *UAS-UAS-RedStinger* (Barolo et al., 2004), *UAS-GCaMP6m* (Chen et al., 2013), *UAS-Calnexin14D* (Harvard *Drosophila* stock centre), *UAS-amo* (Gao et al., 2004) , *UAS-cd4-tdTomato* (Han et al., 2011), *UAS-Draper-II* (Logan et al., 2012), *UAS-Parvalbumin* (Mortimer et al., 2013) , *UAS-sSpitz*$^{CS}$ (Ghiglione et al., 2002), *UAS-EcR*$^{\Delta C655}$ (Cherbas et al., 2003), *UAS-GFP-MYC-2x-FYVE* (Wucherpfennig et al., 2003)), and *UAS-GC3Ai* (Schott et al., 2017). The following UAS lines were made as part of this work: *UAS-HA:PKD2, UAS-HA:amo*, *UAS-amo* and *UAS-PKD2* (all inserted into *attP2*); see below for details or their generation.

The following *GAL4*-independent reporter lines were used: *srpHemo-3x-mCherry* (Gyoergy et al., 2018), *srpHemo-H2A-3x-mCherry* (Gyoergy et al., 2018), *srp-GMA* (James Bloor, University of Kent), *VT17559-RFP, VT32897-RFP, VT57089-RFP, VT62766-RFP* (Coates et al., 2021)

The following *Drosophila* mutants and deficiencies were used: *amo*$^{1}$ (Watnick et al., 2003), *amo*$^{ko67}$ (Gao et al., 2004), *simu*$^{2}$ (Kurant et al., 2008), *repo*$^{03702}$ (Xiong *et al.*, 1994), *crq*$^{ko}$ (Guillou *et al.*, 2016), *Df(3L)H99* (White et al., 1994) and *Df(2L)BSC407*.

All transgenes and mutations were crossed into a *w*$^{1118}$ background, which itself was often used as a negative control.

### 2.1.3 Balancer chromosomes

Fluorescently-labelled balancer chromosomes were used to enable genotyping of *Drosophila* embryos and larvae (Casso *et al.*, 2000). The fluorescent balancer *CyO dfd-nvYFP* was used for alleles and genes on chromosome 2, while *TM6b dfd-nvYFP* was used for chromosome 3 (abbreviated to *CyO dfd* and *TM6b dfd*) unless otherwise stated. Both these balancer chromosomes possess a nvYFP under the control of the promoter for *deformed* (*dfd*), a homeobox containing transcription factor expressed in the developing head (Le et al., 2006; Regulski et al., 1987). This allows easy selection of embryos lacking the balancer chromosomes, as *dfd-nvYFP* can easily be selected against using a fluorescent stereomicroscope. Embryos of the correct genotype (i.e., lacking balancer chromosomes) were therefore selected at random

prior to imaging.

## 2.2 Imaging *Drosophila* embryos

### 2.2.1 Collection, dechorionation and mounting of embryos

To collect embryos for imaging, adult males and virgin females were placed in a laying cage stoppered with an apple juice agar plate supplemented with yeast paste. Embryos were then harvested from plates left overnight at 22°C, typically within 16-18 hours after changing of the plates. Plates were rinsed with room temperature $dH_2O$ and a paintbrush was used to remove embryos from the plate. Embryos were then placed in a solution of 5% bleach for 1 minute to remove the chorion, before extensive washing with room temperature $dH_2O$ to remove bleach. Embryos were left in water prior to mounting to prevent dehydration.

A Leica M165FC fluorescent stereomicroscope was used to select against fluorescently labelled balancer chromosomes, allowing correct genotyping of embryos. Embryos were staged according to gut morphology (via gut autofluorescence) and picked up using a tungsten needle, with stage 15 embryos used unless stated otherwise. Embryos were mounted ventral-side-up on double-sided, sticky tape (Scotch) attached to a microscope slide and flanked by 22x22mm coverslips before being immersed in a minimal amount of Voltalef oil (VWR) before a 32x22mm coverslip was placed on the flanking coverslips, with the bridging coverslip making contact with the immersion oil for optimal imaging of the embryos (**figure 2.1**). The bridging coverslip was then sealed in place using nail varnish (Superdrug), and the prepared slide kept in the dark at room temperature for 30 minutes prior to imaging to allow acclimatisation of the embryos to the oil.

### 2.2.2 Live imaging of embryonic plasmatocytes

Following the mounting procedure described above, *Drosophila* embryos were imaged using a

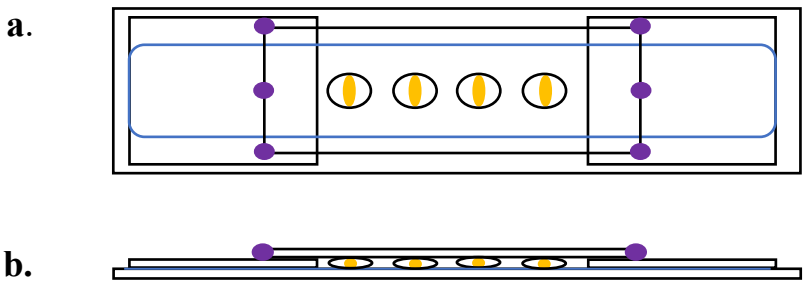


*Figure 2.1 – Schematic of the mounting procedure for live imaging Drosophila embryos*

Top down (a) and lateral (b) view of prepared slide showing 4 embryos (yellow) mounted side by side on double-sided sticky tape (blue) immersed in a minimal drop of oil (black circles). Note the immersion oil touching the top coverslip which is held in place by nail polish (purple).

Perkin Elmer Spinning Disk Confocal microscope with a 40x oil immersion objective lens (planSApo 40x oil, NA 1.3). Embryos were imaged to a depth of 20µm, unless stated otherwise, with z-slices spaced every 1µm. To assay plasmatocyte random migration, z-stacks were taken every 1 minute for 30 minutes, while plasmatocyte dispersal was assayed by imaging stage 13 embryos every 2 minutes for 90 minutes. To measure wound responses, the ventral side of an embryo was ablated using a nitrogen-pumped, Micropoint ablation laser tuned to 435nm (Andor). Embryos were then imaged every 2 minutes for 1 hour, before a final post-wound brightfield image of 35µm depth was taken (**figure 2.2**).

For Lysotracker experiments requiring staining of live embryos, stage 15 dechorionated embryos were selected and transferred to a mixture of peroxide-free heptane (VWR) and 10µm lysotracker red (Thermofisher) in PBS (Oxoid) in a glass vial, which was shaken in the dark for 30 minutes. Embryos were then transferred into a watchmaker's glass containing Halocarbon oil 700 (Sigma), before being mounted as described above.

### 2.2.3 Fixation and immunostaining of embryos

For fixation, embryos were dechorionated as described above, and transferred to glass vials containing a 50:50 mix of 4% formaldehyde (Sigma) in 1xPBS and peroxide-free heptane. These were placed on a shaker at 250 rpm for 20 minutes before the lower heptane phase was removed using a glass Pasteur pipette. Absolute methanol (Fisher) was added to vials which were shaken vigorously and left for 1 minute to allow embryos to 'pop' out of their vitelline

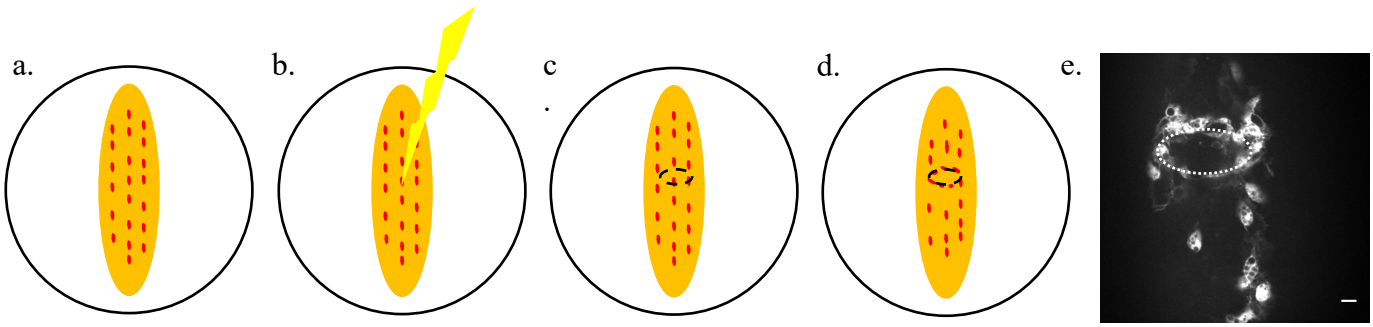


*Figure 2.2 – Schematic of the wounding assay*

a. Stage 15 embryo with plasmatocytes labelled in red, mounted in Voltalef oil ventral-side-up. Note the distinct 3 lines of plasmatocytes on the ventral midline characteristic of stage 15.
b. An epithelial wound is induced using an ablation laser
c. Shows the epithelia immediately post-wounding with the wound outlined
d. Shows plasmatocytes responding to the wound 1-hour after wounding
e. Representative single z-slice of a wild-type embryo 60-minutes post-wound. Scale bar represents 10µm

membrane and sink to the bottom of the vial. A glass Pasteur pipette was used to transfer embryos from the bottom of the glass vial into a 1.5mL microcentrifuge tube where they were washed 3 times with absolute methanol, before being stored at -20°C prior to staining.

For immunostaining, fixed embryos of the same genotype were pooled together into a 1.5mL microcentrifuge tube. The methanol was then removed, and the embryos were washed 3 times with PBTx (PBS with 0.1% Triton-X100 (Sigma)) before being washed with PATx blocking solution (PBTx with 1% BSA (Sigma)) 3 times for 20 minutes on a roller at 60rpm. After the final wash, PATx containing primary antibody was added and the embryos were incubated at 4°C on a roller at 60 rpm overnight. Embryos were kept in the dark wherever possible from this step onwards. After overnight incubations the staining solution was removed and embryos were immediately washed 3 times with PATx, before washing a further 3 times with PATx for 20 minutes on a roller at 60rpm. After the final wash, a 1:200 solution of secondary antibody in PATx was added and the embryos were incubated at room temperature on a roller at 60 rpm for 2 hours. Embryos were then immediately rinsed 3 times with PATx and then a further 3 times with PATx for 20 minutes on a roller at 60rpm, after which the PATx was removed and the embryos were immersed in 1,4-Diazabicyclo[2.2.2]octane (DABCO; Sigma) mountant and

stored at 4°C prior to imaging. DABCO mountant is 2.5% DABCO dissolved in 90% glycerol (Sigma), 10% PBS.

The following primary antibodies were used: mouse anti-Fascin (sn7c; Developmental Studies Hybridoma Bank; used at 1:500) and rat anti-HA (3F10; Sigma; used at 1:200).

The following secondary antibodies were used: Alexa fluor 488 goat anti-mouse (A11029; Life Technologies; used at 1:200), Alexa fluor 568 goat anti-mouse (A11031; Life Technologies; used at 1:200) and Alexa fluor 488 goat anti-rat (AB150157; Abcam; used at 1:1000)

Immunostained embryos were mounted for imaging as described above, with the exception being that a single embryo was mounted per slide, and embryos were immersed in a minimal drop of DABCO mountant as opposed to Voltalef oil.

## 2.3 Imaging *Drosophila* larvae and adults

### 2.3.1 Imaging whole-mount L3 larvae

Wandering third instar larvae were selected with a paintbrush and washed with distilled water, before being transferred to a petri dish lid (Nunc) containing ice-cold water. Larvae were then imaged dorsal side up using a Leica MZ205 fluorescent stereomicroscope with a 10x objective lens at 35x zoom using Leica LAS X software.

### 2.3.2 Imaging whole-mount adults

Newly-eclosed (hatched) virgin females were collected and aged appropriately at 25˚C prior to imaging. Flies were then anaesthetised using $CO_2$ and placed at -20˚C for 3 minutes before being placed on an ice-cold petri dish lid. Flies were orientated laterally and imaged with a Leica MZ205 with a 10x objective lens at 35x zoom using Leica LAS X software.

### 2.3.3 Dissection and imaging of *ex vivo* larval and adult hemocytes

Wandering larvae or adult flies were placed into a 75µL droplet of ice-cold S2 media, consisting of Schneider's media (Sigma) supplemented with 10% heat inactivated FBS (Sigma/Gibco) and 1x pen/strep (Sigma/Gibco). Larvae were ripped open at the posterior end using two pairs of size 5 dissection forceps, releasing circulating hemocytes into the S2 media, while adults were cut longitudinally. Carcasses were then gently agitated for 5 seconds to release hemocytes, before being removed from the suspension. The cell suspension was then added to a well of a 96-well plate (Greiner). For adults, two flies were dissected per well, whereas an additional 75µl of S2 media was added to wells containing larval hemocytes. Hemocytes were allowed to settle for up to 90 minutes in a dark, humidified box, prior to fixation with 4% paraformaldehyde (PFA; ThermoFisher) in PBS for 15 minutes. PFA was washed off using 1xPBS and fixed hemocytes were stored at 4°C prior to staining.

To stain hemocytes, fixed cells were permeabilised by washing with 0.1% PBTx for 4 minutes, before thorough washing with 1xPBS. Cells were then stained using a solution containing 2 drops/mL NucBlue (Invitrogen) to label nuclei, and Alexa Fluor 488 Phalloidin (Thermofisher) to label actin filaments. This solution was left on in the dark for up to 30 minutes, before plates were washed thoroughly with 1xPBS. Stained cells were stored at 4˚C and allowed to warm to room temperature prior to imaging using a 10x objective on an ImageExpress Hi Content microscope. Z-offsets were calculated for each channel prior to imaging 9 central fields of view in each well, and images from each well were converted into hyperstacks prior to analysis.

## 2.4 Assays of *Pkd2/amo* function

### 2.4.1 Fertility assays

Single male adult flies were placed in a vial with five $w^{1118}$ virgin females, of no more than 10 days old. Experimental males (e.g., *amo* mutant homozygotes or trans-heterozygotes) were always compared to wild type males ($w^{1118}/Y$), apart from in cases utilising the *GAL4-UAS* system, in which case *GAL4* drivers lacking any *UAS* effectors were used (e.g., $w;amo^{1};da$-*GAL4*). Adult flies were left to breed for 4 days before being removed from the vial. Progeny in the form of adult flies and late-stage pupae were counted after 12 days.

### 2.4.2 Smooth muscle functional assays

Adult flies were placed in a laying cage 24-hours prior to the assay and left at 25°C. 24 hours after incubation, larvae and embryos were rinsed off the plate as described in section 2.1.3, and first instar larvae were transferred to an apple juice agar plate supplemented with yeast containing 0.05% bromophenol blue for 4 hours (as per Gao et al., 2004). After 4 hours at 25°C, larvae were rinsed off the plate as previously described, and were checked for the presence or absence of blue yeast visible in the hindgut using light microscopy. All larvae with blue yeast visible in the hindgut were transferred to an apple juice agar plate supplemented with undyed yeast and left for 1 hour at 25°C. Larvae were then rinsed off again and the absence of blue yeast in the hindgut was checked and scored.

To visualise calcium signalling in the visceral smooth muscle of L1 larvae, L1 larvae expressing *UAS-GCaMP6m* specifically in the visceral smooth muscle (driven by *24b-GAL4*) were selected from apple juice agar plates supplemented with yeast paste, and stuck dorsal-side-up on a slide with double-sided sticky tape. Larvae were then covered with a minimal amount of Voltalef oil, and immediately imaged with a Leica MZ205 with a 10x objective at 50x zoom using Leica LASX software every 200ms for 30 seconds.

## 2.5 Image processing and analyses

### 2.5.1 Image processing

All images were converted to .tif format, despeckled to reduce background noise, and blinded using a Python script prior to analysis, which was performed on Fiji/ImageJ (Schindelin et al., 2012).

### 2.5.2 Quantification of plasmatocyte migration and dispersal

Time-lapse movies showing plasmatocyte dispersal or random migration were processed into maximum intensity projections formed of 15 z-slices, with the appearance of the most

superficial plasmatocyte marking the first slice. To quantify plasmatocyte dispersal, the total number of plasmatocytes at the end of each movie was counted, whereas migration speeds were calculated via the manual tracking tool in Fiji/ImageJ. Outputs from the manual tracking tool were then imported into the Ibidi chemotaxis tool in Fiji/ImageJ, revealing average plasmatocyte velocity per embryo.

### 2.5.3 Quantification of plasmatocyte wound responses

To calculate wound responses, the wound was identified using the post-wound brightfield image and drawn onto the other channels showing plasmatocytes. Wound response was then quantified in terms of plasmatocyte density, a measure of the number of plasmatocytes responding to the wound divided by the area of the wound, which were normalised to the average hemocyte density of the wild-type controls.

### 2.5.4 Quantification of plasmatocyte efferocytosis and phagosomal acidification

To calculate phagocytic indices of embryonic plasmatocytes, a GFP-based Caspase-3 activity indicator (*UAS-GC3Ai*) was expressed under the control of the ubiquitous driver *daughterless-GAL4* (*da-GAL4*) to label apoptotic cells. A *GAL4*-independent plasmatocyte reporter (*serpent-3x-mCherry*) was used in conjunction with *UAS-GC3Ai*, allowing the number of apoptotic cells within plasmatocytes to be calculated, and the phagocytic index to be calculated by dividing the total number of GC3Ai-positive punctae within plasmatocytes by the total number of plasmatocytes within the field of view.

In order to calculate rates of efferocytosis, *UAS-GFP-MYC-2x-FYVE* was expressed in all plasmatocytes (via *serpent-AD, serpent-DBD*) or specifically in subpopulation plasmatocytes (via *serpent-AD, VT-DBD*). Stage 12/13 embryos were imaged every 2 minutes for 1 hour, and the number of FYVE events (the appearance of GFP on the surface of early phagosomes) per plasmatocyte, per embryo, were counted.

In order to quantify phagosome acidification, the number of phagosomes of the 5 most superficial plasmatocytes were counted using the multi-point selection tool on the green channel. The number of these phagosomes which overlapped with Lysotracker Red staining on the red channel were then counted to work out a percentage of phagosome acidification.

### 2.5.5 Quantification of calcium signalling

To quantify the intensity of calcium flashes in response to wounding, pre-wound images of the ventral midline (VML) of embryos ubiquitously expressing *UAS-GCaMP6m* via *da-GAL4* were taken. Embryos were then wounded and imaged either every 10 seconds for 2 minutes, or every minute for 20 minutes. Pre-wound images and post-wound time lapses were concatenated and converted to an average intensity Z-projection in Fiji. To quantify calcium flashes, the polygon selection tool was used to outline either the entire embryo (for 2-minute time-lapses) or the initial flash area (for 20-minute time-lapses), and the mean grey value for these areas was calculated for each time point. Mean grey values were then normalised to the pre-wound mean grey value and plotted against time using GraphPad (Prism).

Rates of intra-plasmatocyte calcium flashes were determined via imaging the VML of stage 12/13 embryos expressing *UAS-GCaMP6m* under control of the plasmatocyte-specific drivers *srp-GAL4* and *crq-GAL4*, with the *GAL4*-independent pan-plasmatocyte reporter *serpent-3x-mCherry* enabling visualisation of cells without elevated cytoplasmic calcium. Embryos were imaged every minute for an hour, with time-lapse movies being converted into maximum intensity projections in Fiji. The number of calcium flashes per plasmatocyte, per embryo was then calculated.

### 2.5.6 Quantification of plasmatocyte subtype proportions

To work out the relative number of macrophages within subpopulations, embryos were imaged as a single z-stack, which was converted into a maximum intensity projection in Fiji. The total number of plasmatocytes, labelled with pan-plasmatocyte reporters (such as *serpent-3x-mCherry* or via *crq-GAL4,UAS-GFP;srp-GAL4,UAS-GFP*) was counted, as were subpopulation plasmatocytes labelled via *VT-GAL4* driving *UAS* reporters, or via *GAL4*-independent *VT-RFP*

lines. The proportion of plasmatocytes within a given subpopulation was then expressed as a percentage of the overall population.

### 2.5.7 Measuring fluorescent intensity of subpopulation cells within adult flies

To work out relative fluorescent intensity as a readout of subpopulation plasmatocyte numbers, a region of interest (ROI) was drawn around entire flies expressing *UAS-RedStinger* driven by *VT-GAL4* using the polygon selection tool in Fiji. The mean grey value of the ROI was then measured.

### 2.5.8 Quantification of *ex vivo* larval and adult plasmatocytes

The total of number of *ex vivo* plasmatocytes were determined via automated counting of nuclei based on the DAPI channel (nucBlue staining). Images within this channel were converted to a binary mask, and the analyse particles tool in Fiji/ImageJ was used to count number of nuclei. Only particles between 50 and 350 square pixels were counted, to exclude autofluorescent debris. Plasmatocytes within subpopulations were counted manually using the multi-point tool in Fiji/ImageJ, and the proportion of plasmatocytes within subpopulations was expressed as a percentage of the overall population.

## 2.6 Molecular biology

### 2.6.1 Generating HA-tagged *amo* cDNA in pUASTattB

The construct UFO12032 containing *amo* cDNA was obtained (DGRC stock number 1641818). The following primers were used to amplify specifically the cDNA, whilst incorporating an N-terminal HA-tag at the 5' end of the cDNA. Bold and underlined text represents where the primers will anneal with template cDNA, italicised text represents HA tag, red text represents restriction sites:

HA-amo Fwd (containing EcoRI site):

5' GTCGACGAATTCATG*TACCCATACGACGTCCCAGACTACGCT*ATGGCCCAGCAGGGTCAGAGT

HA-amo Rev (containing XbaI site):

5’ TACGAGTCTAGACTATTTTTTCTTGTTATGGTAAT

These primers were used with KAPA HiFi HotStart ReadyMix (Roche) to amplify *amo* cDNA from UFO12032 according to the manufacturer’s instructions. PCR products were run on 1% TAE agarose gels to verify amplification, then purified using QIAquick PCR clean up column (QIAgen) according to the manufacturer's instructions.

1µg of purified PCR product was then treated with EcoRI (Promega) and XbaI (Promega) according to the manufacturer’s instructions, while 1µg of pUASTattB (DGRC stock number 1419) was simultaneously digested with the same enzymes. Reactions were run on 1% agarose TAE gels to verify digestion and extracted using a QIAquick Gel Extraction Kit (QIAgen) according to the manufacturer’s instructions.

Purified, digested PCR product and vector were then ligated using T4 DNA ligase (Promega), left out at room temperature for 10 minutes then placed at 4°C overnight. OneShot TOP10 chemically competent cells (Invitrogen) were transformed using 1µL of the ligation reaction according to the manufacturer's instructions, and transformations were plated on LB agar plates supplemented with 100µg/mL ampicillin and grown overnight at 37°C.

5mL LB supplemented with 100µg/mL ampicillin was inoculated with single colonies and grown overnight in a shaking incubator at 37°C. Purified plasmids were recovered from overnight cultures using a QIAprep spin miniprep kit (QIAgen) according to the manufacturer's instructions. Ligations were validated by digesting transformed plasmids with appropriate enzymes and running on 1% agarose TAE gels.

### 2.6.2 Cloning *HA-PKD2* cDNA into pUASTattB

*PKD2* cDNA possessing a 5’ (N-terminal) HA tag in pcDNA3.1(-) was gifted to us by Dr Andrew Streets (University of Sheffield). *HA-PKD2* cDNA was amplified using the following primers,

designed to incorporate restriction sites allowing insertion into pUASTattB. Bold and underlined text represents where the primers will anneal with template cDNA, italicised text represents HA tag, red text represents restriction sites:

HA-PKD2 Fwd (containing XhoI site):

5' GTCGACCTCGAGATG*TACCCATACGACGTCCCAGACTACGCT*GTGAACTCCAGTCGC

HA-PKD2 Rev (containing XbaI site):

5' TACGAGTCTAGATCATACGTGGACATTAGA

These primers were used along with KAPA HiFi polymerase as per *HA-amo* and cloned into pUASTattB using the same approach, but with XhoI (Promega) used instead of EcoRI

### 2.6.3 Generating untagged *amo* cDNA in pUASTattB

*amo* cDNA was cloned into pUASTattB as per section 3.6.1, except that the following forward primer (lacking a 5' HA-tag) was used to amplify *amo* cDNA from UFO12032:

amo Fwd (containing EcoRI site):

5' GTCGACGAATTCATGGCCCAGCAGGGTCAGAGT

### 2.6.4 Generating untagged *PKD2* cDNA in pUASTattB

*PKD2* cDNA was cloned into pUASTattB as per section 3.6.2, except that the following forward primer (lacking a 5' HA-tag) was used to amplify *PKD2* cDNA from pcDNA3.1(-):

PKD2 Fwd (containing XhoI site):

5' GTCGACCTCGAGATGGTGAACTCCAGTCGCGTG

### 2.6.5 Transgenesis of *Drosophila* embryos

Approximately 5µg of purified plasmid DNA was sent to Genetivision Corporation for PhiC31-mediated site-specific insertion into the genome at the attP2 site on chromosome 3.

## 2.7 Cell culture

### 2.7.1 Ethical Approval

Ethical approval for working with innate immune cells from anonymised donors was obtained from the South Sheffield Research Ethics Committee (study number STH13927).

### 2.7.2 Growth of monocyte-derived macrophages from peripheral blood mononuclear cells

Human peripheral blood mononucleated cells (PBMCs) were isolated from a healthy donor and spun down at 1500 rpm for 6 minutes at 20°C. PBMCs were then resuspended in serum-free RPMI and seeded at a density of 800,000 per well in a 96 well Greiner Bio-One Cellstar plate (cat no. 655098). Cells were left to adhere for 1 hour at 37°C, before unadhered cells were washed off and replaced with 150uL RPMI supplemented with Pen-Strep (Lonza) and Foetal Calf Serum (FCS; Sigma), which was replenished every 2-3 days for up to 10 days. Approximately 10% of PBMCs are monocytes, resulting in approximately 80,000 monocyte derived macrophages per well after culturing at 37°C with 5% $CO_2$.

### 2.7.3 Growth of UCL93 and *PKD2* knockout cells

UCL93 is a kidney cell line isolated from the proximal tubular epithelial cells of a healthy, non-cystic kidney. CRISPR-Cas9 has previously been used by our group to remove exon 1 of the *PKD2* gene in UCL93 cells, essentially resulting in a *PKD2* knock-out cell line. 3 different clones of the *PKD2* knockout cell line were used for experiments, c33 c37 and c38. These were compared to the parental line (i.e., UCL93) as a wild-type control.

Cells were grown to confluence in T75 tissue culture flasks containing 10mL of DMEM/F-12

supplemented with 5% Pen-Strep (Lonza), L-Glutamine and 5% Nu Serum (Corning). All cells were grown at 33°C unless otherwise stated and passaged 1:6 into a flask containing fresh media once confluent.

For efferocytosis assays, confluent cells were counted after trypsination using a Bio Rad TC20 automated cell counter, by mixing 5µL of cell suspension with 5µL Trypan Blue (Bio Rad). Live cells were seeded at a density of 35,000 per well in a 96 well Greiner Bio-One CellStar plate and were incubated for 24 hours prior to the efferocytosis assay. Cells were given 150µL fresh media immediately prior to performing this assay.

### 2.7.4 Neutrophil ageing

Due to their abundance in blood and short lifespan before undergoing programmed cell death by apoptosis, neutrophils were tested as an apoptotic target to assay efferocytosis *in vitro.* Neutrophils were isolated from a healthy donor (different to the PBMC donor) and resuspended in RPMI media supplemented with Pen/Strep and FCS. Neutrophils were then plated on a 96-well flexi plate (Corning) at 500,000 cells per well and were given either complete RPMI or Tyrphostin AG825 (Sigma) in RPMI to a final concentration of 25µM to induce apoptosis (Murillo et al., 2001). Neutrophils were then incubated overnight at 37°C for no more than 22 hours, after which cells were spun on a cytospin, and apoptosis verified on a light microscope as per Crowley et al., 2016.

### 2.7.5 Preparing labelled apoptotic neutrophils

Apoptotic neutrophils were pooled in a 15mL Falcon tube before being spun at 2000 rpm for 2 minutes. Cells treated with Tyrphostin were then rinsed with PBS to remove any excess Tyrphostin, before being spun again. Cell pellets were resuspended in a solution of Cell Tracker Red CMTPX (Fisher) diluted to 1µM in serum free RPMI, then incubated at 37°C for up to 30 minutes. Cells were spun again and rinsed with PBS to remove excess dye, and resuspended in complete DMEM/F-12, usually to a final concentration of 20 million/mL.

### 2.7.6 Efferocytosis assay, fixation and staining

Labelled apoptotic neutrophils (section 2.7.5) were added to cells at ratios ranging from 5:1 to 15:1. MDMs were kept at 37°C for 60-90 minutes while UCL93 and *PKD2* knock out cells were kept at 33°C for 90 minutes. After co-incubation, cells were rinsed with ice cold PBS to remove any excess neutrophils. 4% Paraformaldehyde in PBS was added for up to 20 minutes to fix cells, which were then washed 3 times with PBS. Prior to staining, cells were permeabilised with 0.1% Triton X-100 in PBS for 4 minutes, before extensive washing with PBS. A staining solution containing 0.5% Alexa fluor 488 Phalloidin (final concentration 33nM; Thermofisher) and NucBlue (Invitrogen) at 2 drops/mL was added, and cells were left in the dark to stain at room temperature for 30 minutes. The staining solution was then removed, and cells washed extensively with PBS, before storage at 4°C. Plates were kept in the dark at room temperature for at least 30 minutes prior to imaging to prevent any condensation.

### 2.7.7 Efferocytosis assay imaging and quantification

Plates were kept at room temperature for 30 minutes prior to imaging using an ImageXpress High Content microscope. Z-offsets and exposure times were calculated for each channel (Dapi/blue, GFP/green and Texas Red/red) prior to imaging. 12 central fields of view were imaged per well. Images were saved as hyperstacks, with each resulting slice equivalent to one field of view. Images were quantified by calculating the phagocytic index of each well, here defined as:

$$100 \times \frac{Number\ of\ cells\ with\ inclusions}{Total\ number\ of\ cells} \times \frac{Total\ number\ of\ inclusions}{Total\ number\ of\ cells}$$

Apoptotic inclusions were counted manually using the multipoint tool in Fiji, with any apoptotic bodies not overlapping with the green or Dapi/blue channels not counted. The total number of cells was quantified by the automated counting of the number of nuclei on the DAPI channel, as described in section 2.5.7.

# Chapter 3: Developing *Drosophila* as a model to characterise the functional effect of clinically relevant *PKD2* mutations

## 3.1 Introduction

Autosomal dominant polycystic kidney disease (ADPKD) is the most common inherited cause of kidney failure, and one of the most common genetic diseases, affecting between 1 in 400 and 1 in 1000 people worldwide (Iglesias et al., 1983; Leuenroth & Crews, 2009). The vast majority of ADPKD cases are caused by mutations in either *PKD1* or *PKD2*, encoding Polycystin-1 and Polycystin-2, respectively, while a very small number are caused by mutations in other genes, often with extra-renal pathologies (Cornec-Le Gall et al., 2018; Hughes et al., 1995; Peters et al., 1993; Porath et al., 2016). These mutations result in the formation of fluid-filled cysts, originating from tubular epithelial cells of the nephron, which continue to expand, progressively decreasing renal function and ultimately lead to end-stage renal disease. However, though the genetic basis of the disease has been well characterised, and the pathology of the disease is reasonably well understood, the exact molecular mechanisms involved in pathogenesis remain poorly understood.

*PKD1* encodes Polycystin-1 (PC-1), a large transmembrane protein which localises to the plasma membrane and primary cilia, where it is thought to be involved in mechanosensation using its large, extracellular domain (Forman et al., 2005; Harris et al., 1995). *PKD2* encodes Polycystin-2 (PC-2) which is a substantially smaller and relatively simple protein when compared to PC-1 (Hayashi et al., 1997). PC-2 functions as a non-selective, calcium-permeable cation channel which, like PC-1, is known to localise to primary cilia and the plasma membrane (Mochizuki et al., 1996). At the cilia, both Polycystin proteins interact with one another using their C-terminal coiled-coil domains, forming the so called 'Polycystin complex' (Qian et al., 1997; Yu et al., 2009). It is thought that, in the context of this complex, the mechanosensory function of PC-1's extracellular domains in turn modulates PC-2 channel permeability in response to extracellular stimuli such as fluid flow (Hanaoka et al., 2000; Yoder et al., 2002).

However, both Polycystins are expressed independently of one another; while PC-1 is expressed exclusively on the surface of cells, PC-2 localises to the endoplasmic reticulum (ER) as a homotetramer, where it is involved in maintaining calcium homeostasis. This function is achieved not only through its own activity as a calcium channel, but also via the modulation of other calcium channels located on the ER, such as the inositol 1,4,5-triphosphate receptor (IP3R) and the Ryanodine receptor (RyR) (Anyatonwu et al., 2007; Chauvet et al., 2002; Guillaume & Trudel, 2000; Koulen et al., 2002; Y. Li et al., 2005; Shen et al., 2016).

How exactly the loss of functional PC-1 or PC-2 leads to the polycystic phenotype remains to be understood. However, various aspects of the pathophysiology of ADPKD have been characterised, and it is ultimately thought that loss-of-function mutations in either *PKD1* or *PKD2* result in a disruption of polycystin-mediated intracellular calcium homeostasis in tubular epithelial cells. This leads to an increased in adenylyl cyclase activity, resulting in the increased generation of cAMP which, in turn, leads to increased generation of ATP, resulting in increased proliferation and fluid secretion (Belibi et al., 2004; Hanaoka & Guggino, 2000; Pinto et al., 2012). This cyst progenitor will eventually detach from the tubule to form a cyst that will continue to grow and expand, ultimately resulting in patients suffering end stage renal disease (ESRD).

The prognosis of ADPKD is largely dependent on the nature of the mutation, with truncating mutations in *PKD1* being associated with the most severe prognosis and earliest onset of ESRD (55 years). Though there is currently no known cure for ADPKD, patients with frameshifting mutations in *PKD1* can be administered Tolvaptan, an inhibitor of the vasopressin-2 receptor which results in lower levels of cAMP in tubular epithelial cells, impairing cyst expansion (Devuyst & Torres, 2013; Gansevoort et al., 2016; Torres et al., 2012). However, this therapy is only mildly effective and often associated with severe side effects (Watkins et al., 2015), so there is a pressing need to develop other treatments. Non-truncating *PKD1* mutations result in ESRD onset around 68 years of age, while *PKD2* mutations are associated with the mildest phenotype, with ESRD onset at around 79 years of age (Cornec-Le Gall et al., 2013). Both *PKD1* and *PKD2* exhibit marked allelic heterogeneity, with over 2300 variants of *PKD1* having been reported, of which 1225 are considered pathogenic, while *PKD2* has 278 reported variants, of which 196 are pathogenic, according to the ADPKD mutation database (available at

https://pkdb.mayo.edu/variants). Many of these variants are missense, with single amino acid changes seemingly resulting in non-functional protein – however, the functional effects of many of these variants remain to be characterised.

Patient-derived cell lines used to study ADPKD typically arise from type 1 patients with *PKD1* mutations, owing to the fact that these patients are more abundant and ADPKD is often diagnosed earlier. As such, there is less of an opportunity to study the effect of *PKD2* mutations *in vitro*. However, *PKD2* is evolutionarily conserved across both vertebrates and invertebrates, including the fruit fly *Drosophila melanogaster*, whose homolog is known as *almost there* (*amo*) (Watnick et al., 2003). This homolog gets its name from a mutant phenotype wherein sperm homozygous for *amo* loss of function mutations lack Amo on the surface of their tales. Amo-mediated calcium influx is required for the hyperactivation of sperm, resulting in their migration from the sperm storage organ (the spermatheca) to the unfertilised egg; *amo* mutant sperm are therefore unable to enter and fertilise the egg, hence 'almost there' (Gao et al., 2003; Watnick et al., 2003). Amo is also required for the contraction of visceral smooth muscles in larval stages, with mutants taking more time than wild-type controls to clear blue food in pulse chase experiments (Gao et al., 2004). Interestingly, this phenotype is a haploinsufficiency, with loss of a single copy of *amo* still causing a defect, suggesting a role for gene dosage in this phenotype, which is thought to be a factor in ADPKD (Eccles & Stayner, 2014; Sandro Rossetti et al., 2009).

*PKD2* and *amo* share 26% identity at the amino acid level. There are 12 residues associated with pathogenic missense variants in *PKD2*, and interestingly 10 of these are conserved in *amo*, suggesting evolutionary importance of these residues. The functional effect of some of these variants have been characterised, for example the variant $PKD2^{W414G}$ is thought to result in ADPKD due to a loss of ciliary trafficking, while $PKD2^{C331S}$ fails to homotetramerise due to the loss of cysteine residues, preventing effective channel assembly (Cai et al., 2014; Shen et al., 2016). However, the functional effects of other variants remain to be characterised. In this chapter, I aim to exploit the ease of genetic manipulation in *Drosophila* to characterise the functional effect of uncharacterised, pathogenic *PKD2* variants. I will validate the previous published phenotypes implicating *amo* in male fertility and larval smooth muscle contractility using null alleles, in order to establish a suitable genetic background with which to carry out

this functional analysis. I will then exploit the *GAL4-UAS* system to attempt rescue experiments by ubiquitously overexpressing wild-type *amo* and *PKD2*; if *PKD2* is able to rescue *amo* mutant phenotypes, pathogenic variants will be generated and used for further rescue experiments, whereas equivalent mutations will be made on conserved pathogenic residues in *amo* if wild-type *PKD2* is not able to rescue. Male fertility and larval smooth muscle contractility will then be used as functional readouts of these variants, allowing insight into the molecular basis of these pathogenic variants and how they could contribute towards the pathogenesis of ADPKD.

## 3.2 Results

### 3.2.1 *amo* homozygous mutant males are infertile, and infertility can be rescued by ubiquitous overexpression of *amo*

Before characterising the functional effect of pathogenic mis-sense variants of *PKD2* and *amo*, previously reported phenotypes were confirmed using $amo^{1}$ and $amo^{ko67}$, two characterised null alleles of *amo,* in which male infertility and impaired smooth muscle contractility were reported, respectively (Gao et al., 2004; Watnick et al., 2003). $amo^{1}$ contains a premature stop codon in exon 6 resulting in a truncated, non-functional protein, whereas the exact genetic basis of $amo^{ko67}$ has not been clarified: Western blot analysis shows no functional protein present in these mutants, suggesting that it is indeed a null allele (Gao et al., 2004; Watnick et al., 2003). Males homozygous for $amo^{1}$ or $amo^{ko67}$ mutations and wild-type control males were bred with wild-type virgin females for four days, before males and females were removed from the vials, and progeny were then counted two weeks after setting up the experiment. Counting the number of progeny confirmed that both $amo^{1}$ and $amo^{ko67}$ homozygotes are essentially sterile when comparing numbers of *amo* mutants with wild-type controls in the same genetic background, as does placing these alleles in trans to one another (**figure 3.1a**). Furthermore, placing these alleles in trans to *Df(2L)BSC407*, a genetic deficiency deleting ~500kb of chromosome 2L including *amo* also results in a near complete loss of progeny when compared to flies possessing a single copy of functional *amo* (i.e., *Df(2L)BSC407/+*) , suggesting that just one copy of *amo* is required for male fertility in *Drosophila* (**figure 3.1b**).

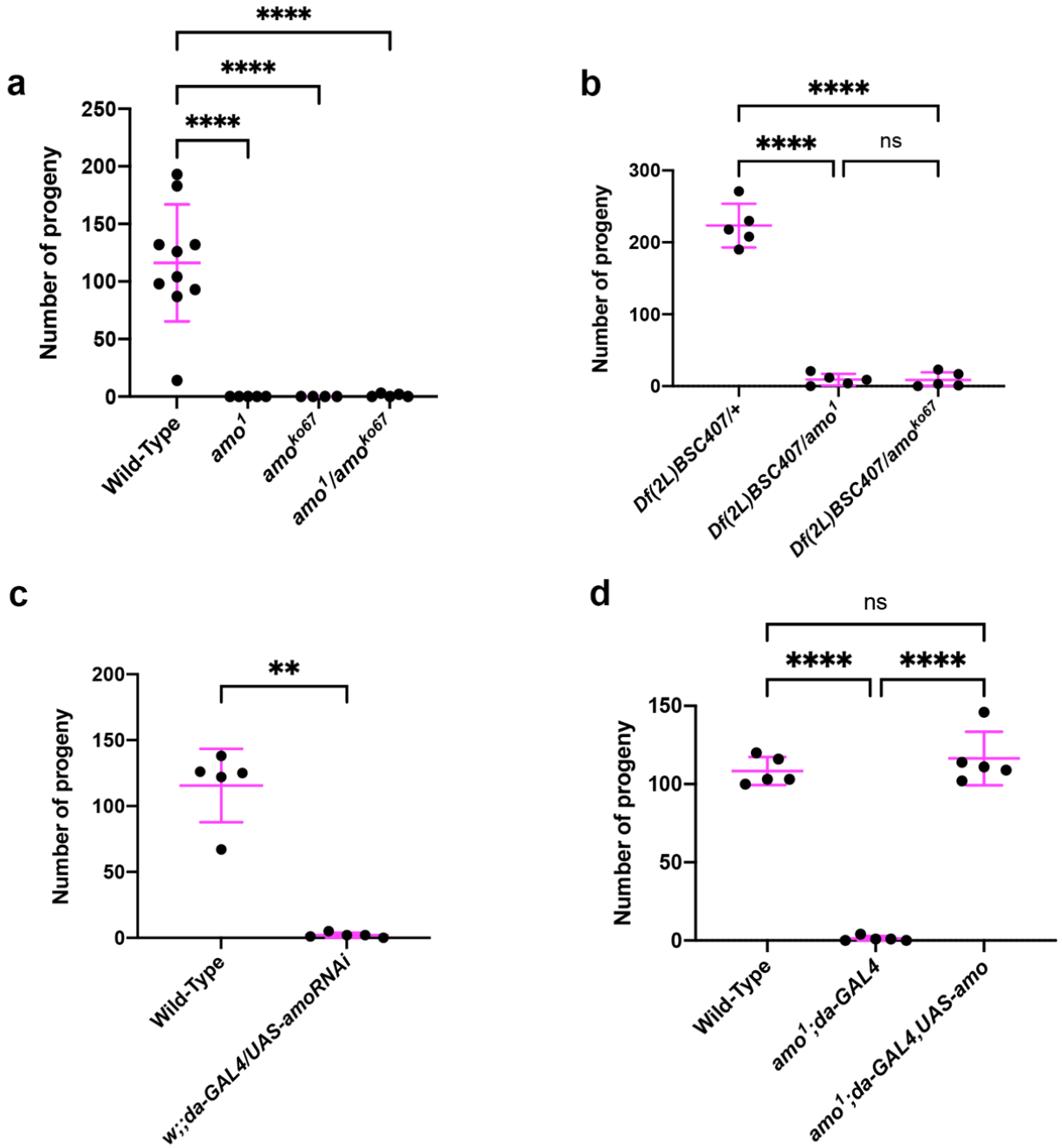


*Figure 3.1 – Amo is required for male fertility in Drosophila*

(a) scatterplot showing number of progeny from wild-type males and *amo* mutant male homozygotes or trans-heterozygotes. (b) scatterplot showing number of progeny from males heterozygous for a genetic deficiency deleting *amo* (*Df(2L)BSC407)* with or without loss-of-function *amo* mutations. (c) scatterplot showing number of progeny from wild-type males and males ubiquitously expressing a hairpin RNA molecule specific to *amo* mRNA. (d) scatterplot showing number of progeny from wild-type males and *amo* mutant males expressing *da-GAL4* with or without *UAS-amo*. All statistical analyses carried out by one-way ANOVA with Holm-Šídák multiple comparisons, apart from (c), which was carried out by a Mann-Whitney test. **p<0.01, ****p<0.0001

RNA interference (RNAi) is another technique which can be used in *Drosophila* to study the effect of gene knockdown, and as such offers an alternative means which to validate these phenotypes as being dependent on *amo* (Heigwer et al., 2018). RNAi-mediated knock-down of *amo* driven by the ubiquitous *GAL4* driver *daughterless* (*da-GAL4/UAS-amo* RNAi) resulted in near complete loss of male fertility in otherwise wild-type flies (**figure 3.1c**), again showing a requirement for *amo* in this process. Furthermore, the fact that *da-GAL4* successfully causes infertility when driving *UAS-amo RNAi* validates this driver as an appropriate tool with which to perform rescue experiments with clinically relevant pathogenic variants of *amo/PKD2* in future experiments.

Consequently, I recombined *da-GAL4* onto the same chromosome as *UAS-amo*, allowing for the ubiquitous expression of wild-type *amo* cDNA in rescue experiments. This recombinant chromosome (*da-GAL4,UAS-amo*) was then crossed into an $amo^{1}$ mutant background, and the fertility of male *amo* homozygous mutants assayed again. It was clearly shown that ubiquitous overexpression of wild-type *amo* completely rescues male infertility in an *amo* mutant background, when compared with $amo^{1}$ mutants expressing *da-GAL4* only. Furthermore, numbers of progeny in the rescue line were comparable to those of wild-type flies (**figure 3.1d**). These data clearly show that $amo^{1}$ can be used as a suitable genetic background with which to characterise the functional effect of pathogenic variants of *amo*, while it will also allow investigation into whether ubiquitous expression of *PKD2* cDNA is capable of rescuing the phenotypes associated with $amo^{1}$.

### 3.2.2 *amo* mutants exhibit impaired smooth muscle contractility

As well as infertility, *amo* mutant *Drosophila* are defective for contractility of the visceral smooth musculature. This phenotype manifests itself upon feeding first instar larvae yeast paste containing a blue dye (bromophenol blue) and checking the clearance of blue food from the hindgut within an hour of transfer to normal, undyed yeast paste (**figure 3.2a**). According to Gao et al., 2004, approximately 10% of $amo^{ko67}$ mutant larvae successfully clear blue food within an hour, as opposed to around 50% of wild-type control larvae, showing a requirement for *amo* in mediating contractility of visceral smooth muscles, at least at this early stage. I therefore sought to investigate whether this phenotype is readily apparent in $amo^{1}$ mutants as

well, with the intention of developing this assay as another tool with which to characterise the functional impact of pathogenic variants of *amo/PKD2*.

Consistent with Gao et al., $amo^{1}$ mutants showed a smaller percentage of excretion positive larvae compared to wild-type controls (figure 3.2b). As with male infertility, this phenotype was successfully rescued via the ubiquitous over-expression of wild-type *amo* using *daughterless-GAL4* (figure 3.2c).

In order to verify that this phenotype is dependent on *amo* functioning as a calcium-permeable cation channel, a genetically-encoded calcium indicator, *UAS-GCaMP6m* (Chen et al., 2013), was recombined with a visceral muscle driver (*24b-GAL4;* Gao et al., 2004). This enabled generation of a calcium reporter specific to visceral smooth muscles. Interestingly, this reporter revealed that *amo* mutants exhibit a decrease in the number of calcium waves propagating down the posterior hindgut relative to wild-type controls (figure 3.2d-e), suggesting that the phenotype is dependent on *amo* functioning as a calcium channel. Calculating the duration of these waves reveals that calcium in *amo* mutant larvae propagates down the smooth musculature surrounding the hindgut at significantly slower speeds than wild type controls, with average times of 6.4 and 5.1 seconds, respectively (figure 3.2f). This suggests that the impaired smooth muscle contractility seen in *amo* mutant larvae may be due to slower rates of peristalsis, due to impaired calcium signalling in the visceral smooth musculature. Furthermore, this previously unreported phenotype could potentially be used as an extra functional readout of missense *amo/PKD2* variants.

### 3.2.3 HA tagged isoforms do not rescue infertility nor smooth muscle contractility

Results in sections 3.2.1-2 show clearly the presence of two phenotypes in $amo^{1}$ mutants, male infertility and larval smooth muscle contractility, both of which can be rescued by the ubiquitous *GAL4-UAS* dependent overexpression of wild-type *amo* cDNA. However, the *UAS-amo* construct used in these rescue experiments was inserted into the genome via P-element-mediated mutagenesis, which inserts transgenic constructs randomly into the genome (Scott Barolo et al., 2004). The ultimate aim of these experiments is to use *Drosophila* as a model with

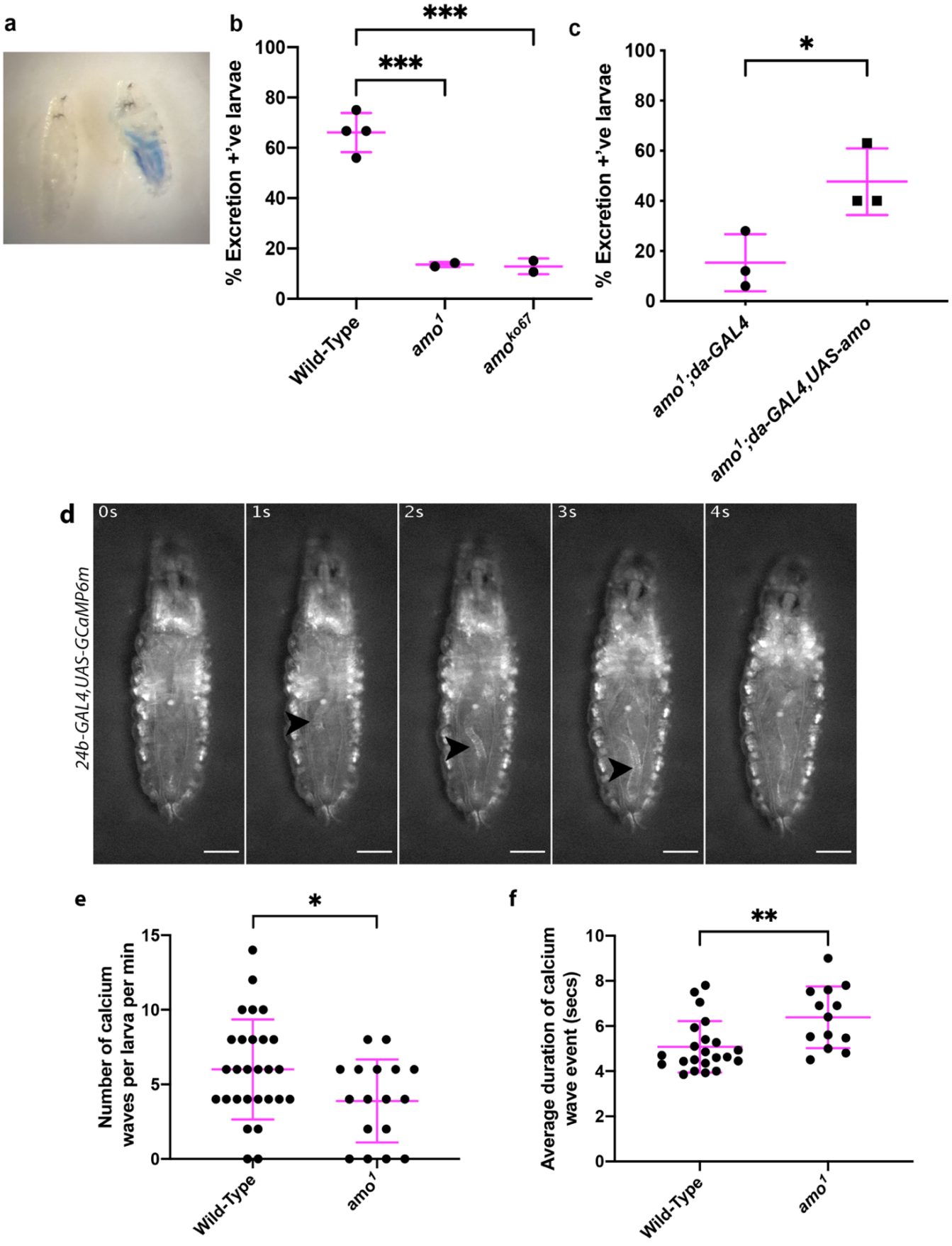
a
b
% Excretion +'ve larvae
100
80
60
40
20
0
***
***
Wild-Type
amo1
amoko67
c
% Excretion +'ve larvae
100
80
60
40
20
0
*
amo1;da-GAL4
amo1;da-GAL4,UAS-amo
d
24b-GAL4,UAS-GCaMP6m
0s
1s
2s
3s
4s
e
Number of calcium waves per larva per min
15
10
5
0
*
Wild-Type
amo1
f
Average duration of calcium wave event (secs)
10
8
6
4
2
0
**
Wild-Type
amo1

*Figure 3.2 – Amo is required for smooth muscle contractility in Drosophila larvae*

(a) example image of excretion-positive (left) and negative (right) first instar larvae. (b) scatterplot showing percentages of excretion positive wild-type and *amo* mutant larvae (***p<0.001). (c) scatterplot showing percentages of excretion-positive *amo* mutant larvae expressing *da-GAL4* with or without *UAS-amo* (p=0.0328). (d) example images of wild-type larva expressing *24b-GAL4,UAS-GCaMP6m* taken from a timelapse movie (images cover 4 seconds of the movie). Note the fluorescent signal (GCaMP6m imaged in the GFP channel) propagating down the hindgut, indicative of intracellular calcium as indicated by arrowheads. (e-f) Scatterplot showing number of calcium waves per larva per minute (e) and average duration of calcium waves (f) between wild-type and *amo* mutants (*n*=28 and 17, p=0.0345 (e) and p=0.0029). Statistical analyses in (b) carried out by one way ANOVA with Holm-Šídák multiple comparisons, (c and e) were carried out by Student's unpaired t-tests and (f) was carried out via Mann-Whitney test. *p<0.05, **p<0.01, ***p<0.001

which to screen the functional effect of missense *PKD2* variants. In order to do this, wild-type controls and the missense variants would need to be inserted into a specific site within the genome in order to negate any insertion site-specific effects which might affect expression levels from different constructs; as such, the use of this P-element insertion is not appropriate for these experiments. Wild-type *amo* and *PKD2* cDNAs were therefore cloned into the *Drosophila* expression vector pUASTattB, which contains an *attB* site, allowing for site-specific insertion into the genome via PhiC31 integrase in the *attP2* site on chromosome 3. An HA tag at the 5' end of each cDNA was included, allowing transgenic expression to be verified by means of immunostaining.

Following transgenesis, male flies containing *UAS-HA:amo* or *UAS-HA:PKD* were crossed to virgin females containing ubiquitous driver *daughterless-GAL4* (*da-GAL4*). When ubiquitously expressed in the embryo via *da-GAL4*, *UAS-HA:PKD2* clearly showed extensive staining compared to wild-type controls that were immunostained in parallel, suggesting that it expresses well when driven by this *GAL4* driver. However, no such staining was observed when *UAS-HA:amo* was expressed via *da-GAL4,* suggesting that this may not be expressing correctly (figure 3.3a).

3 independent *UAS-HA:amo* and *UAS-HA:PKD2* lines generated from separate transgenesis events were used. Lines were then crossed into $amo^{1}$ mutants, in trans to *daughterless-GAL4* in order to try and rescue male infertility. Again, single males were mated with wild-type virgin

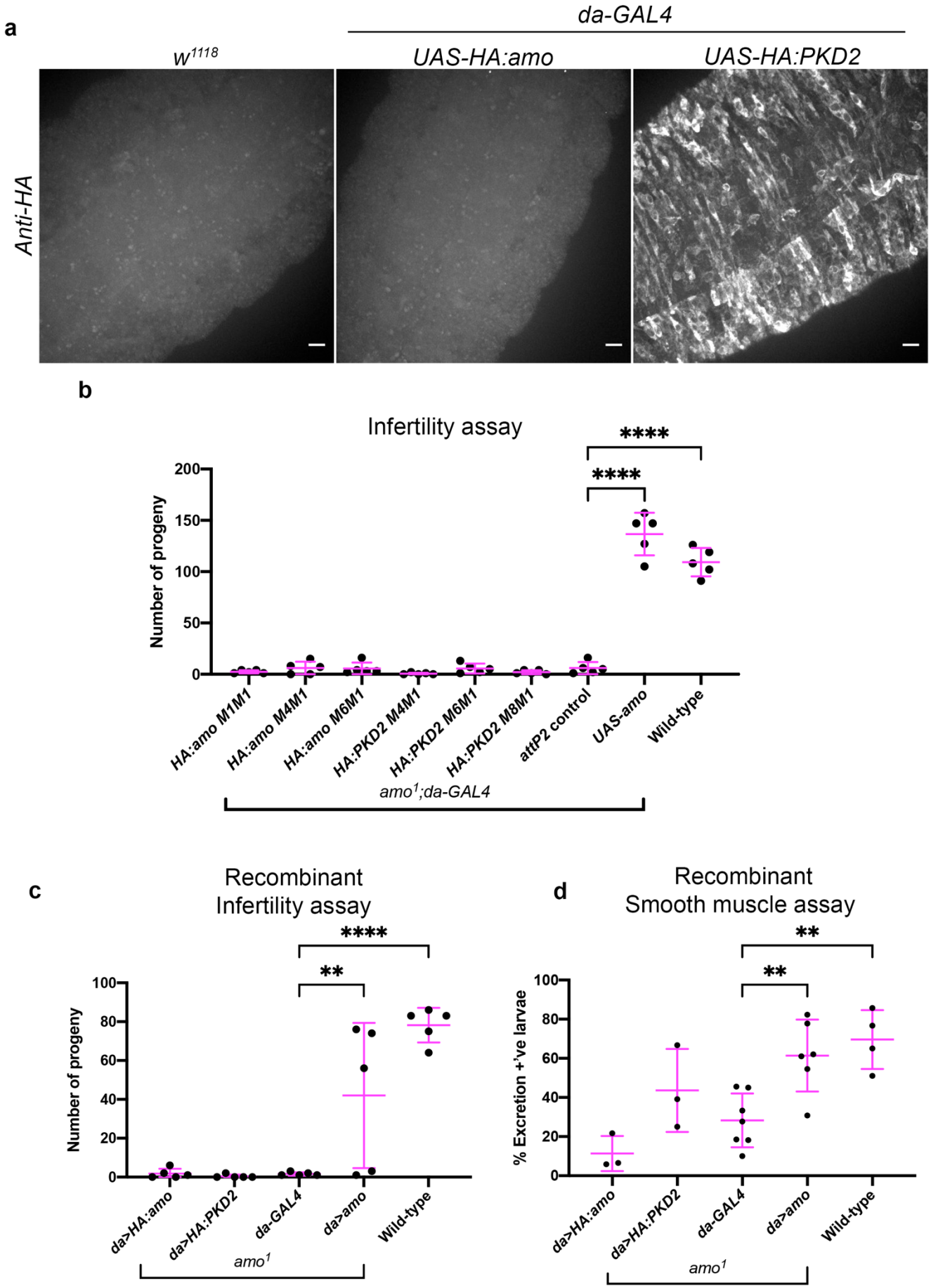
a
da-GAL4
w1118
UAS-HA:amo
UAS-HA:PKD2
Anti-HA
b
Infertility assay
****
****
Number of progeny
200
150
100
50
0
HA:amo M1M1
HA:amo M4M1
HA:amo M6M1
HA:PKD2 M4M1
HA:PKD2 M6M1
HA:PKD2 M8M1
attP2 control
UAS-amo
Wild-type
amo1;da-GAL4
c
Recombinant
Infertility assay
****
**
Number of progeny
100
80
60
40
20
0
da>HA:amo
da>HA:PKD2
da-GAL4
da>amo
Wild-type
amo1
d
Recombinant
Smooth muscle assay
**
**
% Excretion +'ve larvae
100
80
60
40
20
0
da>HA:amo
da>HA:PKD2
da-GAL4
da>amo
Wild-type
amo1

*Figure 3.3 – HA-tagged amo and PKD2 do not rescue male infertility or smooth muscle contractility in amo mutants*

(a) representative maximum projections of anti-HA stained stage 15 embryos. Scale bars indicative of 10µm. (b) scatterplot showing number of progeny from wild-type and *amo* mutant males expressing a single copy of HA tagged *amo* or *PKD2* driven by a single copy of *da-GAL4*. (c) scatterplot showing number of progeny from wild-type and *amo* mutant males expressing two copies of both *da-GAL4* and HA tagged *amo* or *PKD2*. (d) scatterplot showing percentage of excretion positive wild-type and *amo* mutant larvae expressing two copies of both *da-GAL4* and HA tagged *amo* or *PKD2*. All statistical analyses carried out by one way ANOVA with Holm-Šídák multiple comparisons, and only significant different differences between groups are shown on graphs. **p<0.01, ****p<0.0001

females for 4 days before being removed from the vials and progeny then counted after 14 days. Consistent with the lack of detectable expression by HA immunostaining, *UAS-HA:amo* did not rescue male infertility. *UAS-HA:PKD2* also failed to rescue male infertility, despite expressing at apparently high levels based on immunostaining (figure 3.3b). In case the lack of rescue seen in these experiments (as well as the lack of staining seen for *UAS-HA:amo*) was due to a gene dosage effect, *da-GAL4* and *UAS-HA:amo/PKD2* were recombined together on the same chromosome, which enables two copies of both the driver and the rescue construct to be present within the same fly. Again however, neither *HA:amo* or *HA:PKD2* were able to rescue male infertility even with this higher gene dosage (figure 3.3c).

Smooth muscle contractility was also assayed in the presence of two copies of driver and rescue construct in $amo^{1}$ mutant larvae, and similarly to male infertility, neither *HA:amo* or *HA:PKD2* resulted in an increased percentage of excretion-positive larvae (figure 3.3d). These data suggest that *HA:amo* either is not expressed at sufficiently high levels for detection or rescue of function, or that the presence of an N-terminal HA tag results in a non-functional protein, while *HA:PKD2*, which does seem to be expressed based on immunostaining, does not appear to function effectively in *Drosophilla.*

### 3.2.4 Non-HA tagged isoforms of *amo* and *PKD2* do not rescue infertility nor smooth muscle contractility

Overexpression of HA-tagged versions of both *amo* and *PKD2* failed to rescue *amo* mutant phenotypes in *Drosophila*. In case the presence of an N-terminal HA tag was affecting the

translation, localisation and/or folding of the proteins, cDNAs lacking epitope tags were cloned into pUASTattB, allowing the generation of *UAS-amo* and *UAS-PKD2* in the *attP2* site on chromosome 3. As with the HA-tagged rescue constructs, transgenes from 3 independent transgenesis events were crossed into an $amo^{1}$ background, and homozygous mutant males were selected possessing either *UAS-amo* or *UAS-PKD2* together with *da-GAL4* to rescue infertility.

Again, neither *UAS-amo* nor *UAS-PKD2* were able to rescue male infertility when a single copy of either was expressed using a single copy of *da*-GAL4 (figure 3.4a). This suggests that these novel *UAS-amo/PKD2* transgenes either do not express at all, or do not express at sufficient levels to rescue the mutant phenotypes when a single copy is expressed via a single copy of *da-GAL4*. For *UAS-PKD2* however, it is possible that this expresses well (as it did so in the presence of an N-terminal HA tag), and it simply has functionally diverged from *amo* sufficient to no longer function effectively in *Drosophila*.

In order to investigate whether expression of a single copy of non-HA tagged *amo* or *PKD2* cDNA does not express sufficiently to rescue loss of *amo*, *UAS-amo* and *UAS-PKD2* were recombined with *da-GAL4*. This enabled two copies of both the *GAL4* driver and the *UAS-amo/PKD2* cDNAs to be expressed. Again however, neither male infertility (figure 3.4b) nor smooth muscle contractility (figure 3.4c) were rescued when two copies of both driver and transgene were expressed. This suggests that *UAS-amo* is likely not expressing correctly in this insertion site (*attP2*), while *UAS-PKD2* may be expressing without rescuing.

The above results show conclusively that the *UAS-amo* and *UAS-PKD2* transgenes (with or without an N-terminal HA-tag) generated for this study sadly do not rescue previously characterised *amo* mutant phenotypes. As such, clinically relevant pathogenic mutations were unable to be expressed in this system, owing to a lack of a positive control, and this side of my project was finished here.

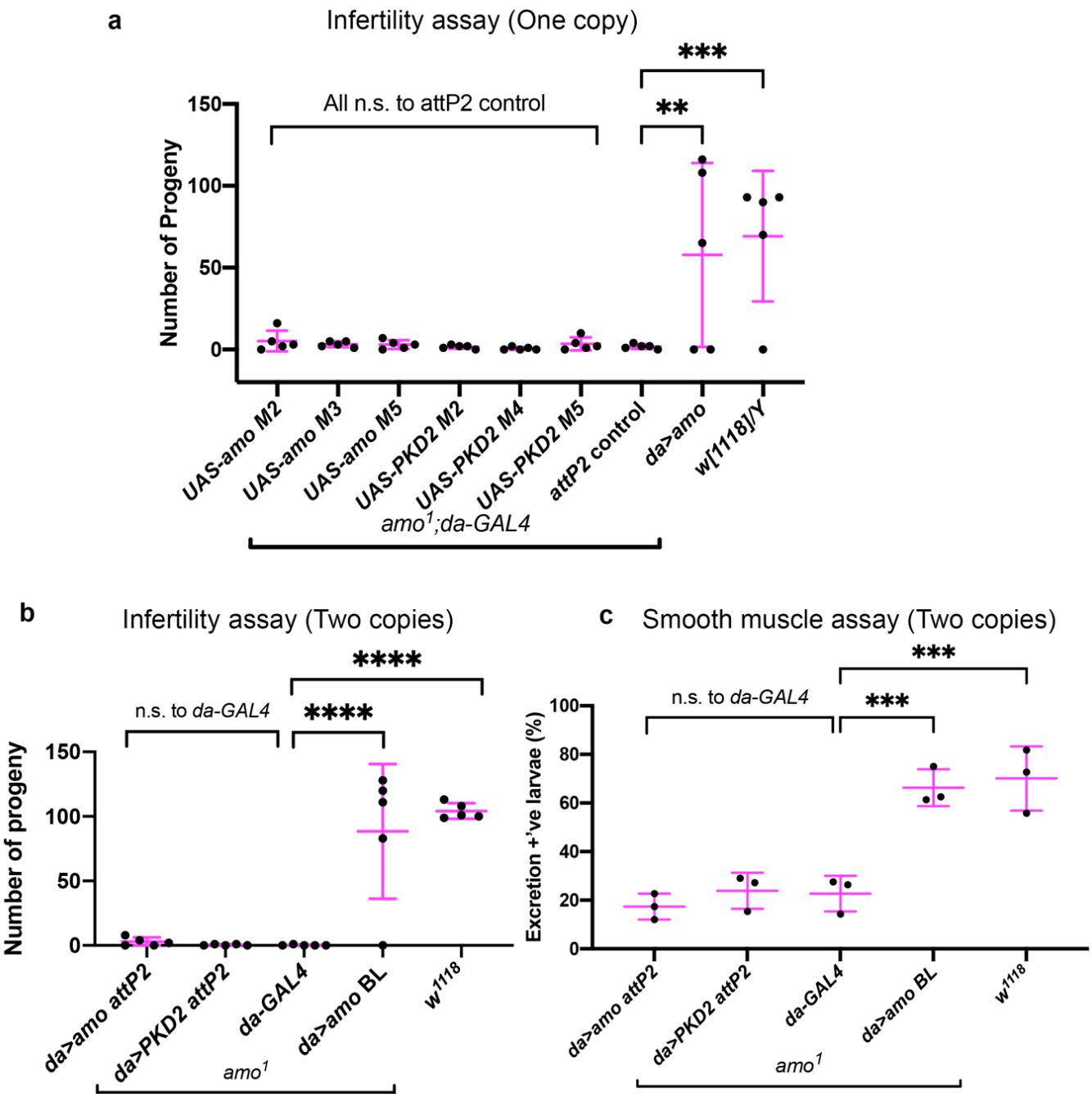


*Figure 3.4 – Non-HA-tagged amo and PKD2 do not rescue male infertility or smooth muscle contractility in amo mutants*

(a) scatterplot showing number of progeny from wild-type and *amo* mutant males expressing a single copy of *amo* or *PKD2* cDNA driven by a single copy of *da-GAL4*. *da>amo* BL represents *da>amo* generated from the P-element generated *UAS-amo* transgene obtained from Bloomington. (b) scatterplot showing number of progeny from wild-type and *amo* mutant males expressing two copies of both *da-GAL4* and *amo* or *PKD2* cDNA. (c) Scatterplot showing percentage of excretion positive wild-type and *amo* mutant larvae expressing two copies of *da-GAL4* and *amo* or *PKD2* cDNA. All statistical analyses carried out by one way ANOVA with Holm-Šídák multiple comparisons. **p<0.01, ***p<.001, ****p<0.0001

## 3.3 Discussion

The major aim of the work carried out in this chapter was to exploit *Drosophila* to develop a model with which to screen pathogenic missense variants of *PKD2* in order to characterise the functional effects of these mutations, an approach which has been exploited for other genetic diseases (Link & Bellen, 2020). Phenotypes previously reported in *amo* mutants, namely male infertility and defective larval smooth muscle contractility, were confirmed using the null allele $amo^{1}$, and these phenotypes were shown to be rescued via the overexpression of wild-type *amo* via the *GAL4-UAS* system, crucially showing that these phenotypes were indeed due to loss of functional *amo* (Gao et al., 2004; Watnick et al., 2003). Furthermore, these results also validate the use of $amo^{1}$, a nonsense variant of *amo*, as a suitable genetic background with which to characterise the functional effect of pathogenic *PKD2* variants, again by use of the *GAL4-UAS* system, with male infertility and larval smooth muscle contractility acting as readouts of *amo/PKD2* function.

cDNAs of both *amo* and *PKD2* containing an HA tag at the 5' end (which would express at the N-terminal of the translated protein) were cloned into the vector pUASTattB, containing 5 copies of *UAS* upstream of the multiple cloning site allowing expression under control of *GAL4*. Crucially, this vector contains an *attB* site, allowing for site specific insertion into the genome, negating any site-specific effects of random insertion caused by P-elements (Bateman et al., 2006). However, staining for the presence of the HA tag seemed to suggest expression of only *PKD2* and not *amo,* when driven by the ubiquitous driver *daughterless-GAL4*, which has previously been shown to rescue both infertility and smooth muscle contractility in *amo* mutants when expressing *UAS-amo* (**figure 3.1-3.2**).

Overexpression of both *HA-amo* and *HA-PKD2* was not sufficient to rescue either male infertility or visceral smooth muscle contractility in $amo^{1}$ mutants. One can assume *HA-PKD2* is expressing at reasonably high levels when driven by *daughterless*, based on the ubiquitous staining seen in **figure 3.3a**. This suggests that in the millions of years since humans and *Drosophila* shared a common ancestor, *PKD2* and *amo* have functionally diverged to such an extent that *PKD2* is unable to compensate for a lack of *amo* in *Drosophila*. Alternatively, the HA tag could result in the protein not localising effectively to where it is needed, although this

is unlikely due to the fact that expression of non-HA tagged *PKD2* also fails to rescue phenotypes associated with loss of *amo*. Furthermore, HA tagged *PKD2* has been shown to express correctly both *in vivo* and *in vitro* (Streets et al., 2013).

Why *UAS-amo,* with or without an N-terminal HA tag, fails to rescue, or indeed express, remains something of a mystery. Sequence analysis shows the *amo* cDNA is entirely as expected, and indeed is the same cDNA as the P-element inserted *UAS-amo* (BL58407) which results show is capable of completely rescuing *amo* mutant phenotypes (figure 3.1-3.2). The N-terminal region of PC-2 contains a domain that is required for the effective oligomerisation of PC-2 subunits into a functional, calcium-permeable homotetramer (Feng et al., 2008). It is possible that the N-terminal HA tag is disrupting correct assembly of Amo, although this remains unlikely given that PC-2 appears to be assembled correctly in the presence of this N-terminal HA tag. Furthermore, the fact that the *UAS-amo* generated for these experiments failed to rescue even in the absence of an N-terminal HA tag suggests that this is improbable.

All transgenic constructs made were inserted into the *attP2* site on chromosome 3L; this site and the vectors used during the cloning procedure have both been used for transgenesis many times (including by our own lab) and there is nothing to suggest that it is less transcriptionally active than other frequently-used landing sites (Coates et al., 2021; Knapp et al., 2015; Pfeiffer et al., 2010). As such, it is unlikely the failures in rescue are due to site-specific effects of this locus. Though other insertion sites were not looked at in this study, it would undoubtedly be of interest to see whether *UAS-amo* in another site would be able to rescue *amo* mutant phenotypes. If one was to successfully generate a rescue construct in a specific site, *Drosophila* it will allow the functional impact of clinically relevant mutations to easily be characterised, through assaying male infertility and smooth muscle contractility.

An alternate strategy could be to manipulate the endogenous *amo* locus via CRISPR/Cas9, an approach which has been used in *Drosophila* to mutagenise endogenous loci (Levi et al., 2020). Such a strategy would easily allow pathogenic point mutations to be introduced and their functional effects investigated. Similarly, the pre-existing P-element construct of *UAS-amo* could also be mutagenised via this approach. Though the insertion site of this transgene has

not been mapped, it would be possible to do so via inverse PCR (Huang et al., 2009), which would allow suitable guides to be designed for CRISPR/Cas9-mediated mutagenesis.

Though most of the data presented in this chapter are either negative or replicating previously published data, a novel phenotype was reported when looking at calcium in the visceral musculature of *amo* mutant larvae. Previously published data showed that Amo is required for visceral smooth muscle contractility in first instar larvae, without revealing what could be happening at the cellular level (Gao et al., 2004). Here, I have shown that *amo* mutants seem to have fewer calcium waves propagating down visceral muscles surrounding the hindgut, which is potentially responsible for the contractility defect. Furthermore, the length of time taken for calcium waves to propagate down the hindgut was significantly increased in *amo* mutants relative to controls.

It has previously been reported that vascular smooth muscle cells from mice heterozygous for *Pkd2* mutations have lower levels of intracellular calcium (Qian et al., 2003). It is therefore possible and indeed likely that the smooth muscle cells surrounding the hindgut of *amo* mutants also possess decreased levels of intracellular calcium, resulting in the decreased number of calcium waves seen in *amo* mutants. Calcium is required in smooth muscle cells for the activation of the enzyme myosin light chain kinase (MLCK) by calmodulin, which ultimately results in contraction of myosin fibres (Mizuno et al., 2008). The calcium required for this comes from the sarcoplasmic reticulum (SR), a specialised store of calcium found in muscle cells, as well as extracellularly (Rossi & Dirksen, 2006). Release of calcium from the SR is known to be largely dependent on RyR and IP3R; these channels release calcium from the SR in response to extracellular calcium entry in a process known as calcium-induced calcium release (CICR) (Collier et al., 2000). Interestingly, the calcium permeability of both RyR and IP3R has been shown to be modulated by Polycystin-2 (Anyatonwu et al., 2007; Y. Li et al., 2005). It is possible therefore that the decreased rates of calcium waves propagating down the larval hindgut may be due to slower CICR from the SR as a result of loss of Amo-mediated modulation of RyR and IP3R. This could explain how these waves not only seem to fire less, but also appear to propagate more slowly down the hindgut, as calcium levels may be sufficient to induce GCaMP fluorescence, which may persist for longer, without being sufficient to induce efficient contraction. Any site-specific rescue construct of *amo* or *PKD2* generated in the future that are

capable of rescuing smooth muscle contractility, could exploit this novel finding to offer an exciting alternative readout for the functional effect of missense variants.

In summary, these results validated the use of *amo*$^{1}$ as a suitable genetic background with which to carry out a functional screen of pathogenic *amo* / *PKD2* variants. It seems that *HA:PKD2*, which expressed at reasonable levels, was unable to rescue any phenotypes associated with loss of *amo.* Unfortunately, however, in these experiments *amo* was unable to be expressed with or without an HA tag when inserted into *attP2*, at least not to sufficient levels to rescue either male infertility or larval smooth muscle contractility. Any work going forward should therefore focus primarily on generating a site-specific *UAS-amo* rescue construct, before introducing equivalent pathogenic mutations at conserved residues of *amo*.

# Chapter 4: Investigating the role of *amo/PKD2* in efferocytosis and immune cell function

## 4.1 Introduction

Autosomal Dominant Polycystic Kidney Disease (ADPKD) is the most common inherited nephropathy, affecting somewhere between 1 in 400 and 1 in 1000 individuals worldwide, accounting for over 12 million patients (Iglesias et al., 1983; Leuenroth & Crews, 2009). The disease is known to be caused by loss-of-function mutations in either of the genes *PKD1* or *PKD2*, encoding Polycystin-1 (PC-1) and PC-2 respectively (Hughes et al., 1995; Peters et al., 1993). The function of PC-1 is relatively poorly understood, due in part to the protein's size and complexity, with numerous functional domains and repeats, although it is known to localise to primary cilia and the plasma membrane, and its expression peaks during developmental stages (Chauvet et al., 2002; Geng et al., 1996). PC-2 however is a member of the Transient Receptor Potential (TRP) family of ion channels, and functions as a non-selective, calcium-permeable cation channel. It localises to the endoplasmic reticulum (ER) and plasma membrane, where it remains constitutively expressed throughout life and plays and important role in the maintenance of intracellular calcium homeostasis, the deregulation of which is ultimately thought to be the major cause of ADPKD (Foggensteiner et al., 2000; Koulen et al., 2002; Mochizuki et al., 1996).

Though the exact mechanisms driving cystogenesis remain poorly understood, ADPKD is undoubtedly driven by the uncontrolled proliferation of tubular epithelial cells. The dysregulation of intracellular calcium signalling, due to loss of function mutations in *PKD1* or *PKD2*, leads to an upregulation of cAMP, ultimately driving proliferation and fluid secretion (Hanaoka & Guggino, 2000). There is also evidence implicating innate immune cells in driving pathogenesis of the polycystic phenotype, namely macrophages (Cassini et al., 2018; Swenson-

Fields et al., 2013). Infiltration of macrophages into the early cyst is known to drive cyst expansion and is directly associated with cyst progression; expression of monocyte chemoattractant protein-1 (MCP-1) in early cysts leads to an initial influx of pro-inflammatory, 'M1-like' macrophages. Following initial infiltration into the nascent cyst, macrophages then shift towards a pro-healing, 'M2-like' activation state, and this behavioural shift drives cyst expansion by driving proliferation in cyst lining cells (Cassini et al., 2018; Karihaloo, 2015; Karihaloo et al., 2011). In this mouse model system, knockout of MCP-1 reduced cyst expansion and improved renal function, showing clearly the important role of both pro- and anti-inflammatory macrophages in the pathogenesis of the polycystic kidney. A separate study looking at both ADPKD and the more severe ARPKD showed that renal epithelial cells isolated from cystic kidneys are capable of polarising naïve BMDMs into a distinct M2-like phenotype, resulting in increased growth and proliferation of cystic cells (Swenson-Fields et al., 2013).

A major function of M2-like macrophages is the phagocytic removal of apoptotic cells as part of a process known as efferocytosis. During efferocytosis, dying cells release chemoattractant 'find me' cues, which are recognised by macrophages and cause their migration towards the site of the dying cell. 'Eat me' cues expressed on the surface of apoptotic cells, such as PS, are then recognised by receptors on the cell surface of phagocytes, initiating phagocytosis. Crucially, efferocytosis is an immunologically silent process, with no inflammatory response initiated; failures in this process however, result in cells undergoing secondary necrosis, wherein the plasma membrane of uncleared apoptotic cells ruptures and releases cytotoxic, pro-inflammatory signals (Silva et al., 2008). The importance of this process is shown by the fact that numerous chronic inflammatory diseases are associated with failures in efferocytosis, such as chronic obstructive pulmonary disease (COPD), atherosclerosis and systemic lupus erythematosus (SLE) (Hodge et al., 2003; Kojima et al., 2017; Abdolmaleki et al., 2018). The polycystic kidney itself is a highly inflamed environment, and the fact that failures in efferocytosis are associated with inflammatory disease hints at the involvement of this process in driving pathogenesis of the disease.

The fruit fly *Drosophila melanogaster* has been used as a model organism for over a century, and so far, 6 Nobel prizes have been awarded to scientific findings exploiting this model. The fact that 75% of all human disease genes are conserved as homologs in *Drosophila* has made

it a commonly used model for various cellular processes and pathologies, including cancer, neurodegenerative disease and metabolic disorders (Halder & Mills, 2011; Lu & Vogel, 2009; Musselman & Kühnlein, 2018). Though much of the research studying efferocytosis has been carried out using *ex vivo* or *in vitro* mammalian models, in the past few decades there has been an increasing amount of research exploiting *Drosophila* to study this process *in vivo* (Wood & Martin, 2017; Zheng et al., 2017).

*Drosophila* contain a population of blood cells called hemocytes, which are divided into 3 lineages: plasmatocytes, crystal cells and lamellocytes. Crystal cells functionally resemble a cross between vertebrate platelets and mast cells, playing an active role in post-wound melanisation, while lamellocytes differentiate in response to parasitism (Wood & Jacinto, 2007). Plasmatocytes, which dominate the hemocytes at around 95% of the overall population, represent the functional equivalent of the vertebrate macrophage. They are highly phagocytic and responsive to both wounding and infection, while they are also highly migratory, secrete extracellular matrix (ECM) and are involved in tissue shaping and remodelling during development of the fly (Wood & Jacinto, 2007; Wood & Martin, 2017). Critically, plasmatocytes are highly effective at mediating efferocytosis, with embryonic plasmatocytes in particular being used to characterise efferocytosis in an *in vivo* system, and the imaging capabilities of the embryo allowing interactions between plasmatocytes and apoptotic cells to be dissected (Roddie et al., 2019; Tardy et al., 2021).

Recent papers have shown that increased numbers of uncleared apoptotic cells, for example due to mutations in the phosphatidylserine (PS) receptor *six microns under* (*simu*), impair other important functions of embryonic macrophages, such as their dispersal, migration and ability to respond to sites of sterile wounding (Roddie et al., 2019; Armitage et al., 2020). It is thought that uncleared apoptotic cells retain plasmatocytes, hereafter referred to as macrophages, in the anterior of the embryo, where the first hematopoietic wave occurs, resulting in the presence of fewer macrophages on the ventral midline (VML) at stage 15. This is potentially caused by the release of 'find me' cues from uncleared apoptotic corpses, which are also thought to 'distract' macrophages on the VML of *Drosophila* embryos, disrupting their basal random migration, resulting in the slower migration speeds seen in *simu* mutants (Roddie et al., 2019). This is also thought to explain the impaired ability of macrophages to respond to

sites of sterile wounding, suggesting that macrophages prioritise signals from apoptotic cells over inflammatory cues from sites of wounding. This is echoed by the fact that overexposure of the EGFR ligand *sSpitz*$^{cs}$, a putative 'find me' cue, dampens wound response, decreases random migration speeds and vacuolation of macrophages on the VML (Tardy et al., 2021).

Efferocytosis can also be impaired by the disruption of calcium signalling, which may in turn perturb macrophage function in ways akin to *simu* mutants. For example, the *Drosophila* junctophilin protein Undertaker (Uta) links ER calcium release channels with the plasma membrane during Draper/Simu-mediated efferocytosis, facilitating effective calcium homeostasis downstream of phagocytosis (Cuttell et al., 2008). *uta* mutants therefore fail to efficiently phagocytose apoptotic corpses, which persist in the organism. It can therefore be speculated that the increased presence of uncleared corpses due to calcium signalling failures would perturb macrophage migration and dispersal in similar ways as loss of *simu*. Calcium is also known to be required for cellular migration, independent of phagocytosis. Extracellular calcium influxes are essential for the effective formation of actin filaments at the leading edge of migrating macrophages (Evans & Falke, 2007), while lysosomal calcium is known to be required for both effective macrophage migration and phagocytic processing in *Drosophila* macrophages (Edwards-Jorquera et al., 2020).

The *Drosophila PKD2* homolog *almost there* (*amo*) has been shown to be required for efferocytosis, with a 50% reduction in the phagocytic index of *amo* mutant macrophages reported, relative to wild type controls (Van Goethem et al., 2012). It is proposed that Amo functions downstream of Simu, where it is required for the maintenance of calcium homeostasis downstream of phagocytosis. If Amo and Simu function in the same pathway, it would be possible that *amo* mutant macrophages exhibit similar phenotypes in terms of their dispersal, migration and wound responsiveness. As well as *amo* in *Drosophila* macrophages, human *PKD2* has been implicated in immune cell function. Magistroni et al. investigated *ex vivo* T lymphocytes derived from type 2 ADPKD patients, and found these cells exhibited aberrant migration speeds, significantly lower levels of ER calcium release in response to ATP stimulation whilst also forming aggregates significantly larger than those formed by control cells (Magistroni et al., 2019). These aggregates were also shown to express significantly greater

levels of inflammatory chemokines including macrophage migration inhibitory factor (MIF), which is known to drive cyst growth in ADPKD (Chen et al., 2015).

The above shows clearly how efferocytosis and calcium signalling are important for the regulation and behaviour of immune cells, while immune cells themselves have been implicated in the progression of ADPKD in multiple studies (Cassini et al., 2018; Chen et al., 2015; Swenson-Fields et al., 2013). The fact that failures in efferocytosis are associated with numerous chronic inflammatory conditions, together with the inflamed nature of the polycystic kidney and the requirement of *amo* and *PKD2* in immune cells in both *Drosophila* and humans suggests that efferocytosis is an attractive candidate pathway to investigate with respect to ADPKD pathogenesis.

Here I test the hypothesis that defective *amo*-mediated efferocytosis disrupts macrophage function in *Drosophila*, which could implicate this process in the pathogenesis of ADPKD. I exploit the imaging capabilities of embryonic *Drosophila* macrophages to enable the characterisation of the effects of *amo* on immune cell behaviour *in vivo*, while using kidney epithelial cells lacking functional *PKD2* to investigate efferocytosis in a mammalian system *in vitro*.

## 4.2 Results

### 4.2.1 *amo*$^{1}$ mutant macrophages exhibit impaired dispersal and migration speeds relative to controls

*Drosophila* macrophages originate in the developing head around stage 10, before following stereotyped migrations routes resulting in their dispersal across the entire embryo by stage 15. One such dispersal route sees macrophages migrating down the ventral midline (VML) during the development of the ventral nerve cord (VNC) from stage 13 of development (Evans et al., 2010; Roddie et al., 2019). Following stage 13, the VNC has fully developed and macrophages then migrate laterally to form a distinctive '3 line' pattern by stage 15, after which they undergo 'random migration' around the VML.

The presence of uncleared apoptotic cells is thought to retain macrophages in the developing head, resulting a delay in their migration down the VML by stage 15. Furthermore, uncleared apoptotic cells are also known to affect the random migration of macrophages on the VML at stage 15 (Roddie et al., 2019). *amo* mutant macrophages in the head of stage 12 embryos have been reported to exhibit a 50% decrease in PI relative to wild-type controls (Van Goethem et al., 2012). It is likely therefore that this would result in a build-up of uncleared apoptotic cells, which could prevent effective macrophage dispersal across the embryo. To test if *amo* mutants exhibit a dispersal phenotype, a null allele of *amo* was used ($amo^{1}$) which contains a premature stop codon, and stage 13 embryos of both control and $amo^{1}$ mutant embryos were imaged until they reached stage 15. Macrophages on the VML of both were then counted, while macrophage random migration speeds at stage 15 were also calculated (**figure 4.1a-b**).

Significantly fewer macrophages were counted on the VML following stage 13 in $amo^{1}$ mutants compared to controls (**figure 4.1c**), consistent with retention of macrophages within the head preventing dispersal, possibly due to the presence of uncleared apoptotic cells. Furthermore, random migration speeds of stage 15 macrophages were also significantly reduced in $amo^{1}$ embryos (**figure 4.1d-f**), and again there were fewer macrophages on the VML of $amo^{1}$ embryos (**figure 4.1g**). The fact that both dispersal and migration of embryonic macrophages are impaired in $amo^{1}$ mutants suggests that defective efferocytosis due to *amo* mutations affects macrophage function beyond simply their ability to phagocytose apoptotic corpses.

### 4.2.2 Genetic removal of apoptosis rescues macrophage dispersal and migration speeds

Previous studies have shown that impaired macrophage migration due to defective efferocytosis, or rather the presence of uncleared apoptotic cells, can be rescued by the removal of apoptosis (Roddie et al., 2019). *Df(3L)H99*, hereafter referred to as *H99*, is a genetic deficiency that removes, among others, 3 key pro-apoptotic genes - *grim, reaper* and *hid* (White et al., 1994). Embryos homozygous for this deficiency therefore lack apoptosis, developing to stage 17 but failing to hatch as first instar larvae. *H99* therefore represents a useful tool with which to study how failures in the apoptotic machinery disrupt macrophage

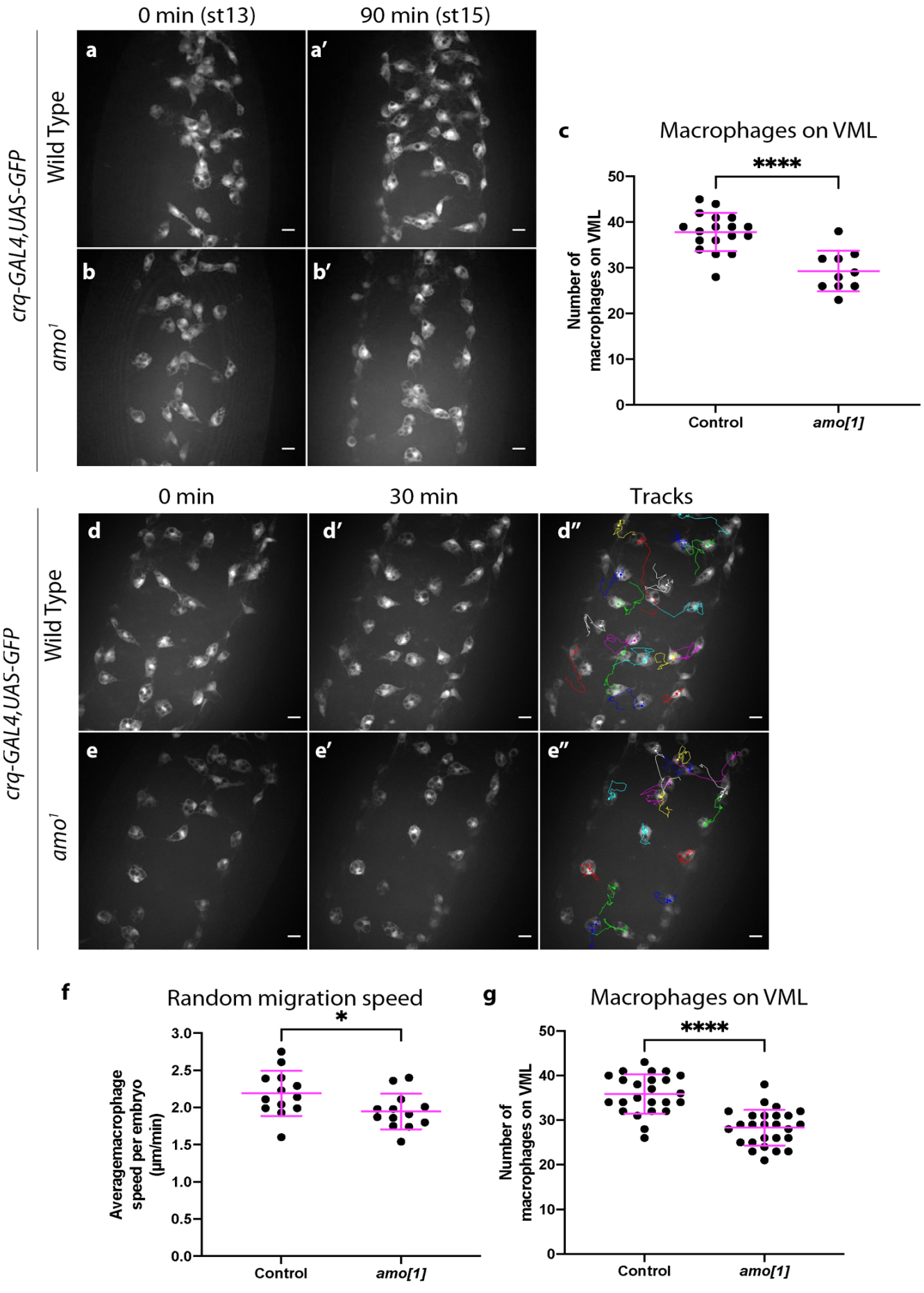
0 min (st13)
90 min (st15)
crq-GAL4,UAS-GFP
Wild Type
amo1
a
a′
b
b′
c
Macrophages on VML
****
Number of macrophages on VML
50
40
30
20
10
0
Control
amo[1]
0 min
30 min
Tracks
d
d′
d″
e
e′
e″
f
Random migration speed
*
Averagemacrophage speed per embryo (µm/min)
3.0
2.5
2.0
1.5
1.0
0.5
0.0
Control
amo[1]
g
Macrophages on VML
****
Number of macrophages on VML
50
40
30
20
10
0
Control
amo[1]

*Figure 4.1 – amo mutant macrophages exhibit impaired dispersal and migration speeds*

(a-b) representative images of the ventral midline of control and *amo*$^{1}$ embryos at stage 13 (a-b) and 90-minutes later at stage 15 (a'-b'). Scale bars denote 10µm. (c) scatterplot showing number of macrophages present on the ventral midline after 90 minutes in control and *amo*$^{1}$ embryos (*n*=10 and 18 respectively, p<0.0001). (d-e) representative images of the ventral midline of wild-type and *amo*$^{1}$ embryos at stage 15, shown 30 minutes later in (d'-e'). (d"-e") Tracks of macrophages over a 30-minute period. Scale bars denote 10µm. (f) Scatterplot showing average migration speed per macrophage, per embryo between control and *amo*$^{1}$ embryos (*n*=13 and 13, p=0.0332). (g) scatterplot showing number of macrophages present on the ventral midline at stage 15 of control and *amo*$^{1}$ embryos (*n*=24 and 26 respectively, p<0.0001). Anterior is up in all images, all statistical comparisons carried out via non-paired t-tests.

function. The removal of apoptosis using this deficiency rescues defects in macrophage migration, dispersal and wound responses seen in *simu* mutants (Roddie et al., 2019), showing that these phenotypes are due to failures in apoptosis and/or apoptotic cell clearance, as opposed to Simu being directly involved in these processes.

To investigate whether *amo*$^{1}$ phenotypes relate to apoptosis, apoptotic cell death was prevented using the *H99* deficiency, to understand the role of Amo in the absence of apoptosis. Loss of Hid, Reaper and Grim has been shown to cause subtle effects on macrophage migration and dispersal, therefore *H99* alone was used as a control and compared to *amo*$^{1}$*;H99* for this experiment . No significant differences were detected in terms of migration speeds or dispersal when comparing *amo*$^{1}$*;H99* to *H99* only controls (**figure 4.2 a-d**). This suggests that the impaired dispersal and migration speed phenotypes seen in *amo*$^{1}$ mutants may depend on the presence of apoptotic cells, as apoptosis-null embryos lack these phenotypes, despite possessing *amo* mutations.

### 4.2.3 Macrophage-specific overexpression of *amo* rescues migration speeds but not dispersal

As mentioned above, *amo*$^{1}$ failed to induce a phenotype on an apoptosis-null genetic background. These data suggest that the observed phenotypes are due to how the embryo deals with apoptotic cells. However, this does not explicitly show the requirement of *amo* in this process. In order to verify loss of *amo* as being responsible for the phenotypes seen above,

a rescue experiment was carried out wherein wild-type *amo* under *UAS* control was expressed specifically in the macrophages using the macrophage-specific driver *crq-GAL4*. Interestingly, overexpression of *amo* in $amo^{1}$ mutant macrophages revealed a significant increase in macrophage random migration speeds compared to $amo^{1}$ controls, although number of macrophages on the VML was still significantly lower than those of control embryos (**figure 4.3a-e**). These results suggest that *amo* has a macrophage-autonomous function in migration, though the fact that macrophage dispersal was still impaired suggests that macrophages may still be retained in the head.

### 4.2.4 Loss of *amo* does not obviously affect phagocytosis of apoptotic cells

A key macrophage function is the removal of apoptotic cells during development of the *Drosophila* embryo, in a process known as efferocytosis (Wood & Martin, 2017). Loss of *amo* has previously been linked to defects in efferocytosis (Van Goethem et al., 2012), therefore I imaged both macrophages (labelled with *srp-3x-mCherry*), and apoptotic cells on the ventral midline to verify this phenotype. Apoptotic cells were labelled via expression of the caspase-ON sensor *UAS-GC3Ai* via the ubiquitous *GAL4* driver *daughterless* (*da*). The GC3Ai sensor becomes fluorescent upon cleavage by caspases in apoptotic cells and can therefore be used to quantify cell death and efferocytosis live *in vivo* (Roddie et al., 2019; Schott et al., 2017). Green fluorescent punctae were counted within macrophages to calculate phagocytic indices in control and *amo* mutant embryos; this was calculated by dividing the number of apoptotic punctae by the total number of macrophages present in the most superficial 10µm of the embryo.

Despite a 50% decrease in relative phagocytic index of *amo* mutants having previously been reported by Van Goethem et al., no such decrease was observed, and macrophage phagocytic indices were essentially the same in both $amo^{1}$ and control embryos at stage 15 (**figure 4.4a-c**). It is worth noting however that Van Goethem et al. imaged macrophages in the head at stage 12, as opposed to the ventral midline at stage 15 as here. However, imaging the head at stage 12 using *da-GAL4,UAS-GC3Ai* in tandem with *serpent-3x-mCherry* also revealed no obvious differences between control and *amo* mutants (data not shown).

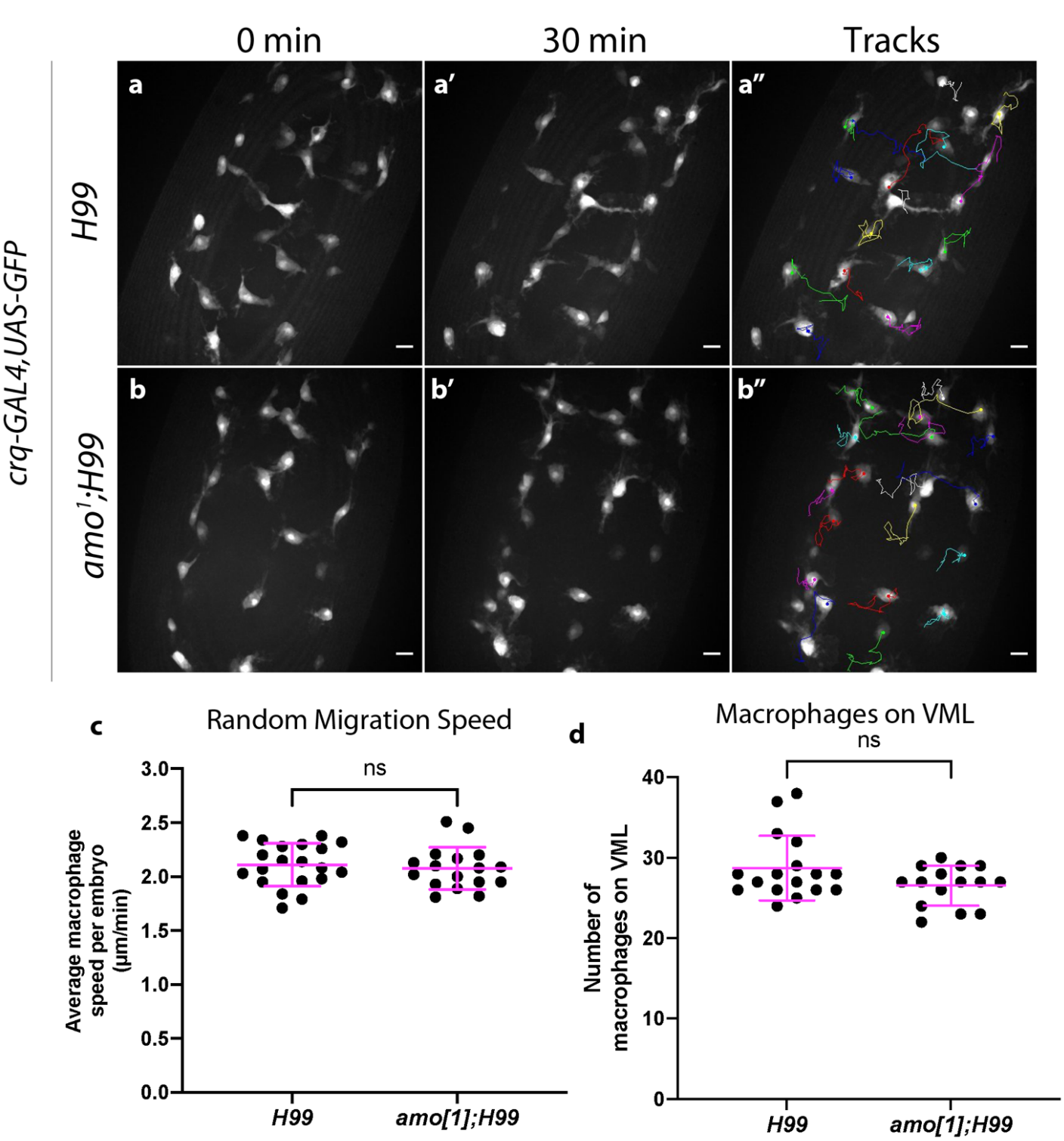


*Figure 4.2 – amo mutant macrophages exhibit no dispersal or migration defects compared to control embryos lacking apoptosis*

(a-b) Representative images of the ventral midline of *H99* and *amo[1];H99* embryos at stage 15, shown 30 minutes later in (a'-b'). (a"-b") Tracks of macrophages over 30 minutes. Scale bars denote 10µm. (c) Scatterplot showing average macrophage migration speeds per embryo between *H99* and *amo[1];H99* embryos (*n*=20 and 17, respectively, p>0.5). (d) Scatterplot showing number of macrophages present on the ventral midline at stage 15 of *H99* and *amo[1];H99* embryos (*n*=17 and 15 respectively, p=0.3033). Anterior is up in all images, statistical comparison in (c) carried out via non-paired t-tests, comparisons in (d) carried out via a Mann-Whitney test. Scale bars denote 10µm

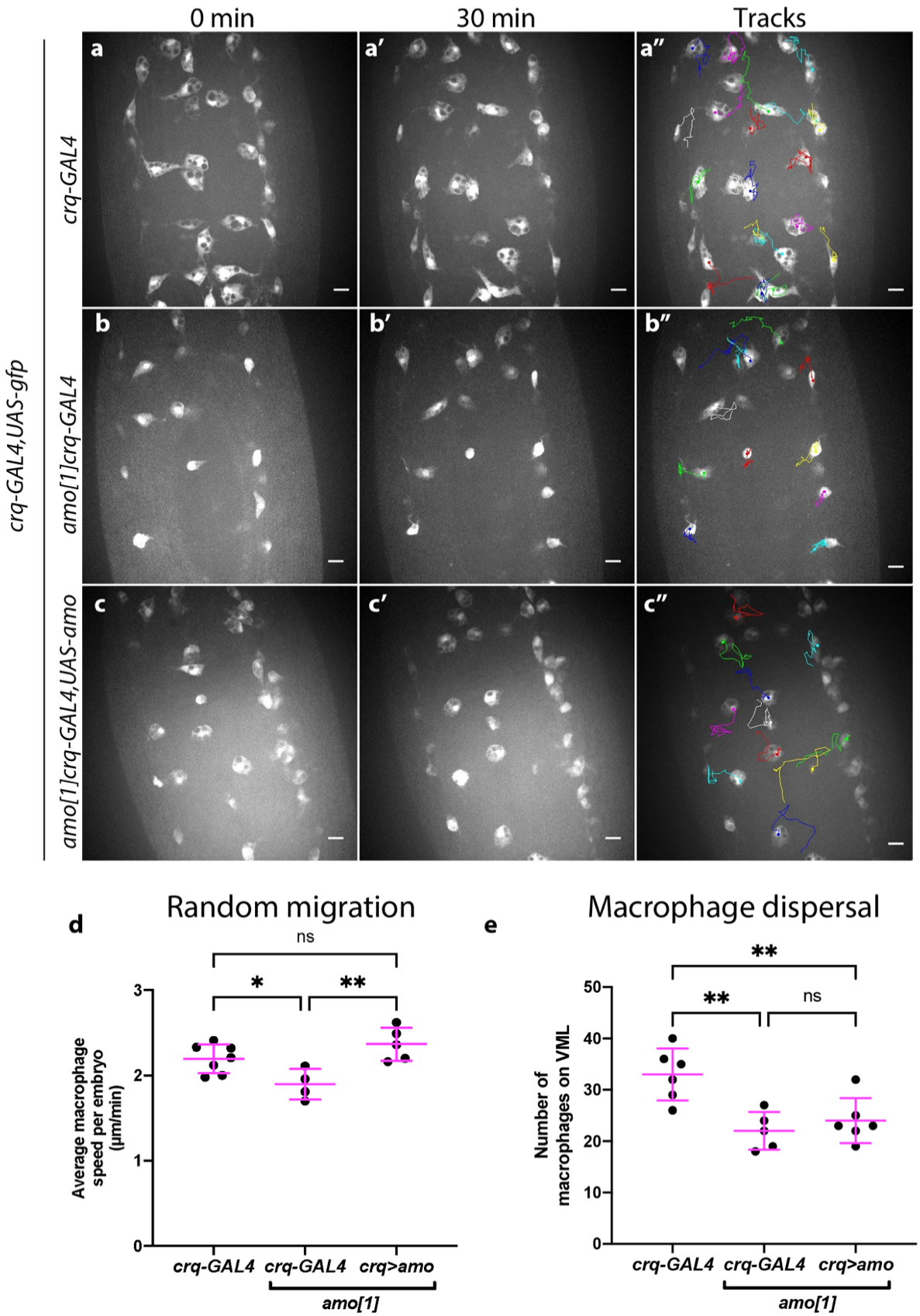
0 min
30 min
Tracks
crq-GAL4,UAS-gfp
crq-GAL4
amo[1]crq-GAL4
amo[1]crq-GAL4,UAS-amo
a
a′
a″
b
b′
b″
c
c′
c″
d
Random migration
Average macrophage speed per embryo (µm/min)
ns
*
**
crq-GAL4
crq-GAL4
crq>amo
amo[1]
e
Macrophage dispersal
Number of macrophages on VML
**
**
ns
crq-GAL4
crq-GAL4
crq>amo
amo[1]

*Figure 4.3 – Macrophage-specific overexpression of amo rescues macrophage migration speeds but not dispersal*

(a-c) representative images of the ventral midline of control (a), *amo*$^{1}$ control (b) and *amo*$^{1}$ rescue (c) embryos at stage 15, shown 30-minutes later in (a'-c'). (a"-c") Tracks of macrophages over 30 minutes. Scale bars denote 10µm. (d-e) scatterplots showing average macrophage migration speed (d) and macrophage number on the ventral midline (e) in wild-type controls, *amo* controls and *amo* rescues ( *n*=6, 4 and 6, respectively). Statistical analyses in (d-e) carried out via one-way ANOVA with Tukey's multiple comparisons. **p<0.01, ****p<0.001

Interestingly the *GAL4*-independent macrophage reporter *serpent-3x-mCherry* showed similar numbers of macrophages on the ventral midline between control and *amo* mutants at stage 15 (**figure 4.4d**), contrasting with results seen when using *crq-GAL4,UAS-GFP* (**figure 4.1g**). This appears to be due to *srp-3x-mCh* labelling significantly fewer macrophages in a control background than *crq-GAL4,UAS-GFP*, suggesting that the expression of one of these reporter lines is substantially weaker than the other, or that one of them may have picked up background mutations altering haematopoiesis or dispersal.

### 4.2.5 Loss of *amo* does not affect the macrophage inflammatory wound response or generation of calcium flashes

Another key immune-relevant behaviour of macrophages is their recruitment to sites of sterile inflammation (Stramer et al., 2005). Such damage can be induced using a high-powered ablation laser, with the generation of hydrogen peroxide downstream of calcium signalling necessary for this process (Razzell et al., 2013). Both defective efferocytosis and calcium signalling impair this process, with macrophages appearing to prioritise 'find me' cues from apoptotic corpses over inflammatory cues caused by wounding, such as hydrogen peroxide. Due to the involvement of *amo* in both calcium homeostasis and efferocytosis, I hypothesised that *amo* mutant macrophages would exhibit an impaired wound response.

Stage 15 embryos were mounted, and a wound was induced on the ventral midline using an ablation laser. Wound responses were measured both in terms of macrophage density, a measure of the number of macrophages at the wound relative to the size of the wound, and by the intensity of calcium flashes as measured by fluorescence of the genetically encoded calcium indicator *UAS-GCaMP6m*, driven via ubiquitously expressed *da-GAL4*.

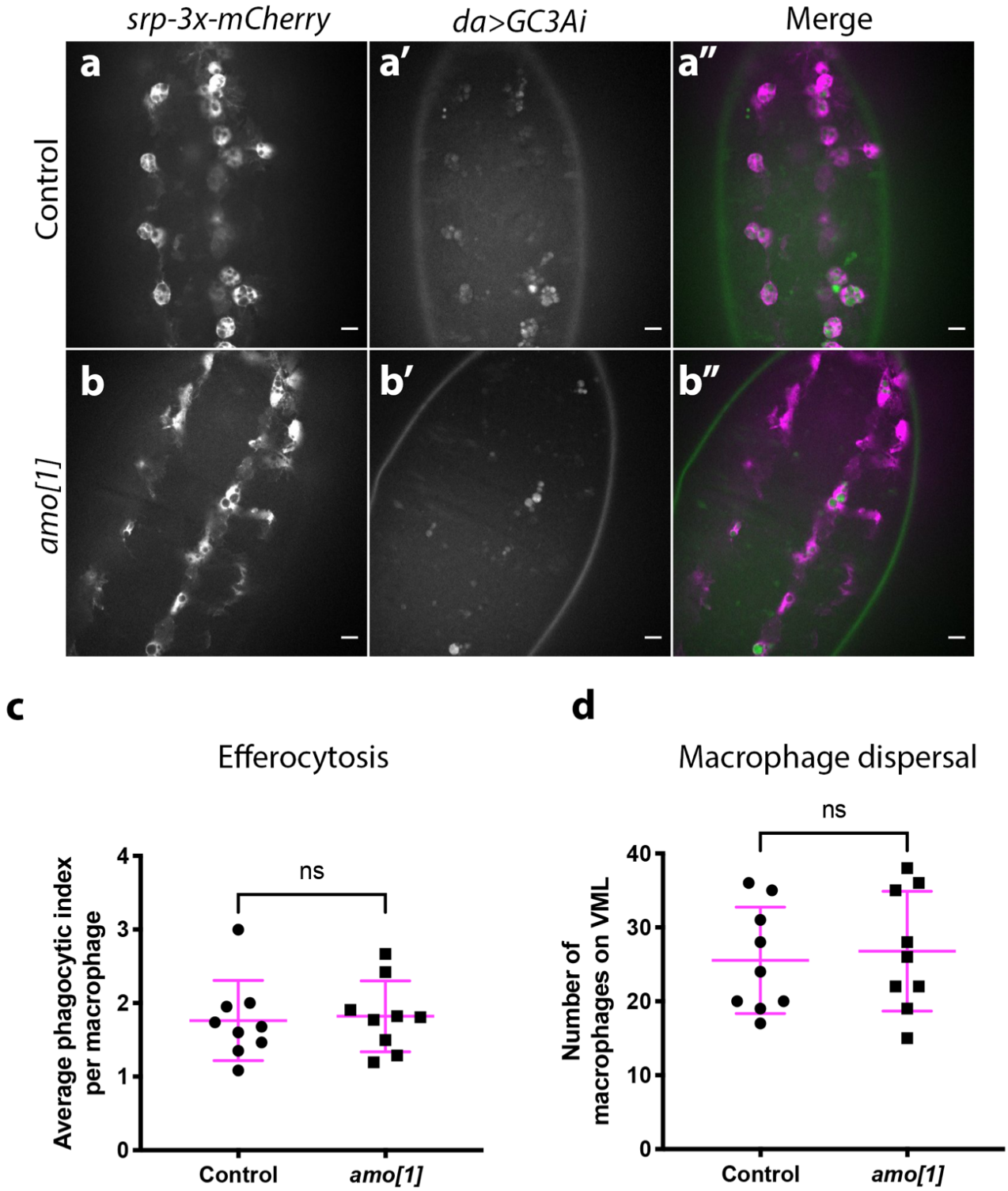


*Figure 4.4 – Loss of amo does not affect the phagocytic index of macrophages on the VML at stage 15*

(a-b) representative z-slices of control (a) and *amo*$^{1}$ (b) embryos at stage 15 with macrophages labelled via *serpent-3x-mCherry* (a-b; purple in merge) and Caspase-3 activity shown with *UAS-GC3Ai* (a'-b'; green in merge). (a"-b") shows merged channels. Scale bars denote 10µm. (c-d) scatterplots showing phagocytic index (total number of engulfed apoptotic cells divided by total number of macrophages (c) and macrophages on the ventral midline (d) between wild-type and *amo*$^{1}$ embryos (*n*=9 and 9). Statistical analyses in (c-d) carried out via non-paired t-tests; ns=not significant.

Perhaps surprisingly, given its reported involvement in efferocytosis and its function as a calcium channel, *amo* mutants exhibited no difference in either macrophage density, or the percentage of macrophages responding to the wound relative to controls (**figure 4.5a-d)**. Consistent with there being no difference in macrophage density in response to wounding, there was also no difference in the generation or persistence of epithelial calcium flashes in *amo* mutants relative to controls (**figure 4.5e-f**), suggesting that *amo* is not required for the propagation of calcium flashes across the epithelia.

The fact that macrophage wound response is not impaired in *amo* mutants is consistent with data showing no apparent differences in efferocytosis between control and *amo* mutant macrophages (**figure 4.4**). It is therefore not particularly surprising that inflammatory wound responses are not impaired by uncleared apoptotic cells, as our data suggests that there may not be sufficient uncleared cells to affect the wound response.

### 4.2.6 Immunostaining macrophages shows no apparent difference in macrophage dispersal

Results so far show that *amo* mutations impair macrophage random migration and dispersal, two phenotypes typically associated with failures in efferocytosis (**figure 4.1**; Roddie et al., 2019). However, when visualising apoptotic cells with a Caspase-3 activity indicator, no differences in efferocytosis were observed between control and *amo* mutant macrophages (**figure 4.4**), and the inflammatory wound response was not impaired in *amo* mutants (**figure 4.5**). These subsequent experiments used the *GAL4*-independent *serpent-3x-mCherry* to label macrophages, and no difference in macrophage numbers on the VML was observed using this reporter, unlike *crq-GAL4,UAS-GFP* which was used in initial experiments.

Due to the apparent discrepancy between control reporters seen above, I sought to see which value is more reflective of wild-type embryos by immunostaining macrophages in wild-type and *amo* mutant embryos lacking any transgenic macrophage reporters (in case the shortfall in macrophages was due to a lack of labelling of cells in one genotype compared to

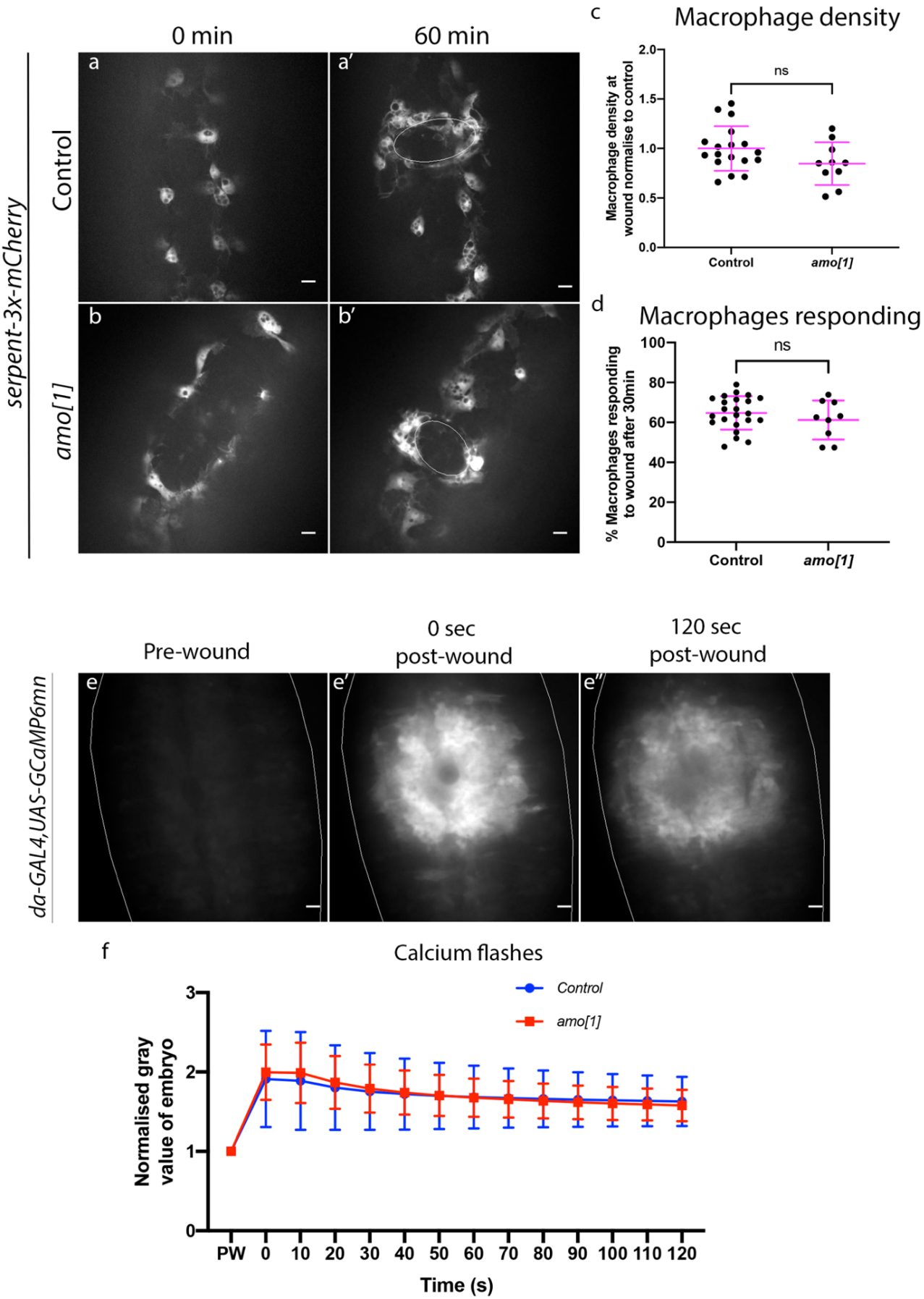
0 min
60 min
serpent-3x-mCherry
Control
amo[1]
a
a′
b
b′
c
Macrophage density
Macrophage density at wound normalise to control
ns
Control
amo[1]
d
Macrophages responding
% Macrophages responding to wound after 30min
ns
Control
amo[1]
Pre-wound
0 sec post-wound
120 sec post-wound
da-GAL4,UAS-GCaMP6mn
e
e′
e″
f
Calcium flashes
Control
amo[1]
Normalised gray value of embryo
PW 0 10 20 30 40 50 60 70 80 90 100 110 120
Time (s)

*Figure 4.5 – Loss of amo does not affect the macrophage wound response or the propagation of epithelial calcium waves*

(a-b) example z-slices before wounding (a-b) and 60-minutes post-wounding (a'-b') of control (a) and *amo*$^{1}$ (b) stage 15 embryos with macrophages labelled using *serpent-3x-mCherry*. Scale bars in denote 10µm. (c-d) scatterplots showing macrophage density (c, *n*=18 and 10) and percentages of macrophages responding to wounds (d, *n*=23 and 9) between control and *amo*$^{1}$ embryos. (e) Example average projection of a stage 15 control embryo ubiquitously expressing *UAS-GCaMP6m* before wounding (e), immediately after wounding (e') and 120-seconds post wounding (e''). Scale bars in denote 10µm. (f) Graph showing grey value of embryos following wounding, measured every 10 seconds for 120 seconds, normalised to pre-wound levels. Statistical analyses (c-d) carried out via non-paired t-tests; ns=not significant.

the other, rather than fewer cells on the VML *per se*). To achieve this, control (*w*$^{1118}$) and *amo* mutant embryos were fixed and immunostained with an anti-Fascin antibody; Fascin is an actin-bundling protein highly enriched in macrophages (Zanet et al., 2009). Embryos were then imaged and macrophage numbers on the VML were quantified (**figure 4.6a-b)**.

Interestingly, the number of macrophages on the VML of stage 15 embryos were no different between wild-type and *amo* embryos (**figure 4.6c)**. The average number of macrophages in wild-type control embryos using this approach was 29, significantly lower than the average of 37 seen when using *crq-GAL4,UAS-GFP* (**figure 4.1c**) and much more consistent with the average of 26 seen using *serpent-3x-mCherry* (**figure 4.4d**). It is therefore possible that the control line of *crq-GAL4,UAS-GFP* used in my initial experiments may have acquired a background mutation affecting embryonic hematopoiesis, and the dispersal and migration phenotypes seen using this control are false positives.

### 4.2.7 Validation of macrophage dispersal using other macrophage reporters.

As anti-Fascin staining suggested that there is in fact no difference in macrophage dispersal between control and *amo*$^{1}$ embryos, different transgenic macrophage reporters were used to analyse macrophage dispersal, while random migration was also be assayed. Both *GAL4*-dependent (*crq-GAL4,UAS-CD4-tdTomato*) and *GAL4*-independent lines (p{*srp-Hemo-GMA}*) were used, to allow comparisons between reporters driven via different promoters.

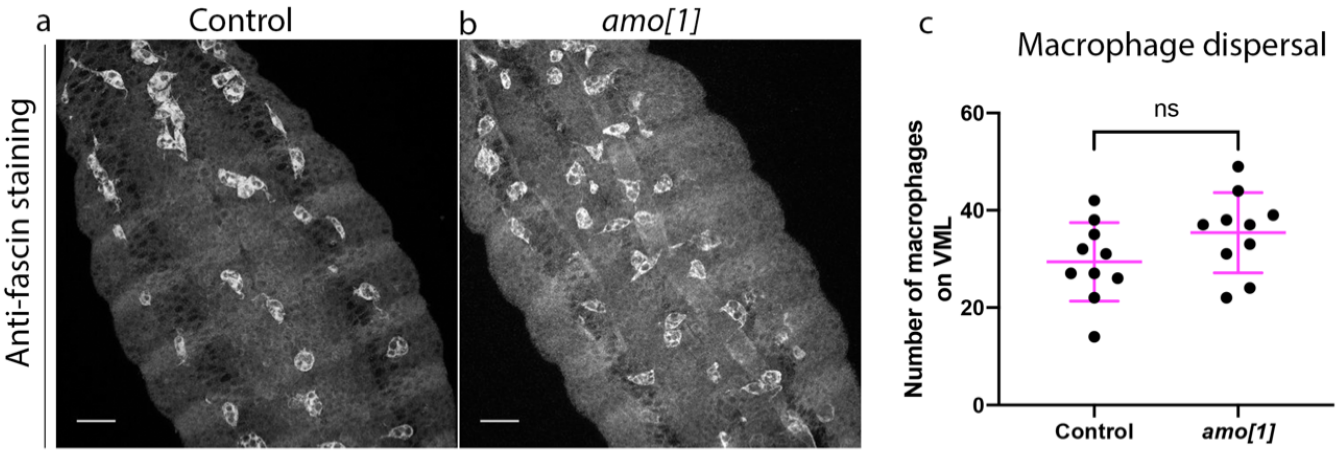


*Figure 4.6 – Immunostaining reveals no apparent difference in macrophage dispersal between control and amo[1] embryos*

(a-b) representative 15 µm maximum projections of stage 15 control (a) and *amo*[1] (b) embryos immunostained using anti-Fascin. Scale bars denote 10µm. (c) scatterplot showing number of macrophages on the ventral midline between control and *amo*[1] embryos (*n*=10 and 10). Statistical analyses carried out via non-paired t-tests (p=0.1187).

Neither *crq-GAL4,UAS-CD4-tdTomato* (figure 4.7a-d) nor *srp-GMA* (figure 4.8a-d) showed any defect in random migration speed when comparing *amo* mutants to controls, nor were there any differences in macrophage numbers on the ventral midline. Taken together, these results cast serious doubt over the validity of the results seen in section 4.2.1, and the fact that no differences in efferocytosis have been observed suggest further that the phenotypes seen in section 4.1.1. are unlikely to be due to failures in apoptotic cell clearance.

### 4.2.8 A new control line reveals no differences in migration speeds of control and *amo* mutant macrophages

Results from section 4.2.7. showed that all macrophage reporters other than wild-type *crq-GAL4,UAS-GFP* show similar numbers of macrophages on the VML in both control and *amo* mutant backgrounds. The fact that the *crq-GAL4,UAS-GFP* control line had significantly greater numbers of macrophages suggests the presence of a possible backround mutation in this control line, which could have arisen due to generations of inbreeding in the stock line. To address this, a

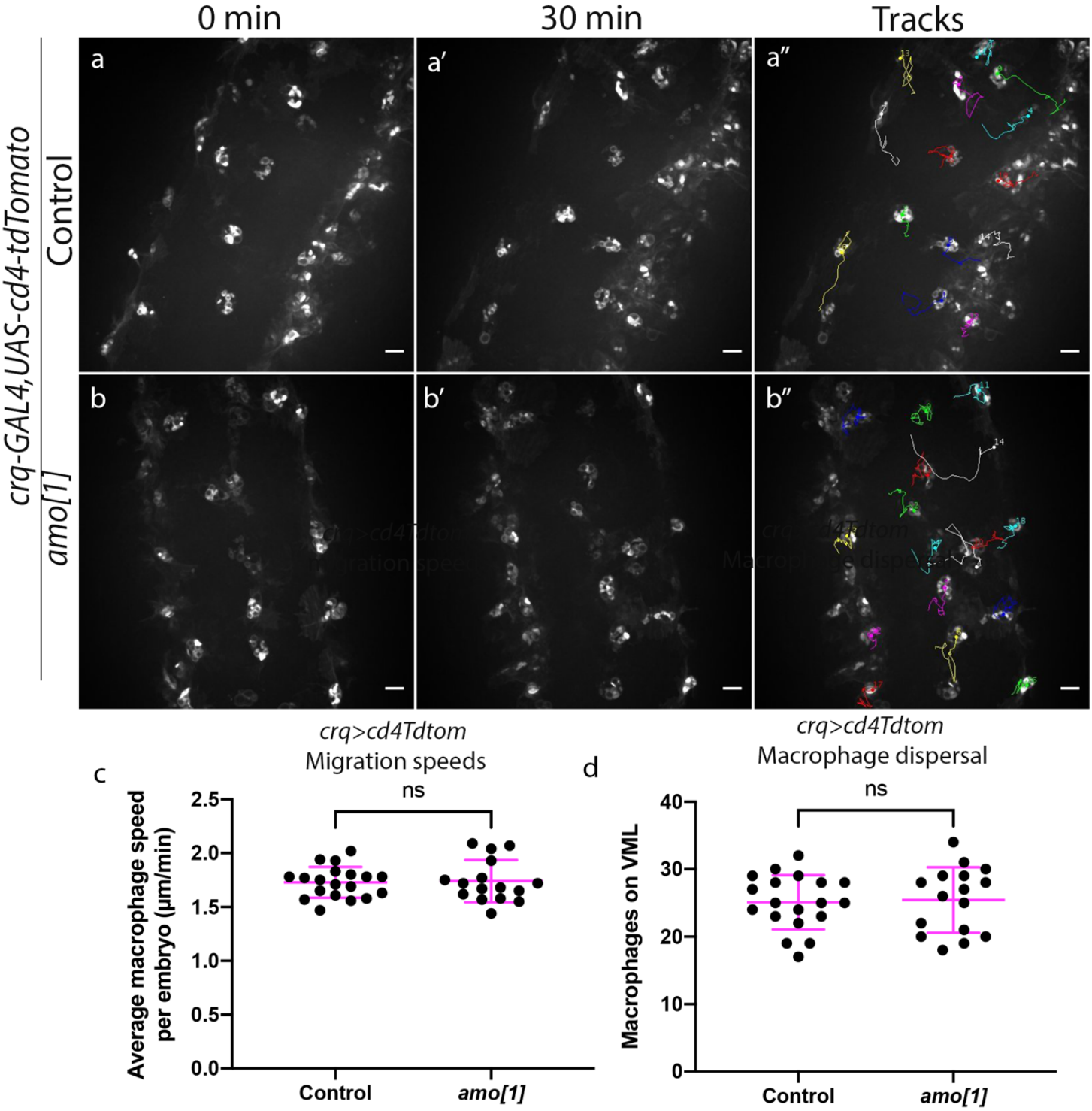


*Figure 4.7 –The GAL4-dependent macrophage reporter crq-GAL4,UAS-cd4-tdTomato shows no difference in migration or dispersal in amo[1] embryos*

(a-b) representative 15µm maximum projections of the ventral midline of control and amo[1] embryos at stage 15. Macrophages labelled via UAS-tdTomato driven by crq-GAL4. (a'-b') Embryos following imaging for 30 minutes. (a''-b'') macrophage tracks over 30 minutes. Scale bars denote 10µm. (c-d) scatterplots showing average migration speed per macrophage, per embryo (c, n=19 and 16) and number of macrophages on the VML at stage 15 (d, n=19 and 16) between control and amo[1] embryos. Statistical analyses carried out via unpaired t-tests; ns=not significant.

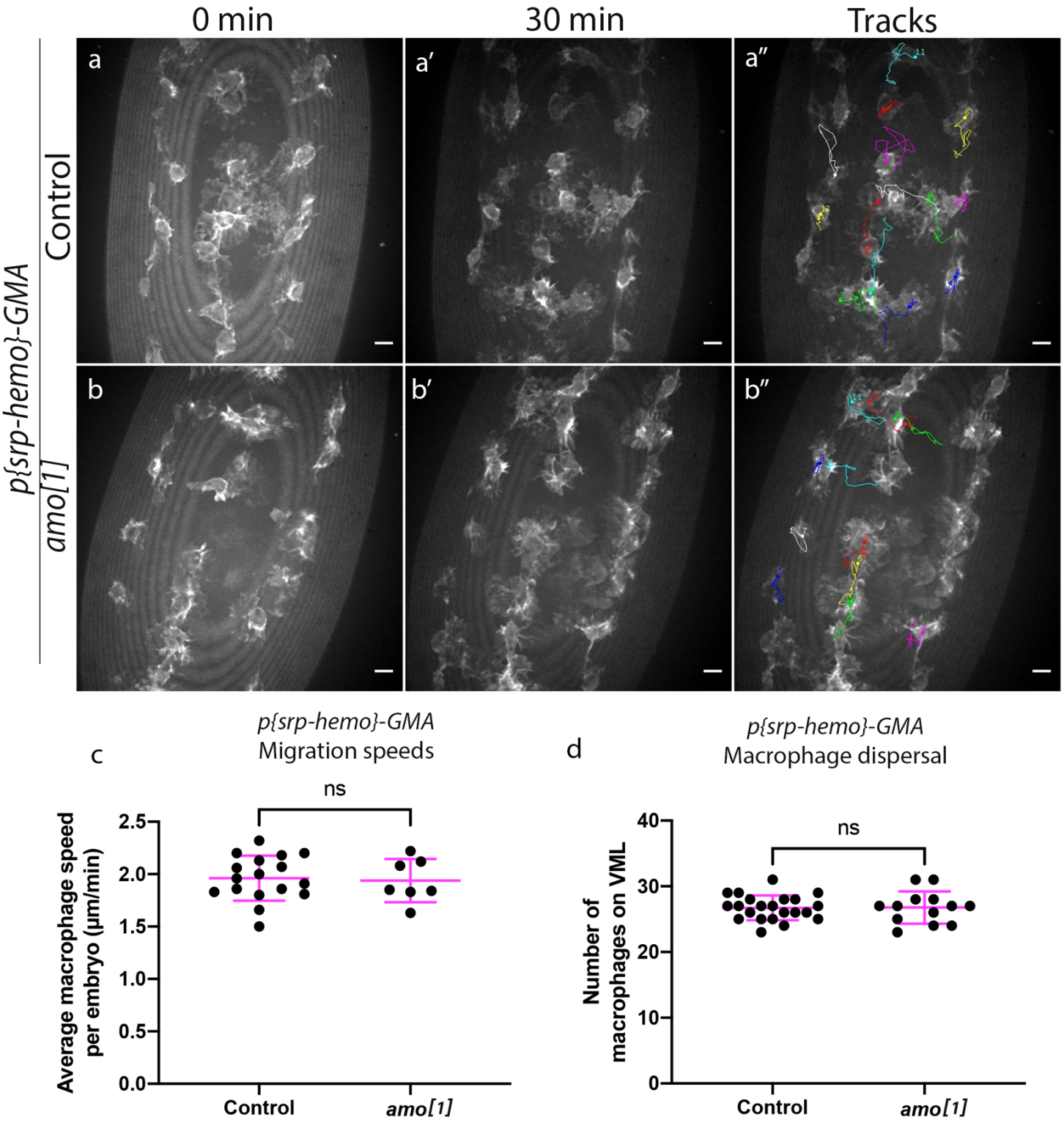


*Figure 4.8 –The GAL4-independent macrophage reporter serpent-GMA shows no difference in migration or dispersal in amo[1] embryos*

(a-b) representative 15μm maximum projections of the ventral midline of control and *amo[1]* embryos at stage 15. Macrophages labelled via *p{srp-GMA}*. (a'-b') embryos following imaging for 30 minutes. (a''-b'') macrophage tracks over 30 minutes. Scale bars denote 10μm. (c-d) scatterplots showing average migration speed per macrophage per embryo (c, *n*=17 and 7) and number of macrophages on the VML at stage 15 (d, *n*=22 and 13) between control and *amo[1]* embryos. Statistical analyses carried out via unpaired t-tests; ns=not significant.

new control line was generated by outcrossing *amo*$^{1}$*;crq-GAL4,UAS-GFP* mutants into a wild-type, balanced background. This new control line was then imaged alongside the 'old' control line and *amo*$^{1}$ mutants, before counting VML macrophages at stage 15 and assaying random migration (**figure 4.9a-c**).

There was a significant increase in random migration speed of macrophages at stage 15 in the 'old' control line compared to both *amo* mutants and the 'new' control line, while there was no significant difference between *amo* mutants and the 'new' control (**figure 4.9d**). The same trend was observed when counting numbers of macrophages on the VML, with the 'old' control line possessing a significantly greater number of macrophages than those of the 'new' control line and *amo* mutants. Again, no significant difference was noticed between the 'new' control line and *amo*$^{1}$ mutants. Importantly, these results suggest that the random migration and dispersal phenotypes reported in *amo* mutants in sections 4.2.1. were likely false positives and could possibly have been due to background mutations present in the control line used for these experiments. Furthermore, these data question whether *amo* mutations do indeed disrupt macrophage function in the embryo as I found no evidence to suggest macrophage function is impaired in *amo* mutant embryos under normal homeostatic conditions

### 4.2.9 *amo* mutant macrophages are as responsive to an increased apoptotic burden as control macrophages

Results so far suggest that *amo* mutations do not affect the ability of *Drosophila* macrophages to mediate efferocytosis. Early results suggested *amo* mutant macrophages have impaired dispersal and random migration speeds, phenotypes associated with impaired efferocytosis (Roddie et al., 2019). Critically, these phenotypes could be rescued by the genetic removal of apoptosis using *H99*, suggesting that the apoptotic machinery is required for this phenotype. However, subsequent data suggested that these results were in fact due to the presence of a background mutation in the control line used, as opposed to failures in *amo*-mediated efferocytosis.

Imaging stage 15 embryos also showed no difference in the phagocytic indices of control and *amo* mutant macrophages (**figure 4.4**). During stage 15 of embryogenesis however, there are

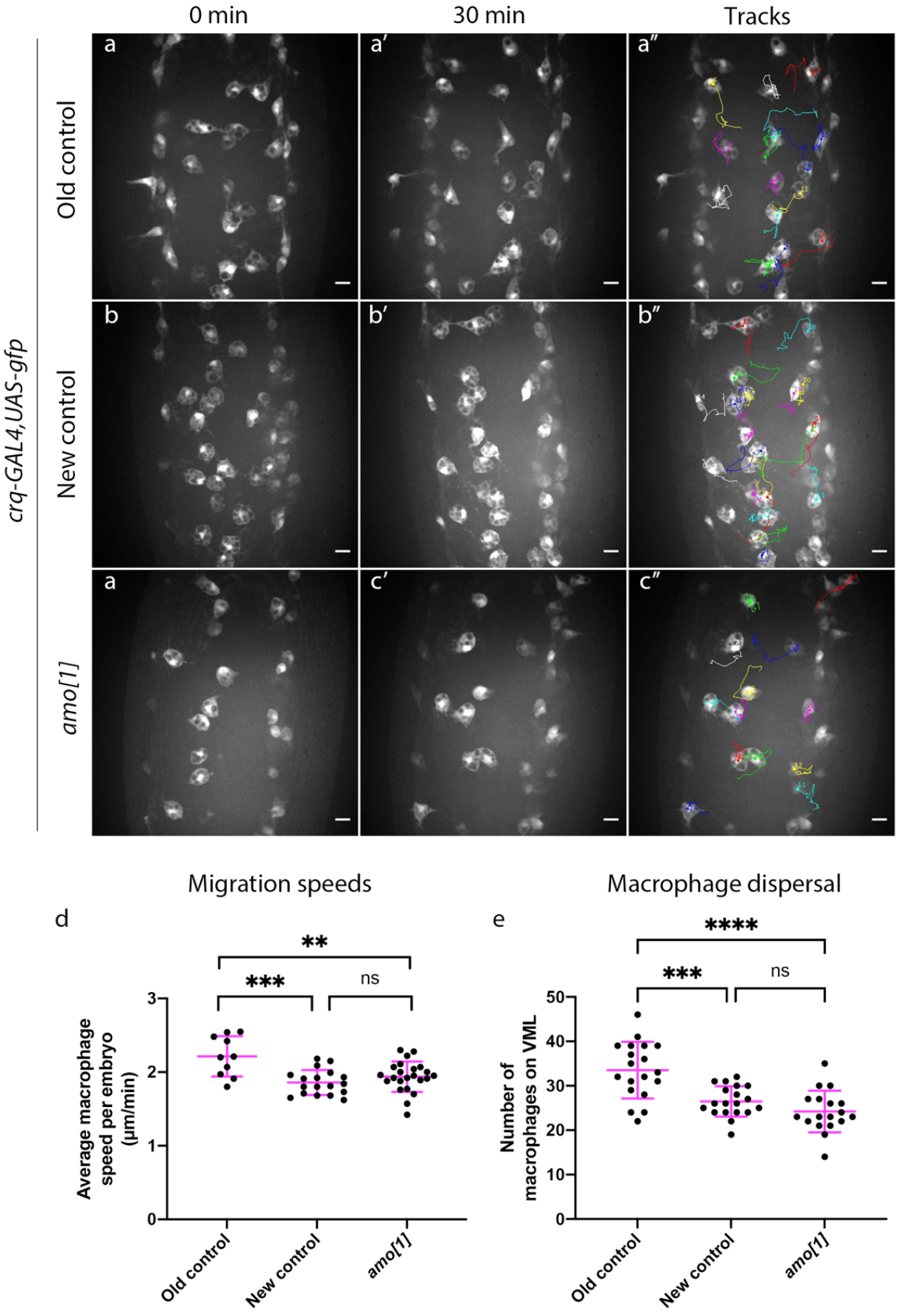
0 min
30 min
Tracks
crq-GAL4,UAS-gfp
Old control
New control
amo[1]
a
a′
a″
b
b′
b″
a
c′
c″
Migration speeds
Macrophage dispersal
d
e
**
***
ns
****
***
ns
Average macrophage speed per embryo (µm/min)
Number of macrophages on VML
0
1
2
3
0
10
20
30
40
50
Old control
New control
amo[1]
Old control
New control
amo[1]

*Figure 4.9 – Outcrossed control reporter lines show no difference in macrophage random migration or dispersal compared to amo mutants*

(a-c) representative 15µm maximum projections of the ventral midline of old and new control (a-b) and *amo*$^{1}$ (c) embryos showing *crq-GAL4,UAS-GFP* tracks over 30 minutes. Scale bars denote 10µm. (d-e) scatterplots showing average migration speed per macrophage per embryo (d, *n*=10, 18 and 23) and number of macrophages on the VML at stage 15 (e, *n*=19, 19 and 19). Statistical analyses carried out via one-way ANOVA with Tukey's multiple comparisons; **p<0.01, ***p<0.001, ****p<0.0001,ns=not significant.

relatively few uncleared apoptotic cells on the VML, with the majority of apoptosis happening in this region between stages 12 and 13 during the period of development when macrophages migrate down the developing ventral nerve cord (VNC). During this process glial cells, representing the other major phagocyte of the developing embryo, mediate efferocytosis along with macrophages. The transcription factor *reversed polarity* (*repo*) is required to enable glial cells to mediate this process, with *repo* mutant glia failing to express the phagocytic receptor *draper*. This results in an increased apoptotic burden being placed upon macrophages, which exhibit the same phenotypes as those caused by failures in macrophage-mediated efferocytosis, namely decreased random migration speed and an impaired wound response (Roddie et al., 2019, Armitage et al., 2020).

To test if *amo* is required for efferocytosis in a background with increased levels of apoptotic cells, a loss-of-function *repo* mutation was introduced (*repo*$^{03702}$ - Armitage et al., 2020; Campbell et al., 1994) to increase the apoptotic burden placed upon macrophages. If *amo* is indeed required in macrophages for efferocytosis, we hypothesised that increasing the phagocytic burden placed upon macrophages would exacerbate the effect of *amo*$^{1}$ mutations and cause a more obvious difference between *amo* mutants and controls in terms of phagocytic index and random migration speeds.

Assaying random migration revealed no difference in macrophage speeds in *repo* single mutants possessing wild-type *amo* when compared to *amo;repo* double mutants (**figure 4.10a-c)**. This suggests that macrophage migration is no more impaired in the absence of *amo* when challenged with pathological levels of uncleared apoptotic cells due to *repo* mutations, further suggesting that *amo* might not in fact be required for efferocytosis.

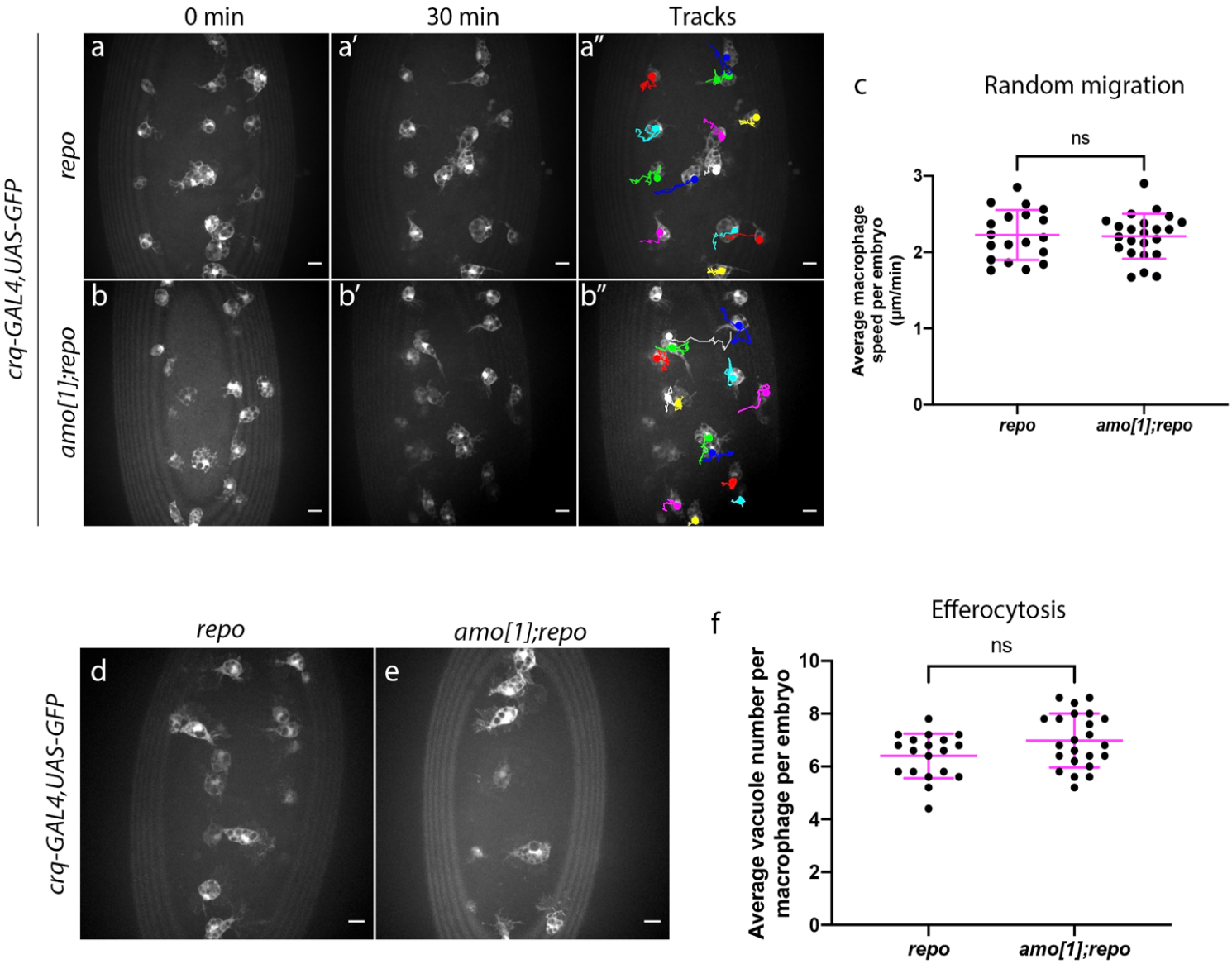


*Figure 4.10 – amo mutant macrophages are as responsive to an increased apoptotic challenge as control macrophages*

(a-b) representative 10µm maximum projections of the ventral midline of stage 15 *repo* (a) and *amo*$^{1}$*;repo (b)* embryos with macrophages labelled via *crq-GAL4,UAS-gfp*. (a'-b'') embryos following 30-minutes of imaging. (a''-b'') macrophage tracks over 30 minutes. (c) scatterplot showing average migration speed per macrophage per embryo (*n*=19 and 23). (d-e) Representative 5µm maximum projections of the ventral midline of *repo* (d) and *amo*$^{1}$*;repo* (e) stage 15 embryos, showing the most superficial macrophages. (f) scatterplot showing average number of vacuoles per macrophage per embryo between *repo* and *amo*$^{1}$*;repo* embryos (*n*=19 and 23). Scale bars in (a,b and e) denote 10µm, statistical analyses in (c and f) carried out via non-parametric t-tests; ns=not significant.

To assay efferocytosis in a *repo* mutant background, average vacuolation of embryonic macrophages were counted. Vacuoles in embryonic macrophages typically represent phagocytosed apoptotic corpses (Evans et al., 2013), so vacuolation can be used as an effective readout of apoptotic cell clearance (**figure 4.10d-e)**. Comparing *repo* single mutants with *amo*$^{1}$*;repo* double mutants revealed no apparent difference in macrophage vacuolation (**figure 4.10f**). As seen when assaying random migration, *amo*$^{1}$ mutant macrophages appear to be no less effective than control macrophages at responding to the increased apoptotic burden placed upon macrophages by *repo* mutations.

In summary, these data suggest that any requirement for *amo* in *Drosophila* efferocytosis is subtle, with mutations in *amo* not affecting macrophage function in ways associated with impaired efferocytosis (Roddie et al., 2019). Though initial data seemed to suggest a requirement for *amo* in macrophage dispersal and migration, it appears that these results were false positives caused by a background mutation in a control line, given that an outcrossed control line yielded no phenotypes. As such, work investigating the effect of *amo* mutations on *Drosophila* macrophage behaviour was ceased.

### 4.2.10 Development of an *in vitro* efferocytosis assay

In parallel to investigating the role of Amo in *Drosophila* efferocytosis, experiments were also taking place investigating the role of PC-2 in mammalian efferocytosis. Kidney epithelial cells are known to mediate efferocytosis as a so called 'non-professional' phagocyte (Ichimura et al., 2008), so one aim of my project was to develop an *in vitro* assay allowing efferocytosis to be quantified, in order to see whether epithelial efferocytosis could be involved in the pathogenesis of ADPKD. The ultimate aim of this assay is to compare the ability of wild type and *PKD2* knockout kidney tubular epithelial cells to mediate efferocytosis to investigate if there is a defect in *PKD2* knockout cells.

Before assessing the ability of wild type and *PKD2* mutant kidney epithelial cell lines to mediate efferocytosis, human monocyte-derived macrophages (MDMs) were used as a 'professional' phagocyte to verify efferocytosis can be assayed and quantified *in vitro*, before moving onto

kidney epithelial cells. Neutrophils were isolated from a healthy donor and aged for no more than 22 hours. Tyrphostin AG825, a tyrosine phosphatase inhibitor, can be used to induce apoptosis in neutrophils (Murillo et al., 2001). MDMs were therefore co-incubated with aged neutrophils or aged neutrophils treated with tyrphostin, which were then fixed, stained and imaged (**figure 4.11a-b)**. The phagocytic index (PI) of MDMs incubated with treated or untreated neutrophils was calculated, and a significantly higher PI was observed when apoptosis was induced in neutrophils via Tyrphostin (**figure 4.11c)**, suggesting that these

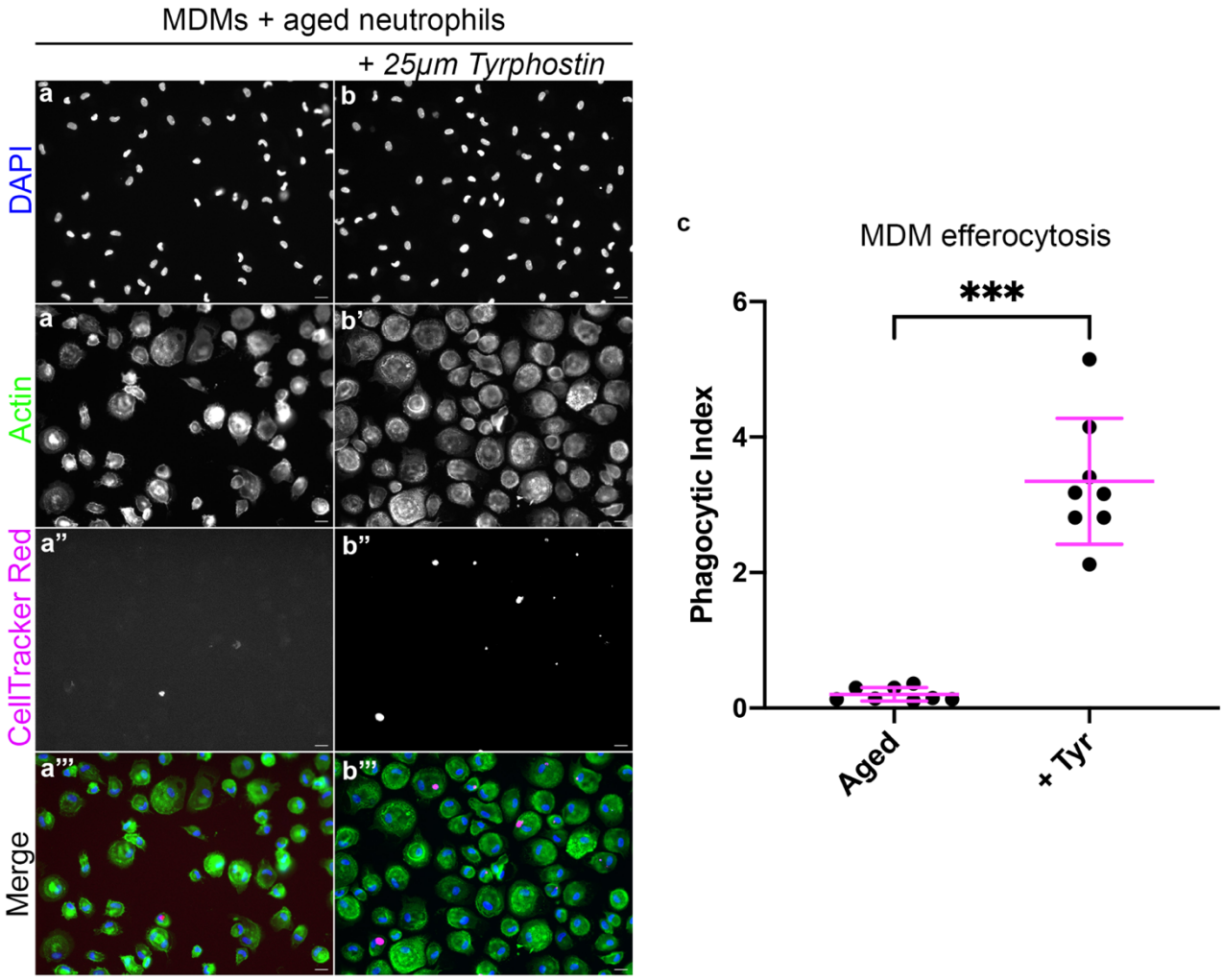


*Figure 4.11 – Monocyte-derived macrophages mediate efferocytosis in vitro, and phagocytose neutrophils treated with tyrphostin more readily*

(a-b'") representative images of *ex vivo* MDMs stimulated with aged neutrophils (a-a'") or aged neutrophils treated with 25μM tyrphostin AG825 (b-b'"). Nuclei are labelled with DAPI (blue in merge; a-b), actin filaments via Phalloidin staining (green in merge; a'-b') and apoptotic neutrophils are via CellTracker Red (magenta in merge; a"-b"). Scale bars denote 20μm. (c) scatterplot comparing phagocytic indices of MDMs stimulated with aged neutrophils and aged neutrophils treated with 25μM tyrphostin AG825 (n=8 and 8, p=0.002). Statistical analysis carried out via Mann-Whitney test. ***p<0.001.

represent a viable apoptotic target for use in an *in vitro* efferocytosis assay looking at kidney epithelial cells.

### 4.2.11 Epithelial cell lines lacking functional *PKD2* show no difference in efferocytosis compared to controls

Following on from quantifying *in vitro* efferocytosis mediated by MDMs, a similar technique was used to try and quantify efferocytosis mediated by renal tubular epithelial cells. Both the ratio of neutrophil to cells and co-incubation time were increased to try and improve the likelihood of efferocytosis events, given that epithelial cells represent 'non-professional' phagocytes, in contrast to the professional MDMs. The ability of a tubular epithelial cell line(UCL93) to mediate efferocytosis was compared to the ability of three independent cell lines (clones 33, 37 and 38) that are null for *PKD2* (Δ*PKD2*). Following co-incubation with Tyrphostin-treated neutrophils, cells were fixed stained and imaged (**figure 4.12a-d)**. It was shown that both wild type UCL93 and the Δ*PKD2* clones are indeed able to mediate efferocytosis of apoptotic neutrophils, albeit at substantially lower rates than MDMs, and there were no differences in PIs between any of the cell lines (**figure 4.12e)**. Internalisation of apparent apoptotic inclusions was validated by running two assays in parallel, one of which was kept at 4˚C to impair membrane dynamics, while the other was kept at 33˚C, and it was shown that the cells at 33˚C did indeed appear to have an increased, albeit non-significant, phagocytic index relative to the 4˚C control cells (**figure 4.12f**).

Similar to *Drosophila* macrophages, it appears that *PKD2* is not required for efferocytosis via renal epithelial cells. However, rates of efferocytosis by epithelial cell lines were found to be very low, reflecting their status as a 'non-professional' phagocyte, therefore any differences between control and *PKD2* knockout cells could be hard to distinguish. As such, the research investigating the role of *amo* and *PKD2* in efferocytosis was ended at this point.

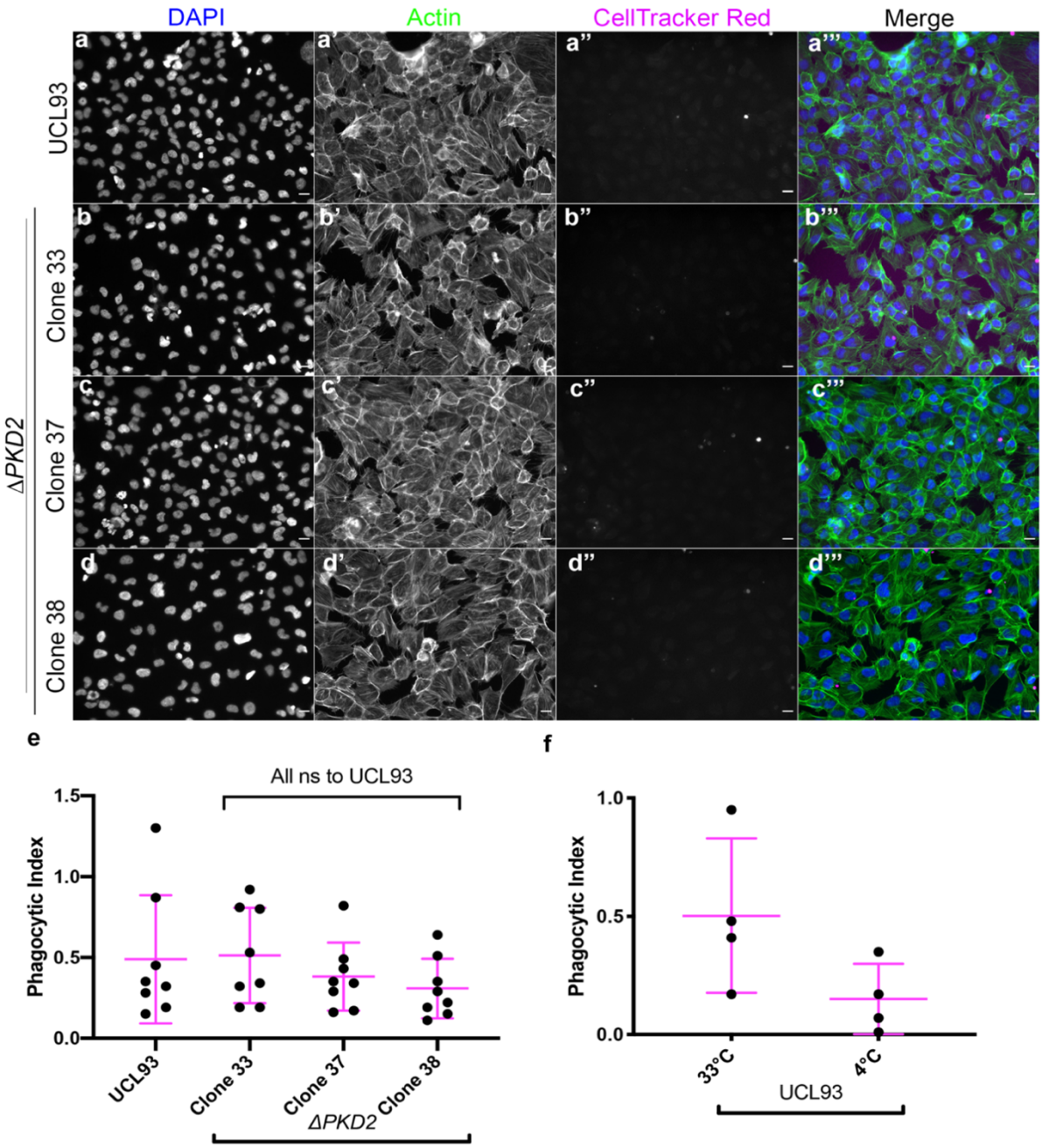


*Figure 4.12 – Loss of PKD2 does not affect efferocytosis of UCL93 cells in vitro*

(a-d''') representative images of wild-type (a-a''') and 3 independent *PKD2* knockout (b-d''') tubular epithelial cell lines stimulated with aged neutrophils treated with 25µM tyrphostin AG825 (b-b'''). Nuclei are labelled with DAPI (blue; a-d), actin filaments via Phalloidin staining (green; a'-d'), and apoptotic neutrophils via CellTracker Red (magenta; a"-d"). Scale bars denote 20µm. (e) scatterplot comparing phagocytic indices of wild type (UCL93) and *PKD2* knockout tubular epithelial cells stimulated with aged neutrophils treated with 25µM tyrphostin AG825 (n=8, 8, 8 and 8, p>0.05). (f) scatterplot comparing phagocytic indices of UCL93 cells stimulated with apoptotic neutrophils incubated at 33°C or 4°C (n=4 and 4, p>0.05). Statistical analysis in (e) and (f) carried out via one-way ANOVA with Tukey's multiple comparisons and Mann-Whitney tests, respectively.

## 4.3 Discussion

The overarching aim of this work was to characterise the functional effect of *amo* mutations at the macrophage level, with the hope that this would implicate novel pathways in the pathogenesis of ADPKD. I investigated whether defective efferocytosis in *amo* mutants impairs macrophage function in ways akin to mutations in other genes required for efferocytosis, such as *simu* (Roddie et al., 2019). However, results seem to suggest that *amo* is not in fact required for efferocytosis, with *amo* mutant macrophages exhibiting none of the phenotypes typically associated with failures in this process. Initial data suggested that *amo* mutations do indeed impair macrophage migration and dispersal, but I was unable to validate this further or reproduce it using alternative reporter lines and genetic backgrounds. Therefore, these initial phenotypes are most likely due to a background mutation in the original control line used as a control (*crq-GAL4,UAS-GFP*). Stage 15 macrophages exhibited no defects in efferocytosis under basal conditions, nor in a mutant background with high levels of apoptosis. Furthermore, human kidney epithelial cell lines lacking *PKD2* exhibited no difference in *in vitro* efferocytosis compared to controls, suggesting that *PKD2* function is not required for efferocytosis in mammals as well as *Drosophila*.

### 4.3.1 The effect of *amo* mutations on macrophage dispersal and random migration

Initial results showed the presence of two phenotypes associated with defective efferocytosis, namely impaired macrophage dispersal and random migration speeds, in *amo* mutants. These phenotypes were apparently rescued when removing apoptosis using the deficiency *Df(3L)H99,* suggesting that these phenotypes were, in some part at least, related to how embryonic macrophages process apoptotic cells. Random migration speeds in *amo* mutants appeared to be able to be rescued by the expression of *amo* specifically in the macrophages using *crq-GAL4,UAS-amo*, suggesting that *amo* is required in the macrophages for effective random migration. However, this rescue experiment failed to rescue the dispersal of macrophages, suggesting that functional *amo* in macrophages only is insufficient to prevent their retention in the head. Ubiquitous rescue experiments were planned, wherein *UAS-amo* would have been driven by the ubiquitous *da-GAL4* driver in order to see if the macrophage

dispersal phenotype could be rescued. However, this would have required the use of *GAL4*-independent macrophage reporters (e.g., *srp-3x-mCherry*) and I was unable to show any phenotypes when using this reporter/background.

Anti-Fascin staining was used to validate the dispersal phenotype seen when using *crq-GAL4,UAS-GFP*. However, no differences in macrophage dispersal between wild-type and *amo* mutant embryos were observed using this approach. Similarly, the use of other macrophage reporters also failed to recapitulate these phenotypes, suggesting that the phenotypes in question were specific to the use of *crq-GAL4,UAS-GFP.* It is well known that generations of inbreeding and genetic drift can lead to stocks of *Drosophila* acquiring so-called background mutations (Dworkin et al., 2009). Background mutations are capable of affecting any number of developmental processes, introducing phenotypes, which can be considered false positives as they are likely unrelated to the gene of interest. In order to see if there were any background mutations present in the *crq-GAL4,UAS-GFP* control line, I generated a 'new' line by outcrossing $amo^{1}$ from $amo^{1}$*;crq-GAL4,UAS-GFP* and assayed macrophage dispersal and migration. No difference was seen between $amo^{1}$ and the 'new' control, while the 'old' control had significantly more macrophages on the VML at stage 15, suggesting that the apparent phenotypes observed were in fact due to possible background mutations in the 'old' control line.

What exactly this background mutation seems to be affecting however remains to be seen. It is possible that it could be affecting the apoptotic machinery, given that recombination of the *H99* genomic deficiency with this control reporter seems to rescue the enhanced macrophage dispersal. However, it is possible that the generation of this recombinant line outcrossed the background mutation responsible for the phenotypes, or the mutation could have arisen after the *H99, crq-GAL4,UAS-GFP* recombinant. As there is an increased number of macrophages on the VML at stage 15 in this 'old' control line, it is possible that the background mutation could be affecting haematopoiesis, while the fact that macrophages migrate faster in this background suggests that there could be a gain of function mutation affecting the migration machinery of macrophages. As there was still an increased number of macrophages when this control line was crossed to *crq-GAL4,UAS-amo* (for experiments described in section 4.3), one can speculate that this background mutation is causing a dominant effect. Though it would

undoubtedly be interesting to map this background mutation and identify potentially novel regulators of the hematopoietic and migratory machinery, technical and temporal limitations ultimately made this unrealistic.

### 4.3.2 The effect of *amo* mutations on the inflammatory wound response

When inducing epithelial wounds on the VML of stage 15 embryos, no defect was observed in *amo* mutants either in terms of macrophage behaviours or in propagation of calcium waves through the wounded epithelium. It is known that embryonic macrophages prioritise 'find-me' cues from dying cells over wound cues (Roddie et al., 2019); the fact that *amo* mutant macrophages are equally responsive as control macrophages further suggests that there is no build-up of uncleared apoptotic cells distracting the macrophages. This is further supported via live imaging of apoptosis using the GC3ai reporter, and the ability of *amo* mutant macrophages to respond to an increased apoptotic challenge in *repo* mutant embryos.

The inflammatory wound response is known to be a calcium-dependent process; wounding generates calcium flashes which propagate across epithelial gap junctions leading to activation of DUOX and resulting in the generation of hydrogen peroxide, a potent wound signal necessary for the recruitment of macrophages to sites of damage (Razzell et al., 2013). As failures in calcium signalling can result in a dampened wound response, the role of *amo* as a calcium-permeable cation channel suggested it could potentially be involved in the propagation of these signals. Furthermore, unpublished data from our lab has implicated the Sarcoplasmic/Endoplasmic Reticulum Calcium ATPase (SERCA) in this process, suggesting that ER-resident calcium could be involved in this process. Given the function of *amo/PKD2* as an ER-resident calcium channel, it was thought that the generation or propagation of these wound induced flashes could be impaired in an *amo* mutant background. However, the use of a ubiquitously expressed calcium indicator suggested there are no differences in the generation or spread of this initial wound signal. This is consistent with results seeing no difference in wound responses at the macrophage level, suggesting loss of *amo* does not impact this response. Though one could have expected *amo* to be involved in this process, owing to its function as a calcium-permeable cation channel, there is no evidence to suggest

that it is expressed in the epithelia, or even in the embryonic stages at all, with previous studies failing to detect *amo* mRNA earlier than larval stages (Watnick et al., 2003). This, however, does seem to go against the reported requirement for *amo* in embryonic efferocytosis (Van Goethem et al., 2012), with this reported phenotype suggesting that *amo* must be expressed during embryonic stages. It is therefore possible that, assuming *amo* is indeed expressed in embryonic stages, transcript levels are too low to be detected by reverse-transcript PCR or *in situ* hybridisation.

### 4.3.3 The role of *amo*/*PKD2* in efferocytosis

The use of a genetically-encoded Caspase-3 indicator showed no apparent differences in the phagocytic index of *amo* mutant and control macrophages at stage 15, despite a 50% reduction in PI having previously been reported when using acridine orange to label apoptotic cells (Van Goethem et al., 2012). The majority of developmental apoptosis and efferocytosis in the VML occurs between stages 12 and 13 as glia and macrophages work in concert to shape the developing VNC (Evans et al., 2010), and by stage 15, macrophages with defective efferocytosis generally show differences in PI when compared to controls (Roddie et al., 2019; Shklyar et al., 2014). The fact that no difference was observed here suggests that *amo* is not in fact required for efferocytosis.

For my experiments, a genetically-encoded Caspase-3 activity indicator was used to label apoptotic cells (Schott et al., 2017), in contrast with the Acridine Orange (AO) staining used by Van Goethem *et al.*. It is therefore possible that failures to replicate the phenotype could be due to the use of a different approach to label apoptotic cells. However, a genetically-encoded caspase 3 activity indicator is arguably going to offer a more effective readout of efferocytosis specifically, compared to AO which simply labels acidified intracellular compartments (Thomé et al., 2016). The differences in the phagocytic index of *amo* mutant macrophages reported by Van Goethem et al. could therefore be due to decreased acidification of phagosomes in *amo* mutants, as opposed to impaired efferocytosis. Non-acidified phagosomes would not be labelled via AO staining, so it is possible that *amo* mutant macrophages are as capable at

phagocytosing apoptotic cells as control cells, and that the phenotype reported by Van Goethem et al. may be a false positive.

Alternatively, it is possible that Van Goethem et al. identified a novel requirement for Amo in autophagy, as AO staining would label acidified autophagosomes i.e., phagosomes formed during autophagy. Recent work has shown a requirement for *PKD2* in autophagy in human cell lines (Peña-Oyarzun et al., 2021); it is therefore possible that the results seen by Van Goethem et al. (suggesting a decreased PI in *amo*$^{1}$ macrophages) are in fact indicative of fewer autophagosomes within these macrophages, although this is somewhat speculative.

Further evidence suggesting there is no difference in efferocytosis between control and *amo* mutant macrophages can be gleaned by looking at expression levels of reporters driven *croquemort-GAL4*. Expression of *croquemort* is upregulated in response to apoptotic cell engulfment (Zheng et al., 2021), so failures in efferocytosis result in less activity of this promoter and therefore less *crq-GAL4* dependent expression of *UAS* reporters. The fact that both *UAS-GFP* and *UAS-cd4tdTomato* express highly when driven by *crq-GAL4* control in *amo* mutants suggests that activity of the *crq* promoter is no different in *amo* mutants than control embryos.

All the results discussed so far have investigated the role of *amo* in efferocytosis in the context of stage 15 embryos under basal levels of apoptosis and uncleared apoptotic cells. Compared to earlier developmental stages, there is relatively little efferocytosis at stage 15, although imaging macrophages at this stage can still reveal defects in efferocytosis (Roddie et al., 2019). Macrophages can be challenged with an increased apoptotic burden by introducing *repo* mutations (Armitage et al., 2020). There were no observable differences in the migration speed or vacuolation of *amo* mutant macrophages compared to controls in a *repo* mutant background. If *amo* was indeed required for effective efferocytosis, either at the engulfment or digestion stages, one would expect to see decreased or increased numbers of apoptotic vacuoles within macrophages when challenged by increased apoptotic cells. As there are no apparent differences between control and *amo* mutant macrophages, a requirement for *amo* in effective efferocytosis seems increasingly unlikely, or at the very least any defects are subtle enough for other macrophage functions to not be perturbed. The allele used for these

experiments, *amo*$^{1}$, contains a premature stop codon in exon 6 (Watnick et al., 2003), resulting in a truncated protein that would likely be targeted for nonsense-mediated decay; it is therefore highly unlikely that the lack of functional differences observed between control and *amo* mutant macrophages is due to *amo*$^{1}$ encoding a functional protein. Furthermore, the Arginine residue mutated in this allele resides in the middle of a stretch of ten amino acids conserved in *PKD2*, suggesting that this region of the protein is essential for its function.

The presence of null alleles has been known to result in physiological adaptation, which can lead to related genes compensating for the lack of the mutated gene (El-Brolosy & Stainier, 2017). It is therefore possible that the lack of any phenotypes seen in *amo*$^{1}$ mutants is due to compensatory changes that negate the loss of *amo* in this background. In order to fully determine this, *amo* could be knocked down using *GAL4/UAS* mediated RNAi in concert with *GAL80,* a temperature sensitive inhibitor of *GAL4* (Fujimoto et al., 2011). Allowing embryos to develop to stage 15 before heat shocking to remove GAL4 inhibition would therefore allow the effect of acute loss of Amo on macrophage function and behaviour to be investigated. However, perdurance of protein is likely to be an issue with this approach (persistence of protein, despite efficient targeting of mRNA), therefore a "knock sideways" approach or rapid targeted destruction (e.g., via nanobodies; Van et al., 2021) may be more suitable. These approaches would require new transgenics that were not practical in the timeline of this project. Furthermore, genetic compensation seems somewhat unlikely given the fact that the *amo*$^{1}$ allele was used by Van Goethem et al. when the requirement for Amo in efferocytosis was first proposed.

In the kidney, tubular epithelial cells are known to mediate efferocytosis in response to acute tissue injury via the expression of Kidney injury molecule-1 (KIM-1), a phosphatidylserine receptor (Ichimura et al., 2008). In order to test whether *PKD2* could be required in this process, an *in vitro* efferocytosis assay was developed using immortalised tubular epithelial cell lines. Phagocytosis of apoptotic neutrophils were compared between control cell lines and cell lines lacking functional *PKD2*, with no difference in PI reported in *PKD2* knockout lines. It is worth noting that the number of phagocytic events observed in these cell lines were remarkably low, reflective of tubular epithelia as 'non-professional' phagocytes. As such, it is difficult to conclusively say that epithelial-mediated efferocytosis is not *PKD2* dependent.

Expression of KIM-1 is significantly upregulated in response to acute kidney injury (Yang et al., 2015), so there may be insufficient basal expression of KIM-1 in UCL93 cells to confer an effective phagocytic phenotype on this cell line. Though UCL93 cells appeared to exhibit very low rates of efferocytosis, a similar assay carried out using MDMs showed much higher rates of efferocytosis. Given that *PKD2* has already been implicated in immune cell function (Magistroni et al., 2019), it would be of interest to investigate the phagocytic capacity of macrophages derived from type 2 ADPKD patients.

### 4.3.4 Final conclusions

Taken together, results presented in this chapter suggest that Amo is not in fact involved in efferocytosis in *Drosophila* under normal conditions. No defects in macrophage function typically associated with impaired apoptotic cell clearance were reported, nor was there any evidence of impaired clearance mediated via *amo* mutant macrophages. This is despite Amo having previously being reported to be involved in this process, and human *PKD2* known to be involved in immune cell functions (Magistroni et al., 2019; Van Goethem et al., 2012). It is possible that Amo may be involved in later stages of efferocytosis, such as the phagosome acidification/maturation stages, with disruption to this process insufficient to impair macrophage function *in vivo*.

However, there remains a wealth of evidence implicating apoptotic cells, immune cells, and inflammatory responses in the pathogenesis of ADPKD, and efferocytosis remains an attractive candidate pathway worth investigating with respect to this process (Cassini et al., 2018; Chen et al., 2015; Karihaloo, 2015). Though a causative role for Amo/PKD2 -mediated efferocytosis was not categorically identified in this study, this does not rule out efferocytosis as being involved in the pathogenesis of ADPKD. Work in the future should therefore investigate failures in efferocytosis in the context of higher models (namely mice), and also with respect to *PKD1* mutations, as well as *PKD2*.

# Chapter 5: Investigating specification of macrophage subpopulations in *Drosophila*

## 5.1 Introduction

Macrophage heterogeneity is a key feature of vertebrate innate immune systems, allowing macrophages to carry out their various functions in different microenvironments as both specialised, tissue-resident populations, and as monocyte-derived macrophages (Gordon & Taylor, 2005). These important functions include phagocytosis of pathogens, secretion of extracellular matrix, responding to wounds and removing apoptotic cells (Wynn et al., 2013). Historically categorised as being M1 or M2, being pro- and anti-inflammatory respectively, it is now widely accepted that macrophages exist on a 'spectrum' of activation states, wherein they are able to shift towards more pro- or anti-inflammatory phenotypes in response to different stimuli (Murray, 2017). Though the M1-M2 paradigm is largely considered outdated, pro- and anti-inflammatory macrophage populations are often still referred to as 'M1-like' and 'M2-like' respectively, with the former typically associated with enhanced wound responses and microbicide, whereas the latter are associated with more proliferative, pro-healing roles (Gordon & Martinez, 2010).

Pro-inflammatory, M1-like macrophages are stimulated by cytokines such as IFNγ (produced by $T_H1$ cells), or by the recognition of bacterial lipopolysaccharides (LPS) by Toll-like receptor 4 (TLR4) on the surface of naïve, non-polarised, macrophages and monocytes (Orecchioni et al., 2019). Cytokines such as interleukin-4 (IL-4) and IL-13 are known to inhibit the activation of macrophages to this pro-inflammatory state, and result in the establishment of 'alternatively activated', anti-inflammatory M2-like macrophages, which typically are associated with pro-healing behaviours, such as efferocytosis, the phagocytic clearance of apoptotic cells (Gordon & Martinez, 2010).

Aberrant polarisation of macrophages towards more pro- or anti-inflammatory activation states has been implicated in numerous chronic inflammatory diseases, such as COPD, which is associated with an increased population of M2-like macrophages, and atherosclerosis, whose progression is largely driven by M1-like macrophages (Bobryshev et al., 2016; Vlahos & Bozinovski, 2014). Interestingly, in the context of Autosomal Dominant Polycystic Kidney Disease (ADPKD), a relatively common genetic nephropathy, initiation of the disease is thought to be driven by pro-inflammatory M1-like macrophages, which then shift towards a more pro-proliferative, M2-like phenotype, further driving disease progression. This shows the pathological implications of aberrant macrophage polarisation, whilst also highlighting the importance of understanding the processes underlying this phenomenon (Cassini et al., 2018; Karihaloo, 2015; Karihaloo et al., 2011). Given the link between altered macrophage phenotypes and ADPKD, we sought to use the fly model to investigate how macrophage heterogeneity is affected upon loss of *amo/Pkd2* and manipulation of other pathways relevant to ADPKD, namely calcium signalling and apoptotic cell clearance.

The fruit fly *Drosophila melanogaster* has been used as a model organism for well over a century, and in relatively recent years has increasingly been used to understand innate immunity (Evans et al., 2003; Buchon et al., 2014; Wood and Martin, 2017). *Drosophila* possess three populations of blood cells, collectively known as hemocytes, the most abundant of which are plasmatocytes, highly migratory phagocytes representing the functional equivalent of the vertebrate macrophage. Crystal cells, which functionally resemble a cross between platelets and mast cells, and are required for melanisation during wound healing, and lamellocytes, large encapsulating cells which only differentiate in response to parasitic infection (Wood & Jacinto, 2007).

As mentioned above, plasmatocytes of the *Drosophila* innate immune system are functionally analogous to macrophages, and plasmatocyte will be used interchangeably with macrophage from now on. These cells carry out many of the same functions, such as responding to wounds, fighting infection and phagocytosing apoptotic corpses, and exploit similar machinery to vertebrate macrophages when carrying out these functions (Evans et al., 2013; Wood & Martin, 2017). Furthermore, they express various receptors homologous to those expressed on vertebrate macrophages, such as *croquemort (crq)*, homologous to the CD36 scavenger

receptor expressed on the cell surface of vertebrate macrophages, while transcription factors required for their differentiation, such as *serpent* (*srp*) are related to similar factors required in vertebrate systems (Franc et al., 1996; Winick et al., 1993).

Though plasmatocytes and vertebrate macrophages are clearly functionally analogous, a drawback of using plasmatocytes to model macrophage biology is the fact that historically they have been considered a homogenous population of cells, in stark contrast to the highly heterogeneous macrophages within vertebrates. The study of plasmatocyte function and behaviour *in vivo* however, hints at the presence of heterogeneity within these cells, as, for example, plasmatocytes exhibit a wide range of migration speeds during development, suggesting that some cells may have different programming enabling enhanced migration (Evans et al., 2013; Roddie et al., 2019). Furthermore, wounding the ventral midline (VML) of stage 15 embryos reveals some plasmatocytes that readily respond to sites of wounding while other cells at a similar distance to the wound site fail to respond equally, if indeed at all (Evans et al., 2015; Roddie et al., 2019).

Coates et al. followed up these behavioural differences by looking at the activity of non-coding enhancer elements in *Drosophila* in the publicly available Vienna Tiles array database (available at http://enhancers.starklab.org; Kvon et al., 2014). By investigating enhancers that appeared to be active in some plasmatocytes, but not all, they were able to identify functionally distinct subpopulations of plasmatocytes (Coates et al., 2021). These subpopulations behaved in a potentially pro-inflammatory manner, exhibiting an enhanced wound-response compared to the overall population, while also appearing to phagocytose fewer apoptotic cells (Coates et al., 2021). Interestingly, the authors showed that the pan-plasmatocyte overexpression of *cnx14D*, a gene whose ORF is located proximal to one of the non-coding enhancer elements (*VT62766*), enhances the wound responsiveness of the overall plasmatocyte population (Coates et al., 2021). *cnx14D* encodes Calnexin14D, a calcium-binding chaperone protein known to localise to the ER (Christodoulou et al., 1997). The fact that overexpression of this gene seems to enhance wound responsiveness in the fly potentially implicates ER-resident calcium stores in the establishment of this putative pro-inflammatory subpopulation.

This study also suggested the existence of plasticity and potentially polarisation within *Drosophila* plasmatocytes, as well as their heterogeneity. Mutations in the transcription factor *reversed polarity (repo*) result in an increased phagocytic burden placed upon plasmatocytes (Armitage et al., 2020), due to failures in the differentiation of glial cells, the other major efferocyte during embryogenesis (Shklyar et al. 2014; Sonnenfeld and Jacobs 1995; Xiong et al. 1994). It was shown that the presence of a *repo* mutation resulted in a striking, significant decrease in the relative numbers of plasmatocytes within subpopulations (Coates et al., 2021). This is consistent with these subpopulations potentially being pro-inflammatory, as apoptotic cell clearance is a typical anti-inflammatory behaviour. Furthermore, this also suggests that plasmatocytes may be capable of polarisation in response to their environment, with plasmatocytes polarising away from a pro-inflammatory phenotype in a high-apoptotic background, as evidenced by the decreased wound responsiveness of *repo* mutant plasmatocytes (Armitage et al., 2020). This potential polarisation could possibly be mediated by the prolonged exposure of plasmatocytes to find-me cues released by dying cells, a hypothesis which is supported by recent work showing how mis-expression of a putative find-me cue, the EGFR ligand sSpitz$^{cs}$, results in an impaired wound response (Tardy et al., 2021).

Further evidence of plasmatocyte heterogeneity is revealed at the transcriptional level, as well as the behavioural and phenotypic. Independent RNA sequencing (RNAseq) studies looking at larval hemocytes have been carried out, grouping together multiple clusters of plasmatocytes based on transcriptional profile similarities (Cattenoz et al., 2020; Tattikota et al., 2020). One of these studies compared transcriptional profiles between embryonic and larval plasmatocytes, further showing how plasmatocytes are more plastic than previously considered, with differential gene expression observed at these different developmental stages. The steroid hormone ecdysone is involved in changing plasmatocyte behaviour during *Drosophila* development (Regan et al., 2013; Sampson et al., 2013; Tan et al., 2014), so it too is a candidate involved in establishing functionally-distinct plasmatocyte subpopulations.

The above functional and transcriptional evidence clearly suggests that *Drosophila* macrophages (i.e., plasmatocytes) could in fact represent a heterogeneous population of cells, with the potential for both pro-inflammatory and anti-inflammatory subpopulations existing (Cattenoz et al., 2020; Coates et al., 2021; Tattikota et al., 2020). Exposure of macrophages to

apoptotic cells has been shown to cause a shift towards more anti-inflammatory phenotypes in vertebrates (Fadok et al., 1998), while in *Drosophila,* numbers of putative pro-inflammatory macrophages seem to decrease in mutants that place a high apoptotic burden upon macrophages (Coates et al., 2021). The fact that the polycystic kidney is associated with high levels of uncleared apoptotic cells and altered macrophage phenotype suggests that aberrant macrophage polarisation due to failures in efferocytosis may contribute towards the pathogenesis of ADPKD (Cassini et al., 2018; Peintner & Borner, 2017; Swenson-Fields et al., 2013).

Herein, I investigate the processes determining the fate of pro-inflammatory macrophage subpopulations within *Drosophila*, with a particular focus on the role of *amo/Pkd2*, efferocytosis and calcium signalling. Due to the unparalleled imaging capabilities of the *Drosophila* embryo, the majority of this work focuses on macrophages at this developmental stage. Various mutant *Drosophila* lines with impaired efferocytosis were investigated, while the *GAL4-UAS* system has also been exploited to manipulate certain signalling pathways, specifically within macrophages.

**N.b., the results in this chapter include and expand upon findings published as part of Coates et al., (2021), a publication on which I am second author.**

## 5.2 Results

### 5.2.1 Subpopulation macrophages show decreased rates of phagocytosis

*Drosophila* macrophages originate in the developing head around stage 10 of embryogenesis, and follow a stereotypical migration path across the embryo, with some macrophages infiltrating the germband while others migrate down the developing ventral nerve cord (VNC) from stage 12, removing apoptotic glia and neurons from the developing nervous system (Crozatier & Meister, 2007; Sonnenfeld & Jacobs, 1995). Efferocytosis is an anti-inflammatory behaviour, typically mediated by 'M2-like' macrophages, and there is marked variability in

phagocytosis between embryonic macrophages when counting numbers of phagocytic vacuoles as a proxy of phagocytosis, further suggesting heterogeneity within *Drosophila.* Coates et al., exhibited 4 distinct plasmatocyte subpopulations based on the activity of *VT-GAL4* enhancer trap lines: *VT17559, VT32897, VT57089* and *VT62766* (Coates et al., 2021; Kvon et al., 2014). These subpopulations exhibited an enhanced wound response and were also found to possess fewer of these phagosomal vacuoles. This shows that these subpopulations exhibit an impaired 'M2-like' behaviour as well as an enhanced 'M1-like' behaviour, further hinting that these subpopulations may be pro-inflammatory.

Though subpopulation macrophages exhibit a significant decrease in phagosomal vacuoles, it remains unclear whether this is due to decreased rates of efferocytosis by subpopulation macrophages, or slower processing of apoptotic phagosomes. In order to validate the apparent decrease in phagocytosis by subpopulation macrophages, efferocytosis was imaged dynamically using *UAS-GFP-MYC-2x-FYVE*. This reporter binds to the phospholipid PI3P on the surface of developing phagosomes and can therefore be used to visualise rates of phagocytosis live and *in vivo* (Wucherpfennig et al., 2003; Roddie et al., 2019). *UAS-GFP-MYC-2x-FYVE* was expressed specifically in subpopulations via the split-*GAL4* system, with the GAL4 activation domain being driven via the *serpent* promoter (*srp-AD)*, and the GAL4 DNA-binding domain driven via the VT enhancer (VT-DBD). Only in cells expressing both *srp*-AD and *VT-DBD* will a complete GAL4 protein form, and activate transcription of *UAS* transgenes (Coates et al., 2021; Pfeiffer et al., 2010).

Rates of *MYC-2x-FYVE*-positive phagosome formation were scored in stage 13 embryos (figure 5.1a-d) and compared to the overall macrophage population (with *UAS-GFP-MYC-2x-FYVE* driven via *srp-AD, srp-DBD;* figure 5.1e). Consistent with the decrease seen in terms of vacuole numbers, all 4 subpopulation macrophages exhibited decreased rates of phagosome formation when compared to the overall macrophage population, wherein split-*GAL4* transgenes under the control of the *serpent* enhancer region were used to drive expression of *UAS-GFP-MYC-2x-FYVE* (figure 5.1f). These results validate the decrease seen in raw vacuole numbers as being due to decreased rates of phagocytosis, while also further suggesting macrophage heterogeneity is conserved in *Drosophila*, as there are evidently macrophage subpopulations with differing levels of phagocytic capabilities. Furthermore, this is consistent with these

subpopulation macrophages potentially being more pro-inflammatory than the overall population, as efferocytosis is a typical anti-inflammatory behaviour.

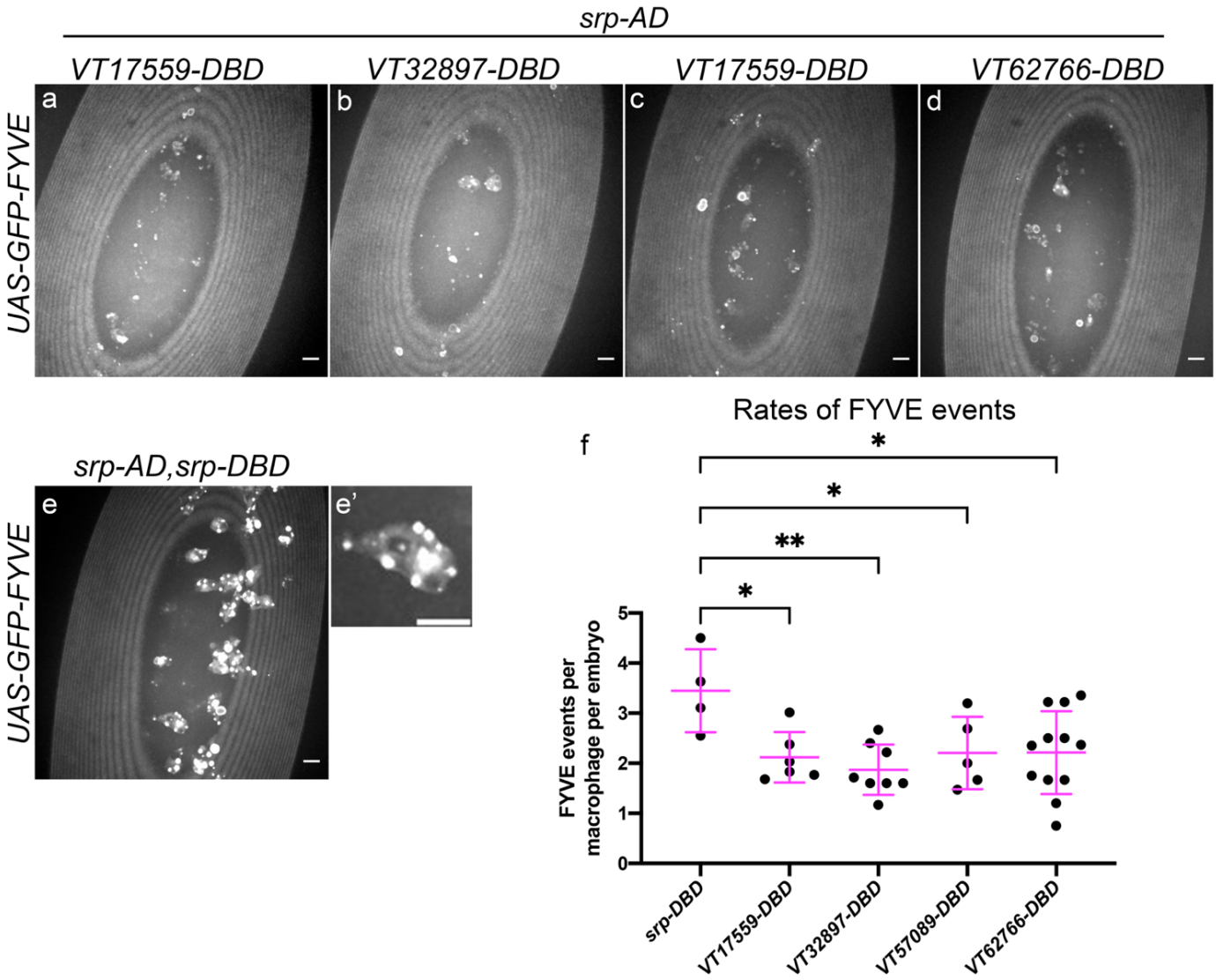


*Figure 5.1 – Subpopulation macrophages show decreased rates of efferocytosis*

(a-e) representative maximum projection images of the VML of stage 13 embryos showing nascent phagosomes labelled via *UAS-GFP-myx-2x-FYVE* either in subpopulation macrophages specifically (a-d) or the entire macrophage population (e). (e') example zoom of macrophage expressing *UAS-GFP-myx-2x-FYVE*. Note bright punctae, indicative of nascent phagosomes. Anterior is up on all images, scale bars indicate 10µm. (f) scatterplot showing the number of FYVE events per macrophage per embryo, wherein FYVE-GFP is recruited to early phagosomes. *n* = 4, 6, 8, 5 and 12, respectively. Statistical analyses carried out via one-way ANOVA with Dunnett's multiple comparison test. * and ** represent $p<0.05$ and $p<0.01$, respectively.

### 5.2.2 Overexposure of macrophages to apoptotic cells via loss of Simu does not cause a decrease in subpopulation macrophages

The macrophages associated with these non-coding (*VT-GAL4*) enhancer element were found to be more wound responsive than the overall macrophage population, whilst also exhibiting decreased rates of efferocytosis consistent with typically pro-inflammatory behaviours (Coates et al., 2021, **figure 5.1**). Loss-of-function mutations affecting the phosphatidylserine receptor Simu result in embryonic macrophages failing to effectively mediate efferocytosis, resulting in a build-up of uncleared apoptotic cells around the ventral midline (Roddie et al., 2019). This build-up of dying cells is sufficient to impair macrophage dispersal, migration and wound responsiveness, hypothesised to be due to the presence of 'find-me' cues released from uncleared corpses 'distracting' them, impairing these functions.

Wound responsiveness and migratory capacity are two typical pro-inflammatory behaviours. As these behaviours are both impaired in *simu* mutants, I sought to investigate the effect of this mutation on macrophage subpopulations, which are associated with these typically pro-inflammatory behaviours. *simu* mutations were therefore introduced, and the VML of stage 15 embryos was imaged. All macrophages were labelled via the *GAL4*-independent reporter *serpent-3x-mCherry* (Gyoergy et al., 2018) with subpopulation macrophages labelled via *UAS-eGFP* expression driven via the split-GAL4 system, allowing percentages of macrophages within subpopulations to be calculated. (**figure 5.2a-d'**).

Interestingly, none of the subpopulations exhibited decreased proportions in *simu* mutants, while there was actually an increased proportion of *VT57089* macrophages. *VT62766* macrophages also exhibited a trend suggesting a small, albeit non-significant, increase **(figure 5.2e)**. This suggests that exposure to excessive levels of apoptotic cells or their 'find-me' cues may not drive macrophages out of these subpopulations. Interestingly, this result actually contrasts with the situation in *repo* mutants, a high-apoptotic background, where there are decreased numbers of subpopulation macrophages, thought to be due to the high levels of apoptotic cells present in this genetic background (Coates et al., 2021). It is therefore possible that effective phagocytosis, or at the very least recognition of phosphatidylserine on apoptotic cell surfaces, is required for the effect seen in *repo* mutants.

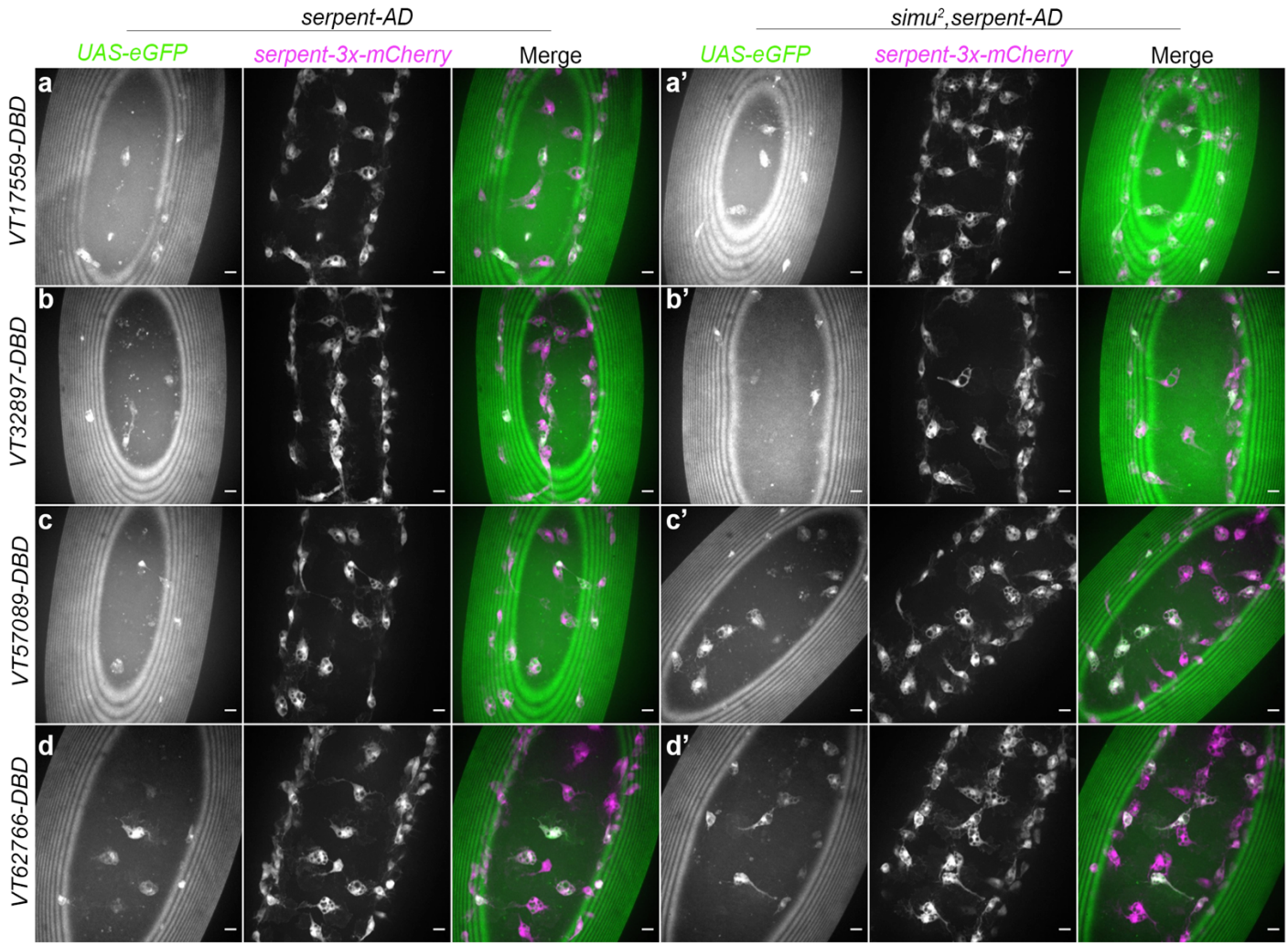
serpent-AD
simu2,serpent-AD
UAS-eGFP
serpent-3x-mCherry
Merge
UAS-eGFP
serpent-3x-mCherry
Merge
a
a'
b
b'
c
c'
d
d'
VT17559-DBD
VT32897-DBD
VT57089-DBD
VT62766-DBD

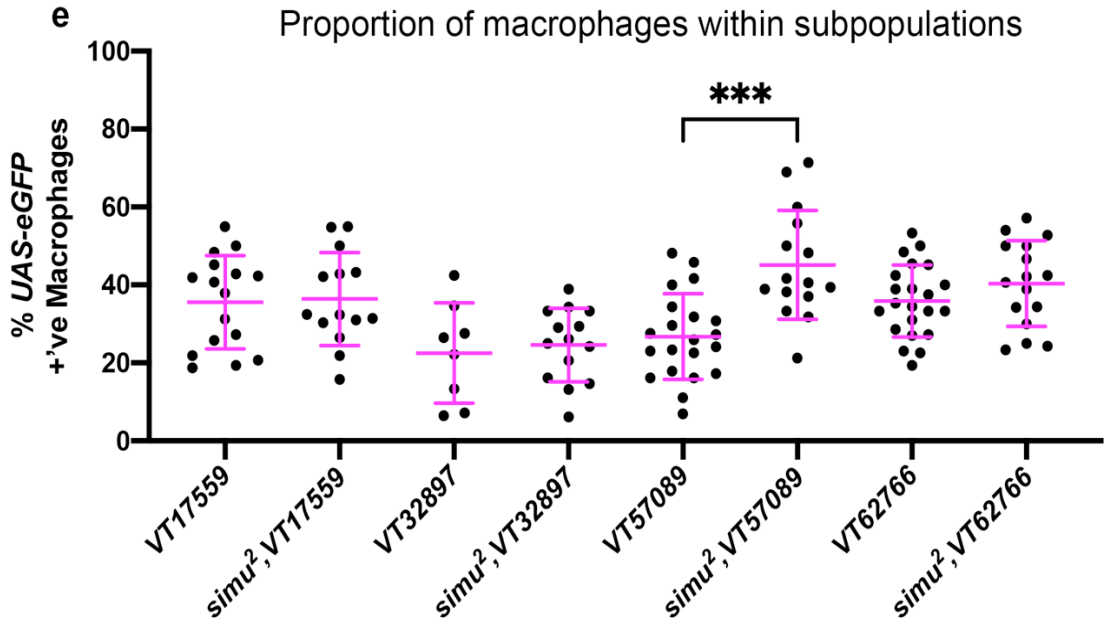
e
Proportion of macrophages within subpopulations
% UAS-eGFP +'ve Macrophages
100
80
60
40
20
0
***
VT17559
simu2;VT17559
VT32897
simu2;VT32897
VT57089
simu2;VT57089
VT62766
simu2;VT62766

*Figure 5.2 – Overexposure of macrophages to apoptotic cells is not sufficient to cause a decrease in pro-inflammatory subpopulations*

(a-d) representative images of the ventral midline of control (a-d) and *simu*$^{2}$ (a'-d') embryos at stage 15. *UAS-eGFP* shows macrophages labelled via split-*GAL4* (green in merge), while *serpent-3x-mCherry* labels every macrophage (magenta in merge). Anterior is up in all images, scale bars denote 10µm. (e) scatterplot showing proportion of macrophages within subpopulations in control and *simu*$^{2}$ embryos. *n*=16, 14, 8 ,14, 21, 15, 22 and 16, respectively. Only significantly different results shown on the graph (p=0.0003), all statistical comparisons carried out via non-paired t-tests. ***P<0.001.

### 5.2.3 *simu* is required for the decreased numbers of certain macrophage subpopulations seen in a *repo* mutant background

As well as macrophages, the other major phagocyte in the *Drosophila* embryo are glial cells of the developing nervous system (Sonnenfeld & Jacobs, 1995). These cells are specified in part by the transcription factor Repo, mutations in which place an increased apoptotic burden upon macrophages sufficient to impair their migration and wound responsiveness, while also causing decreased numbers within putative pro-inflammatory macrophage subpopulations (Halter et al., 1995; Shklyar et al., 2014; Armitage et al., 2020; Coates et al., 2021). Previous results suggest that the presence of high levels of apoptotic cells, due to loss of *simu*, is not sufficient to cause a decrease in the proportions of macrophages within subpopulations (**figure 5.2**). This suggests that the decreased proportions of subpopulations seen in *repo* mutants may depend on effective recognition and/or engulfment of apoptotic corpses via apoptotic cell receptors such as Simu.

Given the different results seen in *simu* and *repo* mutants in terms of macrophage subpopulations, *simu;repo* double mutants were made. This was with the intention of preventing *simu*-dependent efferocytosis in a *repo* mutant background and to block the decrease in subpopulations previously observed in *repo* mutants. The absence of *simu* does not result in a complete lack of efferocytosis, as shown by a modest but significant increase in phagosome number of *simu* mutant macrophages (Roddie et al., 2019). However, levels of uncleared apoptotic cells in *simu* mutant embryos are sufficiently high to disrupt macrophage dispersal, migration and wound responses, clearly showing how the absence of *simu* causes pathological levels of uncleared apoptotic corpses. The use of *simu* mutants should therefore

significantly impair the ability of macrophages to mediate efferocytosis, and potentially block the decreased number of subpopulation macrophages seen in *repo* mutants embryos.

Again, the VML of stage 15 embryos was imaged, with the total macrophage population being labelled via *serpent-H2A-3x-mChery*, while subpopulation macrophages were labelled with *VT-GAL4* driving expression of *UAS-stinger,* a rapidly maturing GFP variant that localises to the nucleus (Kvon et al., 2014; Barolo et al., 2018; Gyoergy et al., 2018). Proportions of macrophages within subpopulations were then calculated and compared between wild-type, *simu* single mutant, *repo* single mutant and *simu;repo* double mutant embryos.

Though all subpopulations were decreased in a *repo* mutant background (as per Coates et al.), the effect of loss of both *simu* and *repo* function was surprisingly variable between different subpopulations (figure 5.3a-d and 5.4a-d). *VT17559* and *VT32897* had similarly low numbers in *repo* and *simu;repo* double mutants, while both wild-type and *simu* single mutant controls had similar numbers (figure 5.3c-d). This suggests that the decrease in numbers within either of these subpopulations is not regulated by *simu*-mediated efferocytosis.

However, results were more interesting for subpopulations labelled via other VT lines: *VT57089*-labelled cells exhibited an increase in *simu* only mutants (consistent with results seen in figure 5.2e), and a similar increase was observed in *simu;repo* double mutants for this subpopulation (figure 5.4c). This increase was not significantly different from wild-type or *simu* only controls, but *simu* only controls were significantly higher than wild-type, suggesting that *simu;repo* double mutants have numbers somewhere in between these two controls. Finally, *VT62766*-labelled cells, which exhibited the largest decrease in their numbers in *repo* mutants relative to controls, also showed increased numbers in *simu* mutants relative to wild-type, similar to *VT57089* (figure 5.4d). However, unlike *VT57089* the increase seen in *simu* only mutants was not seen in *simu;repo* double mutants, which instead had almost identical numbers to *repo* single mutants. This increase in the *VT62766* subpopulation in *simu* only mutants was not seen in experiments described in 5.2.2, possibly due to those experiments having used *UAS-eGFP* to label subpopulation macrophages, as opposed to the more-sensitive

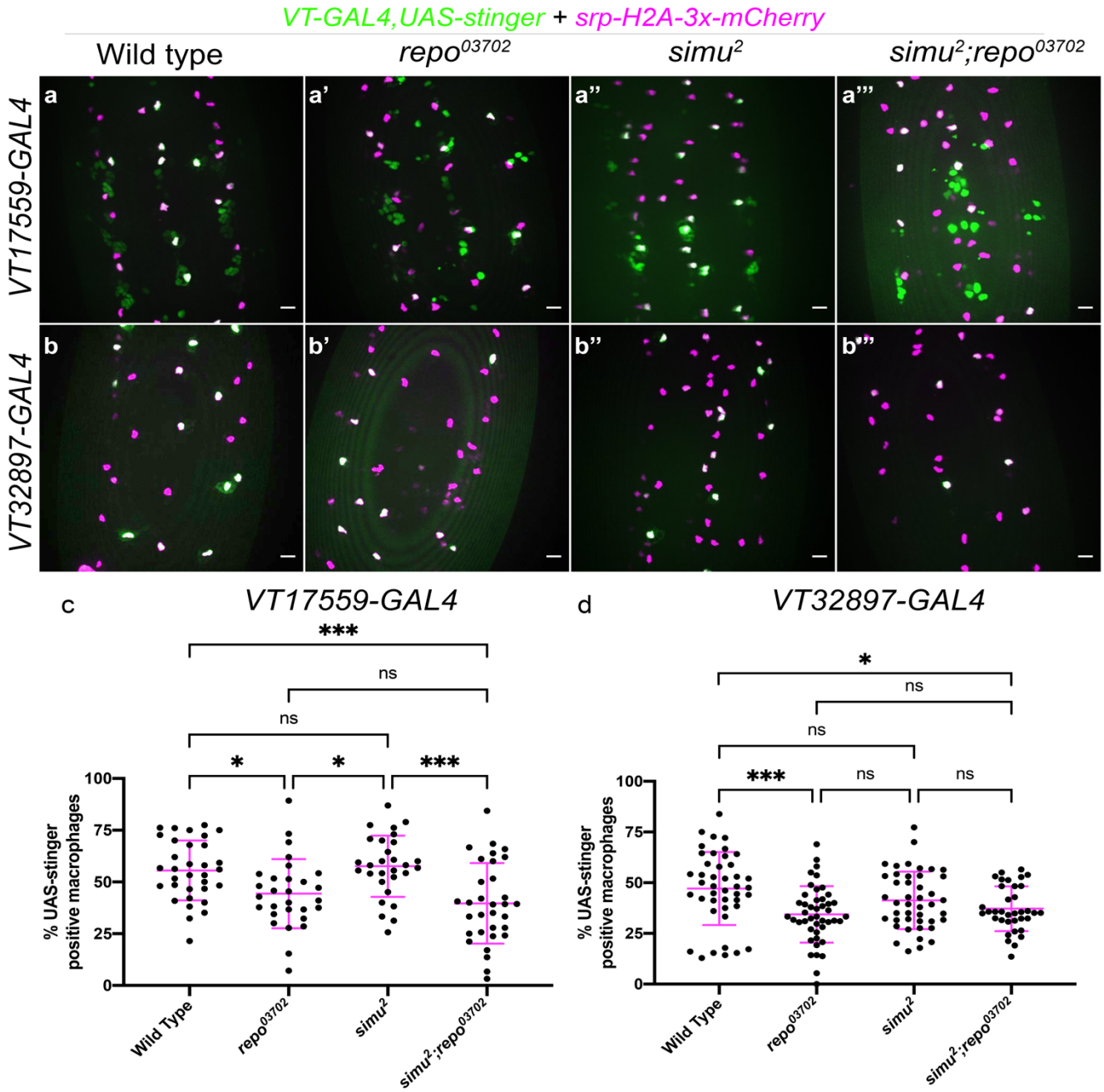


*Figure 5.3 – simu-dependent efferocytosis is not required for the shift out of the VT17559 or VT32897 subpopulations in repo mutants*

(a-b''') representative maximum projection images of the ventral midline of control (a-b), *repo*$^{03702}$ single mutants (a'-b'), *simu*$^{2}$ single mutant (a''-b'') and *simu*$^{2}$*;repo*$^{03702}$ double mutant (a'''-b''') embryos at stage 15. *UAS-stinger* shows subpopulation macrophages labelled via *VT-GAL4* (green in merge), while *serpent-H2A-3x-mCherry* labels every macrophage (magenta in merge). Anterior is up in all images, scale bars denote 10µm. (c) scatterplot showing proportion of macrophages within the *VT17559* subpopulation. *n*=33, 29, 29 and 32 respectively. (d) scatterplot showing proportion of macrophages within the *VT32897* subpopulation. *n*=44, 45, 43 and 36 respectively Statistical analyses carried out via one-way ANOVA with Dunnett's multiple comparison test. * , **and *** represent p<0.05, p<0.01, and p<0.001, respectively.

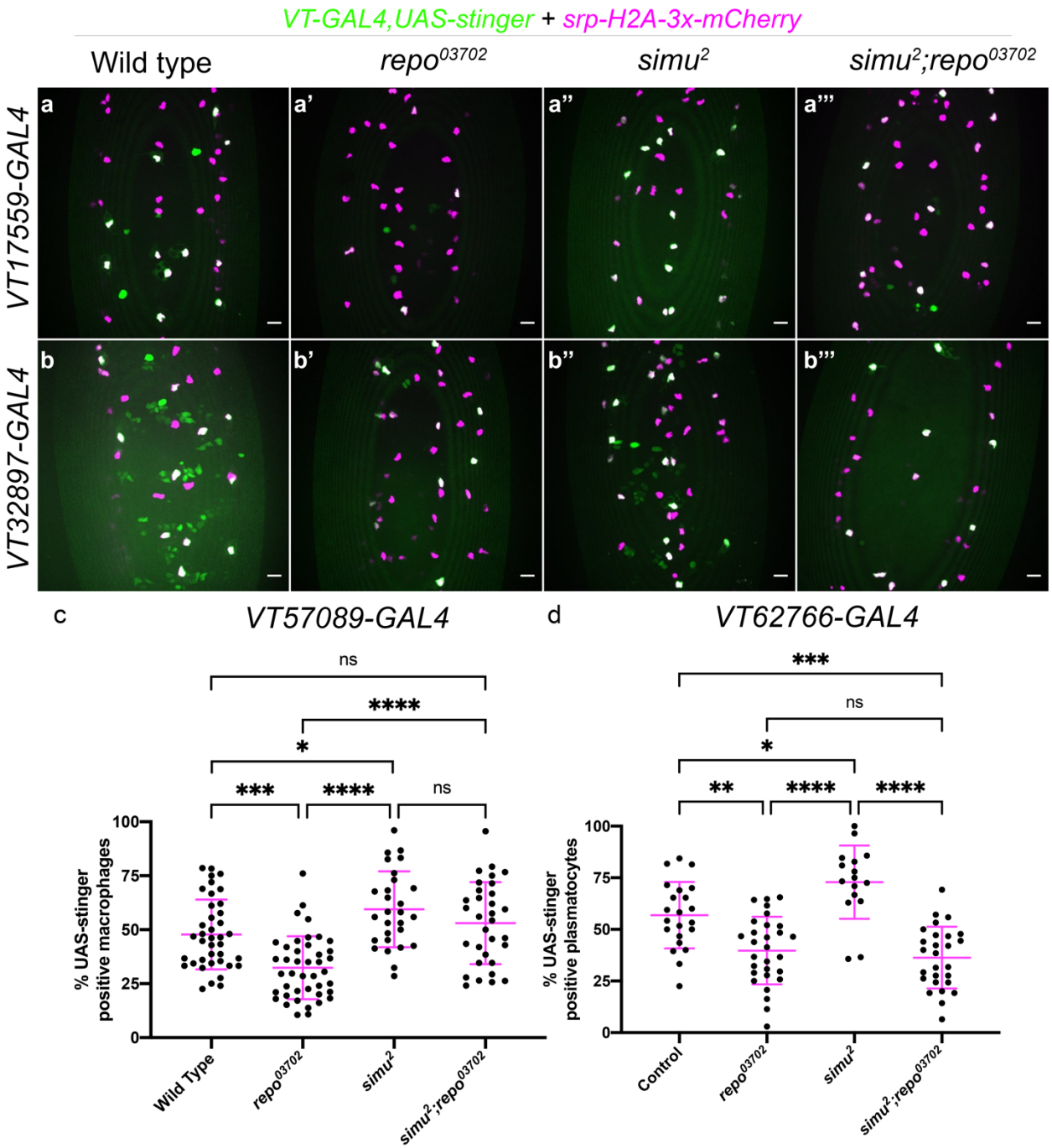


*Figure 5.4 – simu-dependent efferocytosis is required for the shift out of the VT57089 subpopulation in repo mutants, but not VT62766*

(a-b''') representative maximum projection images of the ventral midline of control (a-b), *repo*$^{03702}$ single mutants (a'-b'), *simu*$^{2}$ single mutant (a''-b'') and *simu*$^{2}$*;repo*$^{03702}$ double mutant (a'''-b''') embryos at stage 15. *UAS-stinger* shows subpopulation macrophages labelled via *VT-GAL4* (green in merge), while *serpent-H2A-3x-mCherry* labels every macrophage (magenta in merge). Anterior is up in all images, scale bars denote 10µm. (c) scatterplot showing proportion of macrophages within the *VT57089* subpopulation. *n*=39, 42, 28 and 32 respectively. (d) scatterplot showing proportion of macrophages within the *VT62766* subpopulation. *n*=22, 29, 16 and 27 respectively Statistical analyses carried out via one-way ANOVA with Dunnett's multiple comparison test. * , **, *** and **** represent p<0.05, p<0.01, p<0.001 and p<0.0001, respectively.

*UAS-stinger* that was used for subsequent experiments. Similarly, different drivers were used as the first set of experiments utilised split-*GAL4* drivers, instead of the *VT-GAL4* used in this experiment.

Overall, these results suggest that the decreased numbers of *VT17559, VT32897* and *VT62766* subpopulations seen in *repo* mutants is not due to *simu*-dependent apoptotic cell processing, as this decrease is still observed even when efferocytosis is hindered using *simu* mutations. Though both *VT57089* and *VT62766* exhibited significant increases in the absence of *simu*, the use of *simu;repo* double mutants, only retained numbers of *VT57089* macrophages suggesting that the decrease in this subpopulation exclusively is dependent on Simu-mediated efferocytosis. Furthermore, these differences also suggest that these subpopulations do not completely overlap with one another, and their regulation may be determined by distinct processes.

As mentioned above, efferocytosis is not completely blocked in a *simu* mutant background. It could therefore be the case that processing of apoptotic cells downstream of other apoptotic cell receptor dependent efferocytosis (e.g., *draper, croquemort)* is still causing the decreased numbers of *VT17559, VT32897* and *VT62766*-labelled cells in *repo* mutants, while decreases in *VT57089* may be specific to downstream processing of Simu-dependent efferocytosis. Alternatively, it is possible that interactions between glial cells and macrophages could be required for the specification of these subpopulations, with subpopulations failing to establish effectively in backgrounds lacking functional glial cells.

### 5.2.4 The calcium-permeable cation channel Amo is required for the decrease of *VT57089* subpopulation macrophages in a *repo* mutant background, and is involved in phagosome acidification

Given the fact that the results above show the phosphatidylserine receptor Simu is required for the decreased numbers of the potentially pro-inflammatory *VT57089* subpopulation seen in a *repo* mutant background, I sought to investigate whether molecular players downstream of Simu are involved in the decrease in macrophage numbers seen in this specific subpopulation. The calcium-permeable cation channel Amo/Pkd2 has previously been reported to be required for efferocytosis by embryonic macrophages in *Drosophila*, where it is

thought to be involved in the regulation of calcium homeostasis downstream of Simu (Van Goethem et al., 2012).

In order to investigate whether *amo* mutants cause a similar effect on the *VT57089* subpopulation as *simu*, a loss of function *amo* allele (*amo*$^{1}$; Watnick et al., 2003) was introduced and the VML of stage 15 embryos was imaged as previously. Again, *srp-3x-mCherry* was used to label all macrophages, while *UAS-eGFP* was driven via the split *GAL4* system to label *VT57089* subpopulation macrophages (figure 5.5a-b"). Unlike *simu* mutations, which exhibited an increased proportion of *VT57089* macrophages, no differences were observed between *amo* mutants and control embryos (figure 5.5c).

As *amo* mutants did not exhibit an increase in *VT57089* under normal conditions, I sought to investigate the effect of a high apoptotic challenge on the *VT57089* subpopulation in *amo* mutants. In order to see if *amo*$^{1}$ phenocopies *simu*$^{2}$ and prevents the decreased numbers seen in *repo* mutants, I crossed *amo*$^{1}$ into a *repo* mutant background to generate *amo;repo* double mutants. The ventral midline of stage 15 embryos was then imaged, and the raw number of *UAS-stinger* positive cells within the *VT57089* subpopulation in *amo;repo* double mutants was compared to the numbers seen in *repo* single mutants (figure 5.5d-e). As the genetics for this experiment did not permit for a pan-macrophage reporter to be present, embryos were imaged for 15 minutes and only cells clearly migrating (as one would expect of macrophages at stage 15) were counted.

Consistent with *VT57089* numbers in *simu;repo* double mutants (figure 5.4c), *amo;repo* double mutant embryos exhibited a significantly increased number of macrophages within the *VT57089* subpopulation when compared to *repo* single mutants (figure 5.5f), suggesting that *amo* could indeed be working downstream of Simu-dependent efferocytosis in preventing the establishment of this subpopulation. However, as mentioned above, these experiments lacked a pan-macrophage reporter. It is therefore possible that this result was simply due to an increase in the overall macrophage population, with no difference in the proportion of macrophages within the *VT57089* subpopulation.

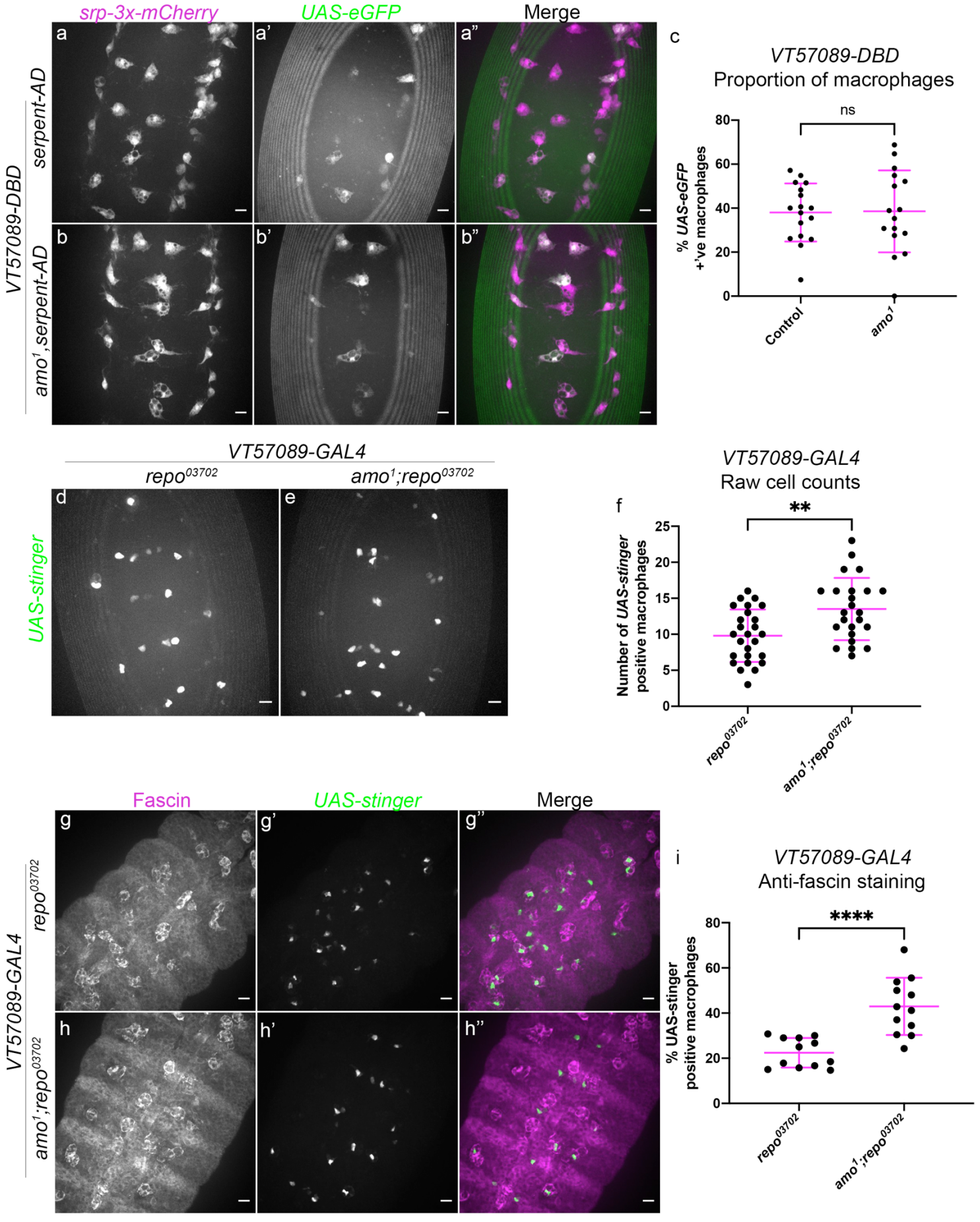
srp-3x-mCherry
UAS-eGFP
Merge
VT57089-DBD
serpent-AD
amo1,serpent-AD
a
a'
a"
b
b'
b"
c
VT57089-DBD
Proportion of macrophages
ns
% UAS-eGFP +'ve macrophages
Control
amo1
VT57089-GAL4
repo03702
amo1;repo03702
UAS-stinger
d
e
f
VT57089-GAL4
Raw cell counts
**
Number of UAS-stinger positive macrophages
repo03702
amo1;repo03702
Fascin
UAS-stinger
Merge
VT57089-GAL4
repo03702
amo1;repo03702
g
g'
g"
h
h'
h"
i
VT57089-GAL4
Anti-fascin staining
****
% UAS-stinger positive macrophages
repo03702
amo1;repo03702

*Figure 5.5 – The calcium permeable cation channel Amo is required for the shift out of the VT57089 subpopulation seen in repo mutants*

(a-b") representative images of the ventral midline of control (a-a") and *amo*$^{1}$ (b-b") embryos at stage 15. *serpent-3x-mCherry* labels every macrophage (magenta in merge – a,b), while *UAS-eGFP* shows *VT57089* macrophages labelled via *split-GAL4* (green in merge – a',b'). Anterior is up in all images, scale bars denote 10µm. (c) scatterplot showing the proportion of macrophages within the *VT57089* subpopulation in control and *amo*$^{1}$ embryos. *n*=17 and 16, respectively. (d-e) representative maximum projection images of the ventral midline of *repo*$^{03702}$ single mutant (d) and *amo*$^{1}$*;repo*$^{03702}$ double mutant (e) embryos at stage 15. *UAS-stinger* shows cells labelled via *VT57089-GAL4* (green). Anterior is up in all images, scale bars denote 10µm. (f) scatterplot showing the raw number of *VT57089* positive cells between *repo*$^{03702}$ single mutants and *amo*$^{1}$*;repo*$^{03702}$ double mutants. *n*=26 and 24 respectively. (g-h") representative maximum projection images of the ventral midline of *repo*$^{03702}$ single mutant (g-g") and *amo*$^{1}$*;repo*$^{03702}$ double mutant (h-h") embryos at stage 15. Macrophages have been labelled via Fascin staining (magenta in merge – g,h), with *VT57089* positive cells labelled via *UAS-stinger* (green in merge – g',h'). Anterior is up in all images, scale bars denote 10µm. (i) scatterplot showing proportion of macrophages within the *VT57089* subpopulation between *repo*$^{03702}$ single mutant (a) and *amo*$^{1}$*;repo*$^{03702}$ double mutant embryos based on anti-Fascin staining. *n*=12 and 13, respectively. Statistical analyses in (c) and (f) carried out via non-paired *t*-tests. Statistical analysis in (i) carried out via Mann-Whitney tests. ** and **** represent p<0.01 and p<0.0001 respectively.

In order to validate the apparent increase in the *VT57089* subpopulation seen in *amo;repo* double mutants, embryos were fixed and stained for Fascin, an actin-bundling protein enriched in macrophages (Zanet et al., 2009), allowing the proportion of macrophages within the *VT57089* subpopulation to be calculated (**figure 5.5g-h"**). Again, a significant increase was observed in *amo;repo* double mutants compared to *repo* single mutants, with *repo* single mutants having ~22% *UAS-stinger* positive macrophages, compared to ~43% for *amo;repo* double mutants (**figure 5.5i**), further suggesting an involvement of Amo in mediating the decrease proportion of *VT57089* subpopulation macrophages seen in *repo* mutants.

Despite *amo* mutants phenocopying *simu* and rescuing numbers within the *VT57089* subpopulation in a *repo* background, no changes were observed in a wild-type background (**figure 5.5c**). This possibly suggests that, though Amo is required downstream of Simu in efferocytosis, loss of *amo* only affects the ability of the macrophage to process apoptotic cells in a high apoptotic background (i.e., *repo* mutants), with any effects being subtle in a 'normal' apoptotic background. To test this hypothesis, acidified phagosomes were stained using Lysotracker Red, and the proportion of acidified phagosomes compared between *repo* single

mutants and *amo;repo* double mutants, with macrophages being labelled via *croquemort-GAL4,UAS-GFP* (figure 5.6a-c). This approach revealed that phagosome acidification was significantly lower in *amo;repo* double mutants compared to *repo* single mutant controls, suggesting that *amo* is in some part required for acidification, phagolysosomal fusion and/or phagosome maturation (figure 5.6d). Furthermore, this result suggests that signalling downstream of these processes, or indeed the processes themselves, could be required for programming of the *VT57089* subpopulation.

### 5.2.5 Loss of *simu* causes increased proportions of macrophage subpopulations in larvae

Previous results suggesting that the presence of uncleared apoptotic cells due to loss of Simu does not cause a decrease in putative pro-inflammatory subpopulations have so far only been carried out in the embryo. The fact that there is a significant increase in numbers within the *VT57089* subpopulation suggests that failures of macrophages to phagocytose apoptotic cells can result in increased numbers of pro-inflammatory macrophages. Though the *VT62766* subpopulation also appeared to exhibit a slight, albeit non-significant increase, two other putative pro-inflammatory subpopulations exhibited no such increase in the absence of Simu, suggesting that this might not be the case.

Embryos were imaged at stage 15, roughly 16 hours after egg laying, and roughly 8 hours after the differentiation of macrophages at stage 11. It may therefore be that certain subpopulations have not been exposed to signals from the uncleared apoptotic corpses caused by *simu* mutations for a sufficient period of time to cause an effect, be it an increase or a decrease in their proportions. In order to see the effect of prolonged exposure to apoptotic cells on macrophage subpopulations, *simu* mutant and control *Drosophila* were reared to the third larval instar stage (figure 5.7a-d'), and their hemocytes imaged *ex vivo*.

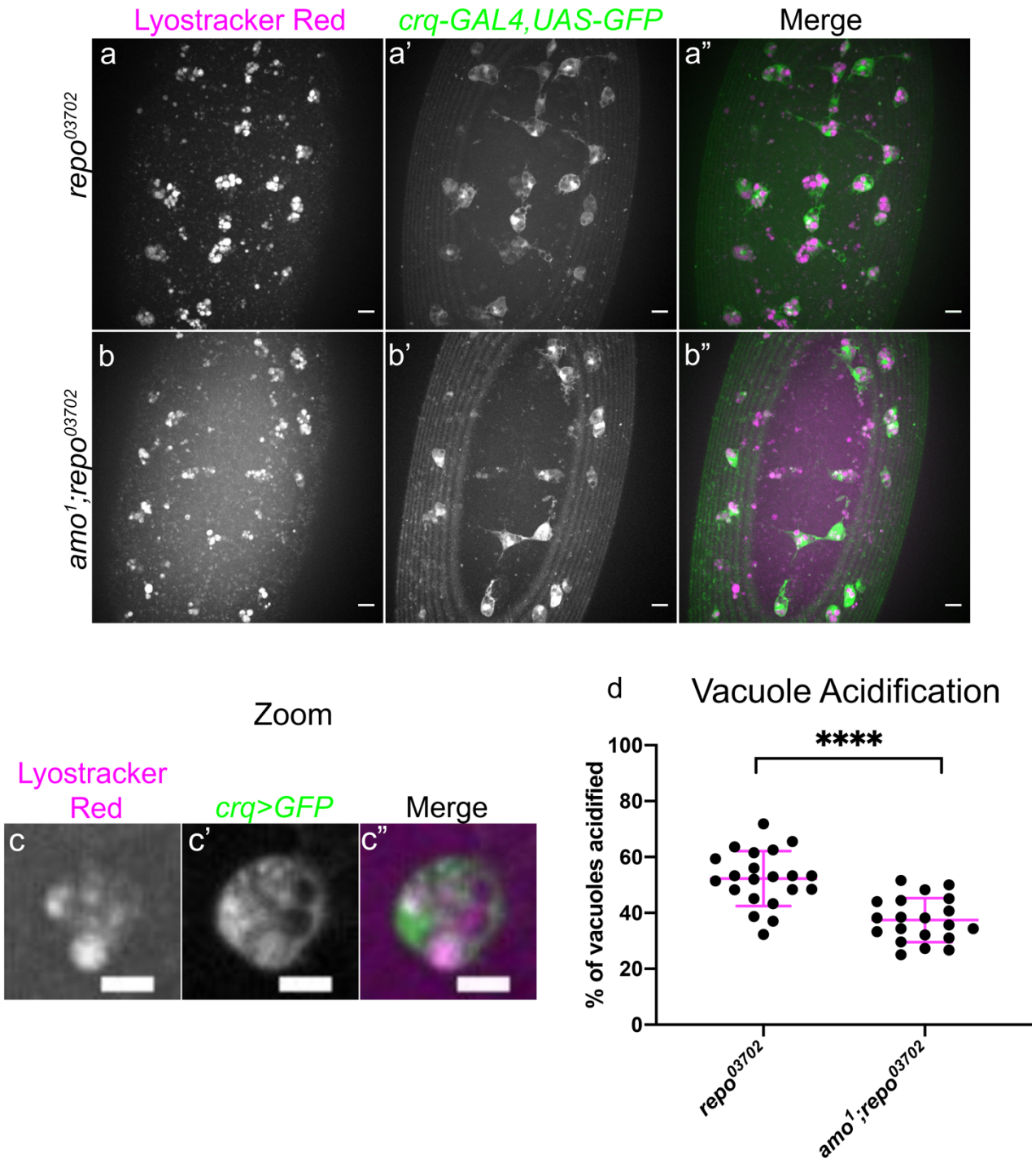


*Figure 5.6 – Amo is required for effective phagosome acidification*

(a-b") representative maximum projection images of the ventral midline of *repo*$^{03702}$ single mutant (a-a") and *amo*$^{1}$*;repo*$^{03702}$ double mutants (b-b"), embryos at stage 15. Lysotracker Red shows acidified phagosomes (a-b), while all macrophages are labelled via *crq-GAL4,UAS-eGFP* (a'-b') . Anterior is up in all images, scale bars denote 10µm. (c-c") zoom of a representative macrophage showing both acidified and non-acidified phagosomes. Scale bar denotes 5µm. (d) scatterplot showing proportion of vacuoles counted which were lysotracker red positive (i.e., acidified). *n*=21 and 20, respectively. Statistical analyses carried out via unpaired *t*-tests, **** represents p<0.0001.

We found that *VT62766*-labelled cells were present in significantly increased proportions in *simu* mutants relative to controls (**figure 5.7e**), consistent with this subpopulation being increased in *simu* mutant embryos (**figure 5.4d**). Another subpopulation, *VT32897* which was unaffected by *simu* mutations in the embryo (**figure 5.3d**), was also shown to be significantly increased in *simu* mutant macrophages *ex vivo* (**figure 5.7e**). Perhaps strangely, *VT57089*, which was significantly increased in *simu* mutant embryos (**figure 5.4c**), exhibited no significant increase in larval macrophages, although there was a trend hinting at a slight increase (**figure 5.7e**). Finally, *VT17559* showed no increase in *simu* mutants, and there was in fact a trend suggesting a decrease, though this was not significant (**figure 5.7e**).

### 5.2.6 Loss of *simu* causes increased proportions of macrophage subpopulations in the adult

Results from the previous sections show that the absence of *simu,* in both embryos and larvae, can cause significant increases in specific macrophage subpopulations, with all subpopulations other than *VT17559* exhibiting an increase in either the embryonic or larval stages in *simu* mutants. Though imaging macrophages of *simu* mutant larvae *ex vivo* allows the effect of long-term exposure of macrophage subpopulations to uncleared apoptotic cells to be characterised, comparatively little apoptosis and efferocytosis occurs during these developmental stages. Pupal development, however, is associated with high levels of apoptotic cell death during the gross tissue remodelling during metamorphosis (Jiang et al., 1997; Zirin et al., 2013). Interestingly, while larval development is associated with the largest decrease in subpopulation macrophage numbers, subpopulation cells return in large numbers in the pupa (Coates et al., 2021).

As pupal development takes place over 4-5 days, whereas embryogenesis takes less than 24 hours, imaging newly eclosed adult *Drosophila* allows the effect of much longer exposure of macrophages to apoptotic cells to be determined. Newly-eclosed virgin female adults of control and *simu* mutants were therefore collected and imaged at 1-day old, and the fluorescent intensity (mean gray value - MGV) of the fly was measured as a readout of numbers

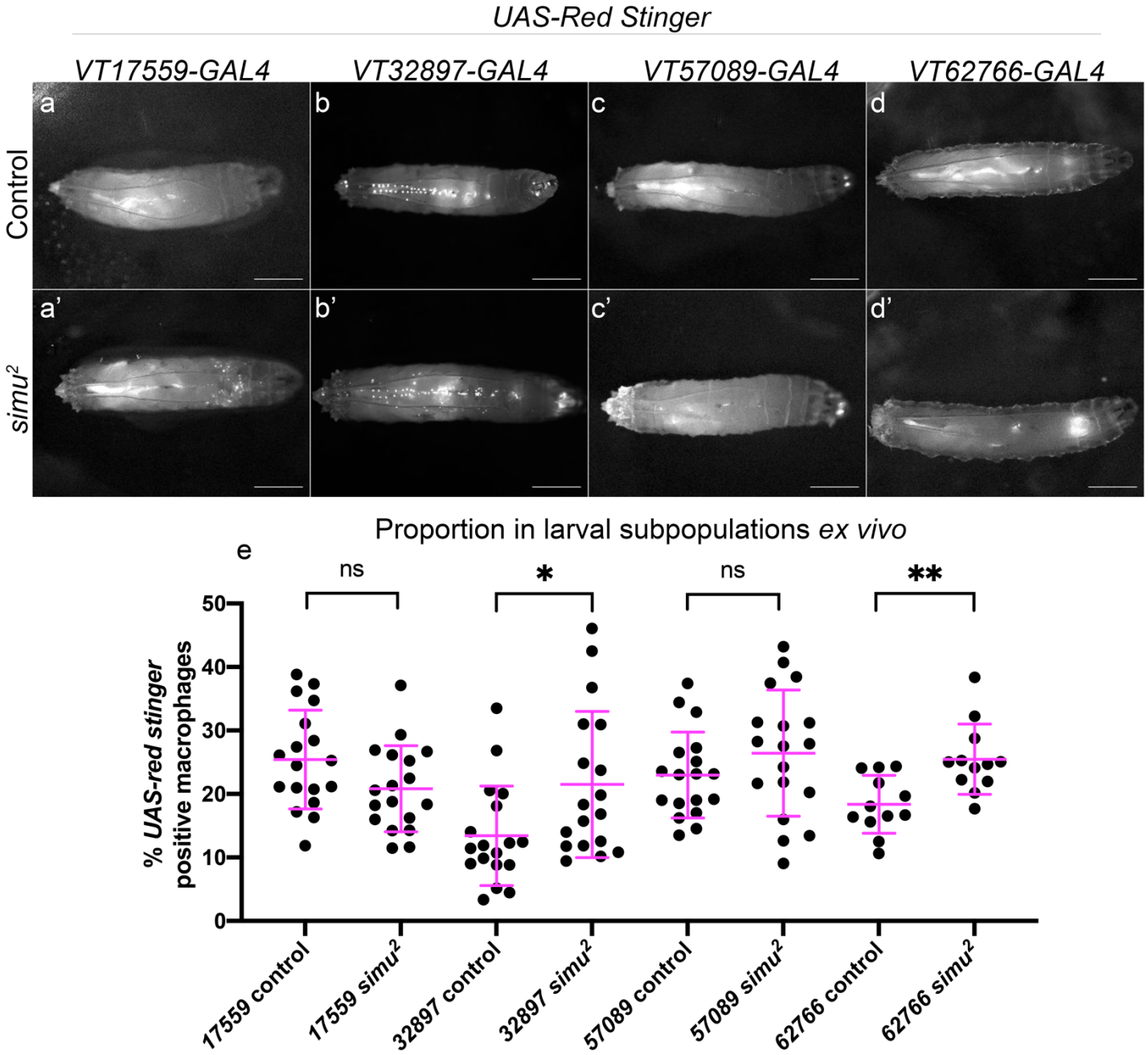


*Figure 5.7 – Loss of simu is associated with increased numbers in subpopulations in L3 larvae*

(a-d') representative images of L3 wandering larvae with subpopulation macrophages labelled via *VT-GAL4* driving *UAS-Red Stinger* in control (a-d) and *simu*$^2$ mutants (a'-d'). Scale bars denote 1mm. (e) scatterplot showing proportion of *ex vivo* macrophages within subpopulations of control and *simu*$^2$ mutant adult virgin females. *n*=18, 18, 18, 18, 18, 18, 18, 12 and 12 respectively. Statistical analyses carried out via unpaired *t*-tests, * and ** represent $p<0.05$ and $p<0.01$, respectively.

within each subpopulation. Subpopulation cells were labelled via *UAS-Red Stinger* driven by *VT-GAL4* (figure 5.8a-d').

Consistent with the increase seen in *VT57089* at embryonic stages, 3 of the 4 putative subpopulations exhibited a significant increase in MGV in *simu* mutants compared to wild type, with *VT57089* actually showing no significant difference although there was a trend suggesting a slight increase (figure 5.8e). However, the increased fluorescence seen in these adults does not necessarily equate to increased numbers within the subpopulations, as it could simply be a result of increased enhancer activity resulting in increased reporter levels within a single cell, or even due to increased non-macrophage *VT-GAL4* activity due to loss of *simu*. To address this, 1-day old virgin females were dissected to recover their blood cells, which were then fixed, allowing the proportions of macrophages within subpopulations to be calculated post staining (figure 5.8f). A significant increase in macrophages within the *VT17559* subpopulation was observed in *simu* mutants, while the *VT32897* subpopulation also showed an increase which was not statistically significant. The *VT57089* and *VT62766* subpopulations, which both contain substantially fewer macrophages than the other two subpopulations, exhibited no increase, with *VT62766* actually showing a small but significant decrease in *simu* mutants, despite an apparent increase when measuring MGV. However, this is possibly explained by the comparatively small numbers within this subpopulation, and the increased number of cells extracted from the hemolymph of *simu* mutants, which consistently had significantly more macrophages within the field of view than controls, suggesting a possible shift of macrophages away from tissue residency (figure 5.8g).

It has been shown that numbers of macrophages within these *VT* enhancers associated subpopulations decreases drastically as adult flies age, with macrophages largely disappearing from subpopulations within two weeks, the exception being *VT32897* cells which appear to persist (Coates et al., 2021). Previous results show that exposure of macrophages to high levels of apoptotic cells during development is capable of causing changes in the number of macrophages within certain subpopulations (figure 5.4c-d, figure 5.7e, figure 5.8e-f; Coates et al., 2021). Therefore, I sought to investigate whether prolonging apoptotic cell exposure results in subpopulation macrophages persisting for longer than usual. In order to achieve this, control and *simu* mutant virgin females were collected and aged for 4 weeks, before being imaged and

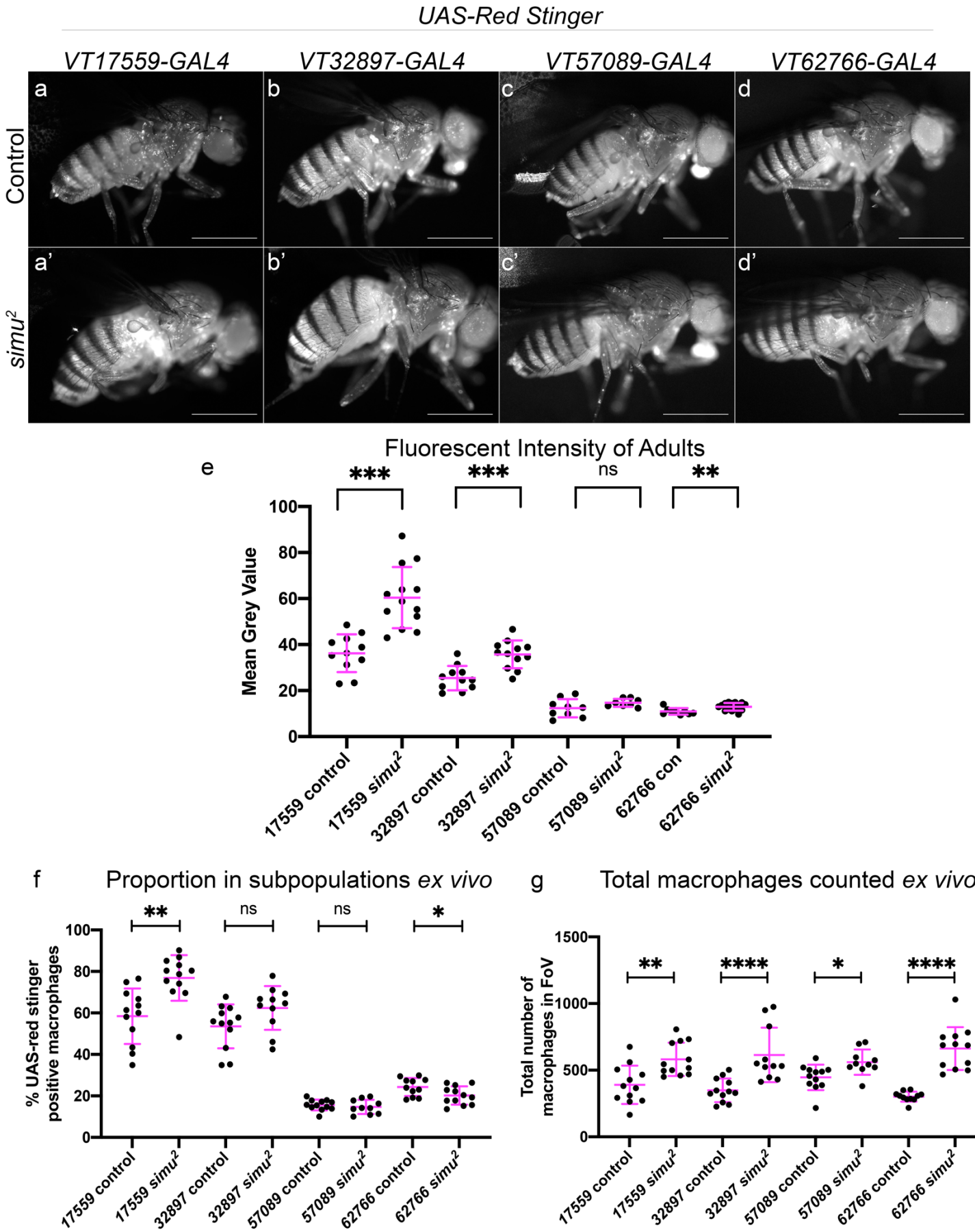
UAS-Red Stinger
VT17559-GAL4
VT32897-GAL4
VT57089-GAL4
VT62766-GAL4
Control
simu2
a
b
c
d
a'
b'
c'
d'
e
Fluorescent Intensity of Adults
Mean Grey Value
***
***
ns
**
17559 control
17559 simu2
32897 control
32897 simu2
57089 control
57089 simu2
62766 con
62766 simu2
f
Proportion in subpopulations ex vivo
% UAS-red stinger positive macrophages
**
ns
ns
*
62766 control
62766 simu2
g
Total macrophages counted ex vivo
Total number of macrophages in FoV
****
****

*Figure 5.8 – Loss of simu is associated with increased numbers in subpopulations in 1-day old adults*

(a-d') representative images of 1-day old adult virgin females with subpopulation macrophages labelled via *VT-GAL4* driving *UAS-Red Stinger* in control (a-d) and *simu*$^{2}$ mutants (a'-d'). Scale bars denote 1mm. (e) scatterplot showing mean grey values of control and *simu*$^{2}$ mutant adult virgin females. *n*=11, 13, 11, 12, 9, 8, 9 and 14, respectively. (f) scatterplot showing proportion of *ex vivo* macrophages within subpopulations of control and *simu*$^{2}$ mutant adult virgin females. *n*=12, 12, 12, 11, 12, 10, 11 and 12, respectively. (g) scatterplot showing the total number of *ex vivo* macrophages in the field of view between control and *simu*$^{2}$ mutant adult virgin females. *n*=12, 12, 12, 11, 12, 10, 11 and 12 respectively. Statistical analyses in (e-g) carried out via unpaired *t*-tests. *, **, *** and **** represent p<0.05, p<0.01, p<0.001 and p<0.0001, respectively.

quantified via their MGV (**figure 5.9a-d'**). A significant increase in MGV was observed in 2 of the 4 subpopulations (*VT17559* and *VT62766*) in *simu* mutants, while a third had a trend suggesting an increase (*VT57089*). However, these were only modest increases and images showed no dramatic increases of subpopulations in *simu* mutants compared to controls. These results suggest that, though there does appear to be still be an increase in subpopulations in these aged *simu* mutant adults, possibly due to the presence of uncleared apoptotic cells, this does not entirely prevent the disappearance of these subpopulations, which is generally observed from 1-2 weeks post eclosion (Coates et al., 2021).

### 5.2.7 Loss of *amo* causes increased proportions of macrophage subpopulations in the adult

Previous results show clearly that, in the absence of *simu*, there is a significant increase in the number of subpopulation macrophages in newly-eclosed adult *Drosophila*. The calcium-permeable cation channel Amo has been shown to be required downstream of Simu in order to mediate decrease in *VT57089* subpopulation seen in *repo* mutants, a background in which an increased phagocytic burden is placed upon macrophages. The effect of *amo* mutations on the decreased number of subpopulations seems to be dependent upon high levels of apoptosis, as no differences were observed between control and *amo* mutant embryos under basal apoptotic conditions (**figure 5.5c**). *repo* mutants are homozygous lethal, preventing the effect of *amo;repo* double mutants to be characterised at other developmental stages.

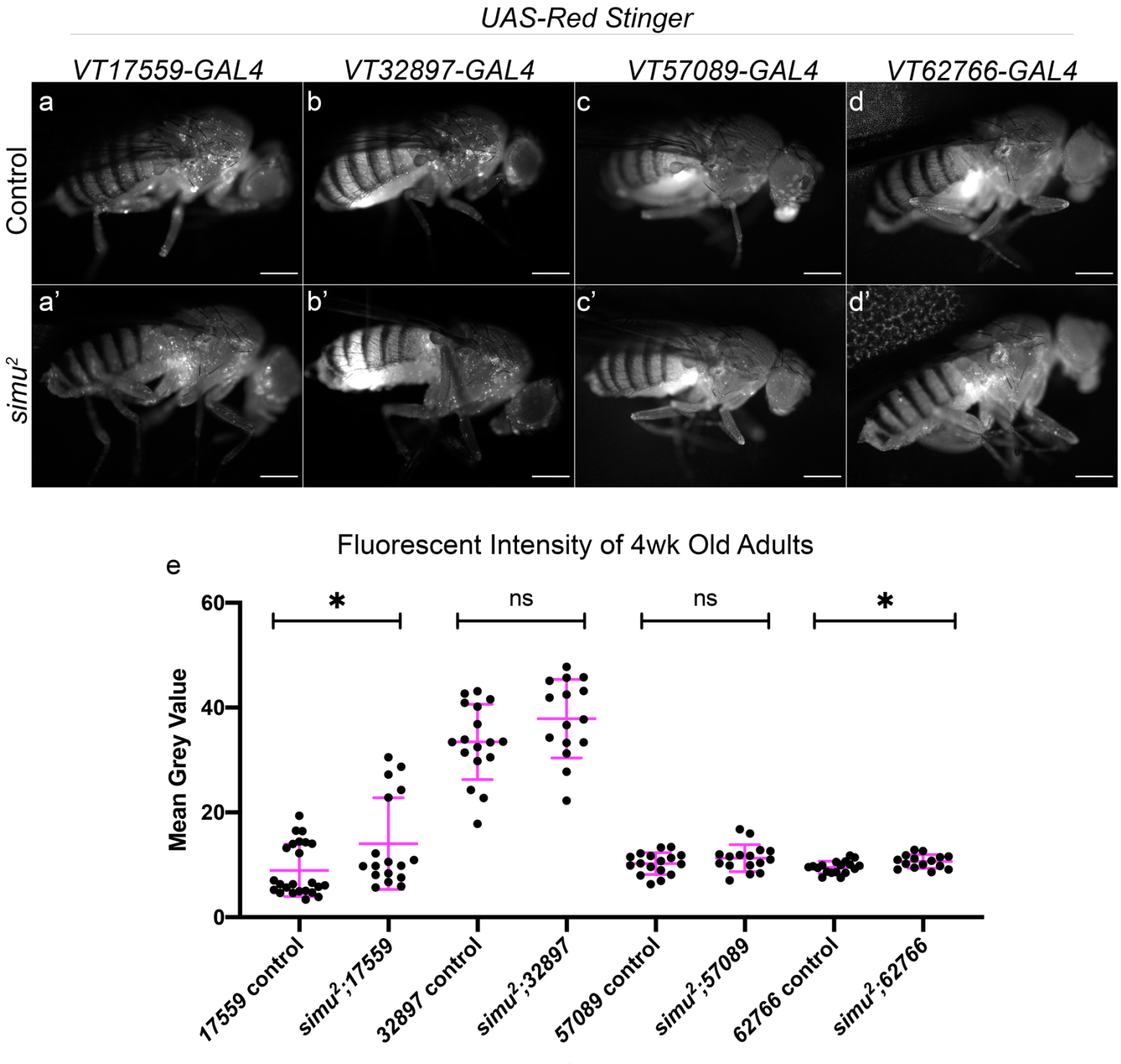


*Figure 5.9 – Loss of simu is associated with increased numbers in subpopulation macrophages in aged adults*

(a-d') representative images of 4 week old adult virgin females with subpopulation macrophages labelled via *VT-GAL4* driving *UAS-Red Stinger* in control (a-d) and *simu*$^2$ mutants (a'-d'). Scale bars denote 500µm. (e) scatterplot showing mean grey values of control and *simu*$^2$ mutant adult virgin females. *n*=24, 17, 17, 15, 17, 16, 18 and 15, respectively. Statistical analyses carried out via unpaired *t*-tests, apart from for *17559* which was not normal data and was therefore carried out via a Mann-Whitney test. * represents $p<0.05$.

However, during metamorphosis there are high levels of apoptosis as vast tissue remodelling takes place (Jiang et al., 1997; Zirin et al., 2013). As such, imaging *Drosophila* adults one-day post eclosion could offer the opportunity to investigate the effect of *amo* mutations on subpopulations following exposure to high levels of apoptotic cells at later stages of development.

As per section 5.2.4, 1-day old virgin female adults were imaged, and MGV measured as a readout of *VT-GAL4* activity (**figure 5.10a-d'**). Interestingly, the *VT17559* subpopulation exhibited a marked increase in fluorescence in the absence of Amo (**figure 5.10e**). This subpopulation was unchanged when attempting to rescue embryonic subpopulations using *simu;repo* double mutants, however there was a significant increase in both fluorescence and *ex vivo* macrophage counts in adult *simu* mutants, with a similar increase in fluorescence being observed in *amo* mutants. However, no other subpopulations exhibited any differences between *amo* mutants and controls, despite Amo previously having been shown to be required downstream of Simu in the departure of macrophages out of the *VT57089* subpopulation (**figure 5.5i**). It is therefore possible that macrophage subpopulations are regulated by different processes at different developmental stages of *Drosophila*, which each pose their own challenges to macrophages and hemocytes in general. Subpopulation macrophages generally seem to disappear during larval stages before re-emerging during pupation (Coates et al., 2021), and potentially the specification of embryonic subpopulations could be carried out by different mechanisms to those driving the subpopulations re-emergence during metamorphosis.

### 5.2.8 Expression of *Draper-II* does not affect macrophage subpopulation numbers in the embryo

Previous results suggest that *simu*-dependent efferocytosis typically removes macrophages from pro-inflammatory subpopulations, as loss of *simu* throughout development is associated with increased number of macrophages within the subpopulations. However, the use of *simu* mutants to try and rescue the decrease in subpopulation numbers seen in *repo* mutants only rescued numbers within the *VT57089* subpopulation. *simu* mutant macrophages exhibit a slight increase in their phagocytic index, suggesting other apoptotic cell receptors are capable

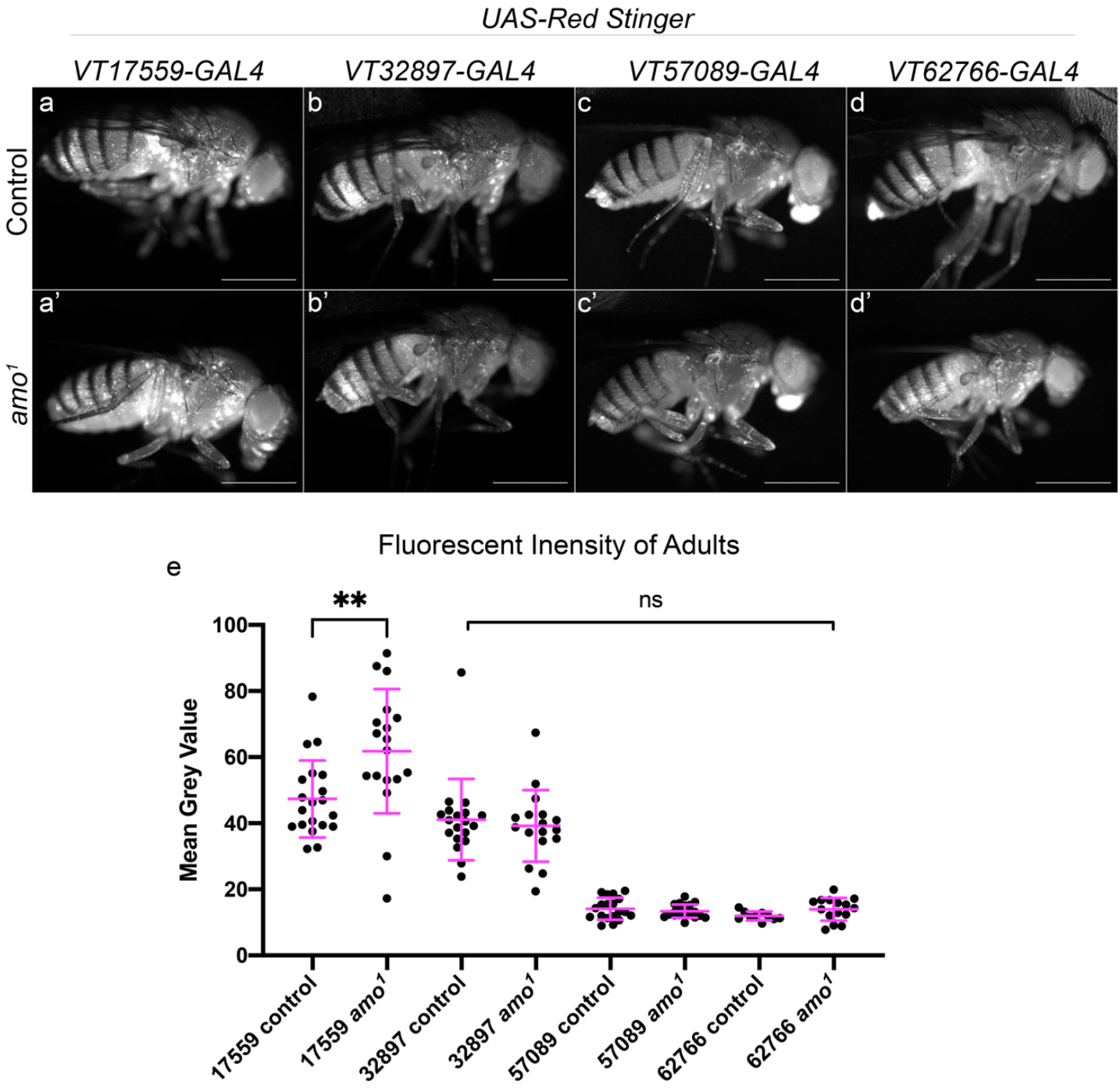


*Figure 5.10 – Loss of amo is associated with increased numbers in the VT17559 subpopulation in one-day old adults*

(a-d') representative images of 1-day old adult virgin females with subpopulation macrophages labelled via *VT-GAL4* driving *UAS-Red Stinger* in control (a-d) and *amo*$^{1}$ mutants (a'-d'). Scale bars denote 1mm. (e) scatterplot showing mean grey values of control and *simu*$^{2}$ mutant adult virgin females. *n*=20, 19, 18, 17, 19, 20, 10 and 15, respectively. Statistical analyses carried out via unpaired *t*-tests, apart from for *32897* which was not normal data and was therefore carried out via a Mann-Whitney test. ** represents p<0.01.

of compensating for the lack of Simu (Roddie et al., 2019). One such receptor is Draper-I, which is expressed by both macrophages and glia and is involved in the phagocytosis of apoptotic corpses. Draper-II is an alternative splice variant of Draper, known to be highly inhibitory towards Draper-I during later stages of the phagocytosis of apoptotic neurons (Logan et al., 2012). Macrophage-specific overexpression of *Draper-II* significantly impairs macrophage wound responsiveness and random migration in ways akin to *simu* mutations, showing that Draper-II can be used to block Draper-I mediated efferocytosis, and suggesting that this in turn causes levels of uncleared apoptotic cells sufficient to perturb macrophage function (Evans et al., 2015).

In order to investigate the effect of Draper-I inhibition on macrophage subpopulations, *UAS-Draper-II* was expressed in all embryonic macrophages via *serpent-GAL4* and *croquemort-GAL4*, and subpopulations were labelled via *GAL4*-independent *VT-RFP* reporters described in Coates et al., 2021 (figure 5.11-12 a-f). Pan-macrophage expression of *UAS-Draper-II* caused no effect on the number of macrophages within subpopulations in a wild-type background (figure 5.11-12, c and f).

I next decided to investigate whether Draper-mediated efferocytosis is required for the reduction in macrophage subpopulation numbers seen in *repo* mutants, and test whether Draper-I inhibition affects subpopulations in a background where macrophages face an increased apoptotic challenge. *repo* mutants are known to cause a decrease in subpopulation numbers; if Draper-I mediated efferocytosis is indeed required for this decrease, inhibition of Draper-mediated efferocytosis should prevent macrophages from effectively carrying out efferocytosis, thus retaining macrophages within the subpopulation. As such, Draper-I was inhibited via *UAS-draper-II*, but this time specifically within macrophage subpopulations, which were labelled via *VT-GAL4* and *UAS-stinger*, while all macrophages were labelled via *serpent-H2A-3x-mCherry*, in order to determine the percentage of macrophages within each subpopulation. When looking at proportions of macrophages within subpopulations, no differences were observed for any subpopulations between *repo* mutants with or without *UAS-draper-II* expression (figure 5.13-14 a-f). This therefore suggests that Draper-mediated efferocytosis, and indeed processes downstream of this, are not in fact responsible for the decrease in subpopulations seen in *repo* mutants.

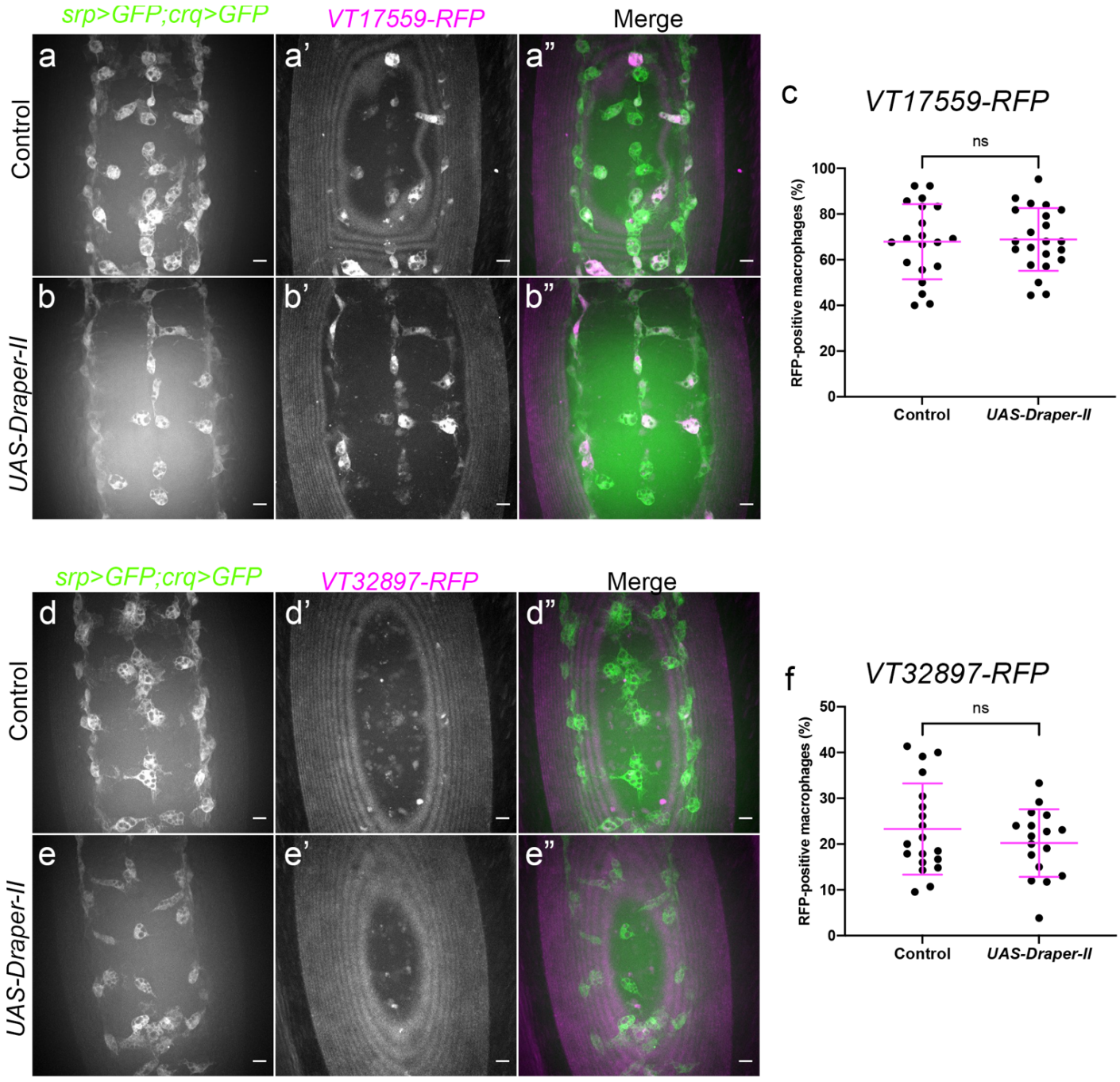


*Figure 5.11 – Pan-macrophage expression of Draper-II causes no effect on the VT17559 or VT32897 subpopulations*

(a-b", d-e") representative maximum projection images of the ventral midline of control embryos (a-a", d-d") and embryos expressing *UAS-Draper-II* specifically in macrophages (b-b",e-e"), at stage 15. Macrophages labelled via *srp-GAL4,UAS-GFP* and *crq-GAL4,UAS-GFP* (a,b,d,e) while subpopulation macrophages are labelled via *VT17559-RFP* (a',b') or *VT32897-RFP* (d',e'). Anterior is up in all images, scale bars denote 10µm. (c,f) scatterplot showing proportion of macrophages within the *VT17559* (c) and *VT32897* (f) subpopulations. (c) *n*= 20 and 22, respectively. (f) *n*= 19 and 17, respectively. Statistical analyses carried out via unpaired *t* tests.

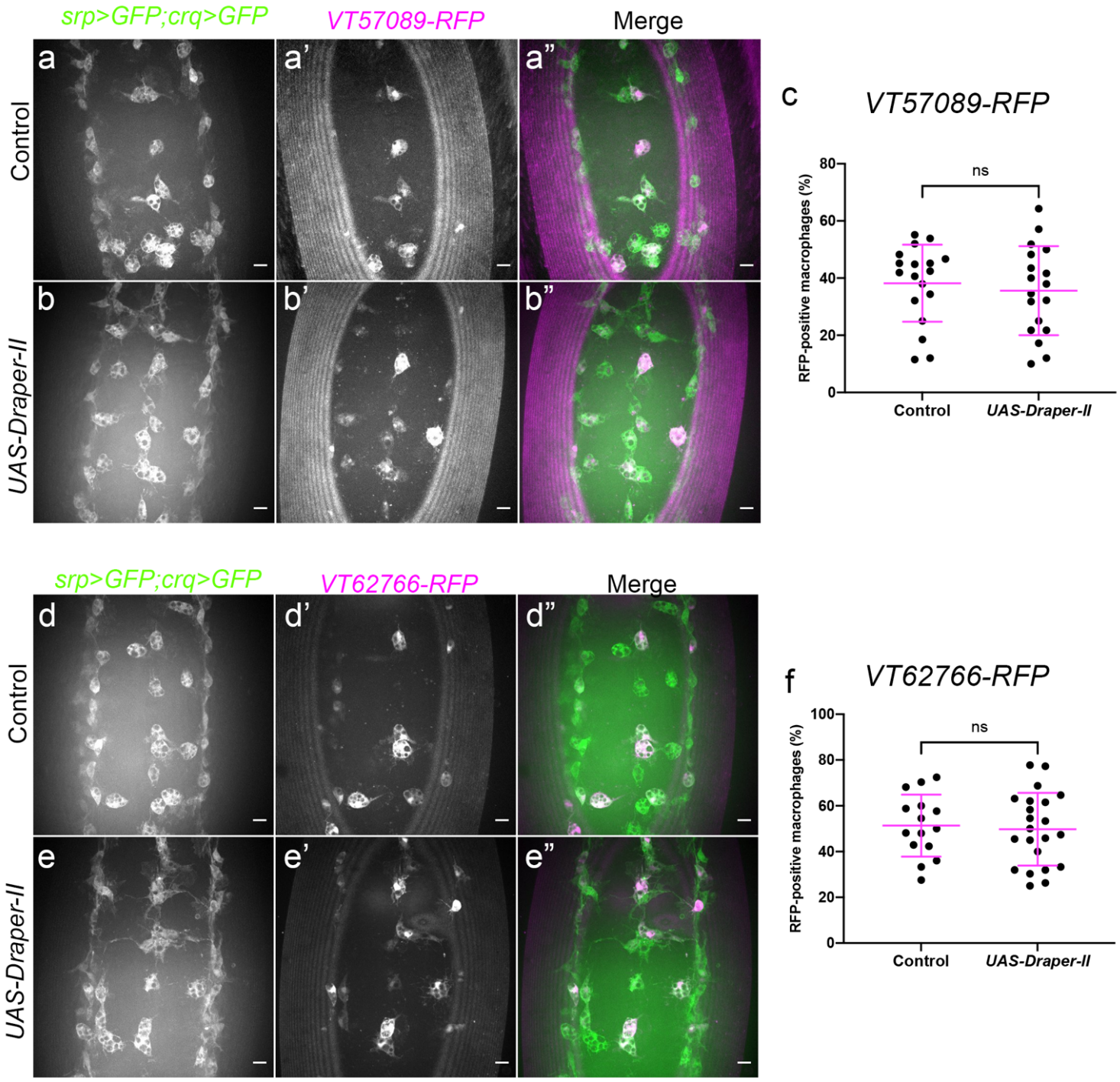


*Figure 5.12 – Pan-macrophage expression of Draper-II causes no effect on the VT57089 or VT62766 subpopulations*

(a-b", d-e") representative maximum projection images of the ventral midline of control embryos (a-a", d-d") and embryos expressing *UAS-Draper-II* specifically in macrophages (b-b",e-e"), at stage 15. Macrophages labelled via *srp-GAL4,UAS-GFP* and *crq-GAL4,UAS-GFP* (a,b,d,e) while subpopulation macrophages are labelled via *VT57089-RFP* (a',b') or *VT62766-RFP* (d',e'). Anterior is up in all images, scale bars denote 10µm. (c,f) scatterplot showing proportion of macrophages within the *VT57089* (c) and *VT62766* (f) subpopulations in the presence and absence of pan-macrophage *Draper-II* expression. (c) *n*= 18 and 18, respectively. (f) *n*= 15 and 22, respectively. Statistical analyses carried out via unpaired *t* tests.

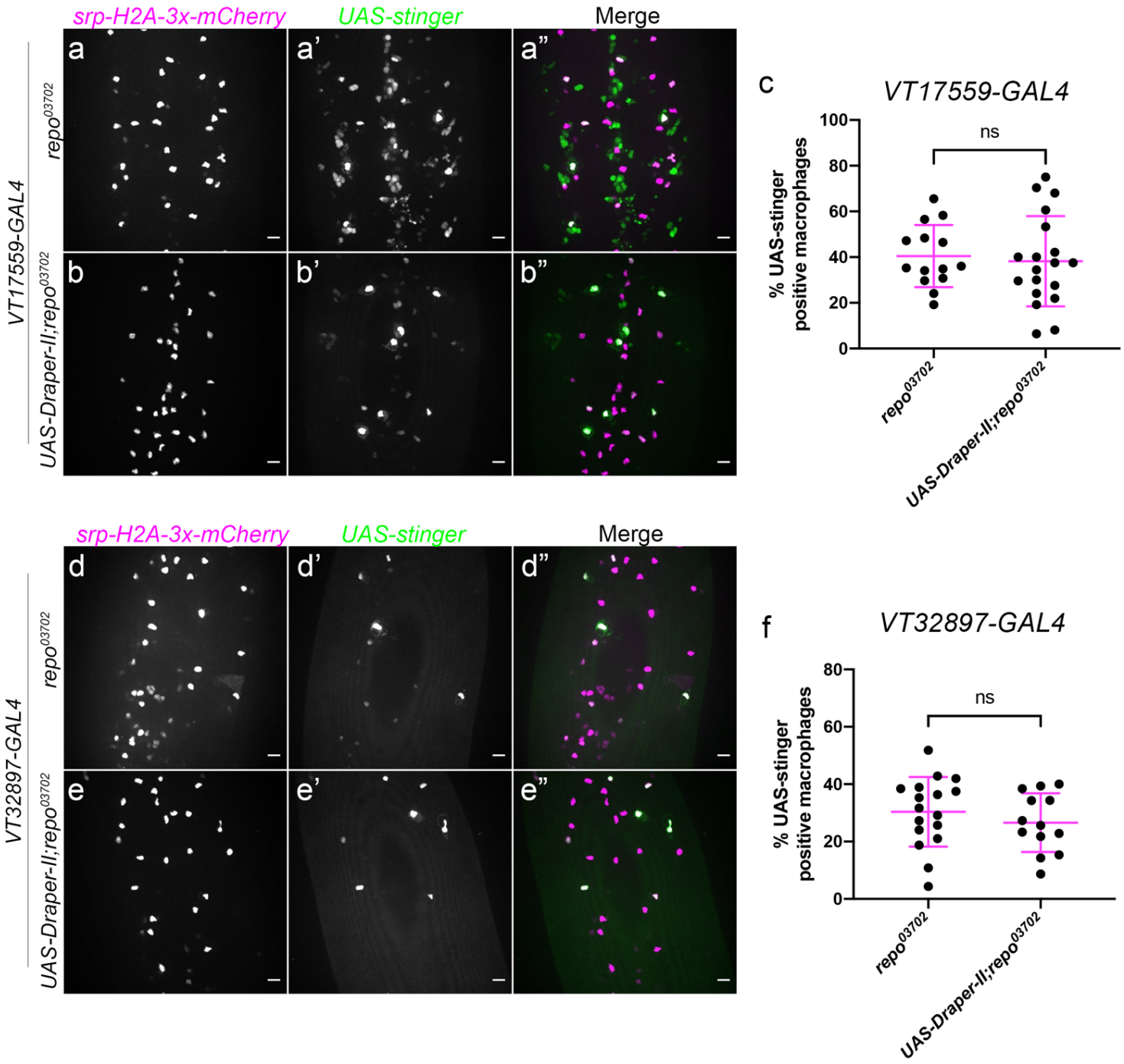


*Figure 5.13 – Subtype specific expression of Draper-II does not rescue the decrease in VT17559 and VT32897 subpopulation numbers caused by repo mutations*

(a-e") representative maximum projection images of the ventral midline of control *repo*$^{03702}$ mutant embryos (a-a", d-d") and *repo*$^{03702}$ embryos expressing *UAS-Draper-II* specifically in subpopulation macrophages (b-b",e-e"), at stage 15. Macrophages labelled via *srp-H2A-3x-mCherry* (a,b,d,e) while subpopulation macrophages are labelled via *UAS-stinger* driven by *VT17559-GAL4* (a',b') or *VT32897-GAL4* (d',e'). Anterior is up in all images, scale bars denote 10µm. (c,f) scatterplot showing proportion of macrophages within the *VT17559* (c) and *VT32897* (f) subpopulations. (c) *n*= 14 and 19, respectively. (f) *n*= 17 and 13, respectively. Statistical analyses carried out via unpaired *t* tests.

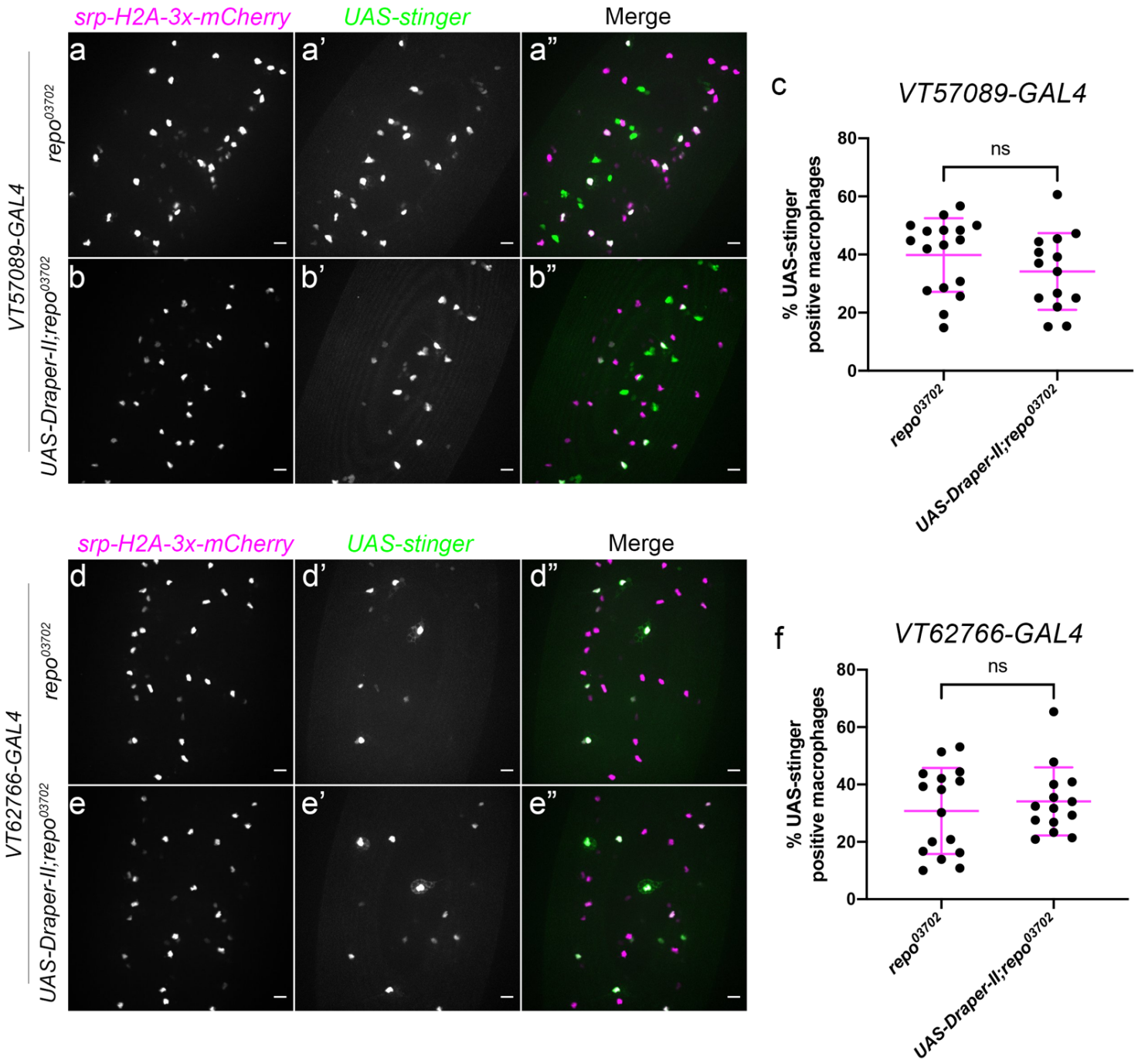


*Figure 5.14 – Subtype specific expression of Draper-II does not rescue the decrease in VT57089 and VT62766 subpopulation numbers caused by repo mutations*

(a-b",d-e") representative maximum projection images of the ventral midline of control *repo*$^{03702}$ mutant embryos (a-a", d-d") and *repo*$^{03702}$ embryos expressing *UAS-Draper-II* specifically in subpopulation macrophages (b-b",e-e"), at stage 15. Macrophages labelled via *srp-H2A-3x-mCherry* (a,b,d,e) while subpopulation macrophages are labelled via *UAS-stinger* driven by *VT57089-GAL4* (a',b') or *VT62766-GAL4* (d',e'). Anterior is up in all images, scale bars denote 10µm. (c,f) scatterplot showing proportion of macrophages within the *VT57089* (c) and *VT62766* (f) subpopulations. (c) *n*= 17 and 14, respectively. (f) *n*= 16 and 14, respectively. Statistical analyses carried out via unpaired *t* tests.

### 5.2.9 Loss of the scavenger receptor Croquemort does not rescue decreased subpopulation numbers seen in *repo* mutants

As well as Simu and Draper, there is a third major receptor expressed on macrophages required for the recognition and engulfment of apoptotic cells in the developing *Drosophila* embryo: Croquemort (Crq). Homologous to the mammalian CD36 scavenger receptor expressed on phagocytic blood cells, Crq is required for apoptotic cell phagocytosis by macrophages specifically, and its expression is known to be upregulated following efferocytosis (Franc et al., 1996, 1999; Zheng et al., 2021). A *crq* null mutation ($crq^{ko92}$; Guillo et al., 2016) was therefore used to investigate if this apoptotic cell receptor is required to cause the decrease in subpopulations seen in *repo* mutants, with proportions of macrophages within subpopulations being compared between *repo* single mutants and *crq;repo*. Subpopulation macrophages were labelled via *VT-GAL4* driving expression of *UAS-stinger*, while macrophages were labelled via anti-Fascin staining of fixed *Drosophila* embryos. No differences in subpopulation proportions were seen between *repo* single mutants and *crq;repo* double mutant embryos, suggesting that *crq*-mediated efferocytosis is not required for the decreased numbers of subpopulation macrophages seen in *repo* mutants (**figure 5.15-16 a-f**).

### 5.2.10 Misexpression of the EGF ligand $sSpitz^{CS}$, a putative find-me cue, within macrophages causes no effect on subpopulation proportions

During apoptosis, dying cells release so called 'find-me' cues in order to attract phagocytic cells, promoting their rapid, immunologically silent clearance via efferocytosis. Relatively recently, it was shown that replacement of dying cells in the adult *Drosophila* midgut is dependent on the release of epidermal growth factor (EGF) ligands to recruit stem cells to the locale of the apoptotic cells (Liang et al., 2017), implicating Spitz, the major EGF ligand during *Drosophila* embryogenesis, as a potential 'find me' cue in *Drosophila*. This was followed up by Tardy et al., who showed that the pan-macrophage overexpression of a secreted isoform of Spitz (*UAS-*$sSpitz^{CS}$) impaired wound responses and migration speeds of embryonic macrophages, suggesting that Spitz could indeed be a signal released by apoptotic cells (Roddie et al., 2019; Tardy et al., 2021).

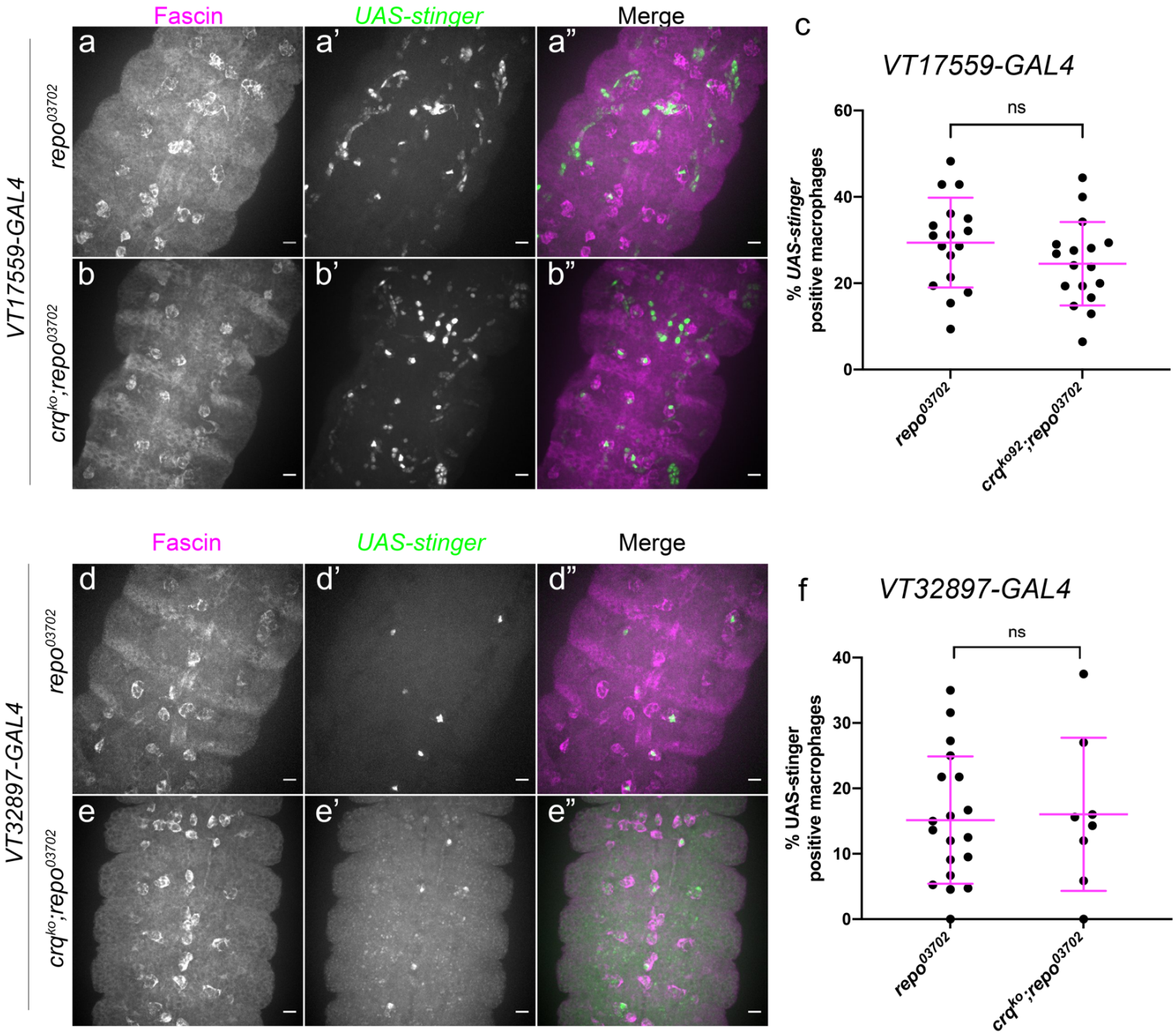


*Figure 5.15 – Loss of croquemort does not rescue the decreases in VT17559 and VT32897 subpopulation numbers seen in repo mutants*

(a-b",d-e") representative maximum projection images of the ventral midline of *repo*$^{03702}$ single mutant (a-a",d-d") and *crq*$^{ko}$*;repo*$^{03702}$ double mutant (b-b",e-e") embryos at stage 15. Macrophages have been labelled via fascin staining (magenta in merge), with subpopulation macrophages being labelled via *UAS-stinger* (green in merge) driven by *VT17559-GAL4* (a-b") or *VT32897-GAL4* (d-e"). Anterior is up in all images, scale bars denote 10µm. (c,f) scatterplot showing proportion of macrophages within the *VT17559* (c) and *32897* (f) subpopulations in *repo*$^{03702}$ single mutants and *crq*$^{ko}$*;repo*$^{03702}$ double mutants. (c) *n*= 17 and 17, respectively. (f) *n*= 19 and 8, respectively. Statistical analysis in (c) and (f) carried out via unpaired *t* tests.

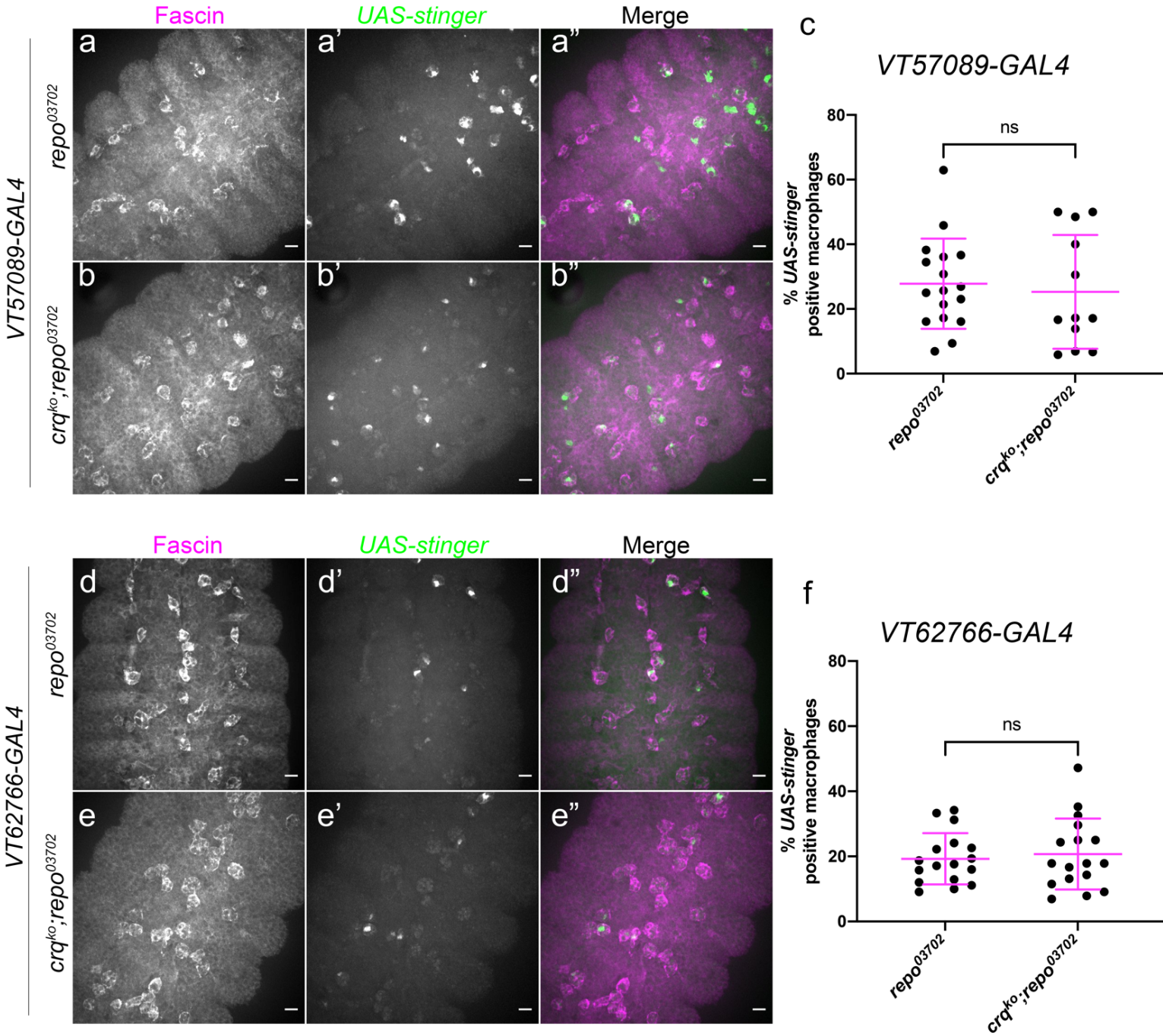


*Figure 5.16 – Loss of croquemort does not rescue the decreases in VT57089 and VT62766 subpopulation numbers seen in repo mutants*

(a-b",d-e") representative maximum projection images of the ventral midline of *repo*$^{03702}$ single mutant (a-a",d-d") and *crq*$^{ko}$*;repo*$^{03702}$ double mutant (b-b",e-e") embryos at stage 15. Macrophages have been labelled via fascin staining (magenta in merge), with subpopulation macrophages being labelled via *UAS-stinger* (green in merge) driven by *VT57089-GAL4* (a-b") or *VT62766-GAL4* (d-e"). Anterior is up in all images, scale bars denote 10µm. (c,f) Scatterplot showing proportion of macrophages within the *VT57089* (c) and *VT62766* (f) subpopulations in *repo*$^{03702}$ single mutants and *crq*$^{ko}$*;repo*$^{03702}$ double mutants. (c) *n*= 17 and 12, respectively. Statistical analysis carried out via Mann-Whitney test. (f) *n*= 17 and 17, respectively. Statistical analysis carried out via unpaired *t* tests.

In order to investigate the effect of this putative 'find-me' cue on macrophage subpopulations, *UAS-sSpitz$^{CS}$* was expressed in embryonic macrophages via *serpent-GAL4* and *crq-GAL4*, while subpopulation macrophages were labelled using *GAL4*-independent *VT-RFP* lines (Coates et al., 2021). As Spitz is known to impair the inflammatory wound response of *Drosophila* macrophages, it can be speculated that overexposure of macrophages to *UAS-sSpitz$^{CS}$* would result in decreased numbers within subpopulations. However, the overexpression of *sSpitz$^{CS}$* resulted in no change in proportion of macrophages within these subpopulations, suggesting that exposure to this cue does not affect subpopulations, despite defects in pro-inflammatory behaviours such as the wound response (**figure 5.17-18 a-f**).

### 5.2.11 Steroid hormone signalling is required for establishing the embryonic *VT62766* macrophage subpopulation

The *Drosophila* embryo, larva, pupa and adult each represent incredibly different environments. As such, as the organism passes through each developmental stage, the challenges faced by macrophage alter, and this is reflected in changes in macrophage behaviour. For example, during embryogenesis, macrophages are highly migratory and phagocytic, facilitating tissue shaping and organogenesis, whereas larval populations are found either circulating in the hemolymph or adhered to the body wall in sessile patches (Leitão & Sucena, 2015; Wood & Martin, 2017). In the context of *Drosophila* development and metamorphosis, the switching of macrophages between different phenotypes is influenced by the activity of the steroid hormone ecdysone (20-hydroxyecdysone) (Regan et al., 2013; Sampson et al., 2013; Tan et al., 2014). In order to test whether ecdysone is responsible for establishing subpopulation identity, a dominant negative isoform of the nuclear ecdysone receptor (*UAS-EcR-B1$^{\Delta C655}$* - hereafter referred to as *EcR-DN*) was expressed specifically in all macrophages via *serpent-GAL4* and *croquemort-GAL4*, with subpopulations labelled via *GAL4*-independent *VT-RFP* reporters and proportion of macrophages within subpopulations being calculated as per section 5.2.7.

The proportion of macrophages within 3 subpopulations exhibited no decrease when expressing *EcR-DN*, suggesting that ecdysone signalling is not responsible for establishing these subpopulations in the embryo. However, the *VT62766* subpopulation exhibited a significant

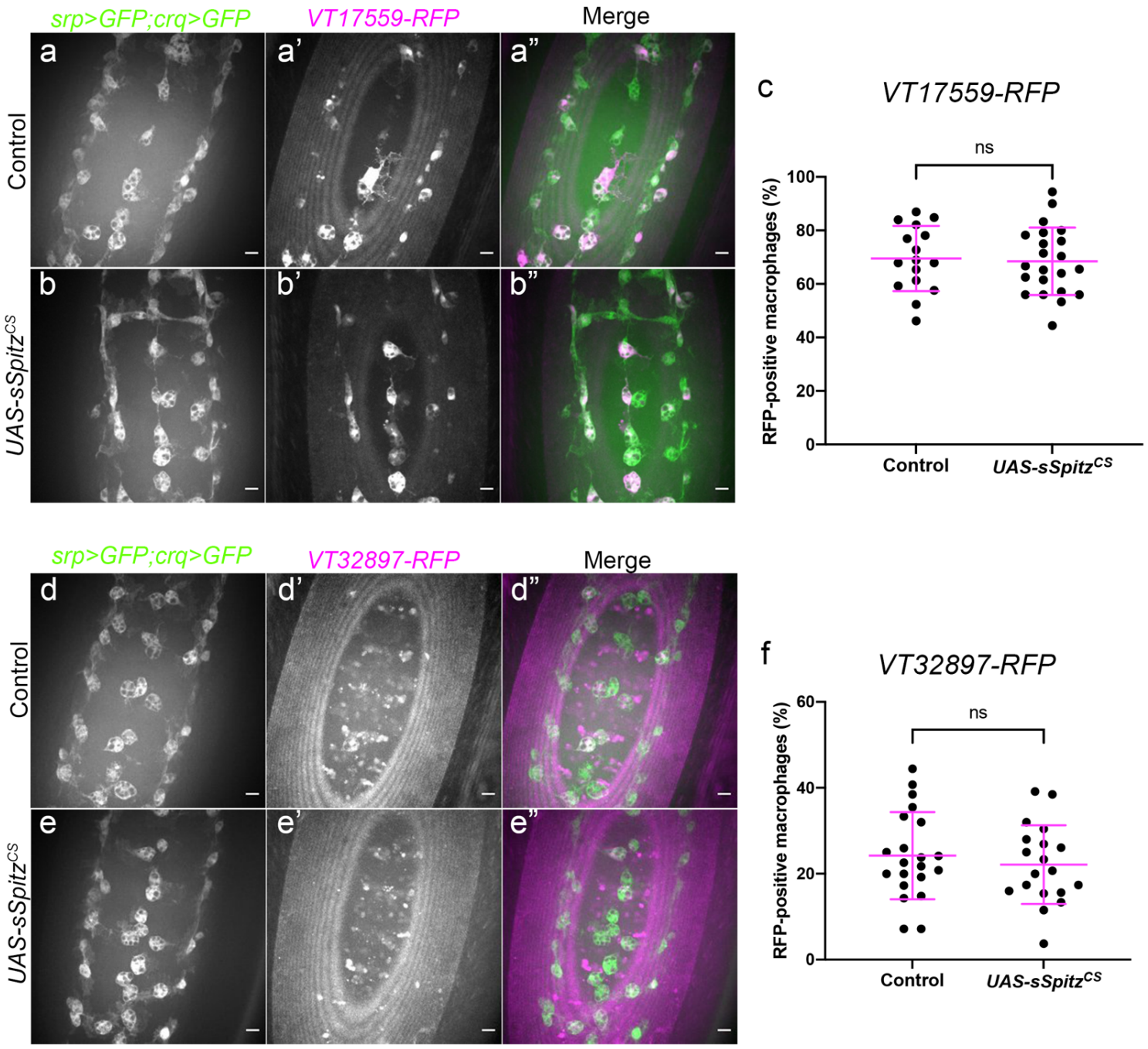


*Figure 5.17 – Pan-macrophage expression of the EGF ligand sSpitz$^{CS}$ causes no effect on the VT17559 or VT32897 subpopulations*

(a-b",d-e") representative maximum projection images of the ventral midline of control embryos (a-a", d-d") and embryos expressing *UAS-sSpitz$^{CS}$* specifically in macrophages (b-b",e-e"), at stage 15. Macrophages labelled via *srp-GAL4,UAS-GFP* and *crq-GAL4,UAS-GFP* (a,b,d,e) while subpopulation macrophages are labelled via *VT17559-RFP* (a',b') or *VT32897-RFP* (d',e'). Anterior is up in all images, scale bars denote 10µm. (c,f) scatterplot showing proportion of macrophages within the *VT17559* (c) and *VT32897* (f) subpopulations in the presence and absence of pan-macrophage *sSpitz$^{CS}$* expression. (c) *n*= 16 and 22, respectively. (f) *n*= 22 and 19, respectively. Statistical analyses carried out via unpaired *t* tests.

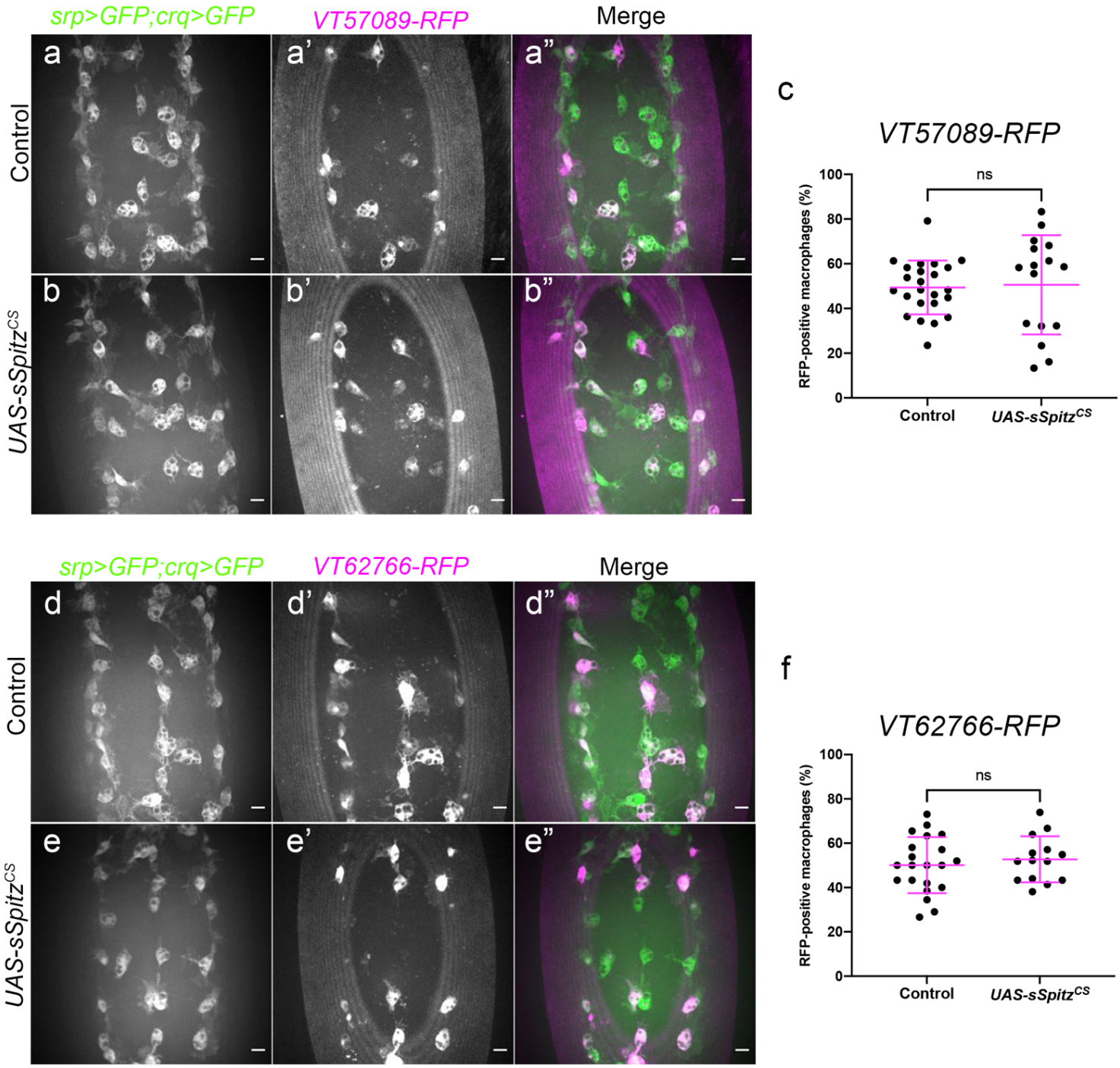


*Figure 5.18 – Pan-macrophage expression of the EGF ligand sSpitz$^{CS}$ causes no effect on the VT57089 or VT62766 subpopulations*

(a-b",d-e") representative maximum projection images of the ventral midline of control embryos (a-a", d-d") and embryos expressing *UAS-sSpitz$^{CS}$* specifically in macrophages (b-b",e-e"), at stage 15. Macrophages labelled via *srp-GAL4,UAS-GFP* and *crq-GAL4,UAS-GFP* (a,b,d,e) while subpopulation macrophages are labelled via *VT57089-RFP* (a',b') or *VT62766-RFP* (d',e'). Anterior is up in all images, scale bars denote 10µm. (c,f) scatterplot showing proportion of macrophages within the *VT57089* (c) and *VT62766* (f) subpopulations in the presence and absence of pan-macrophage *sSpitz$^{CS}$* expression. (c) *n*= 23 and 16, respectively. (f) *n*= 21 and 14, respectively. Statistical analyses carried out via unpaired *t* tests.

decrease of ~30% in the presence of *EcR-DN*, suggesting ecdysone signalling contributes towards establishing this potential pro-inflammatory subpopulation (figure 5.19-20 a-f). The *VT57089* subpopulation also exhibited a trend suggesting a modest, decrease in the presence of *EcR-DN*, although this was not statistically significant (figure 5.20c).

### 5.2.12 Pan-macrophage expression of Parvalbumin causes no effect on macrophage subpopulations proportions

Calcium is a ubiquitous secondary messenger, implicated in many different pathways and processes, including the polarisation of macrophages toward a pro-inflammatory activation state (Chauhan et al., 2018). Furthermore, it has been implicated in phagosomal maturation, as echoed by results from section 5.2.4 showing the requirement of *amo*, a calcium permeable cation channel, in this process. The *VT62766* enhancer lies closest to the locus for the calcium-binding chaperone protein *calnexin-14D* (*cnx14D*), macrophage-specific overexpression of which has been shown to shift the overall macrophage population towards a more wound-responsive state (Coates et al., 2021). Furthermore, intracellular bursts of calcium are known to follow phagocytosis of apoptotic corpses, leading to JNK signalling that upregulates Draper expression, priming macrophages to be able to respond to future sites of wounding (Weavers et al., 2016). Sequestration of intracellular calcium via macrophage-specific overexpression of *parvalbumin* significantly impaired the inflammatory response of these macrophages, showing the importance of calcium signalling in this process (Weavers et al., 2016).

To test if calcium signalling could be involved in the establishment of potentially pro-inflammatory subpopulations in *Drosophila*, *UAS-parvalbumin* was expressed specifically in all macrophages via *srp-GAL4* and *crq-GAL4*, while subpopulations were labelled via *GAL4*-independent *VT-RFP* reporters. Perhaps surprisingly, there were no differences in the proportions of macrophages within any subpopulation when parvalbumin was misexpressed with the aim of sequestering intracellular calcium (figure 5.21-22 a-f). This does not necessarily rule calcium signalling out as being involved in the establishment of pro-inflammatory subpopulations however, as it is possible that there were insufficient levels of Parvalbumin to sequester intracellular calcium sufficiently. This would appear to be unlikely though, as *UAS*

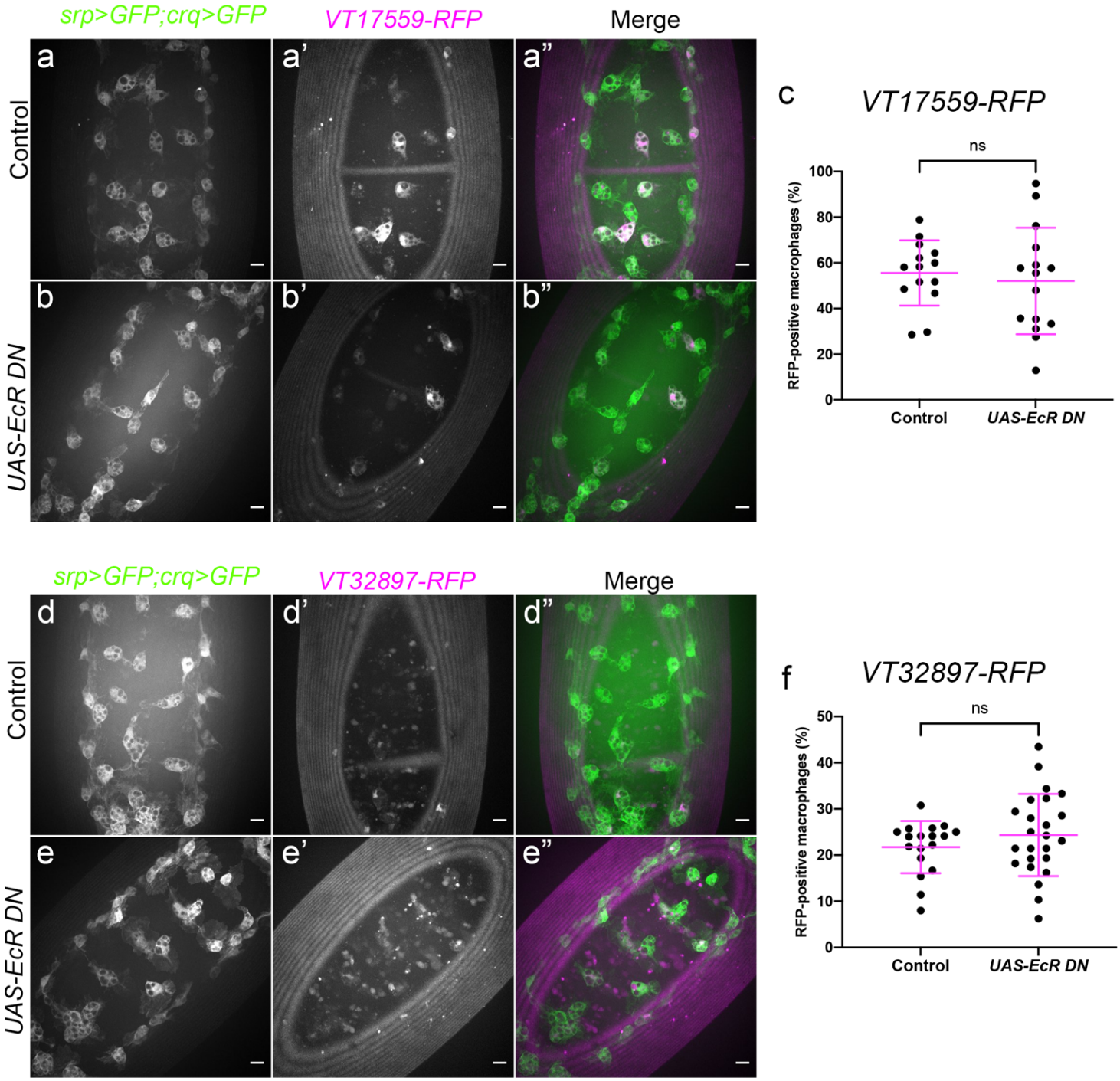


*Figure 5.19 – Pan-macrophage expression of a dominant-negative Ecdysone Receptor causes no effect on the VT17559 or VT32897 subpopulations*

(a-b",d-e") representative maximum projection images of the ventral midline of control embryos (a-a", d-d") and embryos expressing *UAS-EcR$^{\Delta C655}$ (UAS-EcR DN)* specifically in macrophages (b-b",e-e"), at stage 15. Macrophages labelled via *srp-GAL4,UAS-GFP* and *crq-GAL4,UAS-GFP* (a,b,d,e) while subpopulation macrophages are labelled via *VT17559-RFP* (a',b') or *VT32897-RFP* (d',e'). Anterior is up in all images, scale bars denote 10µm. (c,f) scatterplot showing proportion of macrophages within the *VT17559* (c) and *VT32897* (f) subpopulations in the presence and absence of pan-macrophage *UAS-EcR$^{\Delta C655}$* expression. (c) *n*= 14 and 15, respectively. Statistical analysis carried out via unpaired *t* test. (f) *n*= 18 and 24, respectively. Statistical analysis carried out via Mann-Whitney test.

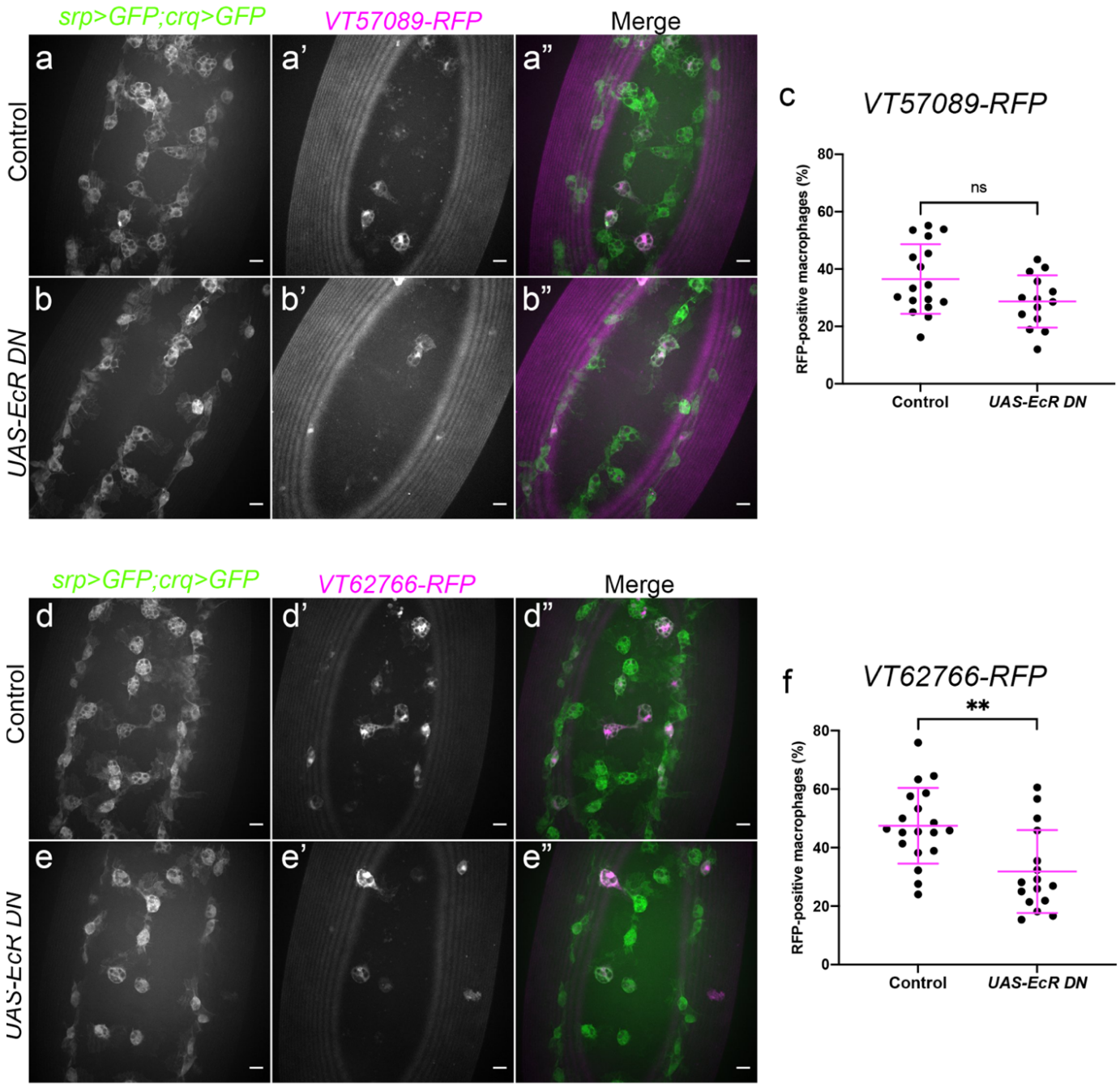


*Figure 5.20 – Pan-macrophage expression of a dominant-negative Ecdysone Receptor causes decreased numbers of VT62766 subpopulation macrophages, but not VT57089*

(a-b",d-e") representative maximum projection images of the ventral midline of control embryos (a-a", d-d") and embryos expressing *UAS-EcR$^{\Delta C655}$ (UAS-EcR DN)* specifically in macrophages (b-b",e-e"), at stage 15. Macrophages labelled via *srp-GAL4,UAS-GFP* and *crq-GAL4,UAS-GFP* (a,b,d,e) while subpopulation macrophages are labelled via *VT17559-RFP* (a',b') or *VT32897-RFP* (d',e'). Anterior is up in all images, scale bars denote 10µm. (c,f) scatterplot showing proportion of macrophages within the *VT57089* (c) and *VT62766* (f) subpopulations in the presence and absence of pan-macrophage *UAS-EcR$^{\Delta C655}$* expression. (c) *n*= 17 and 14, respectively. (f) *n*= 19 and 16, respectively. ** represents p<0.01 Statistical analyses carried out via unpaired *t* tests.

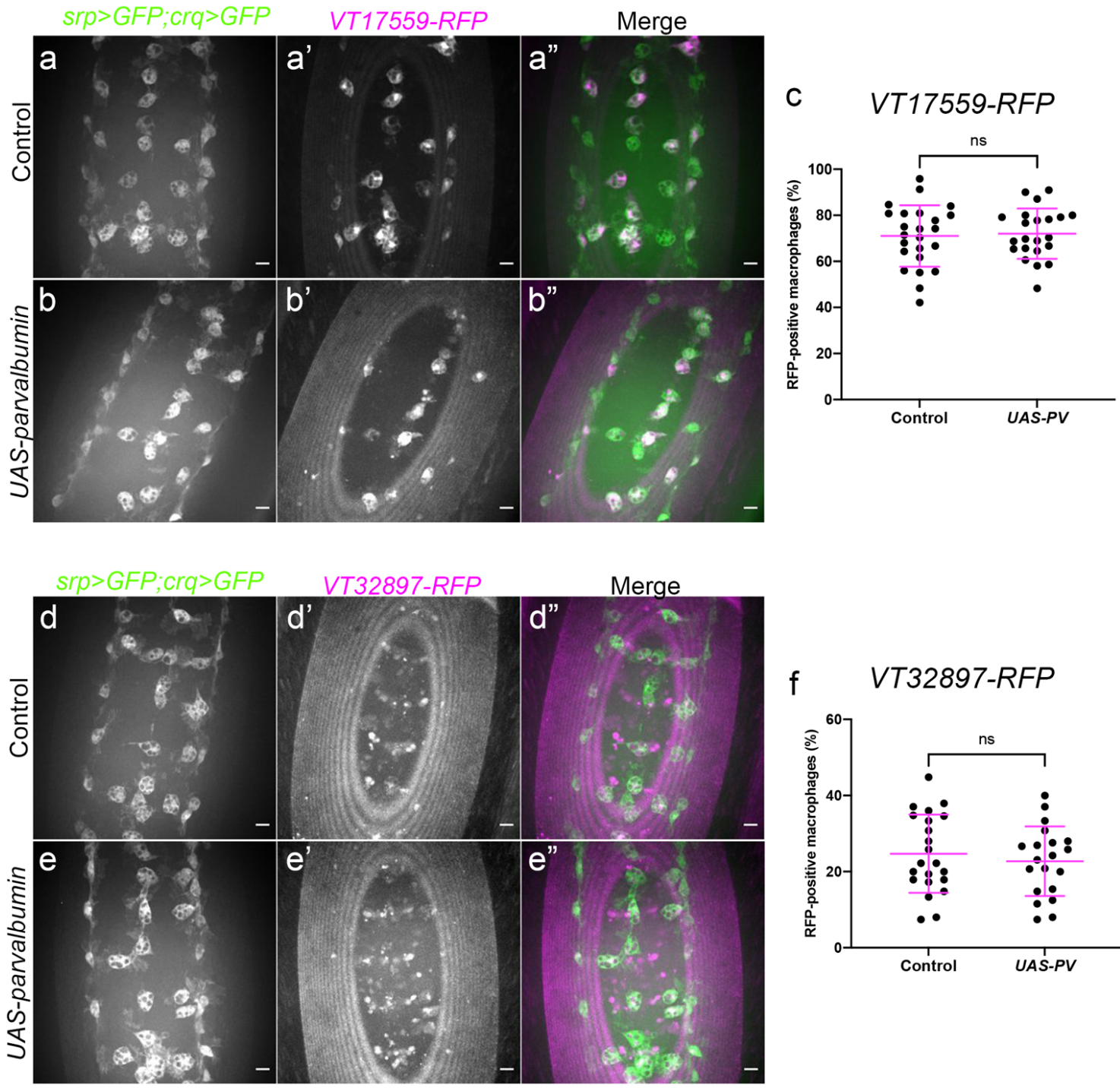


*Figure 5.21 – Pan-macrophage expression of Parvalbumin causes no effect on the VT17559 or VT32897 subpopulations*

(a-b",d-e") representative maximum projection images of the ventral midline of control embryos (a-a", d-d") and embryos expressing *UAS-parvalbumin (UAS-PV)* to sequester intracellular calcium specifically in macrophages (b-b",e-e"), at stage 15. Macrophages labelled via *srp-GAL4,UAS-GFP* and *crq-GAL4,UAS-GFP* (a,b,d,e) while subpopulation macrophages are labelled via *VT17559-RFP* (a',b') or *VT32897-RFP* (d',e'). Anterior is up in all images, scale bars denote 10µm. (c,f) scatterplot showing proportion of macrophages within the *VT17559* (c) and *VT32897* (f) subpopulations in the presence and absence of pan-macrophage *UAS-parvalbumin* expression. (c) *n*= 24 and 22, respectively. (f) *n*= 22 and 20, respectively. Statistical analyses carried out via unpaired *t* tests.

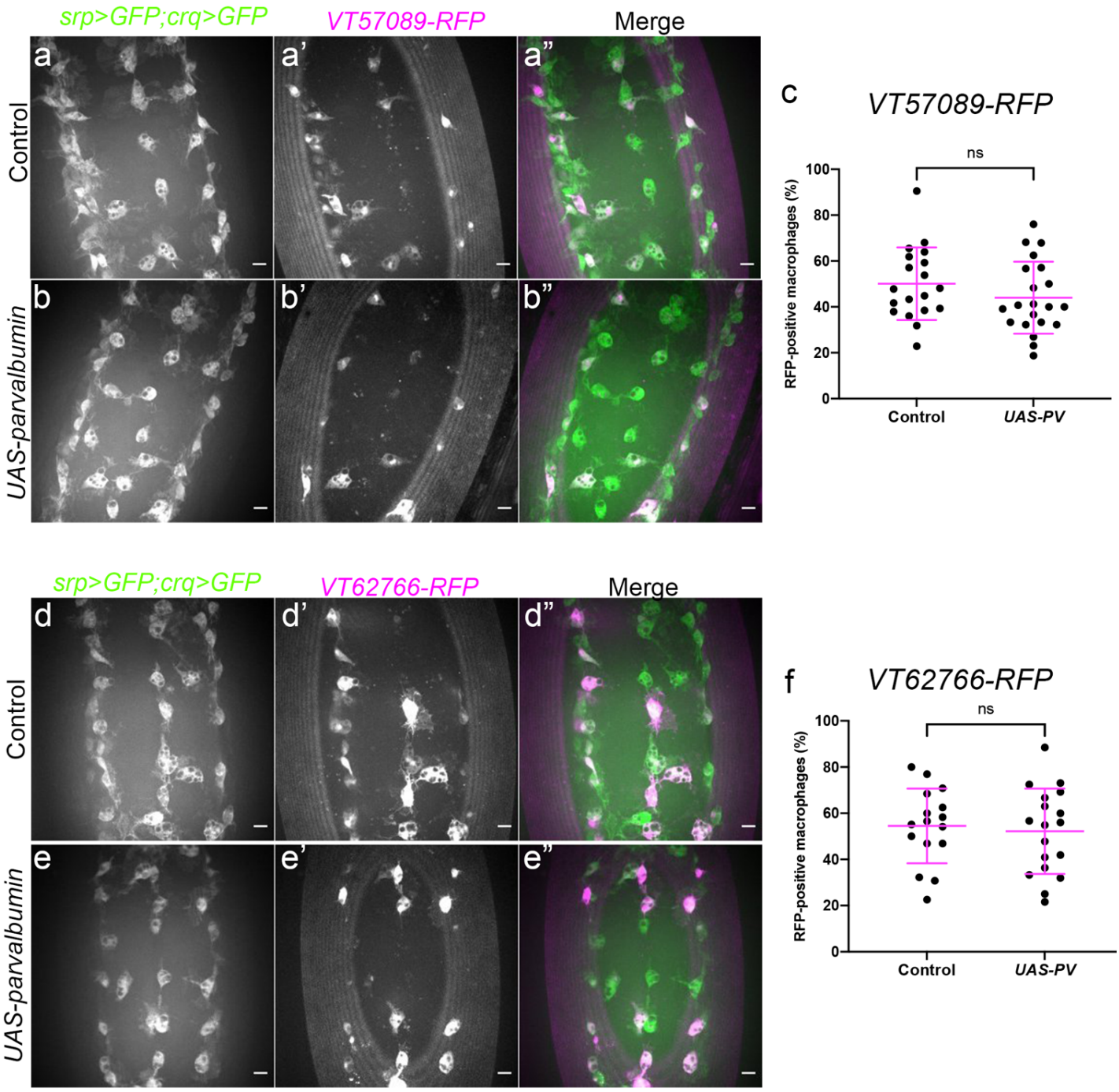


*Figure 5.22 – Pan-macrophage expression of Parvalbumin causes no effect on the VT57089 or VT62766 subpopulations*

(a-b",d-e") representative maximum projection images of the ventral midline of control embryos (a-a", d-d") and embryos expressing *UAS-parvalbumin (UAS-PV)* to sequester intracellular calcium specifically in macrophages (b-b",e-e"), at stage 15. Macrophages labelled via *srp-GAL4,UAS-GFP* and *crq-GAL4,UAS-GFP* (a,b,d,e) while subpopulation macrophages are labelled via *VT57089-RFP* (a',b') or *VT62766-RFP* (d',e'). Anterior is up in all images, scale bars denote 10µm. (c,f) scatterplot showing proportion of macrophages within the *VT17559* (c) and *VT32897* (f) subpopulations in the presence and absence of pan-macrophage *UAS-parvalbumin* expression. (c) *n*= 19 and 21, respectively. (f) *n*= 16 and 18, respectively. Statistical analyses carried out via unpaired *t* tests.

*-parvalbumin* driven by *srp-GAL4* has previously been shown to impair *Drosophila* macrophage wound responses (Weavers et al., 2016).

### 5.2.13 *cnx14D* overexpression augments phagocytosis-associated calcium flashes in macrophages

While enhancers typically regulate the most proximal genetic loci, this is not the case in every example and this holds true of the *VT-GAL4* tilling array library (Kvon et al., 2014). The *VT62766* enhancer element is taken from a genomic region ~12kb downstream of the *cnx14D* ORF on the *Drosophila* X chromosome. Furthermore, it has previously been shown that macrophage-specific overexpression of *cnx14D* enhances the wound-responsiveness of the overall macrophage population, causing the overall macrophage population to behave more similarly to those associated cells marked via *VT62766*-GAL4 (Coates et al., 2021). This therefore suggests *cnx14D* as a candidate gene regulated by the *VT62766* enhancer. However, what *cnx14D* does to enhance the wound-responsiveness of macrophages remains unknown.

The *Dictyostelium* ortholog of *cnx14d* is required for the effective formation of phagocytic cups during the early stages of phagocytosis, suggesting a role of *cnx* in modulating the actin cytoskeleton (Müller-Taubenberger et al., 2001). Effective phagocytosis of apoptotic corpses is known to be an important prerequisite for *Drosophila* macrophages to mount an effective wound response (Weavers et al., 2016). Following phagocytosis, intracellular calcium flashes induce JNK signalling which leads to upregulated expression of *Draper*, 'priming' macrophages to mount an effective wound response (Weavers et al., 2016). The requirement of intracellular calcium flashes for this priming, together with a requirement for *calnexin* in phagocytic cup formation suggests a potential role for *cnx14D* in this process.

To investigate the effect of *calnexin14D* on intracellular calcium dynamics, *UAS-GCaMP6m* was expressed specifically in macrophages via *srp-GAL4* and *crq-GAL4*, and the rate of calcium flashes were compared between macrophages expressing *UAS-cnx14D* and control macrophages lacking *cnx14D* overexpression (**figure 5.23 a-d"**). Embryos were imaged at stage

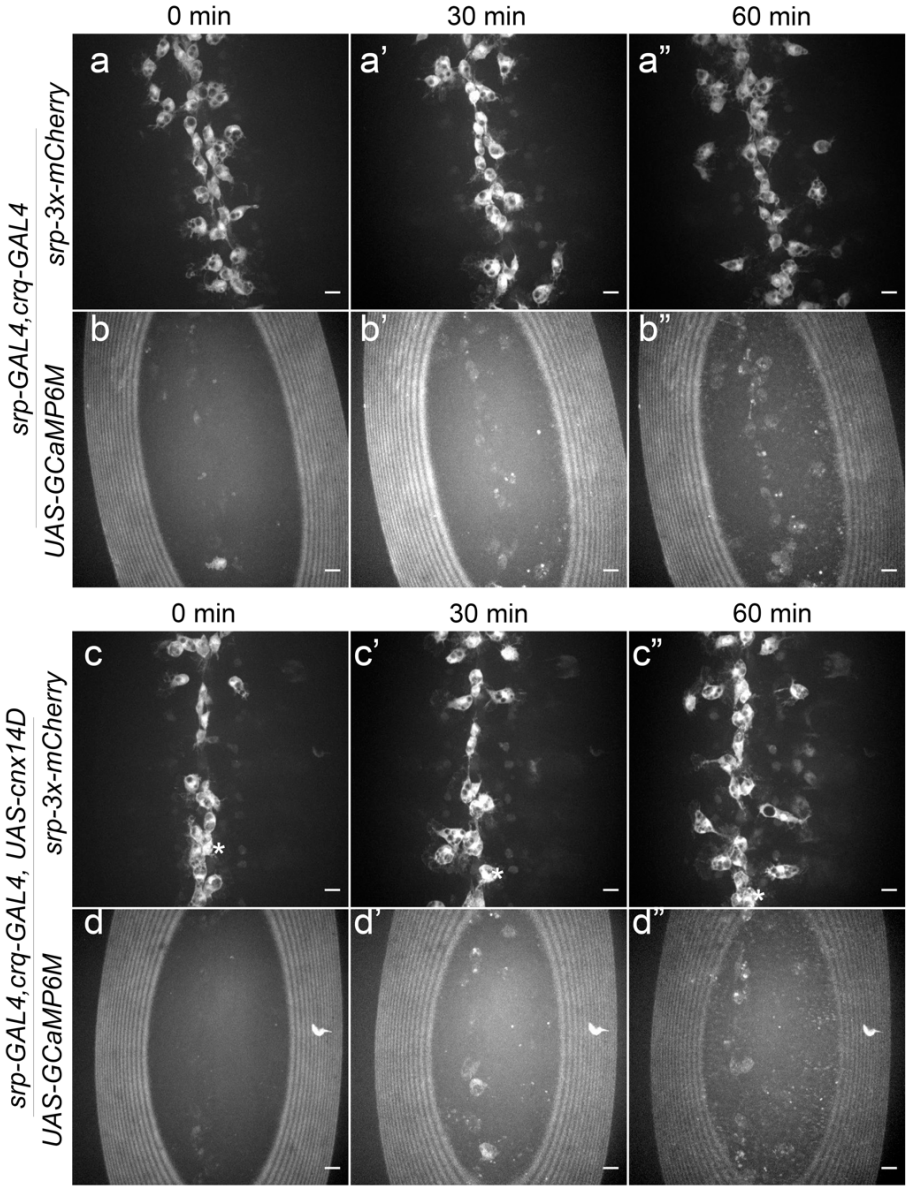
0 min
30 min
60 min
a
a'
a"
b
b'
b"
srp-GAL4,crq-GAL4
srp-3x-mCherry
UAS-GCaMP6M
c
c'
c"
d
d'
d"
srp-GAL4,crq-GAL4, UAS-cnx14D

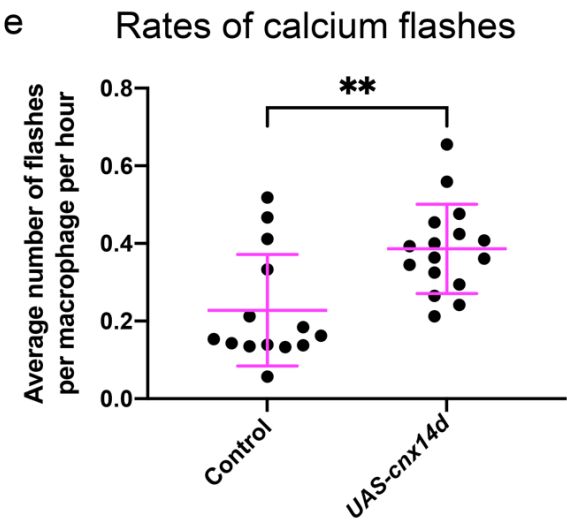
e
Rates of calcium flashes
Average number of flashes per macrophage per hour
0.8
0.6
0.4
0.2
0.0
**
Control
UAS-cnx14d

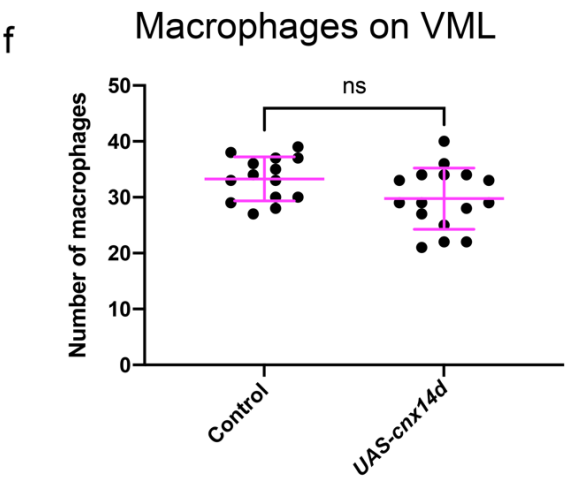
f
Macrophages on VML
Number of macrophages
50
40
30
20
10
0
ns
Control
UAS-cnx14d

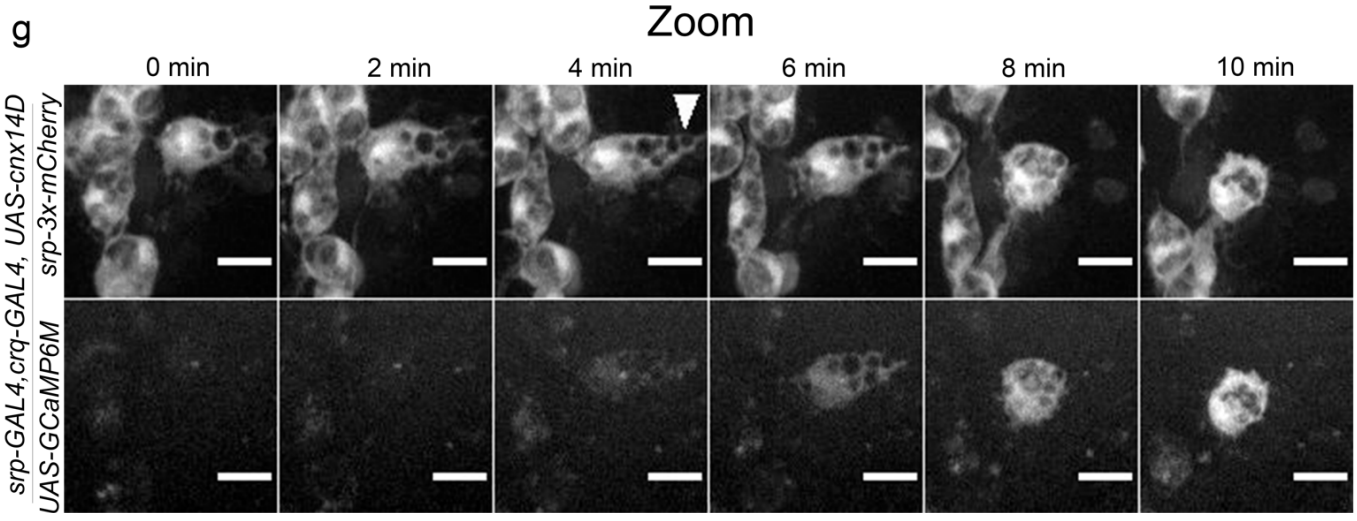
g
Zoom
0 min
2 min
4 min
6 min
8 min
10 min
srp-GAL4,crq-GAL4, UAS-cnx14D
srp-3x-mCherry
UAS-GCaMP6M

*Figure 5.23 – Pan-macrophage overexpression of UAS-calnexin14D causes an increase in rates of phagocytosis associated intra-macrophage calcium flashes*

(a-d") representative maximum projection images of the ventral midline of control embryos (a-b") and embryos expressing *UAS-calnexin14D* specifically in macrophages (c-d"), at stage 13. Macrophages labelled via *srp-3x-mCherry*, with intracellular calcium shown via *UAS-GCaMP6M* driven via *srp-GAL4* and *crq-GAL4* (b-b",d-d"). Anterior is up in all images, scale bars denote 10µm. (e) scatterplot showing average number of calcium flashes per macrophage per embryo in the presence and absence of pan-macrophage *UAS-calnexin14D* expression. *n*=14 and 16 respectively. Statistical analysis carried out via Mann-Whitney test, ** represents p<0.01. (f) scatterplot showing number of macrophages on the VML of stage 13 embryos in the presence and absence of pan-macrophage *UAS-calnexin14D* expression. *n*= 14 and 16, respectively. Statistical analysis carried out via unpaired *t*-test. (g) representative zoomed maximum projection image showing a macrophage expressing *UAS-cnx14D* undergoing phagocytosis over the course of 10 minutes. This macrophage is labelled with a * in (c-c") Note the formation of a new phagosome (white arrowhead). Scale bars denote 10µm.

13 of embryogenesis, when levels of efferocytosis are relatively high during the development of the VNC. Interestingly, *cnx14D* misexpression resulted in a significant increase in the number of flashes per macrophage observed over the course of 1 hour (figure 5.23e), while the total number of macrophages present on the VML was not changed (figure 5.23f). A *GAL4*-indpendent macrophage reporter (*srp-3x-mCherry)* was also present, allowing macrophage morphology to be observed during these movies, and many of these calcium "flashes" were associated with phagocytic events based on macrophage membrane dynamics and the formation of new vacuoles within macrophages (figure 5.23g). This result is consistent with the reported flashes of calcium following the phagocytosis of apoptotic cells (Weavers et al., 2016), suggesting that expression of *cnx14d* augments the priming of macrophages to mediate inflammatory responses.

In summary, these results show that macrophage subpopulation identity can be modulated by the manipulation of pathways associated with Simu-dependent efferocytosis. Data implicates Amo/Pkd2 in the removal of macrophages from putative pro-inflammatory subpopulations, which is of relevance in the context of ADPKD, which is associated with aberrant macrophage polarisation. Interestingly, results suggest that subpopulations are modulated by different pathways at different developmental stages, with certain subpopulations affected by loss of Simu in the adult stages without any effects at earlier stages. The steroid hormone Ecdysone

was also implicated in the establishment of the *VT62766* associated subpopulation, while *calnexin14D*, a gene potentially regulated by the *VT62766* enhancer, seems to be involved in the phagocytic priming of macrophages to mount effect wound responses. See **table 5.1** for a summary of findings presented in this chapter.

*Table 5.1 Summary of the effect on subpopulation macrophages of various mutations and genetic manipulations at different developmental stages*
n.s.=not significant.

| Stage | *VT17559* | *VT32897* | *VT57089* | *VT62766* |
|---|---|---|---|---|
| *simu* embryo (st15) | n.s. | n.s | ↑ | ↑ |
| *simu;repo* embryo (st15) | n.s | n.s | ↑ | n.s |
| *amo* embryo (st15) | n/a | n/a | n.s | n/a |
| *amo;repo* embryo (st15) | n/a | n/a | ↑ | n/a |
| *simu* L3 larvae | n.s | ↑ | n.s | ↑ |
| *simu* adult (1 day old) | ↑ | ↑ | n.s | ↑ (*MGV only) |
| *simu* adult (4 weeks old) | ↑ | n.s | n.s | n.s |
| *amo* adult (1 day old) | ↑ | n.s | n.s | n.s |
| *UAS-drpr-II;repo* embryo (st15) | n.s | n.s | n.s | n.s |
| $crq^{ko92}$*;repo* embryo (st15) | n.s | n.s | n.s | n.s |
| *UAS-*$sSpitz^{CS}$ embryo (st15) | n.s | n.s | n.s | n.s |
| *UAS-*$EcR^{\Delta C655}$ embryo (st15) | n.s | n.s | n.s | ↓ |
| *UAS-parvalbumin* (st15) | n.s | n.s | n.s | n.s |

## 5.3 Discussion

The major aim of this work was to use *Drosophila* as an *in vivo* tool with which to understand the processes underlying macrophage heterogeneity and polarisation, a phenomenon implicated in numerous chronic conditions including ADPKD (Cassini et al., 2018; Karihaloo, 2015; Karihaloo et al., 2011; Parisi et al., 2018). Throughout these experiments I have focused on apoptotic cell clearance and calcium signalling, two processes known to be involved in macrophage polarisation and heterogeneity in both vertebrates and *Drosophila* (Chauhan et

al., 2018; Coates et al., 2021; Weavers et al., 2016). Through the use of apoptotic cell receptor mutants and/or elevation of apoptotic cell challenge, I have shown that Simu-dependent phagocytosis of apoptotic cells is implicated in the decreased number of macrophages within the *VT57089* subpopulation. Additionally, I am able to show that the calcium-permeable cation channel Amo/Pkd2 is required downstream of Simu in this process. Investigating phagosomal acidification and maturation showed a potential requirement for Amo in this process and suggests that effective phagosome maturation is an important process regulating acquisition of specific macrophage subpopulation fates.

These investigations have also revealed a requirement for the steroid hormone Ecdysone receptor in establishing the *VT62766* subpopulation in the embryo. The enhancer element associated with this subpopulation is proximal to the ORF for *cnx14D*, a gene whose misexpression has been shown to enhance wound-responsiveness in embryonic macrophage populations (Coates et al., 2021). Further work showed that this *cnx14d* overexpression results in increased rates of cytosolic calcium flashes within macrophages, a phenomenon associated with phagocytosis and subsequent 'priming' of macrophages to mount an effective inflammatory response (Weavers et al., 2016).

### 5.3.1 The role of apoptotic cell clearance on macrophage subpopulations

Efferocytosis is a typical behaviour of anti-inflammatory 'M2-like' macrophages (Gordon & Martinez, 2010). *repo* mutants place an increased phagocytic burden upon macrophages in the developing *Drosophila* embryo, resulting in increased levels of apoptotic cells both inside and outside macrophages (Armitage et al., 2020). Putative macrophage subpopulations showing pro-inflammatory behaviours were shown to exhibit decreased rates of phagocytosis compared to the overall macrophage population in the developing embryo at stage 13. At this stage of development, the major phagocytic target for macrophages is apoptotic cells, so it is therefore likely that these macrophage subpopulations exhibit decreased rates of efferocytosis, consistent with them possibly representing pro-inflammatory subpopulations. Furthermore, increasing the exposure of macrophages to apoptotic cells is known to cause a shift away from macrophage subpopulations (Coates et al., 2021), further suggesting they are

pro-inflammatory, as causing macrophages to carry out a typically anti-inflammatory function results in the presence of fewer of this macrophage subpopulation. This is consistent with published data looking at human monocyte-derived macrophages, which showed that the production of pro-inflammatory cytokines is inhibited following the phagocytosis of apoptotic neutrophils (Fadok et al., 1998). These data further suggest that *Drosophila* macrophages do indeed represent a heterogeneous population of cells containing subpopulations that behave in a typically pro-inflammatory manner and are more similar to their vertebrate counterparts than previously considered.

Experiments using *simu* mutations show that simply overexposing embryonic macrophages to apoptotic cells is insufficient to cause this 'anti-inflammatory shift', with certain subpopulations actually exhibiting increased numbers in the absence of Simu. This suggests that effective recognition and/or phagocytosis of apoptotic cells is required for these differences. Furthermore, the fact that *simu* mutants exhibit increased numbers of putative pro-inflammatory subpopulations possibly suggests that developmental Simu-mediated efferocytosis may be involved in the establishment of other subpopulation macrophages, which could exhibit typically anti-inflammatory behaviours. Though work carried out has focused on 4 *VT-GAL4* enhancer trap lines which exhibit pro-inflammatory behaviours, many other enhancers appear to be active in only a subset of macrophages (Coates et al., 2021; Kvon et al., 2014). It would be of interest to investigate whether these would exhibit anti-inflammatory behaviours, and whether numbers within these subpopulations are also sensitive to changes in exposure to apoptotic cells.

Subpopulation macrophages are at their lowest levels in late larval stages, with lineage tracing experiments using G-TRACE suggesting macrophages are being reprogrammed as opposed to dying (Coates et al., 2021; Evans et al., 2009). Subpopulation macrophages re-emerge during pupal development and can be found in large numbers in newly-eclosed adults. During metamorphosis in the pupa, tissue remodelling associated with high levels of apoptosis occurs (Jiang et al., 1997; Zirin et al., 2013). Again, *simu* mutations were typically shown to be associated with increased levels of subpopulation macrophages in newly-eclosed adults, further suggesting that Simu-dependent efferocytosis is associated with a shift away from those subpopulations we can label. Interestingly, when bleeding hemocytes from newly

eclosed adult flies, significantly more hemocytes were extracted from *simu* mutants compared to controls. This could possibly be explained by loss of Simu altering localisation of cells in the adult, such that more cells are present in circulation rather than attached or integrated into tissue. This is a potentially attractive hypothesis when one considers the increased proportions of putative pro-inflammatory subpopulations seen in *simu* mutant adults, together with tissue resident macrophages typically being anti-inflammatory, with an increase in putative pro-inflammatory subpopulations being consistent with a shift out of tissue resident populations. An alternative explanation for the increase seen in *simu* mutants could be that it is due to stimulation of macrophage proliferation, though this remains a controversial concept in post-larval stages (Ghosh et al., 2015; Sanchez Bosch et al., 2019).

As the $repo^{03702}$ allele is embryonic lethal in the homozygous state, we have not yet been able to investigate if the apparent anti-inflammatory effect on macrophage subtypes seen in embryonic stages is replicated in adults (Xiong et al., 1994). However, imaging adult *Drosophila* one day after eclosion does seem to suggest that, in the absence of Simu-dependent efferocytosis, there is an increase in certain macrophage subpopulations compared to controls. This further supports the hypothesis that these subpopulations are more pro-inflammatory, due to their increased proportions in backgrounds associated with defective efferocytosis. Whether this increase is simply due to there being less efferocytosis in this mutant background, preventing anti-inflammatory signalling removing macrophages from subpopulations, or pro-inflammatory signals (possibly being released by uncleared apoptotic cells undergoing secondary necrosis) remains to be determined.

As well as Simu, two other major apoptotic cell receptors were investigated in the *Drosophila* embryo: Draper-I and Croquemort. Unlike Simu however, neither affected subpopulations in a *repo* mutant background. Though a loss-of-function allele of *crq* was used ($crq^{ko92}$ - Lien Guillou et al., 2016), it is worth mentioning that Draper-mediated efferocytosis was inhibited by the expression of an inhibitory isoform of Draper (*UAS-Draper-II;* Logan et al., 2012) specifically within subpopulation macrophages. As such, it is possible that expression of *UAS-Draper-II* via *VT-GAL4* transgenes was insufficient to inhibit Draper function fully. However, pan-macrophage expression of *UAS-Draper-II* also did not impact subpopulation numbers, albeit in a 'normal' apoptotic background. For these experiments I used *srp-GAL4* and *crq-GAL4* - these

two *GAL4* drivers have been shown to drive sufficient *Draper-II* expression to impair wound responses and alter macrophage migration speeds (Evans et al., 2015). It is therefore likely that Draper-mediated apoptotic cell processing is not responsible for the shift out of subpopulations. However, it is difficult to conclusively say this without looking at the effect of *draper* mutations on subpopulations. Though null-alleles have been reported (Freeman et al., 2003), genetics did not allow for this to be carried out in this instance, as the chromosomal location of *draper* on chromosome 3L would have required recombination with *VT-GAL4* transgenes, which are inserted in the *attP2* site on chromosome 3L (Coates et al., 2021).

A final efferocytosis related process investigated in subpopulation programming was the exposure of macrophages to sSpitz$^{CS}$, a secreted isoform of the EGF ligand Spitz which has recently been identified as a putative 'find-me' cue in *Drosophila* (Liang et al., 2017; Tardy et al., 2021). Though macrophage-specific overexpression of *sSpitz$^{CS}$* phenocopies apoptotic cell receptor mutations (such as *simu*) by impairing wound responses and random migration (Tardy et al., 2021), no subpopulations exhibited any changes in the presence of sSpitz$^{CS}$. It is worth mentioning however that sSpitz$^{CS}$ has not categorically been confirmed as a 'find-me' cue, it has simply been shown to modulate certain macrophage behaviours. Indeed, the conservation of bona fide 'find-me' cues in *Drosophila* remains a source of some debate, although the fact that wound responses are impaired in backgrounds with high levels of uncleared apoptotic cells suggests that macrophages are prioritising signals from these dying cells over wound signals (Roddie et al., 2019). If categorical 'find-me' cues are eventually defined in *Drosophila*, it would undoubtedly be interesting to investigate their effects on subpopulation macrophages.

### 5.3.2 The role of calcium signalling on macrophage subpopulations

Calcium is a ubiquitous secondary messenger involved in many cellular processes, including phagocytosis, efferocytosis and macrophage polarisation (Chauhan et al., 2018; Nunes & Demaurex, 2010). Calcium is involved in the polarisation of vertebrate macrophages towards more pro-inflammatory activation states via the entry of extracellular calcium through Trpc1 channels in response to IFNγ stimulation (Chauhan et al., 2018). Furthermore, calcium flashes

following apoptotic cell clearance by embryonic *Drosophila* macrophages upregulate *Draper* expression (Weavers et al., 2016). Though Draper is known to be involved in efferocytosis, typically an anti-inflammatory macrophage behaviour, it is also essential for mediating inflammatory wound responses, a quintessentially pro-inflammatory behaviour (Evans et al., 2015). As such, calcium signalling seemed an attractive avenue to explore with respect to macrophage subpopulations. However, it was shown that pan-macrophage expression of Parvalbumin, with the intent of sequestering intracellular calcium, caused no effect on subpopulation specification. It has previously been shown that the pan-macrophage sequestration of intracellular calcium is capable of impairing the inflammatory wound response (Weavers et al., 2016); it would therefore be interesting to see whether the putative pro-inflammatory subpopulations still exhibit enhanced wound-responsiveness in this background. If they are still more responsive than the overall population, it would possibly suggest that the pro-inflammatory programming they receive is independent of calcium.

During Simu-dependent efferocytosis, the calcium-permeable cation channel Amo is understood to mediate calcium homeostasis downstream of phagocytosis (Van Goethem et al., 2012). *simu* mutations rescued the decreased numbers within the *VT57089* subpopulation caused by *repo* mutations, implicating Simu-dependent efferocytosis in this shift. This was phenocopied by loss of *amo*, and it was shown that *amo;repo* double mutants exhibit decrease rates of phagosome maturation compared to *repo* single mutants. Calcium has been reported to be required for phagosome maturation in neutrophils, and the lysosomal calcium channel Trpml has been shown to be required for this process in *Drosophila* (Lundqvist-Gustafsson et al., 2000; Edwards-Jorquera et al., 2020). These results implicate *amo* in this process and suggest that effective phagosome maturation is required for signalling resulting in macrophage reprogramming out of subpopulations (see figure 5.24 for a proposed schematic).

Perhaps confusingly, I failed to conclusively identify *amo*-dependent macrophage phenotypes in chapter 4. This conflicts with previously published data implicating *amo* in efferocytosis (Van Goethem et al., 2012), and the apparent requirement for *amo* in phagosomal maturation (figure 5.6). However, in our hands *amo* mutants only exhibited a phenotype in the presence of a high apoptotic burden (i.e., a *repo* mutant background). Unlike *simu* mutants, there was no increase in *VT57089* subpopulation macrophages in *amo* mutants (i.e., within a 'normal

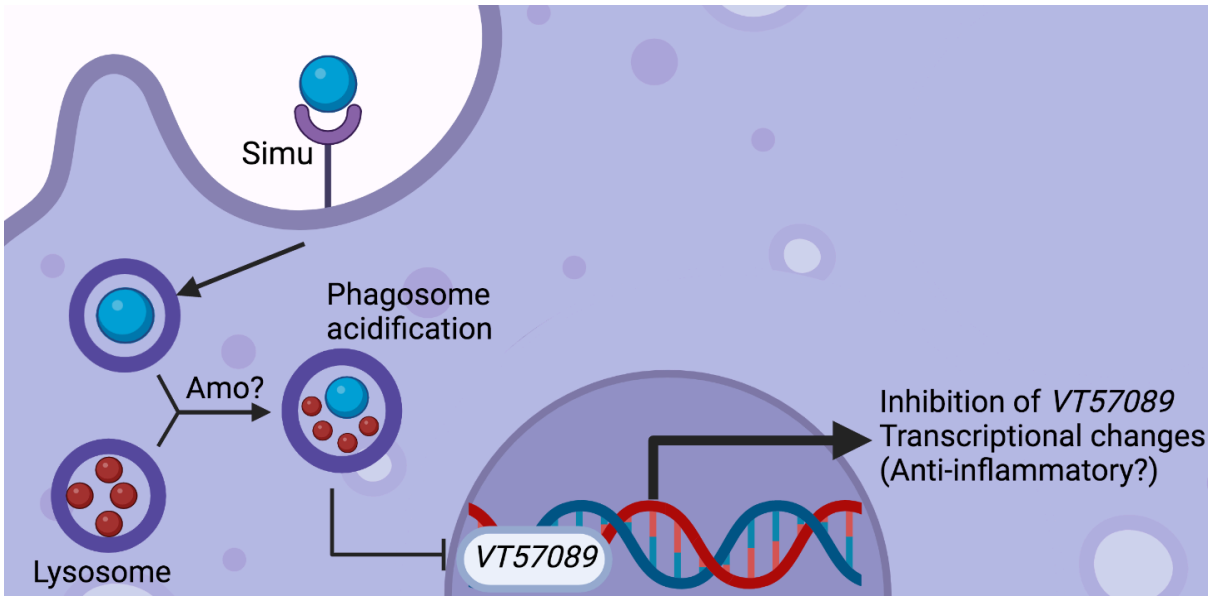


*Figure 5.24 – Proposed mechanism of action for the modulation of the VT57089 subpopulation via Amo and Simu during efferocytosis*

Downstream of Simu-dependent phagocytosis of an apoptotic body, Amo seems to be required for the effective acidification of the phagosome. Signalling downstream of phagosome acidification seems to result in inhibition of *VT57089* activity, and may also result in other transcriptional changes, which may shift the macrophage to a more anti-inflammatory state.

apoptotic' background). Phagosome acidification could simply be slowed down in *amo* mutants, and it is only when there are excessive levels of apoptotic cells that this unveils a phenotype. Consistently, the *VT17559* subpopulation exhibited a significant increase in 1-day old adult *amo* mutants. Metamorphosis is an event associated with high levels of apoptosis due to tissue remodelling (Jiang et al., 1997; Zirin et al., 2013); if loss of *amo* affects subpopulations specifically in a high-apoptosis dependent manner, one would therefore expect newly eclosed *amo* mutant adults to exhibit an increase in subpopulations.

Interestingly, the reported involvement of Amo in phagosome acidification could explain the discrepancies in results seen between chapter 4 of this thesis and the data published by Van Goethem et al. implicating Amo in efferocytosis. As discussed in section 4.3.3, Van Goethem et al. used Acridine Orange (AO) staining as a readout of efferocytosis (Van Goethem et al., 2012). This stains acidified intracellular compartments (Thomé et al., 2016), and a 50% decrease in the number of AO-labelled punctae was reported in *amo* mutant macrophages. If Amo is required for phagosome acidification, as results here suggest, this would explain the

apparent decrease in efferocytosis seen by Van Goethem et al., and how *amo* mutant macrophages exhibited no phenotypic changes associated with defective efferocytosis.

Another possible role for calcium in the control of macrophage subpopulations concerned the calcium-binding chaperone protein Cnx14D. The ORF of *cnx14D* is located 12kb 5' to the locus of the *VT62766* enhancer, and it has previously been shown that pan-macrophage overexpression of *cnx14D* shifts the overall population to a more wound-responsive state (Coates et al., 2021). Combining the pan-macrophage expression of *cnx14D* with a genetically-encoded calcium indicator revealed increased rates of calcium flashes in the presence of *cnx14D*. These flashes often seemed to follow phagocytic events, and as mentioned above, calcium flashes following apoptotic corpse engulfment are known to induce JNK activity and result in upregulation of *Draper* expression, priming macrophages to respond to wounds (Weavers et al., 2016). The *Dictyostelium* ortholog of *cnx14D* is required during phagocytosis for the effective formation of the phagocytic cup, with mutants capable of binding phagocytic targets without internalising them (Müller-Taubenberger et al., 2001). It was shown that the ER localises closely to the base of the nascent phagocytic cup, and the authors speculated that ER-resident calcium, bound by Calnexin, is involved in modulating the actin cytoskeleton during phagocytic cup extension. If *cnx14D* activity in *Drosophila* macrophages is established by *VT62766* enhancer activity, which appears to be active in roughly 50% of macrophages, this would explain the variability of wound responsiveness seen in embryonic macrophages.

### 5.3.3 The role of steroid hormone signalling on macrophage subpopulations

Ecdysone signalling is known to be important in shifting *Drosophila* macrophages towards different behavioural states at various 'checkpoints' throughout development. During metamorphosis, ecdysone levels peak, and this is associated with macrophages shifting to behave in a more phagocytic and motile manner, two behaviours typically considered to be pro-inflammatory (Regan et al., 2013; Sampson et al., 2013). Indeed, culturing *ex vivo* larval hemocytes, typically sessile and non-migratory, with ecdysone induces a migratory phenotype dependent on the action of the nuclear ecdysone receptor, hereafter referred to as EcR (Sampson et al., 2013). Expression of a dominant-negative isoform of the EcR specifically within

embryonic macrophages resulted in a significant decrease in macrophage numbers within the *VT62766* subpopulation, suggesting that Ecdysone plays a role in the establishment of this population. If this dominant-negative EcR impairs the ability of embryonic macrophages to mediate phagocytosis, it could theoretically prevent the 'priming' of macrophages to mount an effective inflammatory response following corpse engulfment, resulting in the decreased numbers seen within this more wound-responsive subpopulation (Weavers et al., 2016). Furthermore, the action of the EcR during embryogenesis is required to enable embryonic macrophages to mount responses to pathogenic bacterial infections (Tan et al., 2014). The phagocytosis of bacteria is a typical behaviour of pro-inflammatory macrophages, so the requirement for EcR in establishing *VT62766* subpopulation macrophages is consistent with this being a pro-inflammatory subpopulation.

This involvement of the EcR in establishing the *VT62766* subpopulation may actually tie in with results investigating the macrophage-specific overexpression of *cnx14D*. This work revealed an increased numbers of phagocytosis-associated calcium flashes in macrophages expressing *cnx14D*, which is known to prime macrophages to mount an effective wound response (Weavers et al., 2016). In response to Ecdysone, the EcR could activate the *VT62766* enhancer in turn leading to transcription of *cnx14D*. This may lead to augmented phagocytosis, and subsequent priming of macrophages to mount an effective wound response (see **figure 5.25** for a proposed schematic).

Though subpopulations become increasingly sparse during larval development, they re-emerge at significant levels following pupation, and persist until early adulthood (Coates et al., 2021). As EcR is known to be involved in macrophage reprogramming during metamorphosis, it would be interesting to see if the presence of a dominant-negative EcR is able to prevent the re-emergence of subpopulation macrophages in the pupae/adult (Regan et al., 2013; Sampson et al., 2013). Unfortunately, the *GAL4*-independent *VT-RFP* reporters made by Coates et al. do not label subpopulations in larval or adult stages at sufficiently bright levels either *in vivo* or *ex vivo* (data not shown). However, EcR is certainly a viable candidate with respect to controlling re-emergence of subpopulations, and future experiments can be carried out to investigate this in more detail. For example, though *VT-RFP* reporters failed to be detectable in the adult or larval stages, expression of *VT-RFP* during pupation has not been investigated. Pupation is

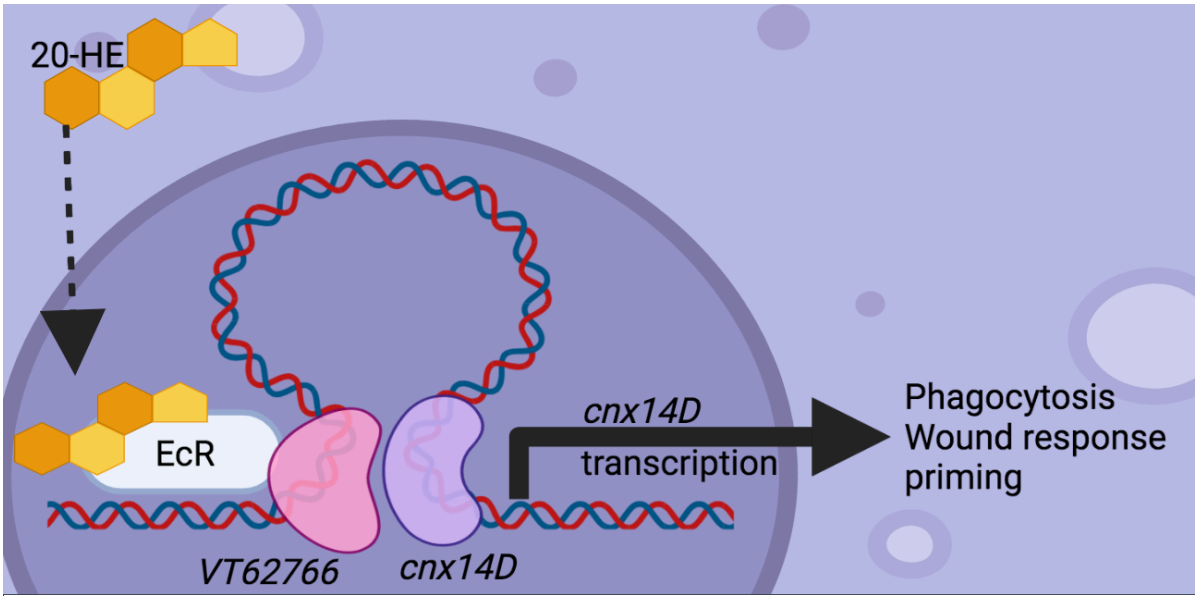


*Figure 5.25 – Proposed mechanism of action for the role of ecdysone in establishing the VT62766 subpopulation*

Pulses of ecdysone (20-HE) at specific developmental timepoints result in the diffusion of ecdysone into the nucleus of a macrophage, where it binds the ecdysone receptor (EcR). The EcR then stimulates *VT62766* enhancer activity (pink), leading to looping of DNA, bringing the *calnexin14D* promoter (purple) in close proximity to the enhancer and leading to transcription of *cnx14D*. Once translated, Cnx14D augments phagocytosis, priming the macrophage to mount an effective wound response, establishing the pro-inflammatory *VT62766* subpopulation

associated with a dramatic increase of *VT* enhancer activity as subpopulations re-emerge (Coates et al., 2021), so it is therefore possible that this would cause increased *VT-RFP* activity, allowing pupal macrophage subpopulations to be visualised. If this is the case, then the role of ecdysone in the re-emergence of subpopulations during pupation could easily be elucidated.

### 5 3.4 Do subpopulation macrophages overlap?

It is worth mentioning that as yet, we are unsure how overlapping these subpopulations are. These subpopulations clearly exhibit differences in terms of their behaviours and specification. For example, subpopulations largely seem to disappear after adults reach ~1-week old, apart from *VT32897* macrophages, which persist for much longer (Coates et al., 2021). However, overlap between subpopulations must occur at the embryonic stage at least, due to each of the 4 enhancers labelling at least 25% of the macrophage population. As such, it is impossible for there not to be a degree of overlap within subpopulations at this stage.

It may therefore be the case that activity of the *VT-GAL4* enhancer is required for establishing specific subpopulations only at specific developmental timepoints. This would be consistent with our data showing that different challenges, for example *simu* mutations, seem to affect subpopulations in different ways at different developmental stages. If this was the case, it may be that apparent changes in subpopulations are actually reflective of changes in enhancer activity, either at a certain stage in development or in response to certain challenges, and not necessarily due to altered numbers within a specific subpopulation.

Another caveat to be taken into consideration is that subpopulation macrophages were generally labelled using either *UAS-stinger* or *UAS-redStinger*. These two reporters both rapidly mature (Barolo et al., 2004), and therefore offer a somewhat binary readout of *VT-GAL4* activity. As such, these do not discriminate between differential activity levels of *VT* enhancer elements within macrophages, which may not be reflective of the situation *in vivo*.

### 5 3.5 Concluding remarks

In this chapter, I have sought to understand how *Drosophila* can be used to understand processes underlying macrophage heterogeneity and polarisation, with a particular focus on processes relevant to ADPKD, namely efferocytosis and calcium signalling. I have shown how Simu-dependent efferocytosis is required for the shift out of the *VT57089* subpopulation seen in *repo* mutants, and that a loss of *simu*, required for anti-inflammatory efferocytosis, is typically associated with increased proportions of macrophages within putative pro-inflammatory subpopulations, at all developmental stages this has been investigated in.

Downstream of *simu*, I have implicated the *Drosophila PKD2* homolog *amo* in modulating the apparent shift out of the *VT57089* subpopulation and revealed a possible role for Amo in phagolysosomal maturation. I have also revealed that the calcium-binding chaperone protein Calnexin14D is associated with increased rates of phagocytosis-associated calcium flashes which are known to prime macrophages for mediating inflammatory wound responses. Finally, I have shown that the steroid hormone Ecdysone is required for the establishment of a pro-

inflammatory subpopulation of embryonic macrophages, a result which possibly implicated Ecdysone in the re-emergence of subpopulation macrophages in *Drosophila* adults.

Overall, these results reveal that *Drosophila* macrophages continue to be more complicated than first thought and validate their use as a model of macrophage heterogeneity. The fact that the different macrophage subpopulations generally respond in different ways to different stimuli at different developmental stages shows clearly how complex these cells, once thought to be homogeneous, actually are. Furthermore, that we are able to understand the processes driving macrophages into and out of certain subpopulations suggests that *Drosophila* could be used as a model of macrophage polarisation, a process that, like heterogeneity, was once thought to be limited to vertebrates. Having a comparatively simple model of studying this phenomenon will allow crucial insight into understanding this process, which is implicated in numerous chronic diseases.

N.b., in a bid to try to reveal which genes could be regulated by the *VT* enhancers, I have carried out targeted DamID (TaDa) in order to carry out transcriptional profiling of the *Drosophila* macrophage subpopulations (Marshall et al., 2016; Southall et al., 2013). Unfortunately, the data was not analysed in sufficient time to include it in this thesis, but I hope to use it as the basis of a primary research paper.

# Chapter 6: Final discussion

## 6.1 Project summary

The major aim of this project was to investigate how *Drosophila* could be used to further our understanding of the pathogenesis of ADPKD. This was to be achieved through three parts, firstly by using two previously-reported phenotypes (Gao et al., 2004; Watnick et al., 2003) caused by *amo/Pkd2* mutations as functional readouts of pathogenic *amo/PKD2* variants (chapter 3). Secondly, a reported involvement of *amo/Pkd2* in efferocytosis (Van Goethem et al., 2012) was investigated further, in order to see if defects caused by this mutation had adverse consequences on macrophage function and behaviour, to assess whether this could contribute to ADPKD pathogenesis (chapter 4). Finally, the specification and polarisation of recently discovered *Drosophila* macrophage subpopulations was investigated (Coates et al., 2021), in a bid to understand how macrophage polarisation can be modulated via disrupted calcium signalling and efferocytosis (chapter 5), processes related to ADPKD pathogenesis (Cassini et al., 2018; Karihaloo et al., 2011; Swenson-Fields et al., 2013). Understanding these processes in a comparatively simple model would offer further insight into how they could contribute towards ADPKD.

The results presented in the first two chapters proved inconclusive. A reporter generated for the first strand of this project revealed a novel phenotype in *amo* mutant larvae, showing that calcium waves propagating down the visceral smooth musculature were both slower and less frequent in *amo* mutants. Though this would have offered an interesting functional readout of pathogenic variants, along with defecation rates and male fertility, I was unable to successfully generate control lines that expressed wild-type *amo* for rescue experiments. Results looking into the effect of *amo* mutations on macrophage function were also mixed, as initial data seemed to suggest that *amo* mutant macrophages exhibited phenotypes typically associated with defective efferocytosis as per Roddie et al., 2019. However, experiments using other macrophage reporters/genetic backgrounds failed to recapitulate these phenotypes, nor were any gross defects in efferocytosis identified. The use of different control lines in subsequent

experiments seemed to show that these initial phenotypes were false positives, likely caused by background mutations.

Investigations into the specification and polarisation of *Drosophila* macrophage subpopulations was more successful, with various processes having been shown to be involved. Simu-dependent apoptotic cell clearance appeared to modulate macrophage subpopulations across development, with effects generally most pronounced in adults. It was also shown that Amo, possibly downstream of Simu, was involved in this process, although these results depended on challenge with high levels of apoptosis. The *Drosophila* steroid hormone receptor EcR was also implicated in the establishment of one sub-population, associated with the *VT62766* enhancer, which may modulate expression of *calnexin14D*. Calnexin14D itself seemed to be involved in phenotypic changes associated with this putative pro-inflammatory subpopulation, by being implicated in the priming of macrophages to mount an effective wound response (Weavers et al., 2016).

### 6.1.1 The use of *Drosophila* to model pathogenic *Pkd2* variants

Both *PKD1* and *PKD2* exhibit marked allelic heterogeneity, further compounding efforts to understand the function of the two Polycystin proteins and understand their role in pathogenesis of ADPKD (Magistroni et al., 2003; Sandro Rossetti et al., 2001). Numerous missense variants of *PKD2* have been characterised, many of which have yet to have their functional impact clarified (Grieben et al., 2017, Yu et al., 2011). One of the aims of this project was to exploit *Drosophila* as a model to transgenic *PKD2* variants to be expressed in an *amo* null background, with male infertility and visceral muscle contraction representing functional readouts. Crucially, these transgenic lines were to be inserted into the genome at specific sites, controlling for expression levels and negating the potential for site-specific effects seen via random insertion into the genome (Bateman et al., 2006).

Following transgenesis, it appeared that *PKD2* was able to express at reasonable levels based on immunostaining. However, neither male infertility nor larval smooth muscle contractility were rescued on expression of this transgene, suggesting that PC-2 and Amo have functionally diverged. As such, the screening of pathogenic variants would therefore be limited to

introducing mutations on conserved residues on Amo. However, the wild-type *UAS-amo* control line generated for this study did not appear to express, nor did it rescue even when expressed as an untagged isoform. As such, I was unable to carry out the planned screening of patient-associated variants, as there was insufficient time to repeat the transgenesis using different insertion sites or different cloning approaches.

An interesting phenotype was revealed using a novel reporter for calcium within the visceral smooth muscle (*24b-GAL4,UAS-GCaMP6m*). It has previously been shown by Gao et al. that *amo* mutant *Drosophila* are haploinsufficient for mediating visceral smooth muscle contractility (Gao et al., 2004), and this reporter reveals that this defect appears to be due to the function of Amo as a calcium-permeable cation channel, with *amo* mutant larvae exhibiting fewer calcium waves propagating down the smooth muscle surrounding the visceral hindgut when compared to controls. These waves also propagated at slower speeds in *amo* mutants, suggesting that Amo is required for the effective release of calcium from the sarcoplasmic reticulum (SR) which is ultimately essential for the contraction of myosin fibres in muscle cells (Mizuno et al., 2008). This is consistent with Amo/PC-2 being involved in the modulation of the SR calcium-release channels RyR and IP3R, both of which are essential for mediating calcium induced calcium entry during smooth muscle contraction (Anyatonwu et al., 2007; Collier et al., 2000; Y. Li et al., 2005). This phenotype would make an interesting means with which to test the involvement of such channels and other downstream effectors.

Though I was not able to achieve my ultimate aim of screening pathogenic variants, the fact that human *PKD2* is unable to rescue *amo* mutant phenotypes is undoubtedly of relevance to the field. Furthermore, the calcium wave phenotypes seen in the visceral smooth musculature will offer additional functional readouts of *amo* mutants to be gleaned, should a site-specific *UAS-amo* rescue construct successfully be generated.

### 6.1.2 The role of Amo in apoptotic cell clearance and macrophage behaviour

The polycystic kidney is a highly-inflamed environment and is associated with influx of macrophages and high levels of uncleared apoptotic cells (Cassini et al., 2018; Karihaloo, 2015;

Karihaloo et al., 2011; Peintner & Borner, 2017; Swenson-Fields et al., 2013). *Drosophila* has previously been used to show how failures in efferocytosis, such as via *simu* mutations, are sufficient to impair macrophage function and behaviour (Armitage et al., 2020; Evans et al., 2015; Roddie et al., 2019). Given that *Drosophila Pkd2/amo* has been implicated in apoptotic cell clearance (Van Goethem et al., 2012), together with the fact that calcium signalling is also required for effective efferocytosis and the inflammatory wound response (Cuttell et al., 2008; Weavers et al., 2016), we sought to investigate if *amo* mutations impaired macrophage function in ways characteristic of defective efferocytosis.

Initial experiments revealed decreased number of macrophages on the ventral midline (VML) of stage 15 embryos which also exhibited slower random migration speeds, two phenotypes typically associated with defective apoptotic cell clearance (Roddie et al., 2019). The genetic removal of three pro-apoptotic genes (*hid, reaper* and *grim*) using the *H99* genomic deficiency rescued these defects, suggesting that they were dependent on the interaction of macrophages with apoptotic cells. Similarly, over-expression of *amo* in an *amo* mutant background also appeared to rescue macrophage random migration speeds, suggesting that this phenotype was indeed caused by loss of functional Amo in the macrophages.

Next, I investigated apoptotic clearance via the use of a genetically encoded capsase-3 activity indicator, which revealed no apparent differences in efferocytosis between *amo* mutant macrophages compared to controls. These embryos were imaged at stage 15, where there is comparatively little apoptosis relative to the earlier stages where the phenotype was reported (Van Goethem et al., 2012). However, *simu* mutant macrophages exhibit different numbers of apoptotic vacuoles at stage 15 relative to controls (Roddie et al., 2019), so one may still expect to see an effect in *amo* mutants at this stage, especially considering Amo is proposed to be involved in efferocytosis downstream of Simu (Van Goethem et al., 2012).

The experiments investigating efferocytosis in control and *amo* mutant embryos utilised the *GAL4*-independent reporter *serpent-3x-mCherry* to label macrophages (Gyoergy et al., 2018), unlike previous experiments which utilised *croquemort-GAL4,UAS-GFP*. Curiously, *serpent-3x-mCherry* failed to recapitulate the dispersal phenotype seen using *croquemort-GAL4,UAS-GFP*, with a large discrepancy in the number of macrophages seen on the VML of control embryos.

The use of other reporter lines, both *GAL4*-dependent and independent, to assay macrophage random migration and dispersal revealed no differences between *amo* mutants and controls, and the subsequent use of an outcrossed *croquemort-GAL4,UAS-GFP* control revealed an apparent background mutation in the previously used controls that seemed to augment both macrophage random migration and dispersal.

It is therefore difficult to say whether or not failures in *amo*-mediated efferocytosis do impair macrophage functions in ways one would expect. It appears that any defects are likely subtle, and insufficient to impair macrophage dispersal or migration, and wound responses were also unaffected in *amo* mutants. Work presented in chapter 5 revealed a possible role for Amo in acidification of phagosomes, suggesting that the previously reported phenotype implicating Amo in apoptotic cell clearance may have been due to failures in acidification, as opposed to efferocytosis. This could explain why phenotypes typical of defective efferocytosis were not observed in *amo* mutants. Crucially, no defects were noticed in *amo;repo* double mutants when compared to *repo* only mutants, suggesting that *amo;repo* double mutants are no less able to mediate efferocytosis in response to a high apoptotic challenge than *repo* only controls.

### 6.1.3 The specification and polarisation of *Drosophila* macrophage subpopulations

The final major aim of this project was to use *Drosophila* as a model with which to understand the processes underlying macrophage heterogeneity and polarisation, two processes associated with numerous inflammatory diseases including ADPKD (Abdolmaleki et al., 2018; Cassini et al., 2018; Cornwell et al., 2018; Harris & Torres, 2014; Karihaloo et al., 2011). Recently discovered subpopulations of *Drosophila* macrophages (Coates et al., 2021), which exhibit typical pro-inflammatory behaviours, were challenged with various mutations, and numerous pathways were manipulated. I primarily focused on efferocytosis and calcium signalling, both of which are relevant in the context of ADPKD, and investigated other pathways potentially implicated in *Drosophila* macrophage polarisation, such as steroid hormone and EGF signalling.

When studying the effect of apoptotic cell clearance on 4 distinct macrophage subpopulations, loss of Simu, a major apoptotic cell receptor, was typically associated with increased proportions of subpopulation macrophages at all developmental stages, suggesting that Simu-mediated efferocytosis may be involved in the removal of macrophages out of subpopulations. Significantly, *simu* mutations were able to block the decrease in the *VT57089* subpopulation seen in *repo* mutant embryos, showing that Simu-dependent efferocytosis is required for this decrease. Interestingly, *amo* mutants were shown to phenocopy the effect of *simu* mutants in blocking the decreased proportions of *VT57089* seen in *repo* mutants, suggesting that Amo may be required downstream of Simu in causing this effect (or operate in a parallel, but necessary pathway).

Lysotracker staining revealed decreased phagosome acidification in *amo;repo* double mutants when compared to *repo* single mutants, suggesting that this process may be involved in modulating the departure of macrophages out of this subpopulation. Interestingly, zebrafish PC-1 is required for the acidification of autophagosomes, with it being essential for effective autophagolysosomal fusion (Peintner et al., 2020). Loss of *PKD1* results in activation of Calpain proteases, which degraded Lamp1 on the surface of lysosomes. Given the calcium dependence of Calpain activity and the disruption of calcium homeostasis associated with loss of Amo/PKD2, it is possible that similar aberrant activation of Calpains occurs in Amo mutants, degrading Lamp1 on the surface of lysosomes and preventing phagolysosomal fusion. Whether this is occurring *in vivo* or not, targeting phagosome maturation could offer a novel therapeutic target with respect to ADPKD.

Though Simu and Amo were implicated in modulating the shift out of *VT57089* subpopulation macrophages in *repo* mutants, we are still unsure what could be causing the effect seen in the other 3 subpopulations. In a bid to try and elucidate what could be modulating these shifts, other apoptotic cell receptors were investigated. However, neither Croquemort nor Draper mediated efferocytosis seemed to modulate the decreased numbers of subpopulations seen in *repo* mutants, suggesting that interactions between macrophages and glial cells may be required for the establishment of certain subpopulations. Alternatively, there is the potential that some of these populations are overlapping and differences between responses to different stimuli may represent differences in enhancer regulation rather than alterations in

subpopulations. This will be, in part, addressed via transcriptional profiling approaches (e.g., our targeted DamID work, which is near completion).

The action of the steroid hormone Ecdysone induces striking phenotypic changes in macrophage behaviour at various developmental stages in *Drosophila*, particularly at the onset of metamorphosis when macrophages shift to become highly phagocytic and motile (Regan et al., 2013; Sampson et al., 2013; Tan et al., 2014). Pan-macrophage expression of a dominant-negative isoform of the Ecdysone receptor resulted in significantly fewer numbers of *VT6766* subpopulation cells, suggesting this hormone may help establish this subpopulation. The *VT62766* enhancer may be acting upon *cnx14D*, based on its relative proximity to the *cnx14D* ORF, and data suggesting that *cnx14D* overexpression enhances the priming of macrophages to mount an effective immune response (Coates et al., 2021; Weavers et al., 2016). A mechanism has been proposed, wherein *cnx14D* is expressed downstream of EcR, resulting in the establishment the *VT62766* subpopulation, members of which are primed to mount an effective immune response (**figure 5.24).**

### 6.1.4 Future work

This project has identified several pathways regulating subpopulation identity, via mechanisms relevant to ADPKD. These require further investigation to understand them in greater detail. However, attempts to use *Drosophila* to model pathogenic *amo/PKD2* variants were unsuccessful, and experimental design may need to change if this was to be pursued in the future. Though expression of *UAS-amo* in *attP2* was not successful, transgenic rescue constructs can be inserted into other sites, using different transgenesis vectors. If expression of *UAS-amo* is successful in another insertion site, pathogenic mutations can easily be introduced at residues conserved in *PKD2* via site-directed mutagenesis, allowing insight into the functional impact of these variants.

Though results investigating the role of *amo/PKD2* in apoptotic cell clearance largely seem to suggest failures in this process may not contribute towards ADKPD pathogenesis, other experiments should be carried out before categorically ruling this out. For example, the ability

of *Drosophila* macrophages lacking Amo to mediate efferocytosis was only assayed at the embryonic stage. It would therefore be of interest to investigate the effect of *amo* mutations at different developmental stages using *ex vivo* macrophages from larvae, pupae and adults. Indeed, given the relatively late age of ADPKD onset, these experiments would offer valuable insight into how the impact of loss Amo/PC-2 may change with increased ageing. As well as *Drosophila*, further experiments should also be carried out in in mammalian cells to investigate the role of PC-2 in efferocytosis. In our experiments, we investigated efferocytosis in renal tubular epithelial cells, which mediated efferocytosis at incredibly low levels with or without *PKD2* expression, possibly due to low levels of endogenous KIM-1 expression (a phosphatidylserine receptor upregulated in response to acute kidney injury (Ichimura et al., 2008; Yang et al., 2015)). Cell lines could possibly be transfected to induce KIM-1 expression in order to stimulate epithelial efferocytosis which would enable a more effective comparisons of control and *PKD2* knockout cells to be made. It would also be interesting to investigate if MDMs, which appear to mediate *in vitro* efferocytosis at much higher rates than tubular epithelial cells, could be isolated from ADPKD patients, and used for efferocytosis assays. Furthermore, this project has focussed on *PKD2*, due to the involvement of *amo* in efferocytosis – given the increased severity of patients possessing *PKD1* mutations, it would be worth investigating if *PKD1* mutant cell lines or MDMs from patients are less effective at mediating efferocytosis.

Given the somewhat contrasting results seen in chapters 4 and 5 in terms of the role of Amo in efferocytosis, future work should be done to try and validate the apparent requirement for Amo in phagosomal acidification. CharON (Caspase and pH Activated Reporter, Fluorescence ON) is a recently developed reporter containing both a GC3Ai-related Caspase activity indicator and red-fluorescent pH sensor (Raymond et al., 2022). This reporter would allow dynamic changes in phagosome acidification to be visualised over time, and also would not cause any stress to embryos. This is in stark contrast to lysotracker staining, wherein embryos have to be treated with heptane in order to let the dye pass through the vitelline membrane.

Future experiments investigating macrophage subpopulations in *Drosophila* should investigate the overlap of the subtypes identified by Coates et al. with one another, to reveal whether these populations are in fact distinct. This can theoretically be achieved relatively easily, either

via the use of two *GAL4*-independent reporters (e.g., *VT-RFP* with *VT-GFP*), or via *GAL4*-independent reporters in tandem with a *GAL4*-dependent reporter (e.g., *VT-RFP* with *VT-GAL4,UAS-stinger*). Characterising similarities and differences between different subpopulations could enable greater insight into how each of these are specified, and how they might respond to different environmental challenges.

Subpopulation macrophages all exhibit a significant decrease in response to the high apoptotic challenge presented by *repo* mutations. However, we are unsure of whether this represents a 'shift' away from a more pro-inflammatory activation state, or failures in subpopulations being specified in this background in the first place. Using the GAL4/UAS system in concert with a temperature sensitive variant of GAL80 (a negative regulator of GAL4 activity), apoptosis can be induced in a specific tissue at a specific time via heat-shocking embryos (McGuire et al., 2003; Wing et al., 1999). It would be of interest to investigate if acute induction of apoptosis is associated with dynamic changes in subpopulation reporter activity, which would show whether this 'shift' is in fact due to polarisation in response to environmental challenge.

Most subpopulations exhibited increased numbers in newly-eclosed *simu* mutant adults. I hypothesise that this is due to decreased efferocytosis occurring during metamorphosis, causing chronic challenge with high numbers of apoptotic cells. This has the impact that fewer macrophages shift out of subpopulations (or become specified according to their normal fate), compared to their normal re-emergence by adult stages (Coates et al., 2021). This hypothesis could be tested by imaging control and *simu* mutant pupae expressing the pan-macrophage reporter *serpent-3x-mCherry* (Gyoergy et al., 2018) together with *da-GAL4,UAS-GC3Ai* to label apoptotic cells (Roddie et al., 2019; Schott et al., 2017). This would allow dynamic interactions between apoptotic cells and macrophages to be seen, with any defects in efferocytosis to be characterised. A separate interesting experiment investigating pupal macrophages would be the effect of a dominant-negative EcR on subpopulation macrophages. EcR does seem to play a role in the establishment of the *VT62766* subpopulation at embryonic stages. Though EcR is known to be involved in establishing embryonic immunity in *Drosophila* (Tan et al., 2014), it also plays major roles in driving metamorphosis, an event associated with both altered macrophage activation state and the re-emergence of subpopulations (Coates et al., 2021; Regan et al., 2013; Sampson et al., 2013). It would therefore be of interest to see whether

ecdysone is involved in the re-emergence of macrophage subpopulations at the onset of metamorphosis.

Another important experiment which was carried out as part of this project was the transcriptional profiling of subpopulations, but unfortunately results from this experiment were not analysed in sufficient time to include in this thesis. A targeted DNA adenine methyltransferase identification (Targeted DamID/TaDa) approach was used, wherein a DNA modifying enzyme (DNA adenine methyltransferase – Dam) fused to RNA polymerase II was expressed specifically in subpopulation macrophages via the GAL4/UAS system (Marshall et al., 2016; Southall et al., 2013). This ultimately generates a library of modified DNA, representing regions of the genome that are actively transcribed in specific macrophage populations. Following Next Generation sequencing, comparisons can be made between the profiles of subpopulations and control cells, in this instance where the *serpent* promoter was driving expression of the Dam fusion protein. This approach may reveal distinct mechanisms regulating different subpopulations, as well as those common to subpopulations which may be relatively downregulated in *serpent* controls. We hope to use these results as the basis of a primary research paper.

### 6.1.5 Covid statement

When the pandemic struck in March 2020, I had just begun the cloning to generate transgenic *UAS-amo* and *UAS-PKD2*. I was to carry this out with the help of lab members who are very experienced in this; however, when I returned to the lab strict social distancing measures were in place, and I had to carry out this work by myself, resulting in it taking much longer than it otherwise would have done. Furthermore, when we were allowed to return to the lab it was on a shift basis, where I was generally in from 9am-1pm meaning I had limited time in the lab to catch up on all the important practical work that had been missed. In addition, the time taken to get sequencing results back and receive transgenic flies both took significantly longer than we had anticipated when planning this project, meaning we were unable to recoup any of the time lost to lockdowns. As such, generation of the transgenic flies took much longer than we had anticipated, and when these appeared to not successfully rescue as expected, we did

not have sufficient time remaining to generate transgenics expressing *UAS-amo* at a different insertion site, resulting in a somewhat shortened results chapter.

Following resumption of work on campus, progress was significantly slowed by continuing hybrid working patterns. This delayed communications, particularly where internal facilities were relied upon that had yet to fully resume. This caused delays to other strands of work, such as our TaDa approach and also meant microscopy access was at times restricted.

As well as during the national lockdown, I missed out on a significant amount of lab work due to having to self-isolate for over a week on two occasions for coronavirus, once in January 2021 (due to contact tracing) and once in July 2021 (due to a cohabitee testing positive). Having fortunately avoided it for over two years I contracted coronavirus at the end of May 2022, and I was ill for over a week of the final few weeks of my write-up period. I also had to regularly provide cover for lab colleagues when they had to self-isolate (which happened numerous times), meaning I had less time available to carry out my own experiments.

# Appendix

Standard *Drosophila* medium recipe:

- 1 Litre Cold tap water
- 80g Medium Cornmeal
- 18g Dried Yeast
- 10g Soya Flour
- 80g Malt Extract
- 40g Molasses
- 8g Agar
- 25mL 10% Nipagin in Absolute Ethanol
- 4mL Propionic Acid

Apple juice agar plate recipe:

- 400mL Distilled water
- 15g agar
- 100mL apple juice
- 7.5mL 10% Nipagin in absolute ethanol

# Bibliography


Abdolmaleki, F., Farahani, N., Hayat, S. M. G., Pirro, M., Bianconi, V., Barreto, G. E., & Sahebkar, A. (2018). The Role of Efferocytosis in Autoimmune Diseases. *Frontiers in Immunology*, *9*(JUL), 1645. https://doi.org/10.3389/FIMMU.2018.01645

Abrams, J. M., White, K., Fessler, L. I., & Steller, H. (1993). Programmed cell death during Drosophila embryogenesis. *Development*, *117*(1).

Adams, J. M., & Cory, S. (2007). The Bcl-2 apoptotic switch in cancer development and therapy. *Oncogene*, *26*(9), 1324–1337. https://doi.org/10.1038/sj.onc.1210220

Anyatonwu, G. I., Estrada, M., Tian, X., Somlo, S., & Ehrlich, B. E. (2007). Regulation of ryanodine receptor-dependent calcium signaling by polycystin-2. *Proceedings of the National Academy of Sciences of the United States of America*, *104*(15), 6454. https://doi.org/10.1073/PNAS.0610324104

Ariza, M., Alvarez, V., Marín, R., Aguado, S., López-Larrea, C., Alvarez, J., Menéndez, M. J., & Coto, E. (1997). A family with a milder form of adult dominant polycystic kidney disease not linked to the PKD1 (16p) or PKD2 (4q) genes. *Journal of Medical Genetics*, *34*(7), 587–589. http://www.ncbi.nlm.nih.gov/pubmed/9222969

Armitage, E. L., Roddie, H. G., & Evans, I. R. (2020). Overexposure to apoptosis via disrupted glial specification perturbs Drosophila macrophage function and reveals roles of the CNS during injury. *Cell Death & Disease 2020 11:8*, *11*(8), 1–18. https://doi.org/10.1038/s41419-020-02875-2

Audrézet, M.-P., Cornec-Le Gall, E., Chen, J.-M., Redon, S., Quéré, I., Creff, J., Bénech, C., Maestri, S., Le Meur, Y., & Férec, C. (2012). Autosomal dominant polycystic kidney disease: Comprehensive mutation analysis of PKD1 and PKD2 in 700 unrelated patients. *Human Mutation*, *33*(8), 1239–1250. https://doi.org/10.1002/humu.22103

Barnes, P. J., Burney, P. G. J., Silverman, E. K., Celli, B. R., Vestbo, J., Wedzicha, J. A., & Wouters, E. F. M. (2015). Chronic obstructive pulmonary disease. *Nature Reviews Disease Primers 2015 1:1*, *1*(1), 1–21. https://doi.org/10.1038/nrdp.2015.76

Barolo, S., Carver, L. A., & Posakony, J. W. (2000). GFP and β-Galactosidase Transformation Vectors for Promoter/Enhancer Analysis in Drosophila. *Https://Doi.Org/10.2144/00294bm10*, *29*(4), 726–732.

https://doi.org/10.2144/00294BM10

Barolo, Scott, Castro, B., & Posakony, J. W. (2004). New Drosophila transgenic reporters: Insulated P-element vectors expressing fast-maturing RFP. *BioTechniques*, *36*(3), 436–442. https://doi.org/10.2144/04363ST03/ASSET/IMAGES/LARGE/FIGURE3.JPEG

Barr, M. M., DeModena, J., Braun, D., Nguyen, C. Q., Hall, D. H., & Sternberg, P. W. (2001). The Caenorhabditis elegans autosomal dominant polycystic kidney disease gene homologs lov-1 and pkd-2 act in the same pathway. *Current Biology : CB*, *11*(17), 1341–1346. http://www.ncbi.nlm.nih.gov/pubmed/11553327

Bassé, F., Stout, J. G., Sims, P. J., & Wiedmer, T. (1996). Isolation of an erythrocyte membrane protein that mediates Ca2+-dependent transbilayer movement of phospholipid. *The Journal of Biological Chemistry*, *271*(29), 17205–17210. http://www.ncbi.nlm.nih.gov/pubmed/8663431

Bateman, J. R., Lee, A. M., & Wu, C. T. (2006). Site-Specific Transformation of Drosophila via ϕC31 Integrase-Mediated Cassette Exchange. *Genetics*, *173*(2), 769. https://doi.org/10.1534/GENETICS.106.056945

Belibi, F. A., Reif, G., Wallace, D. P., Yamaguchi, T., Olsen, L., Li, H., Helmkamp, G. M., & Grantham, J. J. (2004). Cyclic AMP promotes growth and secretion in human polycystic kidney epithelial cells. *Kidney International*, *66*(3), 964–973. https://doi.org/10.1111/j.1523-1755.2004.00843.x

Bhunia, A. K., Piontek, K., Boletta, A., Liu, L., Qian, F., Xu, P.-N., Germino, F. J., & Germino, G. G. (2002). PKD1 Induces p21waf1 and Regulation of the Cell Cycle via Direct Activation of the JAK-STAT Signaling Pathway in a Process Requiring PKD2. *Cell*, *109*(2), 157–168. https://doi.org/10.1016/S0092-8674(02)00716-X

Bisgrove, B. W., Snarr, B. S., Emrazian, A., & Yost, H. J. (2005). Polaris and Polycystin-2 in dorsal forerunner cells and Kupffer's vesicle are required for specification of the zebrafish left–right axis. *Developmental Biology*, *287*(2), 274–288. https://doi.org/10.1016/j.ydbio.2005.08.047

Blanco-Obregon, D., Katz, M. J., Durrieu, L., Gándara, L., & Wappner, P. (2020). Context-specific functions of Notch in Drosophila blood cell progenitors. *Developmental Biology*, *462*(1), 101–115. https://doi.org/10.1016/J.YDBIO.2020.03.018

Bobryshev, Y. V., Ivanova, E. A., Chistiakov, D. A., Nikiforov, N. G., & Orekhov, A. N. (2016). Macrophages and Their Role in Atherosclerosis: Pathophysiology and Transcriptome

Analysis. *BioMed Research International*, *2016*. https://doi.org/10.1155/2016/9582430

Bogdanova, N., Dworniczak, B., Dragova, D., Todorov, V., Dimitrakov, D., Kalinov, K., Hallmayer, J., Horst, J., & Kalaydjieva, L. (1995). Genetic heterogeneity of polycystic kidney disease in Bulgaria. *Human Genetics*, *95*(6), 645–650. http://www.ncbi.nlm.nih.gov/pubmed/7789949

Boulet, M., Renaud, Y., Lapraz, F., Benmimoun, B., Vandel, L., & Waltzer, L. (2021). Characterization of the Drosophila Adult Hematopoietic System Reveals a Rare Cell Population With Differentiation and Proliferation Potential. *Frontiers in Cell and Developmental Biology*, *9*. https://doi.org/10.3389/FCELL.2021.739357/FULL

Brückner, K., Kockel, L., Duchek, P., Luque, C. M., Rørth, P., & Perrimon, N. (2004). The PDGF/VEGF Receptor Controls Blood Cell Survival in Drosophila. *Developmental Cell*, *7*(1), 73–84. https://doi.org/10.1016/J.DEVCEL.2004.06.007

Buchon, N., Silverman, N., & Cherry, S. (2014). Immunity in Drosophila melanogaster--from microbial recognition to whole-organism physiology. *Nature Reviews. Immunology*, *14*(12), 796–810. https://doi.org/10.1038/NRI3763

Bulley, S., Fernández-Peña, C., Hasan, R., Leo, M. D., Muralidharan, P., Mackay, C. E., Evanson, K. W., Moreira-Junior, L., Mata-Daboin, A., Burris, S. K., Wang, Q., Kuruvilla, K. P., & Jaggar, J. H. (2018). Arterial smooth muscle cell PKD2 (TRPP1) channels regulate systemic blood pressure. *ELife*, *7*. https://doi.org/10.7554/eLife.42628

Bycroft, M., Bateman, A., Clarke, J., Hamill, S. J., Sandford, R., Thomas, R. L., & Chothia, C. (1999). The structure of a PKD domain from polycystin-1: implications for polycystic kidney disease. *The EMBO Journal*, *18*(2), 297–305. https://doi.org/10.1093/emboj/18.2.297

Cabrero, P., Terhzaz, S., Romero, M. F., Davies, S. A., Blumenthal, E. M., & Dow, J. A. T. (2014). Chloride channels in stellate cells are essential for uniquely high secretion rates in neuropeptidestimulated Drosophila diuresis. *Proceedings of the National Academy of Sciences of the United States of America*, *111*(39), 14301–14306. https://doi.org/10.1073/PNAS.1412706111/SUPPL_FILE/PNAS.201412706SI.PDF

Cai, Y., Fedeles, S. V, Dong, K., Anyatonwu, G., Onoe, T., Mitobe, M., Gao, J.-D., Okuhara, D., Tian, X., Gallagher, A.-R., Tang, Z., Xie, X., Lalioti, M. D., Lee, A.-H., Ehrlich, B. E., & Somlo, S. (2014). Altered trafficking and stability of polycystins underlie polycystic kidney disease. *The Journal of Clinical Investigation*, *124*(12), 5129–5144.

https://doi.org/10.1172/JCI67273

Campbell, G., Göring, H., Lin, T., Spana, E., Andersson, S., Doe, C. Q., & Tomlinson, A. (1994). RK2, a glial-specific homeodomain protein required for embryonic nerve cord condensation and viability in Drosophila. *Development*, *120*(10), 2957–2966. https://doi.org/10.1242/DEV.120.10.2957

Caroli, A., Perico, N., Perna, A., Antiga, L., Brambilla, P., Pisani, A., Visciano, B., Imbriaco, M., Messa, P., Cerutti, R., Dugo, M., Cancian, L., Buongiorno, E., De Pascalis, A., Gaspari, F., Carrara, F., Rubis, N., Prandini, S., Remuzzi, A., … ALADIN study group. (2013). Effect of longacting somatostatin analogue on kidney and cyst growth in autosomal dominant polycystic kidney disease (ALADIN): a randomised, placebo-controlled, multicentre trial. *The Lancet*, *382*(9903), 1485–1495. https://doi.org/10.1016/S0140-6736(13)61407-5

Cassini, M. F., Kakade, V. R., Kurtz, E., Sulkowski, P., Glazer, P., Torres, R., Somlo, S., & Cantley, L. G. (2018). Mcp1 Promotes Macrophage-Dependent Cyst Expansion in Autosomal Dominant Polycystic Kidney Disease. *Journal of the American Society of Nephrology*, *29*(10), 2471–2481. https://doi.org/10.1681/ASN.2018050518

Casso, D., Ramírez-Weber, F.-A., & Kornberg, T. B. (2000). GFP-tagged balancer chromosomes for Drosophila melanogaster. *Mechanisms of Development*, *91*(1–2), 451–454. https://doi.org/10.1016/S0925-4773(00)00248-3

Cattenoz, P. B., Sakr, R., Pavlidaki, A., Delaporte, C., Riba, A., Molina, N., Hariharan, N., Mukherjee, T., & Giangrande, A. (2020). Temporal specificity and heterogeneity of Drosophila immune cells. *The EMBO Journal*, *39*(12). https://doi.org/10.15252/embj.2020104486

Ćelić, A. S., Petri, E. T., Benbow, J., Hodsdon, M. E., Ehrlich, B. E., & Boggon, T. J. (2012). Calcium-induced conformational changes in C-terminal tail of polycystin-2 are necessary for channel gating. *Journal of Biological Chemistry*, *287*(21), 17232–17240. https://doi.org/10.1074/JBC.M112.354613/ATTACHMENT/27FBFCAA-C112-4EB5-908A-FA81EB2E6009/MMC1.PDF

Celio, M. R., & Heizmann, C. W. (1982). Calcium-binding protein parvalbumin is associated with fast contracting muscle fibres. *Nature 1982 297:5866*, *297*(5866), 504–506. https://doi.org/10.1038/297504a0

Chang, M. Y., Ma, T. L., Hung, C. C., Tian, Y. C., Chen, Y. C., Yang, C. W., & Cheng, Y. C. (2017). Metformin Inhibits Cyst Formation in a Zebrafish Model of Polycystin-2 Deficiency.

*Scientific Reports 2017 7:1*, *7*(1), 1–12. https://doi.org/10.1038/s41598-017-07300-x

Chapman, A. B., Stepniakowski, K., & Rahbari-Oskoui, F. (2010). Hypertension in Autosomal Dominant Polycystic Kidney Disease. *Advances in Chronic Kidney Disease*, *17*(2), 153–163. https://doi.org/10.1053/j.ackd.2010.01.001

Chauhan, A., Sun, Y., Sukumaran, P., Quenum Zangbede, F. O., Jondle, C. N., Sharma, A., Evans, D. L., Chauhan, P., Szlabick, R. E., Aaland, M. O., Birnbaumer, L., Sharma, J., Singh, B. B., & Mishra, B. B. (2018). M1 Macrophage Polarization Is Dependent on TRPC1-Mediated Calcium Entry. *IScience*, *8*, 85–102. https://doi.org/10.1016/j.isci.2018.09.014

Chauvet, V., Qian, F., Boute, N., Cai, Y., Phakdeekitacharoen, B., Onuchic, L. F., Attié-Bitach, T., Guicharnaud, L., Devuyst, O., Germino, G. G., & Gubler, M.-C. (2002). Expression of PKD1 and PKD2 Transcripts and Proteins in Human Embryo and during Normal Kidney Development. *The American Journal of Pathology*, *160*(3), 973–983. https://doi.org/10.1016/S0002-9440(10)64919-X

Chen, J., Li, M., Yang, C., Yin, X., Duan, K., Wang, J., & Feng, B. (2018). Macrophage phenotype switch by sequential action of immunomodulatory cytokines from hydrogel layers on titania nanotubes. *Colloids and Surfaces. B, Biointerfaces*, *163*, 336–345. https://doi.org/10.1016/J.COLSURFB.2018.01.007

Chen, L., Zhou, X., Fan, L. X., Yao, Y., Swenson-Fields, K. I., Gadjeva, M., Wallace, D. P., Peters, D. J. M., Yu, A., Grantham, J. J., & Li, X. (2015). Macrophage migration inhibitory factor promotes cyst growth in polycystic kidney disease. *Journal of Clinical Investigation*, *125*(6), 2399–2412. https://doi.org/10.1172/JCI80467

Chen, T.-W., Wardill, T. J., Sun, Y., Pulver, S. R., Renninger, S. L., Baohan, A., Schreiter, E. R., Kerr, R. A., Orger, M. B., Jayaraman, V., Looger, L. L., Svoboda, K., & Kim, D. S. (2013). Ultrasensitive fluorescent proteins for imaging neuronal activity. *Nature*, *499*(7458), 295–300. https://doi.org/10.1038/nature12354

Cherbas, L., Hu, X., Zhimulev, I., Belyaeva, E., & Cherbas, P. (2003). EcR isoforms in Drosophila: testing tissue-specific requirements by targeted blockade and rescue. *Development*, *130*(2), 271–284. https://doi.org/10.1242/DEV.00205

Chipuk, J. E., Bouchier-Hayes, L., & Green, D. R. (2006). Mitochondrial outer membrane permeabilization during apoptosis: the innocent bystander scenario. *Cell Death & Differentiation 2006 13:8*, *13*(8), 1396–1402. https://doi.org/10.1038/sj.cdd.4401963

Cho, N. K., Keyes, L., Johnson, E., Heller, J., Ryner, L., Karim, F., & Krasnow, M. A. (2002).

Developmental control of blood cell migration by the Drosophila VEGF pathway. *Cell*, *108*(6), 865–876. https://doi.org/10.1016/S0092-8674(02)00676-1

Christodoulou, S., Lockyer, A. E., Foster, J. M., Hoheisel, J. D., & Roberts, D. B. (1997). Nucleotide sequence of a Drosophila melanogaster cDNA encoding a calnexin homologue. *Gene*, *191*(2), 143–148. https://doi.org/10.1016/S0378-1119(97)00025-5

Coates, J. A., Brooks, E., Brittle, A. L., Armitage, E. L., Zeidler, M. P., & Evans, I. R. (2021). Identification of functionally distinct macrophage subpopulations in drosophila. *ELife*, *10*. https://doi.org/10.7554/ELIFE.58686

Cohen, G. M. (1997). Caspases: the executioners of apoptosis. *The Biochemical Journal*, *326 ( Pt 1)*, 1–16. http://www.ncbi.nlm.nih.gov/pubmed/9337844

Collier, M. L., Ji, G., Wang, Y. X., & Kotlikoff, M. I. (2000). Calcium-induced calcium release in smooth muscle: Loose coupling between the action potential and calcium release. *Journal of General Physiology*, *115*(5), 653–662. https://doi.org/10.1085/JGP.115.5.653/VIDEO-1

Cornec-Le Gall, E., Audrezet, M.-P., Chen, J.-M., Hourmant, M., Morin, M.-P., Perrichot, R., Charasse, C., Whebe, B., Renaudineau, E., Jousset, P., Guillodo, M.-P., Grall-Jezequel, A., Saliou, P., Ferec, C., & Le Meur, Y. (2013). Type of PKD1 Mutation Influences Renal Outcome in ADPKD. *Journal of the American Society of Nephrology*, *24*(6), 1006–1013. https://doi.org/10.1681/ASN.2012070650

Cornec-Le Gall, Emilie, Olson, R. J., Besse, W., Heyer, C. M., Gainullin, V. G., Smith, J. M., Audrézet, M.-P., Hopp, K., Porath, B., Shi, B., Baheti, S., Senum, S. R., Arroyo, J., Madsen, C. D., Férec, C., Joly, D., Jouret, F., Fikri-Benbrahim, O., Charasse, C., … Harris, P. C. (2018). Monoallelic Mutations to DNAJB11 Cause Atypical Autosomal-Dominant Polycystic Kidney Disease. *American Journal of Human Genetics*, *102*(5), 832–844. https://doi.org/10.1016/j.ajhg.2018.03.013

Cornec-Le Gall, Emilie, Torres, V. E., & Harris, P. C. (2018). Genetic Complexity of Autosomal Dominant Polycystic Kidney and Liver Diseases. *Journal of the American Society of Nephrology : JASN*, *29*(1), 13–23. https://doi.org/10.1681/ASN.2017050483

Cornwell, W. D., Kim, V., Fan, X., Vega, M. E., Ramsey, F. V., Criner, G. J., & Rogers, T. J. (2018). Activation and polarization of circulating monocytes in severe chronic obstructive pulmonary disease. *BMC Pulmonary Medicine*, *18*(1). https://doi.org/10.1186/S12890-018-0664-Y

Crowley, L. C., Marfell, B. J., & Waterhouse, N. J. (2016). Morphological analysis of cell death by cytospinning followed by rapid staining. *Cold Spring Harbor Protocols*, *2016*(9), 773–777. https://doi.org/10.1101/PDB.PROT087197

Crozatier, M., & Meister, M. (2007). Drosophila haematopoiesis. *Cellular Microbiology*, *9*(5), 1117–1126. https://doi.org/10.1111/J.1462-5822.2007.00930.X

Cuttell, L., Vaughan, A., Silva, E., Escaron, C. J., Lavine, M., Van Goethem, E., Eid, J.-P., Quirin, M., & Franc, N. C. (2008). Undertaker, a Drosophila Junctophilin, links Draper-mediated phagocytosis and calcium homeostasis. *Cell*, *135*(3), 524–534. https://doi.org/10.1016/j.cell.2008.08.033

Daoust, M. C., Reynolds, D. M., Bichet, D. G., & Somlo, S. (1995). Evidence for a third genetic locus for autosomal dominant polycystic kidney disease. *Genomics*, *25*(3), 733–736. http://www.ncbi.nlm.nih.gov/pubmed/7759112

de Almeida, S., de Almeida, E., Peters, D., Pinto, J. R., Távora, I., Lavinha, J., Breuning, M., & Prata, M. M. (1995). Autosomal dominant polycystic kidney disease: evidence for the existence of a third locus in a Portuguese family. *Human Genetics*, *96*(1), 83–88. http://www.ncbi.nlm.nih.gov/pubmed/7607660

de Gaetano, M., Crean, D., Barry, M., & Belton, O. (2016). M1- and M2-type macrophage responses are predictive of adverse outcomes in human atherosclerosis. *Frontiers in Immunology*, *7*(JUL), 275. https://doi.org/10.3389/FIMMU.2016.00275/BIBTEX

Deltas, C. C. (2001). Mutations of the human polycystic kidney disease 2 (PKD2) gene. *Human Mutation*, *18*(1), 13–24. https://doi.org/10.1002/humu.1145

Denholm, B., Hu, N., Fauquier, T., Caubit, X., Fasano, L., & Skaer, H. (2013). The tiptop/teashirt genes regulate cell differentiation and renal physiology in Drosophila. *Development*, *140*(5), 1100–1110. https://doi.org/10.1242/DEV.088989

Devuyst, O., Chapman, A. B., Shoaf, S. E., Czerwiec, F. S., & Blais, J. D. (2017). Tolerability of Aquaretic-Related Symptoms Following Tolvaptan for Autosomal Dominant Polycystic Kidney Disease: Results From TEMPO 3:4. *Kidney International Reports*, *2*(6), 1132–1140. https://doi.org/10.1016/j.ekir.2017.07.004

Devuyst, O., & Torres, V. E. (2013). Osmoregulation, vasopressin, and cAMP signaling in autosomal dominant polycystic kidney disease. *Current Opinion in Nephrology and Hypertension*, *22*(4), 459–470. https://doi.org/10.1097/MNH.0b013e3283621510

Dewitt, S., & Hallett, M. B. (2002). Cytosolic free $Ca^{2+}$ changes and calpain activation are

required for β integrin–accelerated phagocytosis by human neutrophils. *The Journal of Cell Biology*, *159*(1), 181–189. https://doi.org/10.1083/jcb.200206089

Di Mise, A., Ranieri, M., Centrone, M., Venneri, M., Tamma, G., Valenti, D., & Valenti, G. (2018). Activation of the Calcium-Sensing Receptor Corrects the Impaired Mitochondrial Energy Status Observed in Renal Polycystin-1 Knockdown Cells Modeling Autosomal Dominant Polycystic Kidney Disease. *Frontiers in Molecular Biosciences*, *5*, 77. https://doi.org/10.3389/fmolb.2018.00077

Dong, K., Zhang, C., Tian, X., Coman, D., Hyder, F., Ma, M., & Somlo, S. (2021). Renal plasticity revealed through reversal of polycystic kidney disease in mice. *Nature Genetics 2021 53:12*, *53*(12), 1649–1663. https://doi.org/10.1038/s41588-021-00946-4

Doran, A. C., Yurdagul, A., & Tabas, I. (2020). Efferocytosis in health and disease. In *Nature Reviews Immunology* (Vol. 20, Issue 4, pp. 254–267). https://doi.org/10.1038/s41577-019-0240-6

Dow, J. A. T., Simons, M., & Romero, M. F. (2022). Drosophila melanogaster: a simple genetic model of kidney structure, function and disease. *Nature Reviews. Nephrology*. https://doi.org/10.1038/S41581-022-00561-4

Duvic, B., Hoffmann, J. A., Meister, M., & Royet, J. (2002). Notch signaling controls lineage specification during Drosophila larval hematopoiesis. *Current Biology : CB*, *12*(22), 1923–1927. https://doi.org/10.1016/S0960-9822(02)01297-6

Dworkin, I., Kennerly, E., Tack, D., Hutchinson, J., Brown, J., Mahaffey, J., & Gibson, G. (2009). Genomic Consequences of Background Effects on scalloped Mutant Expressivity in the Wing of Drosophila melanogaster. *Genetics*, *181*(3), 1065. https://doi.org/10.1534/GENETICS.108.096453

Eccles, M. R., & Stayner, C. A. (2014). Polycystic kidney disease - where gene dosage counts. *F1000prime Reports*, *6*, 24. https://doi.org/10.12703/P6-24

Edwards-Jorquera, S. S., Bosveld, F., Bellaïche, Y. A., Lennon-Duménil, A. M., & Glavic, Á. (2020). Trpml controls actomyosin contractility and couples migration to phagocytosis in fly macrophages. *Journal of Cell Biology*, *219*(3). https://doi.org/10.1083/jcb.201905228

El-Brolosy, M. A., & Stainier, D. Y. R. (2017). Genetic compensation: A phenomenon in search of mechanisms. *PLOS Genetics*, *13*(7), e1006780. https://doi.org/10.1371/JOURNAL.PGEN.1006780

Essner, J. J., Amack, J. D., Nyholm, M. K., Harris, E. B., & Yost, H. J. (2005). Kupffer's vesicle is a

ciliated organ of asymmetry in the zebrafish embryo that initiates left-right development of the brain, heart and gut. *Development*, *132*(6), 1247–1260. https://doi.org/10.1242/DEV.01663

Evans, C. J., Hartenstein, V., & Banerjee, U. (2003). Thicker Than Blood: Conserved Mechanisms in Drosophila and Vertebrate Hematopoiesis. *Developmental Cell*, *5*(5), 673–690. https://doi.org/10.1016/S1534-5807(03)00335-6

Evans, C. J., Olson, J. M., Ngo, K. T., Kim, E., Lee, N. E., Kuoy, E., Patananan, A. N., Sitz, D., Tran, P. T., Do, M. T., Yackle, K., Cespedes, A., Hartenstein, V., Call, G. B., & Banerjee, U. (2009). G-TRACE: rapid Gal4-based cell lineage analysis in Drosophila. *Nature Methods 2009 6:8*, *6*(8), 603–605. https://doi.org/10.1038/nmeth.1356

Evans, I R, Ghai, P. A., Urbančič, V., Tan, K.-L., & Wood, W. (2013). SCAR/WAVE-mediated processing of engulfed apoptotic corpses is essential for effective macrophage migration in Drosophila. *Cell Death & Differentiation*, *20*(5), 709–720. https://doi.org/10.1038/cdd.2012.166

Evans, Iwan R, Hu, N., Skaer, H., & Wood, W. (2010). Interdependence of macrophage migration and ventral nerve cord development in Drosophila embryos. *Development (Cambridge, England)*, *137*(10), 1625–1633. https://doi.org/10.1242/dev.046797

Evans, Iwan Robert, Rodrigues, F. S. L. M., Armitage, E. L., & Wood, W. (2015). Draper/CED-1 mediates an ancient damage response to control inflammatory blood cell migration in vivo. *Current Biology : CB*, *25*(12), 1606–1612. https://doi.org/10.1016/j.cub.2015.04.037

Evans, J. H., & Falke, J. J. (2007). Ca2+ influx is an essential component of the positive-feedback loop that maintains leading-edge structure and activity in macrophages. *Proceedings of the National Academy of Sciences*, *104*(41), 16176–16181. https://doi.org/10.1073/pnas.0707719104

Fadeel, B., Xue, D., & Kagan, V. (2010). Programmed cell clearance: Molecular regulation of the elimination of apoptotic cell corpses and its role in the resolution of inflammation. *Biochemical and Biophysical Research Communications*, *396*(1), 7–10. https://doi.org/10.1016/j.bbrc.2010.02.106

Fadok, V. A., Bratton, D. L., Konowal, A., Freed, P. W., Westcott, J. Y., & Henson, P. M. (1998). Macrophages That Have Ingested Apoptotic Cells In Vitro Inhibit Proinflammatory Cytokine Production Through Autocrine/Paracrine Mechanisms Involving TGF-, PGE2,

and PAF. *J. Clin. Invest*, *101*(4), 890–898. http://www.jci.org

Fadok, V. A., de Cathelineau, A., Daleke, D. L., Henson, P. M., & Bratton, D. L. (2001). Loss of Phospholipid Asymmetry and Surface Exposure of Phosphatidylserine Is Required for Phagocytosis of Apoptotic Cells by Macrophages and Fibroblasts. *Journal of Biological Chemistry*, *276*(2), 1071–1077. https://doi.org/10.1074/jbc.M003649200

Feng, S., Okenka, G. M., Bai, C. X., Streets, A. J., Newby, L. J., DeChant, B. T., Tsiokas, L., Obara, T., & Ong, A. C. M. (2008). Identification and Functional Characterization of an N-terminal Oligomerization Domain for Polycystin-2. *Journal of Biological Chemistry*, *283*(42), 28471–28479. https://doi.org/10.1074/JBC.M803834200

Fischer, E., Legue, E., Doyen, A., Nato, F., Nicolas, J.-F., Torres, V., Yaniv, M., & Pontoglio, M. (2006). Defective planar cell polarity in polycystic kidney disease. *Nature Genetics*, *38*(1), 21–23. https://doi.org/10.1038/ng1701

Foggensteiner, L., Bevan, A. P., Thomas, R., Coleman, N., Boulter, C., Bradley, J., Ibraghimov-Beskrovnaya, O., Klinger, K., & Sandford, R. (2000). Cellular and subcellular distribution of polycystin-2, the protein product of the PKD2 gene. *Journal of the American Society of Nephrology : JASN*, *11*(5), 814–827. http://www.ncbi.nlm.nih.gov/pubmed/10770959

Forman, J. R., Qamar, S., Paci, E., Sandford, R. N., & Clarke, J. (2005). The Remarkable Mechanical Strength of Polycystin-1 Supports a Direct Role in Mechanotransduction. *Journal of Molecular Biology*, *349*(4), 861–871. https://doi.org/10.1016/j.jmb.2005.04.008

Franc, N. C., Dimarcq, J.-L., Lagueux, M., Hoffmann, J., & Ezekowitz, R. A. B. (1996). Croquemort, A Novel Drosophila Hemocyte/Macrophage Receptor that Recognizes Apoptotic Cells. *Immunity*, *4*(5), 431–443. https://doi.org/10.1016/S1074-7613(00)80410-0

Franc, N. C., Heitzler, P., Ezekowitz, R. A. B., & White, K. (1999). Requirement for croquemort in phagocytosis of apoptotic cells in Drosophila. *Science*, *284*(5422), 1991–1994. https://doi.org/10.1126/science.284.5422.1991

Freeman, M. R., Delrow, J., Kim, J., Johnson, E., & Doe, C. Q. (2003). Unwrapping Glial Biology: Gcm Target Genes Regulating Glial Development, Diversification, and Function brain barrier that isolates and protects neural tissue. Glia mediate many brain responses to injury and neuro-degenerative diseases (Wyss-Coray and Mucke, 2002), and abnormal glial growth results in gliomas-the most deadly forms of cancer-and other neurological

dis. In *Neuron* (Vol. 38). http://flybase.bio.indiana.

Fu, Y., Huang, X., Zhang, P., van de Leemput, J., & Han, Z. (2020). Single-cell RNA sequencing identifies novel cell types in Drosophila blood. *Journal of Genetics and Genomics*, *47*(4), 175–186. https://doi.org/10.1016/J.JGG.2020.02.004

Fujimoto, E., Gaynes, B., Brimley, C. J., Chien, C. Bin, & Bonkowsky, J. L. (2011). Gal80 Intersectional Regulation of Cell-Type Specific Expression in Vertebrates. *Developmental Dynamics : An Official Publication of the American Association of Anatomists*, *240*(10), 2324. https://doi.org/10.1002/DVDY.22734

Gamberi, C., Hipfner, D. R., Trudel, M., & Lubell, W. D. (2017). Bicaudal C mutation causes myc and TOR pathway up-regulation and polycystic kidney disease-like phenotypes in Drosophila. *PLoS Genetics*, *13*(4). https://doi.org/10.1371/JOURNAL.PGEN.1006694

Gansevoort, R. T., Arici, M., Benzing, T., Birn, H., Capasso, G., Covic, A., Devuyst, O., Drechsler, C., Eckardt, K.-U., Emma, F., Knebelmann, B., Le Meur, Y., Massy, Z. A., Ong, A. C. M., Ortiz, A., Schaefer, F., Torra, R., Vanholder, R., Więcek, A., … Van Biesen, W. (2016). Recommendations for the use of tolvaptan in autosomal dominant polycystic kidney disease: a position statement on behalf of the ERA-EDTA Working Groups on Inherited Kidney Disorders and European Renal Best Practice. *Nephrology, Dialysis, Transplantation : Official Publication of the European Dialysis and Transplant Association - European Renal Association*, *31*(3), 337–348. https://doi.org/10.1093/ndt/gfv456

Gao, Z., Joseph, E., Ruden, D. M., & Lu, X. (2004). Drosophila Pkd2 Is Haploid-insufficient for Mediating Optimal Smooth Muscle Contractility. *Journal of Biological Chemistry*, *279*(14), 14225–14231. https://doi.org/10.1074/jbc.M312223200

Gao, Z., Ruden, D. M., & Lu, X. (2003). PKD2 Cation Channel Is Required for Directional Sperm Movement and Male Fertility. *Current Biology*, *13*(24), 2175–2178. https://doi.org/10.1016/j.cub.2003.11.053

Gattone, V. H., Chen, N. X., Sinders, R. M., Seifert, M. F., Duan, D., Martin, D., Henley, C., & Moe, S. M. (2009). Calcimimetic Inhibits Late-Stage Cyst Growth in ADPKD. *Journal of the American Society of Nephrology : JASN*, *20*(7), 1527. https://doi.org/10.1681/ASN.2008090927

Geng, L., Segal, Y., Peissel, B., Deng, N., Pei, Y., Carone, F., Rennke, H. G., Glücksmann-Kuis, A. M., Schneider, M. C., Ericsson, M., Reeders, S. T., & Zhou, J. (1996). Identification and localization of polycystin, the PKD1 gene product. *The Journal of Clinical Investigation*,

*98*(12), 2674–2682. https://doi.org/10.1172/JCI119090

Gervais, F. G., Xu, D., Robertson, G. S., Vaillancourt, J. P., Zhu, Y., Huang, J., LeBlanc, A., Smith, D., Rigby, M., Shearman, M. S., Clarke, E. E., Zheng, H., Van Der Ploeg, L. H., Ruffolo, S. C., Thornberry, N. A., Xanthoudakis, S., Zamboni, R. J., Roy, S., & Nicholson, D. W. (1999). Involvement of caspases in proteolytic cleavage of Alzheimer's amyloid-beta precursor protein and amyloidogenic A beta peptide formation. *Cell*, *97*(3), 395–406. http://www.ncbi.nlm.nih.gov/pubmed/10319819

Ghiglione, C., Bach, E. A., Paraiso, Y., Carraway, K. L., Noselli, S., & Perrimon, N. (2002). Mechanism of activation of the Drosophila EGF Receptor by the TGFα ligand Gurken during oogenesis. *Development*, *129*(1), 175–186. https://doi.org/10.1242/DEV.129.1.175

Ghosh, S., Singh, A., Mandal, S., & Mandal, L. (2015). Active Hematopoietic Hubs in Drosophila Adults Generate Hemocytes and Contribute to Immune Response. *Developmental Cell*, *33*(4), 478–488. https://doi.org/10.1016/J.DEVCEL.2015.03.014

González-Perrett, S., Kim, K., Ibarra, C., Damiano, A. E., Zotta, E., Batelli, M., Harris, P. C., Reisin, I. L., Arnaout, M. A., & Cantiello, H. F. (2001). Polycystin-2, the protein mutated in autosomal dominant polycystic kidney disease (ADPKD), is a Ca2+-permeable nonselective cation channel. *Proceedings of the National Academy of Sciences of the United States of America*, *98*(3), 1182–1187. http://www.ncbi.nlm.nih.gov/pubmed/11252306

Gordon, S., & Martinez, F. O. (2010). Alternative Activation of Macrophages: Mechanism and Functions. *Immunity*, *32*(5), 593–604. https://doi.org/10.1016/J.IMMUNI.2010.05.007

Gordon, S., & Plüddemann, A. (2017). Tissue macrophages: heterogeneity and functions. *BMC Biology*, *15*(1). https://doi.org/10.1186/S12915-017-0392-4

Gordon, S., & Taylor, P. R. (2005). Monocyte and macrophage heterogeneity. In *Nature Reviews Immunology* (Vol. 5, Issue 12, pp. 953–964). Nat Rev Immunol. https://doi.org/10.1038/nri1733

Goyal, L., McCall, K., Agapite, J., Hartwieg, E., & Steller, H. (2000). Induction of apoptosis by Drosophila reaper, hid and grim through inhibition of IAP function. *The EMBO Journal*, *19*(4), 589. https://doi.org/10.1093/EMBOJ/19.4.589

Grantham, J. J., Geiser, J. L., & Evan, A. P. (1987). Cyst formation and growth in autosomal dominant polycystic kidney disease. *Kidney International*, *31*(5), 1145–1152.

http://www.ncbi.nlm.nih.gov/pubmed/3599654

Guillaume, R., & Trudel, M. (2000). Distinct and common developmental expression patterns of the murine Pkd2 and Pkd1 genes. *Mechanisms of Development*, *93*(1–2), 179–183. https://doi.org/10.1016/S0925-4773(00)00257-4

Gyoergy, A., Roblek, M., Ratheesh, A., Valoskova, K., Belyaeva, V., Wachner, S., Matsubayashi, Y., Sánchez-Sánchez, B. J., Stramer, B., & Siekhaus, D. E. (2018). Tools Allowing Independent Visualization and Genetic Manipulation of Drosophila melanogaster Macrophages and Surrounding Tissues. *G3 (Bethesda, Md.)*, *8*(3), 845–857. https://doi.org/10.1534/g3.117.300452

Halder, G., & Mills, G. B. (2011). Drosophila in cancer research: to boldly go where no one has gone before. *Oncogene 2011 30:39*, *30*(39), 4063–4066. https://doi.org/10.1038/onc.2011.128

Halter, D. A., Urban, J., Rickert, C., Ner, S. S., Ito, K., Travers, A. A., & Technau, G. M. (1995). The homeobox gene repo is required for the differentiation and maintenance of glia function in the embryonic nervous system of Drosophila melanogaster. *Development*, *121*(2), 317–332. https://doi.org/10.1242/DEV.121.2.317

Han, C., Jan, L. Y., & Jan, Y. N. (2011). Enhancer-driven membrane markers for analysis of nonautonomous mechanisms reveal neuron-glia interactions in Drosophila. *Proceedings of the National Academy of Sciences of the United States of America*, *108*(23), 9673–9678. https://doi.org/10.1073/PNAS.1106386108/SUPPL_FILE/SM01.MOV

Han, C., Song, Y., Xiao, H., Wang, D., Franc, N. C., Yeh Jan, L., & Jan, Y. N. (2014). Epidermal Cells Are the Primary Phagocytes in the Fragmentation and Clearance of Degenerating Dendrites in Drosophila. *Neuron*, *81*(3), 544–560. https://doi.org/10.1016/J.NEURON.2013.11.021

Hanaoka, K, & Guggino, W. B. (2000). cAMP regulates cell proliferation and cyst formation in autosomal polycystic kidney disease cells. *Journal of the American Society of Nephrology : JASN*, *11*(7), 1179–1187. http://www.ncbi.nlm.nih.gov/pubmed/10864573

Hanaoka, Kazushige, Qian, F., Boletta, A., Bhunia, A. K., Piontek, K., Tsiokas, L., Sukhatme, V. P., Guggino, W. B., & Germino, G. G. (2000). Co-assembly of polycystin-1 and -2 produces unique cation-permeable currents. *Nature*, *408*(6815), 990–994. https://doi.org/10.1038/35050128

Hanayama, R., Tanaka, M., Miwa, K., Shinohara, A., Iwamatsu, A., & Nagata, S. (2002).

Identification of a factor that links apoptotic cells to phagocytes. *Nature*, *417*(6885), 182–187. https://doi.org/10.1038/417182a

Harris, P C, Ward, C. J., Peral, B., & Hughes, J. (1995). Polycystic kidney disease. 1: Identification and analysis of the primary defect. *Journal of the American Society of Nephrology*, *6*(4). https://jasn.asnjournals.org/content/6/4/1125.long

Harris, Peter C., & Torres, V. E. (2014). Genetic mechanisms and signaling pathways in autosomal dominant polycystic kidney disease. *Journal of Clinical Investigation*, *124*(6), 2315–2324. https://doi.org/10.1172/JCI72272

Hateboer, N., v Dijk, M. A., Bogdanova, N., Coto, E., Saggar-Malik, A. K., San Millan, J. L., Torra, R., Breuning, M., & Ravine, D. (1999). Comparison of phenotypes of polycystic kidney disease types 1 and 2. European PKD1-PKD2 Study Group. *Lancet (London, England)*, *353*(9147), 103–107. http://www.ncbi.nlm.nih.gov/pubmed/10023895

Hayashi, T., Mochizuki, T., Reynolds, D. M., Wu, G., Cai, Y., & Somlo, S. (1997). Characterization of the Exon Structure of the Polycystic Kidney Disease 2 Gene (PKD2). *Genomics*, *44*(1), 131–136. https://doi.org/10.1006/geno.1997.4851

Heigwer, F., Port, F., & Boutros, M. (2018). RNA Interference (RNAi) Screening in Drosophila. *Genetics*, *208*(3), 853–874. https://doi.org/10.1534/GENETICS.117.300077

Herman-Bachinsky, Y., Ryoo, H. D., Ciechanover, A., & Gonen, H. (2007). Regulation of the Drosophila ubiquitin ligase DIAP1 is mediated via several distinct ubiquitin system pathways. *Cell Death & Differentiation 2007 14:4*, *14*(4), 861–871. https://doi.org/10.1038/sj.cdd.4402079

Hodge, S., Hodge, G., Scicchitano, R., Reynolds, P. N., & Holmes, M. (2003). Alveolar macrophages from subjects with chronic obstructive pulmonary disease are deficient in their ability to phagocytose apoptotic airway epithelial cells. *Immunology and Cell Biology*, *81*(4), 289–296. https://doi.org/10.1046/J.1440-1711.2003.T01-1-01170.X

Hofherr, A., Seger, C., Fitzpatrick, F., Busch, T., Michel, E., Luan, J., Osterried, L., Linden, F., Kramer-Zucker, A., Wakimoto, B., Schütze, C., Wiedemann, N., Artati, A., Adamski, J., Walz, G., Kunji, E. R. S., Montell, C., Watnick, T., & Köttgen, M. (2018). The mitochondrial transporter SLC25A25 links ciliary TRPP2 signaling and cellular metabolism. *PLOS Biology*, *16*(8), e2005651. https://doi.org/10.1371/journal.pbio.2005651

HOLDENRIEDER, S., EICHHORN, P., BEUERS, U., SAMTLEBEN, W., SCHOENERMARCK, U., ZACHOVAL, R., NAGEL, D., & STIEBER, P. (2006). Nucleosomal DNA Fragments in

Autoimmune Diseases. *Annals of the New York Academy of Sciences*, *1075*(1), 318–327. https://doi.org/10.1196/annals.1368.043

Holz, A., Bossinger, B., Strasser, T., Janning, W., & Klapper, R. (2003). The two origins of hemocytes in Drosophila. *Development*, *130*(20), 4955–4962. https://doi.org/10.1242/DEV.00702

Hopp, K., Ward, C. J., Hommerding, C. J., Nasr, S. H., Tuan, H. F., Gainullin, V. G., Rossetti, S., Torres, V. E., & Harris, P. C. (2012). Functional polycystin-1 dosage governs autosomal dominant polycystic kidney disease severity. *The Journal of Clinical Investigation*, *122*(11), 4257. https://doi.org/10.1172/JCI64313

Huang, A. M., Rehm, E. J., & Rubin, G. M. (2009). Recovery of DNA sequences flanking P-element insertions in Drosophila: inverse PCR and plasmid rescue. *Cold Spring Harbor Protocols*, *2009*(4). https://doi.org/10.1101/PDB.PROT5199

Hughes, J., Ward, C. J., Peral, B., Aspinwall, R., Clark, K., San Millán, J. L., Gamble, V., & Harris, P. C. (1995). The polycystic kidney disease 1 (PKD1) gene encodes a novel protein with multiple cell recognition domains. *Nature Genetics*, *10*(2), 151–160. https://doi.org/10.1038/ng0695-151

Hume, D. A. (2015). The many alternative faces of macrophage activation. *Frontiers in Immunology*, *6*(JUL), 370. https://doi.org/10.3389/FIMMU.2015.00370/BIBTEX

Ichimura, T., Asseldonk, E. J. P. v., Humphreys, B. D., Gunaratnam, L., Duffield, J. S., & Bonventre, J. V. (2008). Kidney injury molecule–1 is a phosphatidylserine receptor that confers a phagocytic phenotype on epithelial cells. *Journal of Clinical Investigation*, *118*(5), 1657–1668. https://doi.org/10.1172/JCI34487

Iglesias, C. G., Torres, V. E., Offord, K. P., Holley, K. E., Beard, C. M., & Kurland, L. T. (1983). Epidemiology of adult polycystic kidney disease, Olmsted County, Minnesota: 1935-1980. *American Journal of Kidney Diseases : The Official Journal of the National Kidney Foundation*, *2*(6), 630–639. http://www.ncbi.nlm.nih.gov/pubmed/6846334

Imperiali, B., & O'Connor, S. E. (1999). Effect of N-linked glycosylation on glycopeptide and glycoprotein structure. *Current Opinion in Chemical Biology*, *3*(6), 643–649. http://www.ncbi.nlm.nih.gov/pubmed/10600722

Inoue, Y., Sohara, E., Kobayashi, K., Chiga, M., Rai, T., Ishibashi, K., Horie, S., Su, X., Zhou, J., Sasaki, S., & Uchida, S. (2014). Aberrant glycosylation and localization of polycystin-1 cause polycystic kidney in an AQP11 knockout model. *Journal of the American Society of*

*Nephrology : JASN*, *25*(12), 2789–2799. https://doi.org/10.1681/ASN.2013060614

Ito, C., Hikosaka-Kuniishi, M., Yamazaki, H., & Yamane, T. (2022). Multiple cell populations generate macrophage progenitors in the early yolk sac. *Cellular and Molecular Life Sciences : CMLS*, *79*(3). https://doi.org/10.1007/S00018-022-04203-7

Jacinto, R., Sampaio, P., Roxo-Rosa, M., Pestana, S., & Lopes, S. S. (2021). Pkd2 Affects Cilia Length and Impacts LR Flow Dynamics and Dand5. *Frontiers in Cell and Developmental Biology*, *9*. https://doi.org/10.3389/FCELL.2021.624531

Jakubzick, C. V., Randolph, G. J., & Henson, P. M. (2017). Monocyte differentiation and antigen-presenting functions. *Nature Reviews Immunology 2017 17:6*, *17*(6), 349–362. https://doi.org/10.1038/nri.2017.28

Jiang, C., Baehrecke, E. H., & Thummel, C. S. (1997). Steroid regulated programmed cell death during Drosophila metamorphosis. *Development*, *124*(22), 4673–4683. https://doi.org/10.1242/DEV.124.22.4673

Jung, C. H., Ro, S. H., Cao, J., Otto, N. M., & Kim, D. H. (2010). mTOR regulation of autophagy. *FEBS Letters*, *584*(7), 1287. https://doi.org/10.1016/J.FEBSLET.2010.01.017

Jung, S. H., Evans, C. J., Uemura, C., & Banerjee, U. (2005). The Drosophila lymph gland as a developmental model of hematopoiesis. *Development (Cambridge, England)*, *132*(11), 2521–2533. https://doi.org/10.1242/DEV.01837

Karihaloo, A. (2015). Role of Inflammation in Polycystic Kidney Disease. In *Polycystic Kidney Disease*. Codon Publications. https://doi.org/10.15586/CODON.PKD.2015.CH14

Karihaloo, A., Koraishy, F., Huen, S. C., Lee, Y., Merrick, D., Caplan, M. J., Somlo, S., & Cantley, L. G. (2011). Macrophages promote cyst growth in polycystic kidney disease. *Journal of the American Society of Nephrology : JASN*, *22*(10), 1809–1814. https://doi.org/10.1681/ASN.2011010084

Kerr, J. F., Wyllie, A. H., & Currie, A. R. (1972). Apoptosis: a basic biological phenomenon with wide-ranging implications in tissue kinetics. *British Journal of Cancer*, *26*(4), 239–257. http://www.ncbi.nlm.nih.gov/pubmed/4561027

Kim, H., Young Wang, S., Kwak, G., Yang, Y., Chan Kwon, I., Hwa Kim, S., Kim, H., Wang, S. Y., Kwak, G., Kwon, I. C., Yang, Y., & Kim, S. H. (2019). Exosome-Guided Phenotypic Switch of M1 to M2 Macrophages for Cutaneous Wound Healing. *Advanced Science*, *6*(20), 1900513. https://doi.org/10.1002/ADVS.201900513

Kim, J. A., Blumenfeld, J. D., Chhabra, S., Dutruel, S. P., Thimmappa, N. D., Bobb, W. O.,

Donahue, S., Rennert, H. E., Tan, A. Y., Giambrone, A. E., & Prince, M. R. (2016). Pancreatic Cysts in Autosomal Dominant Polycystic Kidney Disease: Prevalence and Association with *PKD2* Gene Mutations. *Radiology*, *280*(3), 762–770. https://doi.org/10.1148/radiol.2016151650

Kim, S., Nie, H., Nesin, V., Tran, U., Outeda, P., Bai, C.-X., Keeling, J., Maskey, D., Watnick, T., Wessely, O., & Tsiokas, L. (2016). The polycystin complex mediates Wnt/Ca(2+) signalling. *Nature Cell Biology*, *18*(7), 752–764. https://doi.org/10.1038/ncb3363

Kinchen, J. M., & Ravichandran, K. S. (2008). Phagosome maturation: going through the acid test. *Nature Reviews. Molecular Cell Biology*, *9*(10), 781–795. https://doi.org/10.1038/nrm2515

Kirsch, S., Pasantes, J., Wolf, A., Bogdanova, N., Münch, C., Markoff, A., Pennekamp, P., Krawczak, M., Dworniczak, B., & Schempp, W. (2008). Chromosomal evolution of the PKD1 gene family in primates. *BMC Evolutionary Biology*, *8*, 263. https://doi.org/10.1186/1471-2148-8-263

Knapp, J. M., Chung, P., & Simpson, J. H. (2015). Generating customized transgene landing sites and multi-transgene arrays in Drosophila using phiC31 integrase. *Genetics*, *199*(4), 919–934. https://doi.org/10.1534/GENETICS.114.173187/-/DC1

Knobel, K. M., Peden, E. M., & Barr, M. M. (2008). Distinct protein domains regulate ciliary targeting and function of C. elegans PKD-2. *Experimental Cell Research*, *314*(4), 825–833. https://doi.org/10.1016/j.yexcr.2007.10.017

Kohno, K., Koya-Miyata, S., Harashima, A., Tsukuda, T., Katakami, M., Ariyasu, T., Ushio, S., & Iwaki, K. (2021). Inflammatory M1-like macrophages polarized by NK-4 undergo enhanced phenotypic switching to an anti-inflammatory M2-like phenotype upon co-culture with apoptotic cells. *Journal of Inflammation (United Kingdom)*, *18*(1), 1–14. https://doi.org/10.1186/S12950-020-00267-Z/FIGURES/7

Kojima, Y., Weissman, I. L., & Leeper, N. J. (2017). The Role of Efferocytosis in Atherosclerosis. *Circulation*, *135*(5), 476–489. https://doi.org/10.1161/CIRCULATIONAHA.116.025684/FORMAT/EPUB

Kokudo, N., Kothary, P. C., Eckhauser, F. E., & Raper, S. E. (1991). Inhibitory effects of somatostatin on rat hepatocyte proliferation are mediated by cyclic AMP. *Journal of Surgical Research*, *51*(2), 113–118. https://doi.org/10.1016/0022-4804(91)90079-2

Köttgen, M., Hofherr, A., Li, W., Chu, K., Cook, S., Montell, C., & Watnick, T. (2011).

Drosophila Sperm Swim Backwards in the Female Reproductive Tract and Are Activated via TRPP2 Ion Channels. *PLoS ONE*, *6*(5), e20031. https://doi.org/10.1371/journal.pone.0020031

Koulen, P., Cai, Y., Geng, L., Maeda, Y., Nishimura, S., Witzgall, R., Ehrlich, B. E., & Somlo, S. (2002). Polycystin-2 is an intracellular calcium release channel. *Nature Cell Biology*, *4*(3), 191–197. https://doi.org/10.1038/ncb754

Kurant, E., Axelrod, S., Leaman, D., & Gaul, U. (2008). Six-microns-under acts upstream of Draper in the glial phagocytosis of apoptotic neurons. *Cell*, *133*(3), 498–509. https://doi.org/10.1016/j.cell.2008.02.052

Kurosaka, K., Takahashi, M., Watanabe, N., & Kobayashi, Y. (2003). Silent cleanup of very early apoptotic cells by macrophages. *Journal of Immunology (Baltimore, Md. : 1950)*, *171*(9), 4672–4679. http://www.ncbi.nlm.nih.gov/pubmed/14568942

Kvon, E. Z., Kazmar, T., Stampfel, G., Yáñez-Cuna, J. O., Pagani, M., Schernhuber, K., Dickson, B. J., & Stark, A. (2014). Genome-scale functional characterization of Drosophila developmental enhancers in vivo. *Nature*, *512*(1), 91–95. https://doi.org/10.1038/nature13395

Lanoix, J., D'Agati, V., Szabolcs, M., & Trudel, M. (1996). Dysregulation of cellular proliferation and apoptosis mediates human autosomal dominant polycystic kidney disease (ADPKD). *Oncogene*, *13*(6), 1153–1160. http://www.ncbi.nlm.nih.gov/pubmed/8808689

Lanot, R., Zachary, D., Holder, F., & Meister, M. (2001). Postembryonic hematopoiesis in Drosophila. *Developmental Biology*, *230*(2), 243–257. https://doi.org/10.1006/DBIO.2000.0123

Le, T., Liang, Z., Patel, H., Yu, M. H., Sivasubramaniam, G., Slovitt, M., Tanentzapf, G., Mohanty, N., Paul, S. M., Wu, V. M., & Beitel, G. J. (2006). A new family of Drosophila balancer chromosomes with a w- dfd-GMR yellow fluorescent protein marker. *Genetics*, *174*(4), 2255–2257. https://doi.org/10.1534/genetics.106.063461

Lebestky, T., Chang, T., Hartenstein, V., & Banerjee, U. (2000). Specification of Drosophila hematopoietic lineage by conserved transcription factors. *Science (New York, N.Y.)*, *288*(5463), 146–149. https://doi.org/10.1126/science.288.5463.146

Leitão, A. B., & Sucena, É. (2015). Drosophila sessile hemocyte clusters are true hematopoietic tissues that regulate larval blood cell differentiation. *ELife*, *2015*(4), 1–38. https://doi.org/10.7554/ELIFE.06166

Leonhard, W. N., van der Wal, A., Novalic, Z., Kunnen, S. J., Gansevoort, R. T., Breuning, M. H., de Heer, E., & Peters, D. J. M. (2011). Curcumin inhibits cystogenesis by simultaneous interference of multiple signaling pathways: In vivo evidence from a Pkd1-deletion model. *American Journal of Physiology - Renal Physiology*, *300*(5), 1193–1202. https://doi.org/10.1152/AJPRENAL.00419.2010/SUPPL_FILE/LEGENDS.PDF

Leuenroth, S. J., & Crews, C. M. (2009). Targeting cyst initiation in ADPKD. *Journal of the American Society of Nephrology : JASN*, *20*(1), 1–3. https://doi.org/10.1681/ASN.2008101118

Levi, T., Sloutskin, A., Kalifa, R., Juven-Gershon, T., & Gerlitz, O. (2020). Efficient in Vivo Introduction of Point Mutations Using ssODN and a Co-CRISPR Approach. *Biological Procedures Online*, *22*(1). https://doi.org/10.1186/S12575-020-00123-7

Li, Q., & Barres, B. A. (2018). *Microglia and macrophages in brain homeostasis and disease*. https://doi.org/10.1038/nri.2017.125

Li, Y., Wright, J. M., Qian, F., Germino, G. G., & Guggino, W. B. (2005). Polycystin 2 interacts with type I inositol 1,4,5-trisphosphate receptor to modulate intracellular Ca2+ signaling. *The Journal of Biological Chemistry*, *280*(50), 41298–41306. https://doi.org/10.1074/JBC.M510082200

Liang, J., Balachandra, S., Ngo, S., & O'Brien, L. E. (2017). Feedback regulation of steady-state epithelial turnover and organ size. *Nature*, *548*(7669), 588–591. https://doi.org/10.1038/nature23678

Liebermann, D. A., & Hoffman, B. (2002). Myeloid differentiation (MyD) primary response genes in hematopoiesis. *Oncogene 2002 21:21*, *21*(21), 3391–3402. https://doi.org/10.1038/sj.onc.1205312

Lien Guillou, A., Troha, K., Wang, H., Franc, N. C., & Buchon, N. (2016). *The Drosophila CD36 Homologue croquemort Is Required to Maintain Immune and Gut Homeostasis during Development and Aging*. https://doi.org/10.1371/journal.ppat.1005961

Link, N., & Bellen, H. J. (2020). Using Drosophila to drive the diagnosis and understand the mechanisms of rare human diseases. *Development (Cambridge, England)*, *147*(21). https://doi.org/10.1242/DEV.191411

Logan, M. A., Hackett, R., Doherty, J., Sheehan, A., Speese, S. D., & Freeman, M. R. (2012). Negative regulation of glial engulfment activity by Draper terminates glial responses to axon injury. *Nature Neuroscience*, *15*(5), 722. https://doi.org/10.1038/NN.3066

London, A., Benhar, I., Mattapallil, M. J., Mack, M., Caspi, R. R., & Schwartz, M. (2013). Functional macrophage heterogeneity in a mouse model of autoimmune CNS pathology. *Journal of Immunology (Baltimore, Md. : 1950)*, *190*(7), 3570. https://doi.org/10.4049/JIMMUNOL.1202076

Long, S., Ahmad, N., & Rebagliati, M. (2003). The zebrafish nodal-related gene southpaw is required for visceral and diencephalic left-right asymmetry. *Development*, *130*(11), 2303–2316. https://doi.org/10.1242/DEV.00436

Lu, B., & Vogel, H. (2009). Drosophila Models of Neurodegenerative Diseases. *Annual Review of Pathology*, *4*, 315. https://doi.org/10.1146/ANNUREV.PATHOL.3.121806.151529

Lundqvist-Gustafsson, H., Gustafsson, M., & Dahlgren, C. (2000). Dynamic Ca2+changes in neutrophil phagosomes A source for intracellular Ca2+during phagolysosome formation? *Cell Calcium*, *27*(6), 353–362. https://doi.org/10.1054/ceca.2000.0130

Magistroni, R., He, N., Wang, K., Andrew, R., Johnson, A., Gabow, P., Dicks, E., Parfrey, P., Torra, R., San-Millan, J. L., Coto, E., Van Dijk, M., Breuning, M., Peters, D., Bogdanova, N., Ligabue, G., Albertazzi, A., Hateboer, N., Demetriou, K., … Pei, Y. (2003). Genotype-renal function correlation in type 2 autosomal dominant polycystic kidney disease. *Journal of the American Society of Nephrology : JASN*, *14*(5), 1164–1174. http://www.ncbi.nlm.nih.gov/pubmed/12707387

Magistroni, R., Mangolini, A., Guzzo, S., Testa, F., Rapanà, M. R., Mignani, R., Russo, G., di Virgilio, F., & Aguiari, G. (2019). TRPP2 dysfunction decreases ATP-evoked calcium, induces cell aggregation and stimulates proliferation in T lymphocytes. *BMC Nephrology*, *20*(1), 355. https://doi.org/10.1186/s12882-019-1540-6

Makhijani, K., Alexander, B., Rao, D., Petraki, S., Herboso, L., Kukar, K., Batool, I., Wachner, S., Gold, K. S., Wong, C., O'Connor, M. B., & Brückner, K. (2017). Regulation of Drosophila hematopoietic sites by Activin-β from active sensory neurons. *Nature Communications 2017 8:1*, *8*(1), 1–12. https://doi.org/10.1038/ncomms15990

Makki, R., Meister, M., Pennetier, D., Ubeda, J. M., Braun, A., Daburon, V., Krzemień, J., Bourbon, H. M., Zhou, R., Vincent, A., & Crozatier, M. (2010). A Short Receptor Downregulates JAK/STAT Signalling to Control the Drosophila Cellular Immune Response. *PLOS Biology*, *8*(8), e1000441. https://doi.org/10.1371/JOURNAL.PBIO.1000441

Márkus, R., Laurinyecz, B., Kurucz, É., Honti, V., Bajusz, I., Sipos, B., Somogyi, K., Kronhamn, J.,

Hultmark, D., & Andó, I. (2009). Sessile hemocytes as a hematopoietic compartment in Drosophila melanogaster. *Proceedings of the National Academy of Sciences of the United States of America*, *106*(12), 4805–4809. https://doi.org/10.1073/PNAS.0801766106/SUPPL_FILE/0801766106SI.PDF

Marshall, O. J., Southall, T. D., Cheetham, S. W., & Brand, A. H. (2016). Cell-type-specific profiling of protein–DNA interactions without cell isolation using targeted DamID with next-generation sequencing. *Nature Protocols 2016 11:9*, *11*(9), 1586–1598. https://doi.org/10.1038/nprot.2016.084

Mascardo, R. N., & Sherline, P. (1982). SOMATOSTATIN INHIBITS RAPID CENTROSOMAL SEPARATION AND CELL PROLIFERATION INDUCED BY EPIDERMAL GROWTH FACTOR. *Endocrinology*, *111*(4), 1394–1396. https://doi.org/10.1210/endo-111-4-1394

McConnachie, D. J., Stow, J. L., & Mallett, A. J. (2021). Ciliopathies and the Kidney: A Review. *American Journal of Kidney Diseases*, *77*(3), 410–419. https://doi.org/10.1053/J.AJKD.2020.08.012

McCracken, J. M., & Allen, L. A. H. (2014). Regulation of Human Neutrophil Apoptosis and Lifespan in Health and Disease. *Journal of Cell Death*, *7*(1), 15. https://doi.org/10.4137/JCD.S11038

McGuire, S. E., Le, P. T., Osborn, A. J., Matsumoto, K., & Davis, R. L. (2003). Spatiotemporal Rescue of Memory Dysfunction in Drosophila. *Science*, *302*(5651), 1765–1768. https://doi.org/10.1126/SCIENCE.1089035

Meister, M., & Lagueux, M. (2003). Drosophila blood cells. *Cellular Microbiology*, *5*(9), 573–580. http://www.ncbi.nlm.nih.gov/pubmed/12925127

Miller, Y. I., Chang, M. K., Funk, C. D., Feramisco, J. R., & Witztum, J. L. (2001). 12/15-lipoxygenase translocation enhances site-specific actin polymerization in macrophages phagocytosing apoptotic cells. *The Journal of Biological Chemistry*, *276*(22), 19431–19439. https://doi.org/10.1074/jbc.M011276200

Milutinovic, J., Fialkow, P. J., Rudd, T. G., Agodoa, L. Y., Phillips, L. A., & Bryant, J. I. (1980). Liver cysts in patients with autosomal dominant polycystic kidney disease. *The American Journal of Medicine*, *68*(5), 741–744. http://www.ncbi.nlm.nih.gov/pubmed/7377224

Mizuno, Y., Isotani, E., Huang, J., Ding, H., Stull, J. T., & Kamm, K. E. (2008). Myosin light chain kinase activation and calcium sensitization in smooth muscle in vivo. *American Journal of Physiology - Cell Physiology*, *295*(2), C358. https://doi.org/10.1152/AJPCELL.90645.2007

Mochizuki, T., Wu, G., Hayashi, T., Xenophontos, S. L., Veldhuisen, B., Saris, J. J., Reynolds, D. M., Cai, Y., Gabow, P. A., Pierides, A., Kimberling, W. J., Breuning, M. H., Deltas, C. C., Peters, D. J., & Somlo, S. (1996). PKD2, a gene for polycystic kidney disease that encodes an integral membrane protein. *Science (New York, N.Y.)*, *272*(5266), 1339–1342. http://www.ncbi.nlm.nih.gov/pubmed/8650545

Morioka, S., Maueröder, C., & Ravichandran, K. S. (2019). Living on the Edge: Efferocytosis at the Interface of Homeostasis and Pathology. *Immunity*, *50*(5), 1149–1162. https://doi.org/10.1016/J.IMMUNI.2019.04.018

Mortimer, N. T., Goecks, J., Kacsoh, B. Z., Mobley, J. A., Bowersock, G. J., Taylor, J., & Schlenke, T. A. (2013). Parasitoid wasp venom SERCA regulates Drosophila calcium levels and inhibits cellular immunity. *Proceedings of the National Academy of Sciences of the United States of America*, *110*(23), 9427–9432. https://doi.org/10.1073/PNAS.1222351110/SUPPL_FILE/SD02.TXT

Mrschtik, M., & Ryan, K. M. (2015). Lysosomal proteins in cell death and autophagy. *The FEBS Journal*, *282*(10), 1858–1870. https://doi.org/10.1111/FEBS.13253

Müller-Taubenberger, A., Lupas, A. N., Li, H., Ecke, M., Simmeth, E., & Gerisch, G. (2001). Calreticulin and calnexin in the endoplasmic reticulum are important for phagocytosis. *EMBO Journal*, *20*(23), 6772–6782. https://doi.org/10.1093/emboj/20.23.6772

Murillo, H., Schmidt, L. J., & Tindall, D. J. (2001). Tyrphostin AG825 triggers p38 mitogen-activated protein kinase-dependent apoptosis in androgen-independent prostate cancer cells C4 and C4-2. *Cancer Research*, *61*(20), 7408–7412. http://www.ncbi.nlm.nih.gov/pubmed/11606371

Murray, P. J. (2017). Macrophage Polarization. *Http://Dx.Doi.Org/10.1146/Annurev-Physiol-022516-034339*, *79*, 541–566. https://doi.org/10.1146/ANNUREV-PHYSIOL-022516-034339

Murray, P. J., & Wynn, T. A. (2011). Protective and pathogenic functions of macrophage subsets. *Nature Reviews Immunology 2011 11:11*, *11*(11), 723–737. https://doi.org/10.1038/nri3073

Musselman, L. P., & Kühnlein, R. P. (2018). Drosophila as a model to study obesity and metabolic disease. *Journal of Experimental Biology*, *121*(Suppl_1). https://doi.org/10.1242/JEB.163881/33977

Nathan, C. F., Murray, H. W., Wlebe, I. E., & Rubin, B. Y. (1983). Identification of interferon-

gamma as the lymphokine that activates human macrophage oxidative metabolism and antimicrobial activity. *Journal of Experimental Medicine*, *158*(3), 670–689. https://doi.org/10.1084/JEM.158.3.670

Nauli, S. M., Alenghat, F. J., Luo, Y., Williams, E., Vassilev, P., Li, X., Elia, A. E. H., Lu, W., Brown, E. M., Quinn, S. J., Ingber, D. E., & Zhou, J. (2003). Polycystins 1 and 2 mediate mechanosensation in the primary cilium of kidney cells. *Nature Genetics*, *33*(2), 129–137. https://doi.org/10.1038/ng1076

Newby, L. J., Streets, A. J., Zhao, Y., Harris, P. C., Ward, C. J., & Ong, A. C. M. (2002). Identification, characterization, and localization of a novel kidney polycystin-1-polycystin-2 complex. *The Journal of Biological Chemistry*, *277*(23), 20763–20773. https://doi.org/10.1074/jbc.M107788200

Nguyen-Chi, M., Laplace-Builhe, B., Travnickova, J., Luz-Crawford, P., Tejedor, G., Phan, Q. T., Duroux-Richard, I., Levraud, J. P., Kissa, K., Lutfalla, G., Jorgensen, C., & Djouad, F. (2015). Identification of polarized macrophage subsets in zebrafish. *ELife*, *4*(JULY 2015). https://doi.org/10.7554/ELIFE.07288

Nielsen, S., Chou, C. L., Marples, D., Christensen, E. I., Kishore, B. K., & Knepper, M. A. (1995). Vasopressin increases water permeability of kidney collecting duct by inducing translocation of aquaporin-CD water channels to plasma membrane. *Proceedings of the National Academy of Sciences of the United States of America*, *92*(4), 1013–1017. http://www.ncbi.nlm.nih.gov/pubmed/7532304

Niethammer, P., Grabher, C., Look, A. T., & Mitchison, T. J. (2009). A tissue-scale gradient of hydrogen peroxide mediates rapid wound detection in zebrafish. *Nature*, *459*(7249), 996–999. https://doi.org/10.1038/nature08119

Nims, N., Vassmer, D., & Maser, R. L. (2003). Transmembrane Domain Analysis of Polycystin-1, the Product of the Polycystic Kidney Disease-1 (PKD1) Gene: Evidence for 11 Membrane-Spanning Domains †. *Biochemistry*, *42*(44), 13035–13048. https://doi.org/10.1021/bi035074c

Nowak, K. L., Farmer-Bailey, H., Wang, W., You, Z., Steele, C., Cadnapaphornchai, M. A., Klawitter, J., Patel, N., George, D., Jovanovich, A., Soranno, D. E., Gitomer, B., & Chonchol, M. (2022). Curcumin Therapy to Treat Vascular Dysfunction in Children and Young Adults with ADPKD: A Randomized Controlled Trial. *Clinical Journal of the American Society of Nephrology : CJASN*, *17*(2), 240–250.

https://doi.org/10.2215/CJN.08950621

Nunes, P., & Demaurex, N. (2010). The role of calcium signaling in phagocytosis. *Journal of Leukocyte Biology*, *88*(1), 57–68. https://doi.org/10.1189/jlb.0110028

Obara, T., Mangos, S., Liu, Y., Zhao, J., Wiessner, S., Kramer-Zucker, A. G., Olale, F., Schier, A. F., & Drummond, I. A. (2006). Polycystin-2 Immunolocalization and Function in Zebrafish. *Journal of the American Society of Nephrology : JASN*, *17*(10), 2706. https://doi.org/10.1681/ASN.2006040412

Okuda, T., Van Deursen, J., Hiebert, S. W., Grosveld, G., & Downing, J. R. (1996). AML1, the target of multiple chromosomal translocations in human leukemia, is essential for normal fetal liver hematopoiesis. *Cell*, *84*(2), 321–330. https://doi.org/10.1016/S0092-8674(00)80986-1

Orecchioni, M., Ghosheh, Y., Pramod, A. B., & Ley, K. (2019). Macrophage Polarization: Different Gene Signatures in M1(LPS+) vs. Classically and M2(LPS–) vs. Alternatively Activated Macrophages. *Frontiers in Immunology*, *0*(MAY), 1084. https://doi.org/10.3389/FIMMU.2019.01084

Parisi, L., Gini, E., Baci, D., Tremolati, M., Fanuli, M., Bassani, B., Farronato, G., Bruno, A., & Mortara, L. (2018). Macrophage Polarization in Chronic Inflammatory Diseases: Killers or Builders? *Journal of Immunology Research*, *2018*. https://doi.org/10.1155/2018/8917804

Parnell, S. C., Puri, S., Wallace, D. P., & Calvet, J. P. (2012). Protein Phosphatase-1α Interacts with and Dephosphorylates Polycystin-1. *PLoS ONE*, *7*(6), e36798. https://doi.org/10.1371/journal.pone.0036798

Patera, F., Cudzich-Madry, A., Huang, Z., & Fragiadaki, M. (2019). Renal expression of JAK2 is high in polycystic kidney disease and its inhibition reduces cystogenesis. *Scientific Reports 2019 9:1*, *9*(1), 1–10. https://doi.org/10.1038/s41598-019-41106-3

Paul, B. M., Consugar, M. B., Ryan Lee, M., Sundsbak, J. L., Heyer, C. M., Rossetti, S., Kubly, V. J., Hopp, K., Torres, V. E., Coto, E., Clementi, M., Bogdanova, N., de Almeida, E., Bichet, D. G., & Harris, P. C. (2014). Evidence of a third ADPKD locus is not supported by re-analysis of designated PKD3 families. *Kidney International*, *85*(2), 383–392. https://doi.org/10.1038/ki.2013.227

PEI, Y., WATNICK, T., HE, N., WANG, K., LIANG, Y., PARFREY, P., GERMINO, G., & GEORGE-HYSLOP, P. ST. (1999). Somatic PKD2 Mutations in Individual Kidney and Liver Cysts

Support a “Two-Hit” Model of Cystogenesis in Type 2 Autosomal Dominant Polycystic Kidney Disease. *Journal of the American Society of Nephrology*, *10*(7).

Peintner, L., & Borner, C. (2017). Role of apoptosis in the development of autosomal dominant polycystic kidney disease (ADPKD). *Cell and Tissue Research*, *369*(1), 27–39. https://doi.org/10.1007/s00441-017-2628-6

Peintner, L., Venkatraman, A., Waeldin, A., Hofherr, A., Busch, T., Voronov, A., Viau, A., Kuehn, E. W., Köttgen, M., & Borner, C. (2020). Loss of PKD1/polycystin-1 impairs lysosomal activity in a CAPN (calpain)-dependent manner. *Autophagy*. https://doi.org/10.1080/15548627.2020.1826716

Peña-Oyarzun, D., Rodriguez-Peña, M., Burgos-Bravo, F., Vergara, A., Kretschmar, C., Sotomayor-Flores, C., Ramirez-Sarmiento, C. A., De Smedt, H., Reyes, M., Perez, W., Torres, V. A., Morselli, E., Altamirano, F., Wilson, C. A. M., Hill, J. A., Lavandero, S., & Criollo, A. (2021). PKD2/polycystin-2 induces autophagy by forming a complex with BECN1. *Autophagy*, *17*(7), 1714–1728. https://doi.org/10.1080/15548627.2020.1782035

Pennekamp, P., Karcher, C., Fischer, A., Schweickert, A., Skryabin, B., Horst, J., Blum, M., & Dworniczak, B. (2002). The ion channel polycystin-2 is required for left-right axis determination in mice. *Current Biology : CB*, *12*(11), 938–943. http://www.ncbi.nlm.nih.gov/pubmed/12062060

Peters, D. J. M., Spruit, L., Saris, J. J., Ravine, D., Sandkuijl, L. A., Fossdal, R., Boersma, J., van Eijk, R., Nørby, S., Constantinou-Deltas, C. D., Pierides, A., Briessenden, J. E., Frants, R. R., van Ommen, G.-J. B., & Breuning, M. H. (1993). Chromosome 4 localization of a second gene for autosomal dominant polycystic kidney disease. *Nature Genetics*, *5*(4), 359–362. https://doi.org/10.1038/ng1293-359

Petri, E. T., Ćelić, A., Kennedy, S. D., Ehrlich, B. E., Boggona, T. J., & Hodsdon, M. E. (2010). Structure of the EF-hand domain of polycystin-2 suggests a mechanism for Ca2+-dependent regulation of polycystin-2 channel activity. *Proceedings of the National Academy of Sciences of the United States of America*, *107*(20), 9176–9181. https://doi.org/10.1073/PNAS.0912295107/-/DCSUPPLEMENTAL

Petrignani, B., Rommelaere, S., Hakim-Mishnaevski, K., Masson, F., Ramond, E., Hilu-Dadia, R., Poidevin, M., Kondo, S., Kurant, E., & Lemaitre, B. (2021). A secreted factor NimrodB4 promotes the elimination of apoptotic corpses by phagocytes in Drosophila. *EMBO*

*Reports*, e52262. https://doi.org/10.15252/EMBR.202052262

Pfeiffer, B. D., Ngo, T. T. B., Hibbard, K. L., Murphy, C., Jenett, A., Truman, J. W., & Rubin, G. M. (2010). Refinement of Tools for Targeted Gene Expression in Drosophila. *Genetics*, *186*(2), 735–755. https://doi.org/10.1534/GENETICS.110.119917

Pinto, C. S., Reif, G. A., Nivens, E., White, C., & Wallace, D. P. (2012). Calmodulin-sensitive adenylyl cyclases mediate AVP-dependent cAMP production and Cl- secretion by human autosomal dominant polycystic kidney cells. *American Journal of Physiology. Renal Physiology*, *303*(10), F1412-24. https://doi.org/10.1152/ajprenal.00692.2011

Porath, B., Gainullin, V. G., Cornec-Le Gall, E., Dillinger, E. K., Heyer, C. M., Hopp, K., Edwards, M. E., Madsen, C. D., Mauritz, S. R., Banks, C. J., Baheti, S., Reddy, B., Herrero, J. I., Bañales, J. M., Hogan, M. C., Tasic, V., Watnick, T. J., Chapman, A. B., Vigneau, C., … Harris, P. C. (2016). Mutations in GANAB , Encoding the Glucosidase IIα Subunit, Cause Autosomal-Dominant Polycystic Kidney and Liver Disease. *The American Journal of Human Genetics*, *98*(6), 1193–1207. https://doi.org/10.1016/j.ajhg.2016.05.004

Qian, F., Germino, F. J., Cai, Y., Zhang, X., Somlo, S., & Germino, G. G. (1997). PKD1 interacts with PKD2 through a probable coiled-coil domain. *Nature Genetics*, *16*(2), 179–183. https://doi.org/10.1038/ng0697-179

Qian, Q., Hunter, L. W., Li, M., Marin-Padilla, M., Prakash, Y. S., Somlo, S., Harris, P. C., Torres, V. E., & Sieck, G. C. (2003). Pkd2 haploinsufficiency alters intracellular calcium regulation in vascular smooth muscle cells. *Human Molecular Genetics*, *12*(15), 1875–1880. http://www.ncbi.nlm.nih.gov/pubmed/12874107

Raymond, M. H., Davidson, A. J., Shen, Y., Tudor, D. R., Lucas, C. D., Morioka, S., Perry, J. S. A., Krapivkina, J., Perrais, D., Schumacher, L. J., Campbell, R. E., Wood, W., & Ravichandran, K. S. (2022). Live cell tracking of macrophage efferocytosis during *Drosophila* embryo development in vivo. *Science*, *375*(6585), 1182–1187. https://doi.org/10.1126/SCIENCE.ABL4430

Razzell, W., Evans, I. R., Martin, P., & Wood, W. (2013). Calcium Flashes Orchestrate the Wound Inflammatory Response through DUOX Activation and Hydrogen Peroxide Release. *Current Biology*, *23*(5), 424–429. https://doi.org/10.1016/j.cub.2013.01.058

Regan, J. C., Brandão, A. S., Leitão, A. B., Mantas Dias, Â. R., Sucena, É., Jacinto, A., & Zaidman-Rémy, A. (2013). Steroid Hormone Signaling Is Essential to Regulate Innate Immune Cells and Fight Bacterial Infection in Drosophila. *PLoS Pathogens*, *9*(10).

https://doi.org/10.1371/journal.ppat.1003720

Regulski, M., McGinnis, N., Chadwick, R., & McGinnis, W. (1987). Developmental and molecular analysis of Deformed; a homeotic gene controlling Drosophila head development. *The EMBO Journal*, *6*(3), 767–777. http://www.ncbi.nlm.nih.gov/pubmed/16453752

Reif, G. A., Yamaguchi, T., Nivens, E., Fujiki, H., Pinto, C. S., & Wallace, D. P. (2011). Tolvaptan inhibits ERK-dependent cell proliferation, $Cl^-$ secretion, and in vitro cyst growth of human ADPKD cells stimulated by vasopressin. *American Journal of Physiology-Renal Physiology*, *301*(5), F1005–F1013. https://doi.org/10.1152/ajprenal.00243.2011

Reiter, L. T., Potocki, L., Chien, S., Gribskov, M., & Bier, E. (2001). A Systematic Analysis of Human Disease-Associated Gene Sequences In Drosophila melanogaster. *Genome Research*, *11*(6), 1114–1125. https://doi.org/10.1101/gr.169101

Riegersperger, M., Herkner, H., & Sunder-Plassmann, G. (2015). Pulsed oral sirolimus in advanced autosomal-dominant polycystic kidney disease (Vienna RAP Study): study protocol for a randomized controlled trial. *Trials*, *16*(1), 182. https://doi.org/10.1186/s13063-015-0692-3

Roddie, H. G., Armitage, E. L., Coates, J. A., Johnston, S. A., & Evans, I. R. (2019). Simu-dependent clearance of dying cells regulates macrophage function and inflammation resolution. *PLOS Biology*, *17*(5), e2006741. https://doi.org/10.1371/JOURNAL.PBIO.2006741

Rogulja-Ortmann, A., Lüer, K., Seibert, J., Rickert, C., & Technau, G. M. (2007). Programmed cell death in the embryonic central nervous system of Drosophila melanogaster. *Development*, *134*(1), 105–116. https://doi.org/10.1242/DEV.02707

Rossetti, S., Hopp, K., Sikkink, R. A., Sundsbak, J. L., Lee, Y. K., Kubly, V., Eckloff, B. W., Ward, C. J., Winearls, C. G., Torres, V. E., & Harris, P. C. (2012). Identification of Gene Mutations in Autosomal Dominant Polycystic Kidney Disease through Targeted Resequencing. *Journal of the American Society of Nephrology*, *23*(5), 915–933. https://doi.org/10.1681/ASN.2011101032

Rossetti, Sandro, Kubly, V. J., Consugar, M. B., Hopp, K., Roy, S., Horsley, S. W., Chauveau, D., Rees, L., Barratt, T. M., van't Hoff, W. G., Niaudet, P., Niaudet, W. P., Torres, V. E., & Harris, P. C. (2009). Incompletely penetrant PKD1 alleles suggest a role for gene dosage in cyst initiation in polycystic kidney disease. *Kidney International*, *75*(8), 848–855.

https://doi.org/10.1038/ki.2008.686

Rossetti, Sandro, Strmecki, L., Gamble, V., Burton, S., Sneddon, V., Peral, B., Roy, S., Bakkaloglu, A., Komel, R., Winearls, C. G., & Harris, P. C. (2001). Mutation Analysis of the Entire PKD1 Gene: Genetic and Diagnostic Implications. *The American Journal of Human Genetics*, *68*(1), 46–63. https://doi.org/10.1086/316939

Rossi, A. E., & Dirksen, R. T. (2006). Sarcoplasmic reticulum: the dynamic calcium governor of muscle. *Muscle & Nerve*, *33*(6), 715–731. https://doi.org/10.1002/MUS.20512

Rothé, B., Gagnieux, C., Leal-Esteban, L. C., & Constam, D. B. (2020). Role of the RNA-binding protein Bicaudal-C1 and interacting factors in cystic kidney diseases. *Cellular Signalling*, *68*, 109499. https://doi.org/10.1016/J.CELLSIG.2019.109499

Rubartelli, A., Poggi, A., & Zocchi, M. R. (1997). The selective engulfment of apoptotic bodies by dendritic cells is mediated by the αvβ3 integrin and requires intracellular and extracellular calcium. *European Journal of Immunology*, *27*(8), 1893–1900. https://doi.org/10.1002/eji.1830270812

Ruggenenti, P., Gentile, G., Perico, N., Perna, A., Barcella, L., Trillini, M., Cortinovis, M., Ferrer Siles, C. P., Reyes Loaeza, J. A., Aparicio, M. C., Fasolini, G., Gaspari, F., Martinetti, D., Carrara, F., Rubis, N., Prandini, S., Caroli, A., Sharma, K., Antiga, L., … SIRENA 2 Study Group. (2016). Effect of Sirolimus on Disease Progression in Patients with Autosomal Dominant Polycystic Kidney Disease and CKD Stages 3b-4. *Clinical Journal of the American Society of Nephrology*, *11*(5), 785–794. https://doi.org/10.2215/CJN.09900915

Russo, R. J., Husson, H., Joly, D., Bukanov, N. O., Patey, N., Knebelmann, B., & Ibraghimov-Beskrovnaya, O. (2005). Impaired formation of desmosomal junctions in ADPKD epithelia. *Histochemistry and Cell Biology*, *124*(6), 487–497. https://doi.org/10.1007/s00418-005-0055-3

Sampson, C. J., Amin, U., & Couso, J. P. (2013). Activation of Drosophila hemocyte motility by the ecdysone hormone. *Biology Open*, *2*(12), 1412–1420. https://doi.org/10.1242/BIO.20136619/-/DC1

Sanchez Bosch, P., Makhijani, K., Herboso, L., Gold, K. S., Baginsky, R., Woodcock, K. J., Alexander, B., Kukar, K., Corcoran, S., Jacobs, T., Ouyang, D., Wong, C., Ramond, E. J. V., Rhiner, C., Moreno, E., Lemaitre, B., Geissmann, F., & Brückner, K. (2019). Adult Drosophila Lack Hematopoiesis but Rely on a Blood Cell Reservoir at the Respiratory Epithelia to Relay Infection Signals to Surrounding Tissues. *Developmental Cell*, *51*(6),

787-803.e5. https://doi.org/10.1016/J.DEVCEL.2019.10.017

Sandford, R., Sgotto, B., Aparicio, S., Brenner, S., Vaudin, M., Wilson, R. K., Chissoe, S., Pepin, K., Bateman, A., Chothia, C., Hughes, J., & Harris, P. (1997). Comparative analysis of the polycystic kidney disease 1 (PKD1) gene reveals an integral membrane glycoprotein with multiple evolutionary conserved domains. *Human Molecular Genetics*, *6*(9), 1483–1489. http://www.ncbi.nlm.nih.gov/pubmed/9285785

Schindelin, J., Arganda-Carreras, I., Frise, E., Kaynig, V., Longair, M., Pietzsch, T., Preibisch, S., Rueden, C., Saalfeld, S., Schmid, B., Tinevez, J. Y., White, D. J., Hartenstein, V., Eliceiri, K., Tomancak, P., & Cardona, A. (2012). Fiji: an open-source platform for biological-image analysis. *Nature Methods*, *9*(7), 676–682. https://doi.org/10.1038/NMETH.2019

Schmelzle, T., & Hall, M. N. (2000). TOR, a central controller of cell growth. *Cell*, *103*(2), 253–262. http://www.ncbi.nlm.nih.gov/pubmed/11057898

Schott, S., Ambrosini, A., Barbaste, A., Benassayag, C., Gracia, M., Proag, A., Rayer, M., Monier, B., & Suzanne, M. (2017). A fluorescent toolkit for spatiotemporal tracking of apoptotic cells in living Drosophila tissues. *Development (Cambridge, England)*, *144*(20), 3840–3846. https://doi.org/10.1242/dev.149807

Schottenfeld, J., Sullivan-Brown, J., & Burdine, R. D. (2007). Zebrafish curly up encodes a Pkd2 ortholog that restricts left-side-specific expression of southpaw. *Development*, *134*(8), 1605–1615. https://doi.org/10.1242/dev.02827

Schrijvers, D. M., De Meyer, G. R. Y., Kockx, M. M., Herman, A. G., & Martinet, W. (2005). Phagocytosis of Apoptotic Cells by Macrophages Is Impaired in Atherosclerosis. *Arteriosclerosis, Thrombosis, and Vascular Biology*, *25*(6), 1256–1261. https://doi.org/10.1161/01.ATV.0000166517.18801.a7

Segawa, K., Kurata, S., Yanagihashi, Y., Brummelkamp, T. R., Matsuda, F., & Nagata, S. (2014). Caspase-mediated cleavage of phospholipid flippase for apoptotic phosphatidylserine exposure. *Science (New York, N.Y.)*, *344*(6188), 1164–1168. https://doi.org/10.1126/science.1252809

Serizier, S. B., & McCall, K. (2017). Scrambled Eggs: Apoptotic Cell Clearance by Non-Professional Phagocytes in the Drosophila Ovary. *Frontiers in Immunology*, *8*, 1642. https://doi.org/10.3389/fimmu.2017.01642

Shaykhiev, R., Krause, A., Salit, J., Strulovici-Barel, Y., Harvey, B.-G., O'Connor, T. P., & Crystal, R. G. (2009). Smoking-dependent reprogramming of alveolar macrophage polarization:

implication for pathogenesis of chronic obstructive pulmonary disease. *Journal of Immunology (Baltimore, Md. : 1950)*, *183*(4), 2867–2883. https://doi.org/10.4049/JIMMUNOL.0900473

Shen, P. S., Yang, X., DeCaen, P. G., Liu, X., Bulkley, D., Clapham, D. E., & Cao, E. (2016). The Structure of the Polycystic Kidney Disease Channel PKD2 in Lipid Nanodiscs. *Cell*, *167*(3), 763-773.e11. https://doi.org/10.1016/j.cell.2016.09.048

Shillingford, J. M., Murcia, N. S., Larson, C. H., Low, S. H., Hedgepeth, R., Brown, N., Flask, C. A., Novick, A. C., Goldfarb, D. A., Kramer-Zucker, A., Walz, G., Piontek, K. B., Germino, G. G., & Weimbs, T. (2006). The mTOR pathway is regulated by polycystin-1, and its inhibition reverses renal cystogenesis in polycystic kidney disease. *Proceedings of the National Academy of Sciences*, *103*(14), 5466–5471. https://doi.org/10.1073/pnas.0509694103

Shklyar, B., Sellman, Y., Shklover, J., Mishnaevski, K., Levy-Adam, F., & Kurant, E. (2014). Developmental regulation of glial cell phagocytic function during Drosophila embryogenesis. *Developmental Biology*, *393*(2), 255–269. https://doi.org/10.1016/J.YDBIO.2014.07.005

Siegel, R. M., Chan, F. K. M., Chun, H. J., & Lenardo, M. J. (2000). The multifaceted role of Fas signaling in immune cell homeostasis and autoimmunity. *Nature Immunology 2000 1:6*, *1*(6), 469–474. https://doi.org/10.1038/82712

Siekhaus, D., Haesemeyer, M., Moffitt, O., & Lehmann, R. (2010). RhoL controls invasion and Rap1 localization during immune cell transmigration in Drosophila. *Nature Cell Biology*, *12*(6), 605. https://doi.org/10.1038/NCB2063

Silva, M. T., do Vale, A., & dos Santos, N. M. N. (2008). Secondary necrosis in multicellular animals: an outcome of apoptosis with pathogenic implications. *Apoptosis*, *13*(4), 463–482. https://doi.org/10.1007/s10495-008-0187-8

Smale, G., Nichols, N. R., Brady, D. R., Finch, C. E., & Horton, W. E. (1995). Evidence for Apoptotic Cell Death in Alzheimer's Disease. *Experimental Neurology*, *133*(2), 225–230. https://doi.org/10.1006/exnr.1995.1025

Sonnenfeld, M. J., & Jacobs, J. R. (1995). Macrophages and glia participate in the removal of apoptotic neurons from theDrosophila embryonic nervous system. *The Journal of Comparative Neurology*, *359*(4), 644–652. https://doi.org/10.1002/cne.903590410

SOROKIN, S. (1962). CENTRIOLES AND THE FORMATION OF RUDIMENTARY CILIA BY

FIBROBLASTS AND SMOOTH MUSCLE CELLS. *The Journal of Cell Biology*, *15*(2), 363. https://doi.org/10.1083/JCB.15.2.363

Southall, T. D., Gold, K. S., Egger, B., Davidson, C. M., Caygill, E. E., Marshall, O. J., & Brand, A. H. (2013). Developmental Cell Resource Cell-Type-Specific Profiling of Gene Expression and Chromatin Binding without Cell Isolation: Assaying RNA Pol II Occupancy in Neural Stem Cells. *Developmental Cell*, *26*, 101–112. https://doi.org/10.1016/j.devcel.2013.05.020

Stein, M., Keshav, S., Harris, N., & Gordon, S. (1992). Interleukin 4 potently enhances murine macrophage mannose receptor activity: a marker of alternative immunologic macrophage activation. *The Journal of Experimental Medicine*, *176*(1), 287–292. https://doi.org/10.1084/JEM.176.1.287

Stramer, B., Wood, W., Galko, M. J., Redd, M. J., Jacinto, A., Parkhurst, S. M., & Martin, P. (2005). Live imaging of wound inflammation in Drosophila embryos reveals key roles for small GTPases during in vivo cell migration. *The Journal of Cell Biology*, *168*(4), 567–573. https://doi.org/10.1083/jcb.200405120

Streets, A. J., Wessely, O., Peters, D. J. M., & Ong, A. C. M. (2013). Hyperphosphorylation of polycystin-2 at a critical residue in disease reveals an essential role for polycystin-1-regulated dephosphorylation. *Human Molecular Genetics*, *22*(10), 1924–1939. https://doi.org/10.1093/HMG/DDT031

Strubl, S., Torres, J. A., Spindt, A. K., Pellegrini, H., Liebau, M. C., & Weimbs, T. (2020). STAT Signaling in Polycystic Kidney Disease. *Cellular Signalling*, *72*, 109639. https://doi.org/10.1016/J.CELLSIG.2020.109639

Suzuki, J., Fujii, T., Imao, T., Ishihara, K., Kuba, H., & Nagata, S. (2013). Calcium-dependent phospholipid scramblase activity of TMEM16 protein family members. *The Journal of Biological Chemistry*, *288*(19), 13305–13316. https://doi.org/10.1074/jbc.M113.457937

Swenson-Fields, K. I., Vivian, C. J., Salah, S. M., Peda, J. D., Davis, B. M., Van Rooijen, N., Wallace, D. P., & Fields, T. A. (2013). Macrophages promote polycystic kidney disease progression. *Kidney International*, *83*(5), 855–864. https://doi.org/10.1038/KI.2012.446/ATTACHMENT/CAEC7B3F-FB9E-4BEB-B555-FF85BB0F8BF0/MMC9.PDF

Tan, K. L., Vlisidou, I., & Wood, W. (2014). Ecdysone Mediates the Development of Immunity in the Drosophila Embryo. *Current Biology*, *24*(10), 1145.

https://doi.org/10.1016/J.CUB.2014.03.062

Tardy, O. R., Armitage, E. L., Prince, L. R., & Evans, I. R. (2021). The Epidermal Growth Factor Ligand Spitz Modulates Macrophage Efferocytosis, Wound Responses and Migration Dynamics During Drosophila Embryogenesis. *Frontiers in Cell and Developmental Biology*, *9*, 851. https://doi.org/10.3389/fcell.2021.636024

Tattikota, S. G., Cho, B., Liu, Y., Hu, Y., Barrera, V., Steinbaugh, M. J., Yoon, S. H., Comjean, A., Li, F., Dervis, F., Hung, R. J., Nam, J. W., Sui, S. H., Shim, J., & Perrimon, N. (2020). A single-cell survey of drosophila blood. *ELife*, *9*, 1–35. https://doi.org/10.7554/ELIFE.54818

Tepass, U., Fessler, L. I., Aziz, A., & Hartenstein, V. (1994). Embryonic origin of hemocytes and their relationship to cell death in Drosophila. *Development (Cambridge, England)*, *120*(7), 1829–1837. http://www.ncbi.nlm.nih.gov/pubmed/7924990

Thomé, M. P., Filippi-Chiela, E. C., Villodre, E. S., Migliavaca, C. B., Onzi, G. R., Felipe, K. B., & Lenz, G. (2016). Ratiometric analysis of Acridine Orange staining in the study of acidic organelles and autophagy. *Journal of Cell Science*, *129*(24), 4622–4632. https://doi.org/10.1242/jcs.195057

Torres, J. A., Kruger, S. L., Broderick, C., Amarlkhagva, T., Agrawal, S., Dodam, J. R., Mrug, M., Lyons, L. A., & Weimbs, T. (2019). Ketosis Ameliorates Renal Cyst Growth in Polycystic Kidney Disease. *Cell Metabolism*, *30*(6), 1007-1023.e5. https://doi.org/10.1016/J.CMET.2019.09.012

Torres, V. E., Chapman, A. B., Devuyst, O., Gansevoort, R. T., Grantham, J. J., Higashihara, E., Perrone, R. D., Krasa, H. B., Ouyang, J., & Czerwiec, F. S. (2012). Tolvaptan in Patients with Autosomal Dominant Polycystic Kidney Disease. *New England Journal of Medicine*, *367*(25), 2407–2418. https://doi.org/10.1056/NEJMoa1205511

Torres, V. E., Harris, P. C., & Pirson, Y. (2007). Autosomal dominant polycystic kidney disease. *The Lancet*, *369*(9569), 1287–1301. https://doi.org/10.1016/S0140-6736(07)60601-1

Tucker, P. K., Evans, I. R., & Wood, W. (2011). Ena drives invasive macrophage migration in Drosophila embryos. *Disease Models & Mechanisms*, *4*(1), 126–134. https://doi.org/10.1242/dmm.005694

Turco, A. E., Clementi, M., Rossetti, S., Tenconi, R., & Pignatti, P. F. (1996). An Italian family with autosomal dominant polycystic kidney disease unlinked to either the PKD1 or PKD2 gene. *American Journal of Kidney Diseases : The Official Journal of the National Kidney*

*Foundation*, *28*(5), 759–761. http://www.ncbi.nlm.nih.gov/pubmed/9158217

Van Den Eijnde, S. M., Boshart, L., Baehrecke, E. H., De Zeeuw, C. I., Reutelingsperger, C. P. M., & Vermeij-Keers, C. (1998). Cell surface exposure of phosphatidylserine during apoptosis is phylogenetically conserved. In *Apoptosis* (Vol. 3). https://link.springer.com/content/pdf/10.1023/A:1009650917818.pdf

Van Goethem, E., Silva, E. A., Xiao, H., & Franc, N. C. (2012). The Drosophila TRPP cation channel, PKD2 and Dmel/Ced-12 act in genetically distinct pathways during apoptotic cell clearance. *PloS One*, *7*(2), e31488. https://doi.org/10.1371/journal.pone.0031488

Van, M. V., Fujimori, T., & Bintu, L. (2021). Nanobody-mediated control of gene expression and epigenetic memory. *Nature Communications 2021 12:1*, *12*(1), 1–12. https://doi.org/10.1038/s41467-020-20757-1

Venegas, V., & Zhou, Z. (2007). Two alternative mechanisms that regulate the presentation of apoptotic cell engulfment signal in Caenorhabditis elegans. *Molecular Biology of the Cell*, *18*(8), 3180–3192. https://doi.org/10.1091/mbc.e07-02-0138

Vien, T. N., Ng, L. C. T., Smith, J. M., Dong, K., Krappitz, M., Gainullin, V. G., Fedeles, S., Harris, P. C., Somlo, S., & DeCaen, P. G. (2021). Disrupting polycystin-2 EF hand Ca2+ affinity does not alter channel function or contribute to polycystic kidney disease. *Journal of Cell Science*, *133*(24). https://doi.org/10.1242/JCS.255562/VIDEO-1

Vlahos, R., & Bozinovski, S. (2014). Role of Alveolar Macrophages in Chronic Obstructive Pulmonary Disease. *Frontiers in Immunology*, *5*(SEP). https://doi.org/10.3389/FIMMU.2014.00435

Wang, S., & Dong, Z. (2020). Is autophagy the culprit of cystogenesis in polycystic kidney disease? *EBioMedicine*, *61*. https://doi.org/10.1016/J.EBIOM.2020.103043

Wang, Y., Zhou, C. J., & Liu, Y. (2018). Wnt Signaling in Kidney Development and Disease. In *Progress in molecular biology and translational science* (Vol. 153, pp. 181–207). https://doi.org/10.1016/bs.pmbts.2017.11.019

Wardle, E. N. (1987). Kupffer cells and their function. *Liver*, *7*(2), 63–75. https://doi.org/10.1111/J.1600-0676.1987.TB00319.X

Watkins, P. B., Lewis, J. H., Kaplowitz, N., Alpers, D. H., Blais, J. D., Smotzer, D. M., Krasa, H., Ouyang, J., Torres, V. E., Czerwiec, F. S., & Zimmer, C. A. (2015). Clinical Pattern of Tolvaptan-Associated Liver Injury in Subjects with Autosomal Dominant Polycystic Kidney Disease: Analysis of Clinical Trials Database. *Drug Safety*, *38*(11), 1103–1113.

https://doi.org/10.1007/s40264-015-0327-3

Watnick, T J, Torres, V. E., Gandolph, M. A., Qian, F., Onuchic, L. F., Klinger, K. W., Landes, G., & Germino, G. G. (1998). Somatic mutation in individual liver cysts supports a two-hit model of cystogenesis in autosomal dominant polycystic kidney disease. *Molecular Cell*, *2*(2), 247–251. http://www.ncbi.nlm.nih.gov/pubmed/9734362

Watnick, Terry J., Jin, Y., Matunis, E., Kernan, M. J., & Montell, C. (2003). A Flagellar Polycystin-2 Homolog Required for Male Fertility in Drosophila. *Current Biology*, *13*(24), 2179–2184. https://doi.org/10.1016/J.CUB.2003.12.002

WC, X., H, O., NH, P., JA, B., & C, M. (1994). repo encodes a glial-specific homeo domain protein required in the Drosophila nervous system. *Genes & Development*, *8*(8), 981–994. https://doi.org/10.1101/GAD.8.8.981

Weavers, H., Evans, I. R., Martin, P., & Wood, W. (2016). Corpse Engulfment Generates a Molecular Memory that Primes the Macrophage Inflammatory Response. *Cell*, *165*(7), 1658–1671. https://doi.org/10.1016/j.cell.2016.04.049

Weavers, H., Prieto-Sánchez, S., Grawe, F., Garcia-López, A., Artero, R., Wilsch-Bräuninger, M., Ruiz-Gómez, M., Skaer, H., & Denholm, B. (2008). The insect nephrocyte is a podocyte-like cell with a filtration slit diaphragm. *Nature 2008 457:7227*, *457*(7227), 322–326. https://doi.org/10.1038/nature07526

Wegierski, T., Steffl, D., Kopp, C., Tauber, R., Buchholz, B., Nitschke, R., Kuehn, E. W., Walz, G., & Köttgen, M. (2009). TRPP2 channels regulate apoptosis through the Ca2+ concentration in the endoplasmic reticulum. *The EMBO Journal*, *28*(5), 490–499. https://doi.org/10.1038/emboj.2008.307

Weimbs, T., Shillingford, J. M., Torres, J., Kruger, S. L., & Bourgeois, B. C. (2018). Emerging targeted strategies for the treatment of autosomal dominant polycystic kidney disease. *Clinical Kidney Journal*, *11*(Suppl 1), i27–i38. https://doi.org/10.1093/ckj/sfy089

Weimbs, T., & Talbot, J. J. (2013). STAT3 Signaling in Polycystic Kidney Disease. *Drug Discovery Today. Disease Mechanisms*, *10*(3–4), e113. https://doi.org/10.1016/J.DDMEC.2013.03.001

White, K., Grether, M., Abrams, J., Young, L., Farrell, K., & Steller, H. (1994). Genetic control of programmed cell death in Drosophila. *Science*, *264*(5159), 677–683. https://doi.org/10.1126/science.8171319

Wing, J. P., Zhou, L., Schwartz, L. M., & Nambu, J. R. (1999). Erratum: Distinct cell killing

properties of the Drosophila reaper, head involution defective, and grim genes (Cell Death and Differentiation (1998) 5 (930-939). *Cell Death and Differentiation*, *6*(2), 212–213. https://doi.org/10.1038/sj.cdd.4400487

Winick, J., Abel, T., Leonard, M. W., Michelson, A. M., Chardon-Loriaux, I., Holmgren, R. A., Maniatis, T., Engel, J. D., & Wilson, D. B. (1993). A GATA family transcription factor is expressed along the embryonic dorsoventral axis in Drosophila melanogaster. *Development (Cambridge, England)*, *119*(4), 1055–1065. http://www.ncbi.nlm.nih.gov/pubmed/7916677

Wodarz, A., Hinz, U., Engelbert, M., & Knust, E. (1995). Expression of crumbs confers apical character on plasma membrane domains of ectodermal epithelia of Drosophila. *Cell*, *82*(1), 67–76. https://doi.org/10.1016/0092-8674(95)90053-5

Wong, K., Valdez, P. A., Tan, C., Yeh, S., Hongo, J.-A., & Ouyang, W. (2010). Phosphatidylserine receptor Tim-4 is essential for the maintenance of the homeostatic state of resident peritoneal macrophages. *Proceedings of the National Academy of Sciences of the United States of America*, *107*(19), 8712–8717. https://doi.org/10.1073/pnas.0910929107

Wood, W., & Jacinto, A. (2007). Drosophila melanogaster embryonic haemocytes: masters of multitasking. *Nature Reviews Molecular Cell Biology*, *8*(7), 542–551. https://doi.org/10.1038/nrm2202

Wood, W., & Martin, P. (2017). Macrophage Functions in Tissue Patterning and Disease: New Insights from the Fly. *Developmental Cell*, *40*(3), 221–233. https://doi.org/10.1016/j.devcel.2017.01.001

Wu, G., D'Agati, V., Cai, Y., Markowitz, G., Park, J. H., Reynolds, D. M., Maeda, Y., Le, T. C., Hou, H., Kucherlapati, R., Edelmann, W., & Somlo, S. (1998). Somatic inactivation of Pkd2 results in polycystic kidney disease. *Cell*, *93*(2), 177–188. http://www.ncbi.nlm.nih.gov/pubmed/9568711

Wucherpfennig, T., Wilsch-Bräuninger, M., & González-Gaitán, M. (2003). Role of Drosophila Rab5 during endosomal trafficking at the synapse and evoked neurotransmitter release. *Journal of Cell Biology*, *161*(3), 609–624. https://doi.org/10.1083/JCB.200211087

Wynn, T. A., Chawla, A., & Pollard, J. W. (2013). Macrophage biology in development, homeostasis and disease. *Nature 2013 496:7446*, *496*(7446), 445–455. https://doi.org/10.1038/nature12034

Xu, D., Ma, Y., Gu, X., Bian, R., Lu, Y., Xing, X., & Mei, C. (2018). Novel Mutations in the PKD1

and PKD2 Genes of Chinese Patients with Autosomal Dominant Polycystic Kidney Disease. *Kidney and Blood Pressure Research*, *43*(2), 297–309. https://doi.org/10.1159/000487899

Yang, L., Brooks, C. R., Xiao, S., Sabbisetti, V., Yeung, M. Y., Hsiao, L.-L., Ichimura, T., Kuchroo, V., & Bonventre, J. V. (2015). KIM-1–mediated phagocytosis reduces acute injury to the kidney. *Journal of Clinical Investigation*, *125*(4), 1620–1636. https://doi.org/10.1172/JCI75417

Ye, M., Grant, M., Sharma, M., Elzinga, L., Swan, S., Torres, V. E., & Grantham, J. J. (1992). Cyst fluid from human autosomal dominant polycystic kidneys promotes cyst formation and expansion by renal epithelial cells in vitro. *Journal of the American Society of Nephrology : JASN*, *3*(4), 984–994. https://doi.org/10.1681/ASN.V34984

Yoder, B. K., Hou, X., & Guay-Woodford, L. M. (2002). The polycystic kidney disease proteins, polycystin-1, polycystin-2, polaris, and cystin, are co-localized in renal cilia. *Journal of the American Society of Nephrology : JASN*, *13*(10), 2508–2516. http://www.ncbi.nlm.nih.gov/pubmed/12239239

Yoo, S. J., Huh, J. R., Muro, I. R., Yu, H., Wang, L., Wang, S. L., Feldman, R. M. R., Clem, R. J., Müller, H. A. J., & Hay, B. A. (2002). Hid, Rpr and Grim negatively regulate DIAP1 levels through distinct mechanisms. *Nature Cell Biology*, *4*(6), 416–424. https://doi.org/10.1038/NCB793

Yu, S., Hackmann, K., Gao, J., Gao, J., He, X., Piontek, K., García-González, M. A., García González, M. A., Menezes, L. F., Xu, H., Germino, G. G., Zuo, J., & Qian, F. (2007). Essential role of cleavage of Polycystin-1 at G protein-coupled receptor proteolytic site for kidney tubular structure. *Proceedings of the National Academy of Sciences of the United States of America*, *104*(47), 18688–18693. https://doi.org/10.1073/pnas.0708217104

Yu, Y., Ulbrich, M. H., Li, M.-H., Buraei, Z., Chen, X.-Z., Ong, A. C. M., Tong, L., Isacoff, E. Y., & Yang, J. (2009). Structural and molecular basis of the assembly of the TRPP2/PKD1 complex. *Proceedings of the National Academy of Sciences*, *106*(28), 11558–11563. https://doi.org/10.1073/pnas.0903684106

Zanet, J., Stramer, B., Millard, T., Martin, P., Payre, F., & Plaza, S. (2009). Fascin is required for blood cell migration during Drosophila embryogenesis. *Development*, *136*(15), 2557–2565. https://doi.org/10.1242/dev.036517

Zheng, Q., Gao, N., Sun, Q., Li, X., Wang, Y., & Xiao, H. (2021). bfc, a novel serpent co-factor for the expression of croquemort, regulates efferocytosis in Drosophila melanogaster. *PLoS Genetics*, *17*(12). https://doi.org/10.1371/JOURNAL.PGEN.1009947

Zheng, Q., Ma, A., Yuan, L., Gao, N., Feng, Q., Franc, N. C., & Xiao, H. (2017). Apoptotic Cell Clearance in Drosophila melanogaster. *Frontiers in Immunology*, *8*, 1881. https://doi.org/10.3389/fimmu.2017.01881

Zhu, P., Sieben, C. J., Xu, X., Harris, P. C., & Lin, X. (2017). Autophagy activators suppress cystogenesis in an autosomal dominant polycystic kidney disease model. *Human Molecular Genetics*, *26*(1), 158–172. https://doi.org/10.1093/HMG/DDW376

Zirin, J., Cheng, D., Dhanyasi, N., Cho, J., Dura, J. M., VijayRaghavan, K., & Perrimon, N. (2013). Ecdysone signaling at metamorphosis triggers apoptosis of Drosophila abdominal muscles. *Developmental Biology*, *383*(2), 275–284. https://doi.org/10.1016/J.YDBIO.2013.08.029